

WCAP-13949

WESTINGHOUSE CLASS 3 (Non-Proprietary)

ANALYSIS OF CAPSULE V SPECIMENS AND
DOSIMETERS AND ANALYSIS OF CAPSULE Z
DOSIMETERS FROM THE DUKE POWER
COMPANY MCGUIRE UNIT 1 REACTOR VESSEL
RADIATION SURVEILLANCE PROGRAM

Westinghouse Energy Systems



9404070239 940324
PDR ADDCK 05000369
P PDR

WESTINGHOUSE CLASS 3 (Non-Proprietary)

WCAP-13949

ANALYSIS OF CAPSULE V SPECIMENS AND
DOSIMETERS AND ANALYSIS OF CAPSULE Z
DOSIMETERS FROM THE DUKE POWER
COMPANY MCGUIRE UNIT 1 REACTOR VESSEL
RADIATION SURVEILLANCE PROGRAM

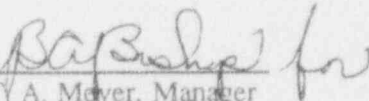
E. Terek
S. L. Zawalick
A. Madeyski
P. A. Peter

February 1994

Work Performed Under Shop Order DXBP-106A

Prepared by Westinghouse Electric Corporation
for the Duke Power Company

Approved by:


T. A. Meyer, Manager
Structural Reliability and
Plant Life Optimization

WESTINGHOUSE ELECTRIC CORPORATION
Nuclear and Advanced Technology Division
P.O. Box 355
Pittsburgh, Pennsylvania 15230-0355

© - 1994 Westinghouse Electric Corporation

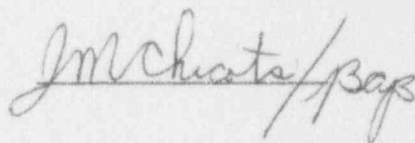
PREFACE

This report has been technically reviewed and verified.

Reviewer:

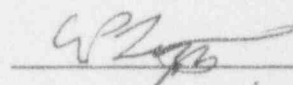
Sections 1 through 5, 7, 8, Appendix A,
Appendix B and Appendix C

J. M. Chicots



Section 6

E. P. Lippincott



Appendix D

B. A. Bishop

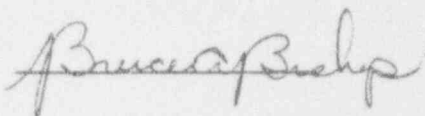


TABLE OF CONTENTS

| <u>Section</u> | <u>Title</u> | <u>Page</u> |
|---|---|-------------|
| 1.0 | SUMMARY OF RESULTS | 1-1 |
| 2.0 | INTRODUCTION | 2-1 |
| 3.0 | BACKGROUND | 3-1 |
| 4.0 | DESCRIPTION OF PROGRAM | 4-1 |
| 5.0 | TESTING OF SPECIMENS FROM CAPSULE V | 5-1 |
| | 5.1 Overview | 5-1 |
| | 5.2 Charpy V-Notch Impact Test Results | 5-3 |
| | 5.3 Tension Test Results | 5-5 |
| | 5.4 Compact Tension Specimen Tests | 5-6 |
| | 5.5 Bend Bar Specimen Tests | 5-6 |
| 6.0 | RADIATION ANALYSIS AND NEUTRON DOSIMETRY | 6-1 |
| | 6.1 Introduction | 6-1 |
| | 6.2 Discrete Ordinates Analysis | 6-2 |
| | 6.3 Neutron Dosimetry | 6-6 |
| | 6.4 Projections of Pressure Vessel Exposure | 6-10 |
| 7.0 | SURVEILLANCE CAPSULE REMOVAL SCHEDULE | 7-1 |
| 8.0 | REFERENCES | 8-1 |
| APPENDIX A LOAD-TIME RECORDS FOR CHARPY SPECIMEN TESTS | | |
| APPENDIX B HEATUP AND COOLDOWN LIMIT CURVES FOR NORMAL OPERATION | | |
| APPENDIX C UPPER SHELF ENERGY EVALUATION | | |
| APPENDIX D JUSTIFICATION FOR USING DIABLO CANYON UNIT 2 SURVEILLANCE WELD DATA FOR THE PREDICTION OF THE MCGUIRE UNIT 1 LOWER SHELL LONGITUDINAL WELD SEAM METAL MECHANICAL PROPERTIES | | |

LIST OF TABLES

| <u>Table</u> | <u>Title</u> | <u>Page</u> |
|--------------|---|-------------|
| 4-1 | Chemical Composition (wt%) of the McGuire Unit 1 Reactor Vessel Surveillance Materials | 4-3 |
| 4-2 | Chemical Composition of Four McGuire Unit 1 Charpy Specimens Removed from Surveillance Capsule V | 4-4 |
| 4-3 | Heat Treatment of the McGuire Unit 1 Reactor Vessel Surveillance Materials | 4-5 |
| 4-4 | Chemistry Results from the NBS Certified Reference Standards | 4-6 |
| 4-5 | Chemistry Results from the NBS Certified Reference Standards | 4-7 |
| 5-1 | Charpy V-notch Data for the McGuire Unit 1 Intermediate Shell Plate B5012-1 Irradiated at 550°F to a Fluence of 2.186×10^{19} n/cm ² (E > 1.0 MeV) (Longitudinal Orientation) | 5-7 |
| 5-2 | Charpy V-notch Data for the McGuire Unit 1 Intermediate Shell Plate B5012-1 Irradiated at 550°F to a Fluence of 2.186×10^{19} n/cm ² (E > 1.0 MeV) (Transverse Orientation) | 5-8 |
| 5-3 | Charpy V-notch Data for the McGuire Unit 1 Surveillance Weld Metal Irradiated at 550°F to a Fluence of 2.186×10^{19} n/cm ² (E > 1.0 MeV) | 5-9 |
| 5-4 | Charpy V-notch Data for the McGuire Unit 1 Heat-Affected-Zone (HAZ) Metal Irradiated at 550°F to a Fluence of 2.186×10^{19} n/cm ² (E > 1.0 MeV) | 5-10 |
| 5-5 | Instrumented Charpy Impact Test Results for the McGuire Unit 1 Intermediate Shell Plate B5012-1 Irradiated at 550°F to a Fluence of 2.186×10^{19} n/cm ² (E > 1.0 MeV) (Longitudinal Orientation) | 5-11 |

LIST OF TABLES (continued)

| <u>Table</u> | <u>Title</u> | <u>Page</u> |
|--------------|---|-------------|
| 5-6 | Instrumented Charpy Impact Test Results for the McGuire Unit 1 Intermediate Shell Plate B5012-1 Irradiated at 550°F to a Fluence of 2.186×10^{19} n/cm ² (E > 1.0 MeV) (Transverse Orientation) | 5-12 |
| 5-7 | Instrumented Charpy Impact Test Results for the McGuire Unit 1 Surveillance Weld Metal Irradiated at 550°F to a Fluence of 2.186×10^{19} n/cm ² (E > 1.0 MeV) | 5-13 |
| 5-8 | Instrumented Charpy Impact Test Results for the McGuire Unit 1 Surveillance Heat-Affected-Zone (HAZ) Metal Irradiated at 550°F to a Fluence of 2.186×10^{19} n/cm ² (E > 1.0 MeV) | 5-14 |
| 5-9 | Effect of 550°F Irradiation to 2.186×10^{19} n/cm ² (E > 1.0 MeV) on the Notch Toughness Properties of the McGuire Unit 1 Reactor Vessel Surveillance Materials | 5-15 |
| 5-10 | Comparison of the McGuire Unit 1 Surveillance Material 30 ft-lb Transition Temperature Shifts and Upper Shelf Energy Decreases with Regulatory Guide 1.99 Revision 2 Predictions | 5-16 |
| 5-11 | Tensile Properties of the McGuire Unit 1 Reactor Vessel Surveillance Materials Irradiated at 550°F to 2.186×10^{19} n/cm ² (E > 1.0 MeV) | 5-17 |
| 6-1 | Calculated Fast Neutron Exposure Rates at the Surveillance Capsule Center | 6-14 |
| 6-2 | Calculated Azimuthal Variation of Fast Neutron Exposure Rates at the Pressure Vessel Clad/Base Metal Interface | 6-15 |
| 6-3 | Relative Radial Distribution of $\phi(E > 1.0 \text{ MeV})$ within the Pressure Vessel Wall | 6-16 |

LIST OF TABLES (continued)

| <u>Table</u> | <u>Title</u> | <u>Page</u> |
|--------------|---|-------------|
| 6-4 | Relative Radial Distribution of $\phi(E > 0.1 \text{ MeV})$ within the Pressure Vessel Wall | 6-17 |
| 6-5 | Relative Radial Distribution of dpa/sec within the Pressure Vessel Wall | 6-18 |
| 6-6 | Nuclear Parameters used in the Evaluation of Neutron Sensors | 6-19 |
| 6-7 | Monthly Thermal Generation During the First Eight Fuel Cycles of the McGuire Unit 1 Reactor | 6-20 |
| 6-8 | Measured Sensor Activities and Reaction Rates Surveillance Capsule U Saturated Activities and Derived Fast Neutron Flux | 6-21 |
| 6-9 | Measured Sensor Activities and Reaction Rates Surveillance Capsule X Saturated Activities and Derived Fast Neutron Flux | 6-22 |
| 6-10 | Measured Sensor Activities and Reaction Rates Surveillance Capsule V Saturated Activities and Derived Fast Neutron Flux | 6-23 |
| 6-11 | Measured Sensor Activities and Reaction Rates Surveillance Capsule Z Saturated Activities and Derived Fast Neutron Flux | 6-24 |
| 6-12 | Summary of Neutron Dosimetry Results Surveillance Capsules U, X, V, and Z | 6-25 |
| 6-13 | Comparison of Measured and Ferret Calculated Reaction Rates at the Surveillance Capsule Center Surveillance Capsules U, X, V, and Z | 6-26 |
| 6-14 | Adjusted Neutron Energy Spectrum at the Center of Surveillance Capsule V | 6-27 |
| 6-15 | Adjusted Neutron Energy Spectrum at the Center of Surveillance Capsule Z | 6-28 |

LIST OF TABLES (continued)

| <u>Table</u> | <u>Title</u> | <u>Page</u> |
|--------------|---|-------------|
| 6-16 | Comparison of Calculated and Measured Neutron Exposure Levels for McGuire Unit 1 Surveillance Capsules U, X, V, and Z | 6-29 |
| 6-17 | Neutron Exposure Projections at Key Locations on the Pressure Vessel Clad/Base Metal Interface | 6-30 |
| 6-18 | Neutron Exposure Values Curves | 6-31 |
| 6-19 | Updated Lead Factors for McGuire Unit 1 Surveillance Capsules | 6-32 |
| 7-1 | McGuire Unit 1 Reactor Vessel Surveillance Capsule Withdrawal Schedule | 7-1 |

LIST OF ILLUSTRATIONS

| <u>Figure</u> | <u>Title</u> | <u>Page</u> |
|---------------|--|-------------|
| 4-1 | Arrangement of Surveillance Capsules in the McGuire Unit 1 Reactor Vessel | 4-8 |
| 4-2 | Diagram Showing the Location of Specimens, Thermal Monitors and Dosimeters | 4-9 |
| 5-1 | Charpy V-Notch Impact Properties for McGuire Unit 1 Reactor Vessel Intermediate Shell Plate B5012-1 (Longitudinal Orientation) | 5-18 |
| 5-2 | Charpy V-Notch Impact Properties for McGuire Unit 1 Reactor Vessel Intermediate Shell Plate B5012-1 (Transverse Orientation) | 5-19 |
| 5-3 | Charpy V-Notch Impact Properties for McGuire Unit 1 Reactor Vessel Surveillance Weld Metal | 5-20 |
| 5-4 | Charpy V-Notch Impact Properties for McGuire Unit 1 Reactor Vessel Weld Heat-Affected-Zone Metal | 5-21 |
| 5-5 | Charpy Impact Specimen Fracture Surfaces for McGuire Unit 1 Reactor Vessel Intermediate Shell Plate B5012-1 (Longitudinal Orientation) | 5-22 |
| 5-6 | Charpy Impact Specimen Fracture Surfaces for McGuire Unit 1 Reactor Vessel Intermediate Shell Plate B5012-1 (Transverse Orientation) | 5-23 |
| 5-7 | Charpy Impact Specimen Fracture Surfaces for McGuire Unit 1 Reactor Vessel Surveillance Weld Metal | 5-24 |
| 5-8 | Charpy Impact Specimen Fracture Surfaces for McGuire Unit 1 Reactor Vessel Heat-Affected-Zone Metal | 5-25 |
| 5-9 | Tensile Properties for McGuire Unit 1 Reactor Vessel Intermediate Shell Plate B5012-1 (Longitudinal Orientation) | 5-26 |

LIST OF ILLUSTRATIONS (continued)

| <u>Figure</u> | <u>Title</u> | <u>Page</u> |
|---------------|--|-------------|
| 5-10 | Tensile Properties for McGuire Unit 1 Reactor Vessel Intermediate Shell Plate B5012-1 (Transverse Orientation) | 5-27 |
| 5-11 | Tensile Properties for McGuire Unit 1 Reactor Vessel Surveillance Weld Metal | 5-28 |
| 5-12 | Fractured Tensile Specimens from McGuire Unit 1 Reactor Vessel Intermediate Shell Plate B5012-1 (Longitudinal Orientation) | 5-29 |
| 5-13 | Fractured Tensile Specimens from McGuire Unit 1 Reactor Vessel Intermediate Shell Plate B5012-1 (Transverse Orientation) | 5-30 |
| 5-14 | Fractured Tensile Specimens from McGuire Unit 1 Reactor Vessel Surveillance Weld Metal | 5-31 |
| 5-15 | Engineering Stress-Strain Curves for Intermediate Shell Plate B5012-1 Tensile Specimens DL4 and DL5 (Longitudinal Orientation) | 5-32 |
| 5-16 | Engineering Stress-Strain Curve for Intermediate Shell Plate B5012-1 Tensile Specimen DL6 (Longitudinal Orientation) | 5-33 |
| 5-17 | Engineering Stress-Strain Curves for Intermediate Shell Plate B5012-1 Tensile Specimens DT4 and DT5 (Transverse Orientation) | 5-34 |
| 5-18 | Engineering Stress-Strain Curve for Intermediate Shell Plate B5012-1 Tensile Specimen DT6 (Transverse Orientation) | 5-35 |
| 5-19 | Engineering Stress-Strain Curves for Weld Metal Tensile Specimens DW4 and DW5 | 5-36 |
| 5-20 | Engineering Stress-Strain Curve for Weld Metal Tensile Specimen DW6 | 5-37 |

LIST OF ILLUSTRATIONS (continued)

| <u>Figure</u> | <u>Title</u> | <u>Page</u> |
|---------------|---|-------------|
| 6-1 | Plan View of a Dual Reactor Vessel Surveillance Capsule | 6-12 |
| 6-2 | Axial Distribution of Neutron Fluence ($E > 1.0$ MeV) Along the 45 Degree Azimuth | 6-13 |

SECTION 1.0

SUMMARY OF RESULTS

The analysis of the reactor vessel materials contained in surveillance Capsule V, the third capsule to be removed from the McGuire Unit 1 reactor pressure vessel and the analysis of the dosimeters contained in capsule Z, the fourth capsule to be removed from the McGuire Unit 1 reactor vessel, led to the following conclusions:

- o Capsule V received an average fast neutron fluence ($E > 1.0$ MeV) of 2.186×10^{19} n/cm² and capsule Z received an average fast neutron fluence ($E > 1.0$ MeV) of 2.285×10^{19} n/cm² after 7.24 effective full power years (EFPY) of plant operation.
- o Irradiation of the capsule V reactor vessel intermediate shell plate B5012-1 Charpy specimens, oriented with the longitudinal axis of the specimen parallel to the major rolling direction of the plate (longitudinal orientation), to 2.186×10^{19} n/cm² ($E > 1.0$ MeV) resulted in a 30 ft-lb transition temperature increase of 85°F and a 50 ft-lb transition temperature increase of 90°F. This results in an irradiated 30 ft-lb transition temperature of 90°F and an irradiated 50 ft-lb transition temperature of 125°F for the longitudinally oriented specimens.
- o Irradiation of the capsule V reactor vessel intermediate shell plate B5012-1 Charpy specimens, oriented with the longitudinal axis of the specimen normal to the major rolling direction of the plate (transverse orientation), to 2.186×10^{19} n/cm² ($E > 1.0$ MeV) resulted in a 30 ft-lb transition temperature increase of 85°F and a 50 ft-lb transition temperature increase of 60°F. This results in an irradiated 30 ft-lb transition temperature of 85°F and an irradiated 50 ft-lb transition temperature of 135°F for transversely oriented specimens.
- o Irradiation of the capsule V weld metal Charpy specimens to 2.186×10^{19} n/cm² ($E > 1.0$ MeV) resulted in a 30 ft-lb transition temperature increase of 175°F and a 50 ft-lb transition temperature increase of 190°F. This results in an irradiated 30 ft-lb transition temperature of 170°F and an irradiated 50 ft-lb transition temperature of 210°F.
- o Irradiation of the capsule V weld Heat-Affected-Zone (HAZ) metal Charpy specimens to 2.186×10^{19} n/cm² ($E > 1.0$ MeV) resulted in a 30 ft-lb transition temperature increase of 135°F and a 50 ft-lb transition temperature increase of 125°F. This results in an irradiated 30 ft-lb transition temperature of 85°F and an irradiated 50 ft-lb transition temperature of 120°F.

- o The average upper shelf energy of the capsule V intermediate shell plate B5012-1 Charpy specimens (longitudinal orientation) resulted in an average energy decrease of 15 ft-lbs after irradiation to 2.186×10^{19} n/cm² (E > 1.0 MeV). This results in an irradiated average upper shelf energy of 125 ft-lbs for the longitudinally oriented specimens.
- o The average upper shelf energy of the capsule V intermediate shell plate B5012-1 Charpy specimens (transverse orientation) resulted in an average energy decrease of 7 ft-lbs after irradiation to 2.186×10^{19} n/cm² (E > 1.0 MeV). This results in an irradiated average upper shelf energy of 94 ft-lbs for the transversely oriented specimens.
- o The average upper shelf energy of the capsule V weld metal Charpy specimens resulted in an average energy decrease of 40 ft-lbs after irradiation to 2.186×10^{19} n/cm² (E > 1.0 MeV). This results in an irradiated average upper shelf energy of 72 ft-lbs for the weld metal specimens.
- o The average upper shelf energy of the capsule V weld HAZ metal Charpy specimens decreased 35 ft-lb after irradiation to 2.186×10^{19} n/cm² (E > 1.0 MeV). This results in an irradiated average upper shelf energy of 83 ft-lbs for the weld HAZ metal.
- o The surveillance Capsule V test results indicate that the surveillance material 30 ft-lb transition temperature increases and average upper shelf energy decreases are less than the Regulatory Guide 1.99, Revision 2 predictions.
- o The calculated end-of-license (32 EFPY) maximum neutron fluence (E > 1.0 MeV) for the McGuire Unit 1 reactor vessel based on the capsule V and Z dosimeters is as follows:

$$\text{Vessel inner radius}^* = 2.016 \times 10^{19} \text{ n/cm}^2$$

$$\text{Vessel 1/4 thickness} = 1.101 \times 10^{19} \text{ n/cm}^2$$

$$\text{Vessel 3/4 thickness} = 2.359 \times 10^{18} \text{ n/cm}^2$$

* Clad/base metal interface

SECTION 2.0 INTRODUCTION

This report presents the results of the examination of the Capsule V test specimens and dosimeters and the results of the examination of the dosimeters from Capsule Z. These capsules are the third and fourth capsules to be removed from the reactor in the continuing surveillance program which monitors the effects of neutron irradiation on the Duke Power Company McGuire Unit 1 reactor pressure vessel materials under actual operating conditions.

The surveillance program for the Duke Power Company McGuire Unit 1 reactor pressure vessel materials was designed and recommended by the Westinghouse Electric Corporation. A description of the surveillance program and the preirradiation mechanical properties of the reactor vessel materials is presented in WCAP-9195, "Duke Power Company William B. McGuire Unit No. 1 Reactor Vessel Radiation Surveillance Program"⁽¹⁾. The surveillance program was planned to cover the 40-year design life of the reactor pressure vessel and was based on ASTM E185-73, "Standard Recommended Practice for Surveillance Tests for Nuclear Reactor Vessels". Capsules "V" and "Z" were removed from the reactor after 7.24 EFPY of exposure and shipped to the Westinghouse Science and Technology Center Hot Cell Facility, where the postirradiation mechanical testing of the Charpy $\sqrt{}$ -notch impact and tensile specimens from capsule "V" was performed.

This report summarizes the testing of and the postirradiation data obtained from surveillance capsules "V" and "Z" removed from the Duke Power Company McGuire Unit 1 reactor vessel and discusses the analysis of the data. For capsule "Z" only the dosimeters were analyzed at this time and the surveillance specimens were placed in storage at the Westinghouse Science and Technology Center Hot Cell Facility.

SECTION 3.0 BACKGROUND

The ability of the large steel pressure vessel containing the reactor core and its primary coolant to resist fracture constitutes an important factor in ensuring safety in the nuclear industry. The beltline region of the reactor pressure vessel is the most critical region of the vessel because it is subjected to significant fast neutron bombardment. The overall effects of fast neutron irradiation on the mechanical properties of low alloy, ferritic pressure vessel steels such as SA533 Grade B Class 1 (base material of the McGuire Unit 1 reactor pressure vessel) are well documented in the literature. Generally, low alloy ferritic materials show an increase in hardness and tensile properties and a decrease in ductility and toughness during high-energy irradiation.

A method for performing analyses to guard against fast fracture in reactor pressure vessels has been presented in "Protection Against Nonductile Failure," Appendix G to Section III of the ASME Boiler and Pressure Vessel Code^[2]. The method uses fracture mechanics concepts and is based on the reference nil-ductility transition temperature (RT_{NDT}).

RT_{NDT} is defined as the greater of either the drop weight nil-ductility transition temperature (NDTT per ASTM E-208^[3]) or the temperature 60°F less than the 50 ft-lb (and 35-mil lateral expansion) temperature as determined from Charpy specimens oriented normal (transverse) to the major working direction of the plate. The RT_{NDT} of a given material is used to index that material to a reference stress intensity factor curve (K_{IR} curve) which appears in Appendix G to the ASME Code^[2]. The K_{IR} curve is a lower bound of dynamic, crack arrest, and static fracture toughness results obtained from several heats of pressure vessel steel. When a given material is indexed to the K_{IR} curve, allowable stress intensity factors can be obtained for this material as a function of temperature. Allowable operating limits can then be determined using these allowable stress intensity factors.

RT_{NDT} and, in turn, the operating limits of nuclear power plants can be adjusted to account for the effects of radiation on the reactor vessel material properties. The changes in mechanical properties of a given reactor pressure vessel steel due to irradiation can be monitored by a reactor surveillance program, such as the McGuire Unit 1 reactor vessel radiation surveillance program^[1], in which a surveillance capsule is periodically removed from the operating nuclear reactor and the

encapsulated specimens tested. The increase in the average Charpy V-notch 30 ft-lb temperature (ΔRT_{NDT}) due to irradiation is added to the initial RT_{NDT} to adjust the RT_{NDT} (ART) for radiation embrittlement. This ART (RT_{NDT} initial + ΔRT_{NDT}) is used to index the material to the K_{IR} curve and, in turn, to set operating limits for the nuclear power plant that take into account the effects of irradiation on the reactor vessel materials.

SECTION 4.0
DESCRIPTION OF PROGRAM

Six surveillance capsules for monitoring the effects of neutron exposure on the McGuire Unit 1 reactor pressure vessel core region (beltline) materials were inserted in the reactor vessel prior to initial plant start-up. The six capsules were positioned in the reactor vessel between the neutron pads and the vessel wall as shown in Figure 4-1. The vertical center of the capsules is opposite the vertical center of the core. The capsules contain specimens made from intermediate shell plate B5012-1 (Heat No. C-4387-2) and weld metal fabricated with 3/16-inch Mil B-4 weld filler wire (tandem wire heat numbers 20291 and 12008) Linde 1092 flux, lot number 3854, which is identical to that used in the actual fabrication of the intermediate shell longitudinal weld seams.

Capsules V and Z were removed after 7.241 effective full power years (EFPY) of plant operation. These capsules contained Charpy V-notch, tensile, and 1/2T compact specimens (1/2T-CT) made from intermediate shell plate B5012-1 and submerged arc weld metal identical to the intermediate shell longitudinal seams and Charpy V-notch specimens from the weld heat affected zone (HAZ) of intermediate shell plate B5012-2.

Test material obtained from the intermediate shell plate (after thermal heat treatment and forming of the plate) was taken at least one plate thickness from the quenched edges of the plate. All test specimens were machined from the 1/4 thickness location of the plate after performing a simulated postweld, stress-relieving treatment on the test material. Specimens from weld metal and HAZ metal were machined from a stress-relieved weldment joining intermediate shell plate B5012-2 and B5012-3. All heat-affected-zone specimens were obtained from the weld heat-affected-zone of intermediate shell plate B5012-2.

Charpy V-notch impact and tension specimens were machined from intermediate shell plate B5012-1 in both the longitudinal orientation (longitudinal axis of the specimen parallel to the major rolling direction of the plate) and transverse orientation (longitudinal axis of the specimen normal to the major rolling direction of the plate). Charpy V-notch and tensile specimens from the weld metal were oriented such that the long dimension of the specimen was normal to the welding direction. The notch of the weld metal Charpy specimens was machined such that the direction of crack propagation in the specimen is in the welding direction.

Capsules V and Z, also, contained 1/2T-CT test specimens from intermediate shell plate B5012-1 machined in both the longitudinal and transverse orientations. 1/2T-CT test specimens from the weld metal were machined such that the simulated crack in the specimen would propagate in the direction of welding. All specimens were fatigue pre-cracked according to ASTM E399.

Each capsule contained one bend bar specimen from intermediate shell plate B5012-1. The bend bar specimen was machined with the longitudinal axis of the specimen oriented normal to the rolling direction of the plate such that the simulated crack would propagate in the rolling direction of the plate. The bend bar specimen was fatigue precracked according to ASTM E399.

The chemical composition and heat treatment of the surveillance material is presented in Tables 4-1 through 4-3. The chemical analysis reported in Table 4-1 was obtained from unirradiated material used in the surveillance program^[1] and irradiated material from capsule U^[4]. In addition, a chemical analysis using Inductively Coupled Plasma Spectrometry was performed on one irradiated Charpy specimen from intermediate shell plate B5012-1 and three weld metal Charpy specimens and is report in Table 4-2. The chemistry results from the NBS certified reference standards are reported in Table 4-4 and 4-5.

Capsules V and Z contained dosimeter wires of pure copper, iron, nickel, and aluminum-0.15 weight percent cobalt wire (cadmium-shielded and unshielded). In addition, cadmium shielded dosimeters of neptunium (Np^{237}) and uranium (U^{238}) were placed in the capsule to measure the integrated flux at specific neutron energy levels.

The capsules contained thermal monitors made from two low-melting-point eutectic alloys and sealed in Pyrex tubes. These thermal monitors were used to define the maximum temperature attained by the test specimens during irradiation. The composition of the two eutectic alloys and their melting points are as follows:

| | |
|------------------------------|------------------------------|
| 2.5% Ag, 97.5% Pb | Melting Point: 579°F (304°C) |
| 1.75% Ag, 0.75% Sn, 97.5% Pb | Melting Point: 590°F (310°C) |

The arrangement of the various mechanical specimens, dosimeters and thermal monitors contained in capsules V and Z is shown in Figure 4-2.

| TABLE 4-1 | | | | |
|--|----------------------------------|---------------------|--|-----------------------------------|
| Chemical Composition (wt%) of the McGuire Unit 1 Reactor Vessel Surveillance Materials | | | | |
| Element | Intermediate Shell Plate B5012-1 | | Surveillance Weld Metal ^(a) | |
| | Westinghouse Analysis | CE Analysis | CE Analysis | Capsule U ^(c) Analysis |
| C | - | 0.21 | 0.10 | - |
| S | - | 0.016 | 0.008 | - |
| N | 0.003 | - | 0.008 | - |
| Co | 0.016 | - | 0.014 | - |
| Cu | 0.087 | 0.13 ^(b) | 0.21 | 0.20 |
| Si | - | 0.23 | 0.24 | 0.23 |
| Mo | - | 0.57 | 0.55 | 0.54 |
| Ni | - | 0.60 | 0.88 | 0.91 |
| Mn | - | 1.26 | 1.36 | 1.19 |
| Cr | 0.068 | - | 0.04 | 0.05 |
| V | 0.003 | - | 0.04 | - |
| P | - | 0.010 | 0.011 | 0.010 |
| Sn | 0.007 | - | 0.007 | - |
| B | <0.003 | - | <0.001 | - |
| Cb | <0.001 | - | <0.01 | - |
| Ti | 0.005 | - | <0.01 | - |
| W | <0.001 | - | <0.01 | - |
| As | 0.008 | - | 0.009 | - |
| Zr | 0.003 | - | <0.001 | - |
| Sb | <0.001 | - | 0.0022 | - |
| Pb | 0.001 | - | <0.001 | - |

- a) Surveillance weld specimens were made of the same weld wire and flux as the intermediate shell longitudinal weld seams (Tandem weld wire heats 20291 and 12008 and Linde 1092 Flux Lot 3854)^[5]
- b) Ladle analysis (Lukens Steel Co.)
- c) Chemical Analysis by Westinghouse on irradiated Charpy weld specimen DW-15 removed from capsule U.^[4]

TABLE 4-2

Chemical Composition of Four McGuire Unit 1 Charpy Specimens
Removed from Surveillance Capsule V

| Element | Concentration in Weight Percent | | | |
|---------|---------------------------------|--------|--------|---------------------|
| | Weld Metal Specimens | | | Base Metal Specimen |
| | DW-22 | DW-24 | DW-25 | DT-25 |
| Fe | 95.848 | 95.880 | 95.851 | 96.002 |
| Co | 0.015 | 0.016 | 0.016 | 0.015 |
| Cr | 0.046 | 0.044 | 0.044 | 0.076 |
| Cu | 0.195 | 0.191 | 0.193 | 0.117 |
| Mn | 1.329 | 1.331 | 1.330 | 1.355 |
| Mo | 0.548 | 0.539 | 0.550 | 0.634 |
| Ni | 0.870 | 0.848 | 0.863 | 0.643 |
| P | 0.013 | 0.014 | 0.015 | 0.011 |
| Ti | 0.006 | 0.006 | 0.006 | 0.007 |
| V | 0.001 | 0.001 | 0.001 | <0.001 |
| Al | <0.022 | <0.022 | <0.022 | <0.024 |
| As | <0.016 | <0.015 | <0.016 | <0.018 |
| B | 0.004 | 0.004 | 0.003 | 0.005 |
| Nb | 0.013 | 0.013 | 0.013 | 0.013 |
| Sn | <0.024 | <0.025 | <0.025 | <0.027 |
| W | <0.039 | <0.040 | <0.040 | <0.043 |
| Zr | <0.010 | <0.010 | <0.010 | <0.011 |
| C | 0.096 | 0.100 | 0.100 | 0.219 |
| S | 0.0106 | 0.0096 | 0.0097 | 0.0133 |
| Si | 0.185 | 0.180 | 0.188 | 0.216 |

Analyses

Metals
Carbon
Sulfur
Silicon

Method of Analysis

ICPS, Inductively Coupled Plasma Spectrometry
LECO Analyzer
LECO Combustion-titration
ASTM Gravimetric

TABLE 4-3

Heat Treatment of the McGuire Unit 1 Reactor Vessel
Surveillance Materials⁽¹⁾

| Material | Temperature (°F) | Time (hr) | Coolant |
|---|-----------------------------|-----------|----------------|
| Surveillance Program Test Plate B5012-1 | Austenitizing: 1600 ± 50 | 4 | Water quenched |
| | Tempered: 1225 ± 25 | 4 | Air cooled |
| | Stress Relief: 1150 ± 25 | 40 | Furnace cooled |
| Weldment | Stress Relief: 1150 ± 25 | 40 | Furnace cooled |

TABLE 4-4

Chemistry Results from the NBS Certified Reference Standards

| Element | Low Alloy Steel: NIST Control Standard | | | |
|---------|--|-----------|----------|-----------|
| | Concentration in Weight Percent | | | |
| | NIST 361 | | NIST 362 | |
| | Measured | Certified | Measured | Certified |
| Fe | 95.442 | 95.600 | 95.370 | 95.300 |
| Co | 0.033 | 0.032 | 0.335 | 0.300 |
| Cr | 0.722 | 0.694 | 0.321 | 0.300 |
| Cu | 0.046 | 0.042 | 0.570 | 0.500 |
| Mn | 0.682 | 0.660 | 1.104 | 1.040 |
| Pb | 0.208 | 0.190 | 0.068 | 0.068 |
| Ni | 2.054 | 2.000 | 0.620 | 0.590 |
| P | 0.020 | 0.014 | 0.038 | 0.041 |
| Ti | 0.022 | 0.020 | 0.030 | 0.084 |
| V | 0.008 | 0.011 | 0.041 | 0.040 |
| Al | <0.022 | 0.021 | 0.089 | 0.095 |
| As | 0.023 | 0.017 | 0.104 | 0.092 |
| B | <0.002 | 0.000 | 0.004 | 0.003 |
| Nb | 0.023 | 0.022 | 0.016 | 0.290 |
| Sn | <0.024 | 0.010 | <0.026 | 0.016 |
| W | <0.020 | 0.017 | 0.209 | 0.200 |
| Zr | <0.009 | 0.009 | 0.204 | 0.190 |
| C | 0.383 | 0.383 | 0.161 | 0.160 |
| S | NA | 0.0140 | 0.0358 | 0.0360 |
| Si | NA | 0.222 | NA | 0.39 |

NA - Not Analyzed

Analyses

Metals

Carbon

Sulfur

Silicon

Method of Analysis

ICPS, Inductively Coupled Plasma Spectrometry

LECO Analyzer

LECO Combustion-titration

ASTM Gravimetric

TABLE 4-5

Chemistry Results from the NBS Certified Reference Standards

| Element | Low Alloy Steel: NIST Control Standard | | | | | |
|---------|--|-----------|----------|-----------|----------|-----------|
| | Concentration in Weight Percent | | | | | |
| | NIST 363 | | NIST 364 | | NIST 365 | |
| | Measured | Certified | Measured | Certified | Measured | Certified |
| Fe | 94.065 | 94.400 | 96.606 | 96.700 | 99.710 | 99.900 |
| Co | 0.052 | 0.048 | 0.175 | 0.150 | 0.008 | 0.007 |
| Cr | 1.416 | 1.310 | 0.073 | 0.063 | <0.022 | 0.007 |
| Cu | 0.118 | 0.100 | 0.302 | 0.249 | 0.007 | 0.006 |
| Mn | 1.598 | 1.500 | 0.277 | 0.255 | 0.008 | 0.006 |
| Mo | 0.024 | 0.028 | 0.551 | 0.490 | <0.006 | 0.005 |
| Ni | 0.339 | 0.300 | 0.155 | 0.144 | 0.044 | 0.041 |
| P | 0.033 | 0.029 | <0.012 | 0.010 | <0.011 | 0.003 |
| Ti | 0.048 | 0.050 | 0.257 | 0.240 | 0.008 | 0.001 |
| V | 0.340 | 0.310 | 0.122 | 0.105 | <0.001 | 0.001 |
| Al | 0.286 | 0.24 | <0.026 | 0.008 | <0.025 | 0.001 |
| As | <0.019 | 0.010 | 0.052 | 0.052 | <0.019 | 0.000 |
| B | <0.002 | 0.001 | 0.015 | 0.011 | <0.002 | 0.000 |
| Nb | 0.050 | 0.049 | 0.042 | 0.157 | 0.012 | 0.000 |
| Sn | 0.103 | 0.104 | <0.030 | 0.008 | <0.028 | 0.000 |
| W | <0.045 | 0.046 | <0.048 | 0.100 | <0.044 | 0.000 |
| Zr | 0.035 | 0.049 | 0.069 | 0.068 | <0.004 | 0.000 |
| C | NA | 0.620 | NA | 0.870 | NA | 0.007 |
| S | NA | 0.0068 | 0.0242 | 0.0250 | NA | 0.0055 |
| Si | NA | 0.74 | NA | 0.065 | NA | 0.008 |

NA - Not Analyzed

Analyses

Metals
Carbon
Sulfur
Silicon

Method of Analysis

ICPS, Inductively Coupled Plasma Spectrometry
LECO Analyzer
LECO Combustion-titration
ASTM Gravimetric

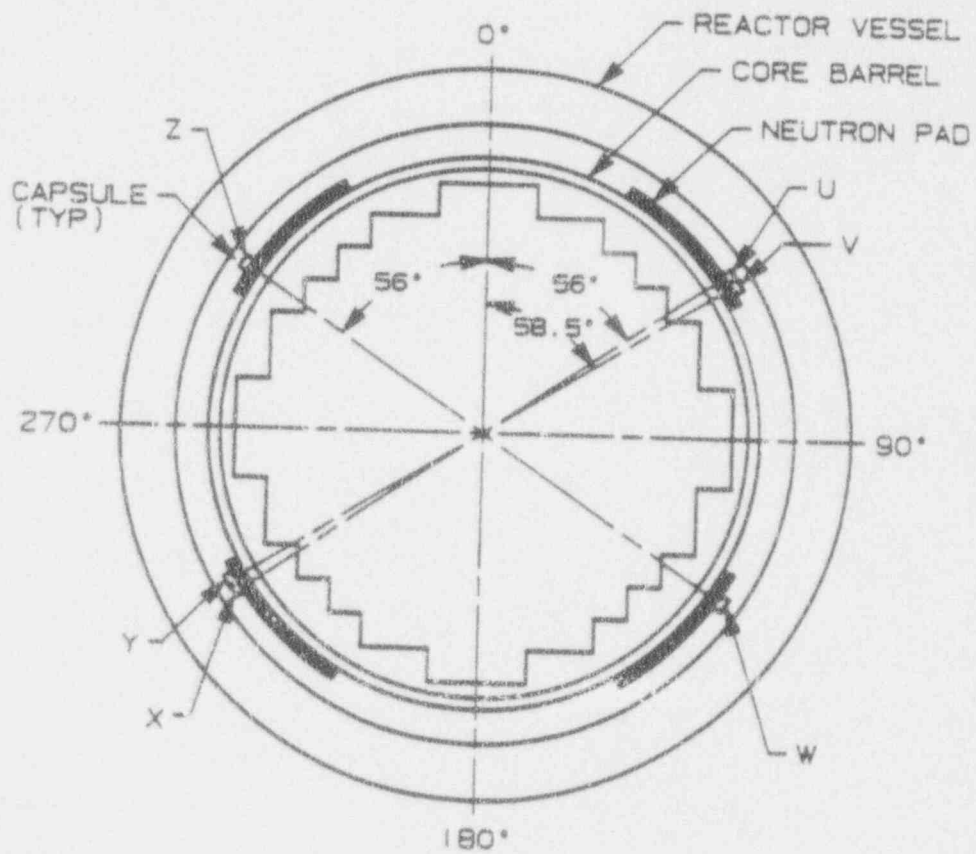
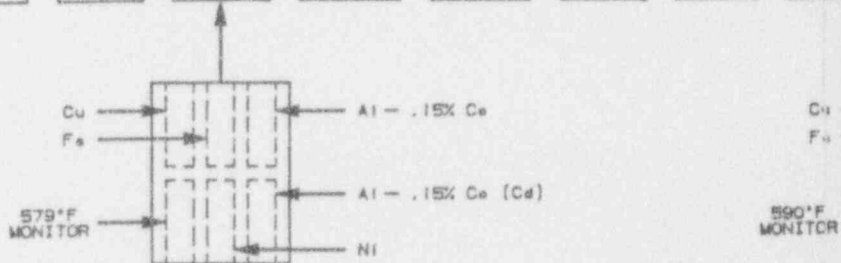
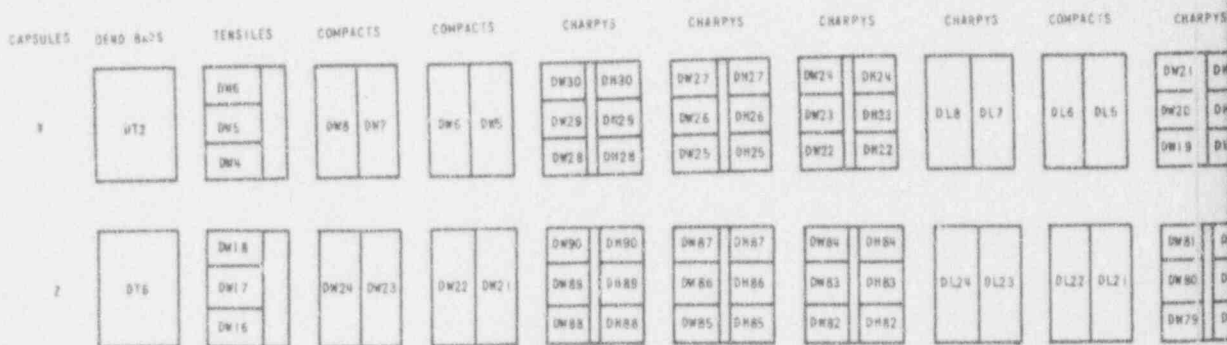


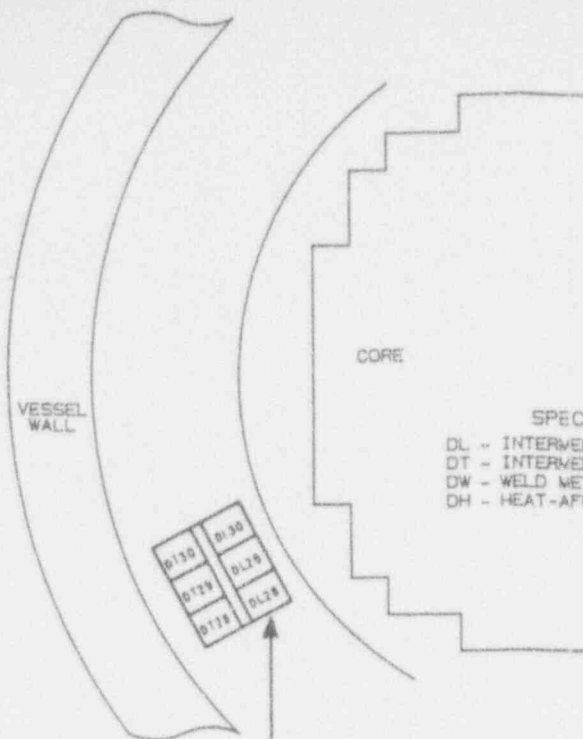
Figure 4-1. Arrangement of Surveillance Capsules in the McGuire Unit 1 Reactor Vessel



← TO TOP OF VESSEL

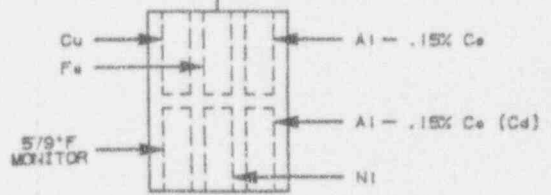
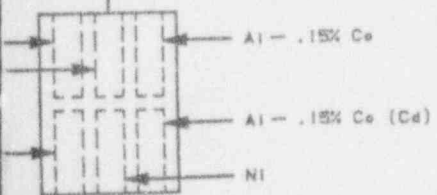
ANSTEC APERTURE CARD

Also Available on Aperture Card



SPECIMEN NUMBERING CODE:
 DL - INTERMEDIATE SHELL PLATE B5012-1 (LONGITUDINAL)
 DT - INTERMEDIATE SHELL PLATE B5012-1 (TRANSVERSE)
 DW - WELD METAL
 DH - HEAT-AFFECTED-ZONE MATERIAL

| CHARPYS | DOSIMETERS | TENSILES | CHARPYS | CHARPYS | CHARPYS | CHARPYS | CHARPYS | CHARPYS | COMPACTS | COMPACTS | TENSILES |
|-------------------------------------|------------|----------------------|-------------------------------------|-------------------------------------|-------------------------------------|-------------------------------------|-------------------------------------|------------------------|----------|----------|----------------------|
| DW10 DH16 DW17 DH17 DW15 DH16 | 307 | DL6 DL5 DL4 | DT30 DL30 DT29 DL29 DT28 DL28 | DT27 DL27 DT26 DL26 DT25 DL25 | DT24 DL24 DT23 DL23 DT22 DL22 | DT21 DL21 DT20 DL20 DT19 DL19 | DT18 DL18 DT17 DL17 DT16 DL16 | DT8 DT7 DT6 DT5 | | | DT4 DT5 DT4 |
| DW78 DH78 DW77 DH77 DW76 DH76 | 311 | DL16 DL17 DL18 | DT90 DL90 DT89 DL89 DT88 DL88 | DT87 DL87 DT86 DL86 DT85 DL85 | DT84 DL84 DT83 DL83 DT82 DL82 | DT81 DL81 DT80 DL80 DT79 DL79 | DT78 DL78 DT77 DL77 DT76 DL76 | DT24 DT23 DT22 DT21 | | | DT18 DT17 DT16 |



CENTER REGION OF VESSEL TO BOTTOM OF VESSEL

Figure 4-2. Diagram Showing the Location of Specimens, Thermal Monitors, and Dosimeters

9403070239-01

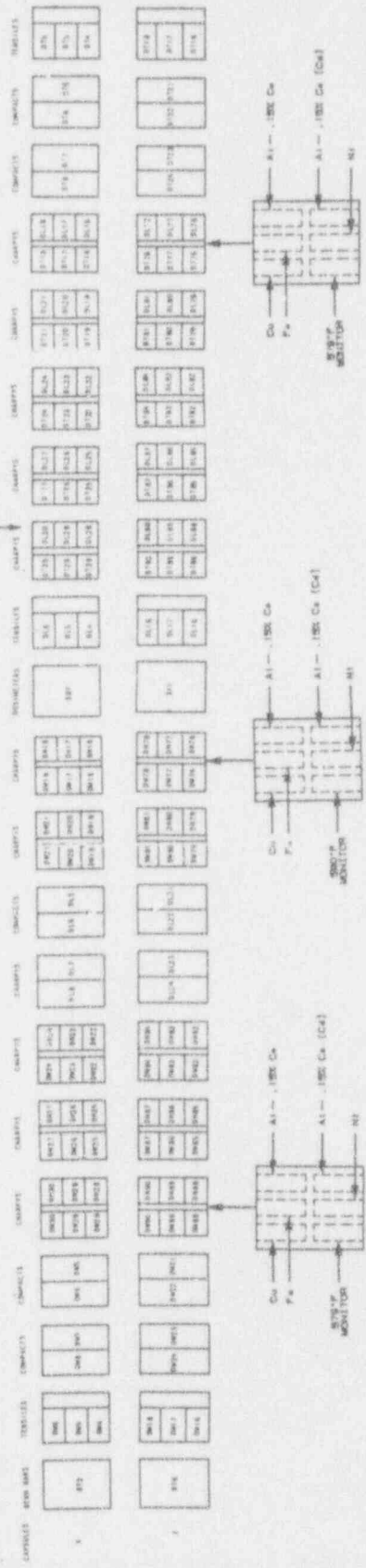
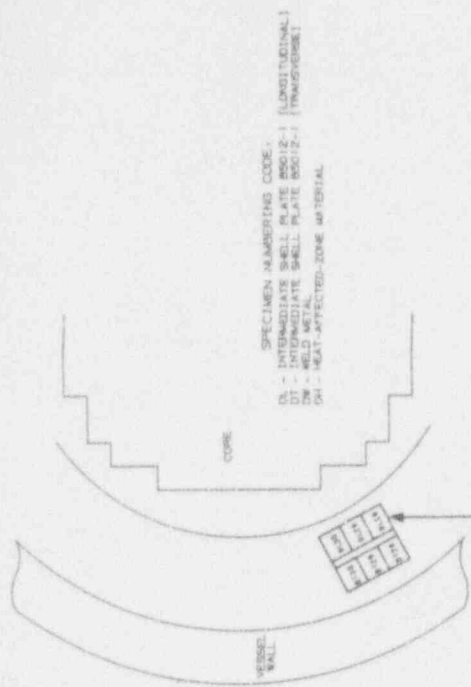


Figure 4-2. Diagram Showing the Location of Specimens, Thermal Monitors, and Dosimeters

SECTION 5.0
TESTING OF SPECIMENS FROM CAPSULE V

5.1 Overview

The Charpy V-notch specimens contained in capsule Z were placed in storage and not tested at this time. The specimens contained in capsule V were tested and the results are reported here.

The post-irradiation mechanical testing of the Charpy V-notch impact specimens and tensile specimens, removed from capsule V, was performed in the Remote Metallographic Facility at the Westinghouse Science and Technology Center. Testing was performed in accordance with 10CFR50, Appendices G and H⁽⁶⁾, ASTM Specification E185-82⁽⁷⁾ and Westinghouse Procedure MHL 8402, Revision 2 as modified by Westinghouse RMF Procedure 8102, Revision 1, and 8103, Revision 1.

Upon receipt of capsules V and Z at the hot cell laboratory, the specimens and spacer blocks were carefully removed, inspected for identification number, and checked against the master list in WCAP-9195⁽⁴⁾. No discrepancies were found.

Examination of the two low-melting point 579°F (304°C) and 590°F (310°C) eutectic alloys indicated no melting of either type of thermal monitor. Based on this examination, the maximum temperature to which the test specimens were exposed was less than 579°F (304°C).

The Charpy impact tests were performed per ASTM Specification E23-92⁽⁸⁾ and RMF Procedure 8103, Revision 1, on a Tinius-Olsen Model 74, 358J machine. The tup (striker) of the Charpy impact test machine is instrumented with a GRC 830I instrumentation system, feeding information into an IBM XT Computer. With this system, load-time and energy-time signals can be recorded in addition to the standard measurement of Charpy energy (E_D). From the load-time curve, the load of general yielding (P_{GY}), the time to general yielding (t_{GY}), the maximum load (P_M), and the time to maximum load (t_M) can be determined. Under some test conditions, a sharp drop in load indicative of fast fracture was observed. The load at which fast fracture was initiated is identified as the fast fracture load (P_F), and the load at which fast fracture terminated is identified as the arrest load (P_A). The energy at maximum load (E_M) was determined by comparing the energy-time record and the load-time record. The energy at maximum load is approximately equivalent to the energy required to initiate a crack in the specimen. Therefore, the propagation energy for the crack

(E_p) is the difference between the total energy to fracture (E_p) and the energy at maximum load (E_M).

The yield stress (σ_Y) was calculated from the three-point bend formula having the following expression:

$$\sigma_Y = (P_{GY} * L) / [B * (W - a)^2 * C] \quad (1)$$

where: L = distance between the specimen supports in the impact machine
B = the width of the specimen measured parallel to the notch
W = height of the specimen, measured perpendicularly to the notch
a = notch depth

The constant C is dependent on the notch flank angle (ϕ), notch root radius (ρ) and the type of loading (ie. pure bending or three-point bending). In three-point bending, for a Charpy specimen in which $\phi = 45^\circ$ and $\rho = 0.010$ ", Equation 1 is valid with $C = 1.21$. Therefore, (for $L = 4W$),

$$\sigma_Y = (P_{GY} * L) / [B * (W - a)^2 * 1.21] = (3.3 * P_{GY} * W) / [B * (W - a)^2] \quad (2)$$

For the Charpy specimen, $B = 0.394$ ", $W = 0.394$ " and $a = 0.079$ " Equation 2 then reduces to:

$$\sigma_Y = (33.3 * P_{GY}) \quad (3)$$

where σ_Y is in units of psi and P_{GY} is in units of lbs. The flow stress was calculated from the average of the yield and maximum loads, also using the three-point bend formula.

Percent shear was determined from post-fracture photographs using the ratio-of-areas methods in compliance with ASTM Specification A370-92^[9]. The lateral expansion was measured using a dial gage rig similar to that shown in the same specification.

Tensile tests were performed on a 20,000-pound Instron, split-console test machine (Model 1115) per ASTM Specification E8-91^[10] and E21-79(1988)^[11], and RMF Procedure 8102, Revision 1. All pull rods, grips, and pins were made of Inconel 718. The upper pull rod was connected through a universal joint to improve axially of loading. The tests were conducted at a constant crosshead speed of 0.05 inches per minute throughout the test.

Extension measurements were made with a linear variable displacement transducer extensometer. The extensometer knife edges were spring-loaded to the specimen and operated through specimen failure. The extensometer gage length was 1.00 inch. The extensometer is rated as Class B-2 per ASTM E83-93^[12].

Elevated test temperatures were obtained with a three-zone electric resistance split-tube furnace with a 9-inch hot zone. All tests were conducted in air. Because of the difficulty in remotely attaching a thermocouple directly to the specimen, the following procedure was used to monitor specimen temperatures. Chromel-alumel thermocouples were positioned at center and each end of the gage section of a dummy specimen in each grip. In the test configuration, with a slight load on the specimen, a plot of specimen temperature versus upper and lower grip and controller temperatures was developed over the range from room temperature to 550°F (288°C). During the actual testing, the grip temperatures were used to obtain desired specimen temperatures. Experiments indicated that this method is accurate to $\pm 2^\circ\text{F}$.

The yield load, ultimate load, fracture load, total elongation, and uniform elongation were determined directly from the load-extension curve. The yield strength, ultimate strength, and fracture strength were calculated using the original cross-sectional area. The final diameter and final gage length were determined from post-fracture photographs. The fracture area used to calculate the fracture stress (true stress at fracture) and percent reduction in area was computed using the final diameter measurement.

5.2 Charpy V-Notch Impact Test Results

The results of the Charpy V-notch impact tests performed on the various materials contained in Capsule V, which was irradiated to 2.186×10^{19} n/cm² ($E > 1.0$ MeV), are presented in Tables 5-1 through 5-8 and are compared with unirradiated results^[1] as shown in Figures 5-1 through 5-4. The transition temperature increases and upper shelf energy decreases for the Capsule V materials are summarized in Table 5-9.

Irradiation of the reactor vessel intermediate shell plate B5012-1 Charpy specimens oriented with the longitudinal axis of the specimen parallel to the major rolling direction of the plate (longitudinal orientation) to 2.186×10^{19} n/cm² ($E > 1.0$ MeV) at 550°F (Figure 5-1) resulted in a 30 ft-lb transitions temperature increase of 85°F and a 50 ft-lb transition temperature increase of 90°F.

This resulted in an irradiated 30 ft-lb transition temperature of 90°F and an irradiated 50 ft-lb transition temperature of 125°F (longitudinal orientation).

The average upper shelf energy (USE) of the intermediate shell plate B5012-1 Charpy specimens (longitudinal orientation) resulted in an energy decrease of 15 ft-lb after irradiation to 2.186×10^{19} n/cm² ($E > 1.0$ MeV) at 550°F. This results in an irradiated average USE of 125 ft-lb (Figure 5-1).

Irradiation of the reactor vessel intermediate shell plate B5012-1 Charpy specimens oriented with the longitudinal axis of the specimen normal to the major rolling direction of the plate (transverse orientation) to 2.186×10^{19} n/cm² ($E > 1.0$ MeV) at 550°F (Figure 5-2) resulted in a 30 ft-lb transition temperature increase of 85°F and a 50 ft-lb transition temperature increase of 60°F. This results in an irradiated 30 ft-lb transition temperature of 85°F and an irradiated 50 ft-lb transition temperature of 135°F (transverse orientation).

The average USE of the intermediate shell plate B5012-1 Charpy specimens (transverse orientation) resulted in an energy decrease of 7 ft-lb after irradiation to 2.186×10^{19} n/cm² ($E > 1.0$ MeV) at 550°F. This results in an irradiated average USE of 94 ft-lb (Figure 5-2).

Irradiation of the surveillance weld metal Charpy specimens to 2.186×10^{19} n/cm² ($E > 1.0$ MeV) at 550°F (Figure 5-3) resulted in a 30 ft-lb transition temperature shift of 175°F and a 50 ft-lb transition temperature increase of 190°F. This results in an irradiated 30 ft-lb transition temperature of 170°F and an irradiated 50 ft-lb transition temperature of 210°F.

The average USE of the surveillance weld metal resulted in an energy decrease of 40 ft-lb after irradiation to 2.186×10^{19} n/cm² ($E > 1.0$ MeV) at 550°F. This resulted in an irradiated average USE of 72 ft-lb (Figure 5-3).

Irradiation of the reactor vessel weld HAZ metal Charpy specimens to 2.186×10^{19} n/cm² ($E > 1.0$ MeV) at 550°F (Figure 5-4) resulted in a 30 ft-lb transition temperature increase of 135°F and a 50 ft-lb transition temperature increase of 125°F. This resulted in an irradiated 30 ft-lb transition temperature of 85°F and an irradiated 50 ft-lb transition temperature of 120°F.

The average USE of the weld HAZ metal resulted in an energy decrease of 35 ft-lb after irradiation to 2.186×10^{19} n/cm² ($E > 1.0$ MeV) at 550°F. This resulted in an irradiated average USE of 83 ft-lb (Figure 5-4).

The fracture appearance of each irradiated Charpy specimen from the various materials is shown in Figures 5-5 through 5-8 and show an increasingly ductile or tougher appearance with increasing test temperature.

A comparison of the 30 ft-lb transition temperature increases and upper shelf energy decreases for the various McGuire Unit 1 surveillance materials with predicted values using the methods of NRC Regulatory Guide 1.99, Revision 2^[13] is presented in Table 5-10 and led to the following conclusions:

- o The 30 ft-lb transition temperature increases for the capsule V surveillance materials are less than the Regulatory Guide 1.99, Revision 2 prediction.
- o The upper shelf energy decreases of the capsule V surveillance materials are less than the Regulatory Guide 1.99, Revision 2 predictions.

5.3 Tension Test Results

The results of the tension tests performed on the various materials contained in capsule V irradiated to 2.186×10^{19} n/cm² (E > 1.0 MeV) are presented in Table 5-11 and are compared with unirradiated results^[1] as shown in Figures 5-9 through 5-11.

The results of the tension tests performed on the intermediate shell plate B5012-1 (longitudinal orientation) indicated that irradiation to 2.186×10^{19} n/cm² (E > 1.0 MeV) at 550°F caused a 9 to 11 ksi increase in the 0.2 percent offset yield strength and a 7 to 10 ksi increase in the ultimate tensile strength when compared to unirradiated data^[1] (Figure 5-9).

The results of the tension tests performed on the intermediate shell plate B5012-1 (transverse orientation) indicated that irradiation to 2.186×10^{19} n/cm² (E > 1.0 MeV) at 550°F caused a 8 to 9 ksi increase in the 0.2 percent offset yield strength and a 4 to 8 ksi increase in the ultimate tensile strength when compared to unirradiated data^[1] (Figure 5-10).

The results of the tension tests performed on the surveillance weld metal indicated that irradiation to 2.186×10^{19} n/cm² (E > 1.0 MeV) at 550°F caused a 20 to 26 ksi increase in the 0.2 percent offset yield strength and a 16 to 20 ksi increase in the ultimate tensile strength when compared to unirradiated data^[1] (Figure 5-11).

The fractured tension specimens for the intermediate shell plate B5012-1 material are shown in Figures 5-12 and 5-13, while the fractured tension specimens for the surveillance weld metal are shown in Figure 5-14.

The engineering stress-strain curves for the tension tests are shown in Figures 5-15 through 5-20.

5.4 Compact Tension Specimen Tests

Per the surveillance capsule testing contract, the 1/2T compact tension (CT) specimens were not tested. The 1/2T CT specimens are being stored at the Westinghouse Science and Technology Center Hot Cell Facility.

5.5 Bend Bar Specimen Tests

Per the surveillance capsule testing contract, the bend bar specimen was not tested. The bend bar specimen is being stored at the Westinghouse Science and Technology Center Hot Cell facility.

TABLE 5-1

| Charpy V-notch Data for the McGuire Unit 1 Intermediate Shell Plate B5012-1 Irradiated at 550°F to a Fluence of 2.186×10^{19} n/cm ² (E > 1.0 MeV) (Longitudinal Orientation) | | | | | | | |
|---|-------------|------|---------------|-----|-------------------|------|--------------|
| Sample Number | Temperature | | Impact Energy | | Lateral Expansion | | Shear (%) |
| | (°F) | (°C) | (ft-lb) | (J) | (mils) | (mm) | |
| DL29 | 25 | -4 | 7 | 9 | 5 | 0.13 | 5 |
| DL17 | 60 | 16 | 18 | 24 | 18 | 0.46 | 10 |
| DL23 | 75 | 24 | 34 | 46 | 27 | 0.69 | 25 |
| DL30 | 100 | 38 | 24 | 33 | 24 | 0.61 | 20 |
| DL22 | 100 | 38 | 40 | 54 | 36 | 0.91 | 30 |
| DL18 | 115 | 46 | 40 | 54 | 38 | 0.97 | 45 |
| DL24 | 125 | 52 | 45 | 61 | 39 | 0.99 | 45 |
| DL16 | 135 | 57 | 60 | 81 | 50 | 1.27 | 65 |
| DL25 | 150 | 66 | 73 | 99 | 55 | 1.40 | 70 |
| DL21 | 175 | 79 | 84 | 114 | 66 | 1.68 | 80 |
| DL20 | 200 | 93 | 90 | 122 | 69 | 1.75 | 85 |
| DL19 | 250 | 121 | 115 | 156 | 86 | 2.18 | 100 |
| DL28 | 300 | 149 | 122 | 165 | 84 | 2.13 | 100 |
| DL26 | 350 | 177 | 135 | 183 | 90 | 2.29 | 100 |
| DL27 | 400 | 204 | 127 | 172 | 77 | 1.96 | 100 |

TABLE 5-2

Charpy V-notch Data for the McGuire Unit 1 Intermediate Shell Plate B5012-1
Irradiated at 550°F to a Fluence of 2.186×10^{19} n/cm² (E > 1.0 MeV)
(Transverse Orientation)

| Sample Number | Temperature | | Impact Energy | | Lateral Expansion | | Shear |
|---------------|-------------|------|---------------|-----|-------------------|------|-------|
| | (°F) | (°C) | (ft-lb) | (J) | (mils) | (mm) | (%) |
| DT26 | 25 | -4 | 12 | 16 | 13 | 0.33 | 10 |
| DT27 | 50 | 10 | 24 | 33 | 24 | 0.61 | 15 |
| DT17 | 65 | 18 | 29 | 39 | 25 | 0.64 | 20 |
| DT20 | 75 | 24 | 32 | 43 | 28 | 0.71 | 25 |
| DT25 | 100 | 38 | 33 | 45 | 28 | 0.71 | 25 |
| DT23 | 115 | 46 | 47 | 64 | 41 | 1.04 | 35 |
| DT29 | 125 | 52 | 52 | 71 | 44 | 1.12 | 50 |
| DT30 | 150 | 66 | 49 | 66 | 43 | 1.09 | 55 |
| DT16 | 175 | 79 | 62 | 84 | 49 | 1.24 | 65 |
| DT24 | 200 | 93 | 77 | 104 | 60 | 1.52 | 75 |
| DT18 | 225 | 107 | 96 | 130 | 72 | 1.83 | 100 |
| DT28 | 250 | 121 | 85 | 115 | 75 | 1.91 | 100 |
| DT19 | 275 | 135 | 93 | 126 | 79 | 2.01 | 100 |
| DT21 | 300 | 149 | 97 | 132 | 80 | 2.03 | 100 |
| DT22 | 325 | 163 | 99 | 134 | 80 | 2.03 | 100 |

TABLE 5-3

Charpy V-notch Data for the McGuire Unit 1 Surveillance Weld Metal
Irradiated at 550°F to a Fluence of 2.186×10^{19} n/cm² (E > 1.0 MeV)

| Sample Number | Temperature | | Impact Energy | | Lateral Expansion | | Shear (%) |
|---------------|-------------|------|---------------|-----|-------------------|------|-----------|
| | (°F) | (°C) | (ft-lb) | (J) | (mils) | (mm) | |
| DW21 | 65 | 18 | 4 | 5 | 6 | 0.15 | 10 |
| DW17 | 100 | 38 | 7 | 9 | 9 | 0.23 | 15 |
| DW27 | 125 | 52 | 23 | 31 | 22 | 0.56 | 30 |
| DW22 | 150 | 66 | 27 | 37 | 24 | 0.61 | 35 |
| DW26 | 160 | 71 | 32 | 43 | | 0.76 | 45 |
| DW24 | 175 | 79 | 34 | 46 | 33 | 0.84 | 45 |
| DW16 | 200 | 93 | 30 | 41 | 29 | 0.74 | 40 |
| DW25 | 200 | 93 | 38 | 52 | 35 | 0.89 | 60 |
| DW19 | 215 | 102 | 60 | 81 | 52 | 1.32 | 95 |
| DW29 | 225 | 107 | 57 | 77 | 49 | 1.24 | 90 |
| DW28 | 250 | 121 | 73 | 99 | 60 | 1.52 | 100 |
| DW18 | 300 | 149 | 64 | 87 | 61 | 1.55 | 100 |
| DW30 | 300 | 149 | 70 | 95 | 61 | 1.55 | 100 |
| DW23 | 350 | 177 | 77 | 104 | 70 | 1.78 | 100 |
| DW20 | 400 | 204 | 76 | 103 | 66 | 1.68 | 100 |

TABLE 5-4

Charpy V-notch Data for the McGuire Unit 1 Heat-Affected-Zone (HAZ) Metal
Irradiated at 550°F to a Fluence of 2.186×10^{19} n/cm² (E > 1.0 MeV)

| Sample Number | Temperature | | Impact Energy | | Lateral Expansion | | Shear |
|------------------|-------------|------|---------------|-----|-------------------|------|-------|
| | (°F) | (°C) | (ft-lb) | (J) | (mils) | (mm) | (%) |
| DH21 | -25 | -32 | 18 | 24 | 17 | 0.43 | 20 |
| DH22 | -5 | -21 | 18 | 24 | 16 | 0.41 | 20 |
| DH18 | 10 | -12 | 7 | 9 | 9 | 0.23 | 10 |
| DH19 | 50 | 10 | 15 | 20 | 14 | 0.36 | 15 |
| DH27 | 65 | 18 | 29 | 39 | 27 | 0.69 | 35 |
| DH24 | 85 | 29 | 18 | 24 | 16 | 0.41 | 25 |
| DH25 | 90 | 32 | 33 | 45 | 27 | 0.69 | 30 |
| DH26 | 100 | 38 | 43 | 58 | 43 | 1.09 | 50 |
| DH16 | 125 | 52 | 53 | 72 | 46 | 1.17 | 60 |
| DH28 | 150 | 66 | 58 | 79 | 47 | 1.19 | 75 |
| DH23 | 200 | 93 | 64 | 87 | 53 | 1.35 | 85 |
| DH30 | 250 | 121 | 70 | 95 | 56 | 1.42 | 100 |
| DH17 | 300 | 149 | 94 | 127 | 78 | 1.98 | 100 |
| DH20 | 350 | 177 | 72 | 98 | 62 | 1.57 | 100 |
| DH29 | 375 | 191 | 94 | 127 | 82 | 2.08 | 100 |

TABLE 5-5

Instrumented Charpy Impact Test Results for the McGuire Unit 1 Intermediate Shell Plate B5012-1
Irradiated at 550°F to a Fluence of 2.186×10^{19} n/cm² (E > 1.0 MeV) (Longitudinal Orientation)

| Sample No. | Test Temp. (°F) | Charpy Energy E _D (ft-lb) | Normalized Energies (ft-lb/in ²) | | | Yield Load P _{GY} (lbs) | Time to Yield t _{GY} (µsec) | Max. Load P _M (lbs) | Time to Max. t _M (µsec) | Fast Fract. Load P _F (lbs) | Arrest Load P _A (lbs) | Yield Stress σ _Y (ksi) | Flow Stress (ksi) |
|------------|-----------------|--------------------------------------|--|------------------------|-------------------------|----------------------------------|--------------------------------------|--------------------------------|------------------------------------|---------------------------------------|----------------------------------|-----------------------------------|-------------------|
| | | | Charpy E _F /A | Max. E _M /A | Prop. E _P /A | | | | | | | | |
| DL29 | 25 | 7 | 56 | 23 | 33 | 2819 | 0.12 | 2919 | 0.13 | 2903 | 212 | 94 | 95 |
| DL17 | 60 | 18 | 145 | 105 | 40 | 3340 | 0.17 | 3808 | 0.31 | 3795 | 245 | 111 | 119 |
| DL23 | 75 | 34 | 274 | 195 | 79 | 3243 | 0.16 | 4095 | 0.48 | 4089 | 951 | 108 | 122 |
| DL30** | 100 | 24 | 193 | - | - | - | - | - | - | - | - | - | - |
| DL22 | 100 | 40 | 322 | 262 | 60 | 3216 | 0.16 | 4212 | 0.61 | 4209 | 531 | 107 | 123 |
| DL18 | 115 | 40 | 322 | 223 | 99 | 3119 | 0.16 | 4023 | 0.55 | 4016 | 1548 | 104 | 119 |
| DL24 | 125 | 45 | 362 | 266 | 97 | 3139 | 0.16 | 4167 | 0.63 | 4154 | 1460 | 104 | 121 |
| DL16 | 135 | 60 | 483 | 289 | 194 | 3017 | 0.15 | 4112 | 0.68 | 4029 | 1381 | 100 | 118 |
| DL25 | 150 | 73 | 588 | 290 | 298 | 2987 | 0.15 | 4183 | 0.68 | 3746 | 2010 | 99 | 119 |
| DL21 | 175 | 84 | 676 | 285 | 391 | 2970 | 0.16 | 4052 | 0.68 | 3503 | 2045 | 99 | 117 |
| DL20 | 200 | 90 | 725 | 283 | 441 | 2986 | 0.17 | 4079 | 0.69 | 3539 | 2125 | 99 | 117 |
| DL19** | 250 | 115 | 926 | - | - | - | - | - | - | - | - | - | - |
| DL28 | 300 | 122 | 982 | 273 | 709 | 2829 | 0.16 | 3919 | 0.67 | * | * | 94 | 112 |
| DL26 | 350 | 135 | 1087 | 276 | 811 | 2854 | 0.17 | 3912 | 0.69 | * | * | 95 | 112 |
| DL27 | 400 | 127 | 1023 | 266 | 757 | 2638 | 0.15 | 3798 | 0.68 | * | * | 88 | 107 |

* Fully ductile fracture.

** Computer data not available due to computer malfunction.

TABLE 5-6

Instrumented Charpy Impact Test Results for the McGuire Unit 1 Intermediate Shell Plate B5012-1
Irradiated at 550°F to a Fluence of 2.186×10^{19} n/cm² (E > 1.0 MeV) (Transverse Orientation)

| Sample No. | Test Temp. (°F) | Charpy Energy E _D (ft-lb) | Normalized Energies (ft-lb/in ²) | | | Yield Load P _{GY} (lbs) | Time to Yield t _{GY} (µsec) | Max. Load P _M (lbs) | Time to Max. t _M (µsec) | Fast Fract. Load P _F (lbs) | Arrest Load P _A (lbs) | Yield Stress σ _y (ksi) | Flow Stress (ksi) |
|------------|-----------------|--------------------------------------|--|------------------------|-------------------------|----------------------------------|--------------------------------------|--------------------------------|------------------------------------|---------------------------------------|----------------------------------|-----------------------------------|-------------------|
| | | | Charpy E _V /A | Max. E _M /A | Prop. E _V /A | | | | | | | | |
| DT26 | 25 | 12 | 97 | 41 | 55 | 3408 | 0.16 | 3507 | 0.17 | 3498 | 364 | 113 | 115 |
| DT27 | 50 | 24 | 193 | 130 | 64 | 3411 | 0.17 | 4020 | 0.35 | 4010 | 596 | 113 | 123 |
| DT17 | 65 | 29 | 234 | 186 | 47 | 3348 | 0.16 | 4183 | 0.46 | 4170 | 336 | 111 | 125 |
| DT20 | 75 | 32 | 258 | 174 | 84 | 3323 | 0.17 | 4027 | 0.44 | 4024 | 878 | 110 | 122 |
| DT25 | 100 | 33 | 266 | 177 | 89 | 3242 | 0.17 | 4026 | 0.46 | 4007 | 1174 | 108 | 121 |
| DT23 | 115 | 47 | 378 | 287 | 91 | 3153 | 0.16 | 4141 | 0.67 | 4099 | 813 | 105 | 121 |
| DT29 | 125 | 52 | 419 | 284 | 135 | 3121 | 0.16 | 4265 | 0.65 | 4249 | 1768 | 104 | 123 |
| DT30 | 150 | 49 | 395 | 230 | 175 | 3057 | 0.16 | 4008 | 0.55 | 3966 | 1946 | 102 | 117 |
| DT16 | 175 | 62 | 499 | 277 | 222 | 3064 | 0.17 | 4020 | 0.67 | 3917 | 1857 | 102 | 118 |
| DT24 | 200 | 77 | 620 | 260 | 360 | 3035 | 0.17 | 4028 | 0.63 | 3652 | 2341 | 101 | 117 |
| DT18 | 225 | 96 | 773 | 285 | 488 | 2899 | 0.15 | 4027 | 0.69 | * | * | 96 | 115 |
| DT28 | 250 | 85 | 684 | 253 | 432 | 2896 | 0.17 | 3877 | 0.63 | * | * | 96 | 112 |
| DT19 | 275 | 93 | 749 | 268 | 481 | 2815 | 0.15 | 3992 | 0.65 | * | * | 94 | 113 |
| DT21 | 300 | 97 | 781 | 263 | 518 | 2745 | 0.14 | 3872 | 0.65 | * | * | 91 | 110 |
| DT22 | 325 | 99 | 797 | 264 | 533 | 2684 | 0.15 | 3883 | 0.67 | * | * | 89 | 109 |

* Fully ductile fracture.

TABLE 5-7

Instrumented Charpy Impact Test Results for the McGuire Unit 1 Surveillance Weld Metal
Irradiated at 550°F to a Fluence of 2.186×10^{19} n/cm² (E > 1.0 MeV)

| Sample No. | Test Temp. (°F) | Charpy Energy E _D (ft-lb) | Normalized Energies (ft-lb/in ²) | | | Yield Load P _{GY} (lbs) | Time to Yield t _{GY} (μsec) | Max. Load P _M (lbs) | Time to Max. t _M (μsec) | Fast Fract. Load P _F (lbs) | Arrest Load P _A (lbs) | Yield Stress σ _Y (ksi) | Flow Stress (ksi) |
|------------|-----------------|--------------------------------------|--|------------------------|-------------------------|----------------------------------|--------------------------------------|--------------------------------|------------------------------------|---------------------------------------|----------------------------------|-----------------------------------|-------------------|
| | | | Charpy E _D /A | Max. E _M /A | Prop. E _P /A | | | | | | | | |
| DW21 | 65 | 4 | 32 | 16 | 16 | 2275 | 0.10 | 2349 | 0.11 | 2346 | 213 | 76 | 77 |
| DW17 | 100 | 7 | 56 | 32 | 24 | 3181 | 0.14 | 3294 | 0.16 | 3268 | 296 | 106 | 108 |
| DW27 | 125 | 23 | 185 | 130 | 56 | 3407 | 0.17 | 3911 | 0.35 | 3892 | 835 | 113 | 122 |
| DW22 | 150 | 27 | 217 | 139 | 78 | 3200 | 0.15 | 3929 | 0.38 | 3917 | 820 | 106 | 118 |
| DW26 | 160 | 32 | 258 | 178 | 79 | 3324 | 0.17 | 4024 | 0.46 | 4018 | 1662 | 110 | 122 |
| DW24 | 175 | 34 | 274 | 177 | 97 | 3226 | 0.16 | 3970 | 0.46 | 3967 | 1663 | 107 | 120 |
| DW16 | 200 | 30 | 242 | 150 | 91 | 3433 | 0.20 | 3999 | 0.41 | 3995 | 1816 | 114 | 123 |
| DW25 | 200 | 38 | 306 | 184 | 122 | 3218 | 0.16 | 3996 | 0.47 | 3980 | 961 | 107 | 120 |
| DW19 | 215 | 60 | 483 | 210 | 273 | 3163 | 0.16 | 4064 | 0.51 | 3965 | 3031 | 105 | 120 |
| DW29 | 225 | 57 | 459 | 212 | 247 | 3309 | 0.18 | 4088 | 0.52 | 4001 | 2951 | 110 | 123 |
| DW28 | 250 | 73 | 588 | 206 | 382 | 3109 | 0.16 | 4024 | 0.51 | * | * | 103 | 118 |
| DW18 | 300 | 64 | 515 | 198 | 318 | 3126 | 0.17 | 3898 | 0.50 | * | * | 104 | 117 |
| DW30 | 300 | 70 | 564 | 200 | 363 | 3082 | 0.16 | 3890 | 0.51 | * | * | 102 | 116 |
| DW23 | 350 | 77 | 620 | 203 | 418 | 3001 | 0.16 | 3885 | 0.52 | * | * | 100 | 114 |
| DW20 | 400 | 76 | 612 | 199 | 413 | 2838 | 0.15 | 3869 | 0.52 | * | * | 94 | 111 |

* Fully ductile fracture.

TABLE 5-8

Instrumented Charpy Impact Test Results for the McGuire Unit 1 Surveillance Heat-Affected-Zone (HAZ) Metal
Irradiated at 550°F to a Fluence of 2.186×10^{19} n/cm² (E > 1.0 MeV)

| Sample No. | Test Temp. (°F) | Charpy Energy E _D (ft-lb) | Normalized Energies (ft-lb/in ²) | | | Yield Load P _{GY} (lbs) | Time to Yield t _{GY} (µsec) | Max. Load P _M (lbs) | Time to Max. t _M (µsec) | Fast Fract. Load P _F (lbs) | Arrest Load P _A (lbs) | Yield Stress σ _Y (ksi) | Flow Stress (ksi) |
|------------|-----------------|--------------------------------------|--|------------------------|-------------------------|----------------------------------|--------------------------------------|--------------------------------|------------------------------------|---------------------------------------|----------------------------------|-----------------------------------|-------------------|
| | | | Charpy E _D /A | Max. E _M /A | Prop. E _P /A | | | | | | | | |
| DH21 | -25 | 18 | 145 | 78 | 67 | 3834 | 0.17 | 3985 | 0.24 | 3978 | 854 | 127 | 130 |
| DH22 | -5 | 18 | 145 | 78 | 67 | 3856 | 0.17 | 3985 | 0.24 | 3979 | 826 | 128 | 130 |
| DH18 | 10 | 7 | 56 | 22 | 35 | 2672 | 0.11 | 2849 | 0.13 | 2829 | 212 | 89 | 92 |
| DH19 | 50 | 15 | 121 | 59 | 62 | 3482 | 0.15 | 3737 | 0.20 | 3727 | 433 | 116 | 120 |
| DH27 | 65 | 29 | 234 | 88 | 146 | 3528 | 0.17 | 3691 | 0.27 | 3688 | 2247 | 117 | 120 |
| DH24 | 85 | 18 | 145 | 88 | 57 | 3521 | 0.17 | 3820 | 0.27 | 3817 | 1144 | 117 | 122 |
| DH25 | 90 | 33 | 266 | 180 | 85 | 3554 | 0.17 | 4178 | 0.44 | 4175 | 916 | 118 | 128 |
| DH26 | 100 | 43 | 346 | 139 | 207 | 3322 | 0.16 | 3969 | 0.37 | 3962 | 2990 | 110 | 121 |
| DH16 | 125 | 53 | 427 | 217 | 210 | 3438 | 0.17 | 4179 | 0.52 | 3882 | 2162 | 114 | 126 |
| DH28 | 150 | 58 | 467 | 270 | 197 | 3284 | 0.16 | 4157 | 0.63 | 4141 | 1001 | 109 | 124 |
| DH23 | 200 | 64 | 515 | 274 | 241 | 3242 | 0.16 | 4081 | 0.64 | 4065 | 2461 | 108 | 122 |
| DH30 | 250 | 70 | 564 | 204 | 360 | 3160 | 0.16 | 3944 | 0.51 | * | * | 105 | 118 |
| DH17 | 300 | 94 | 757 | 279 | 478 | 2935 | 0.16 | 4044 | 0.67 | * | * | 97 | 116 |
| DH20** | 350 | 72 | 580 | - | - | - | - | - | - | - | - | - | - |
| DH29 | 375 | 94 | 757 | 270 | 487 | 2990 | 0.16 | 3880 | 0.67 | * | * | 99 | 114 |

* Computer data not available due to computer malfunction.

** Fully ductile fracture.

TABLE 5-9

Effect of 550°F Irradiation to 2.186×10^{19} n/cm² (E > 1.0 MeV) on the Notch Toughness Properties of the McGuire Unit 1 Reactor Vessel Surveillance Materials

| Material | Average 30 (ft-lb) ^(a) Transition Temperature (°F) | | | Average 35 mil Lateral ^(a) Expansion Temperature (°F) | | | Average 50 ft-lb ^(a) Transition Temperature (°F) | | | Average Energy Absorption ^(a) at Full Shear (ft-lb) | | |
|---------------------------------|--|------------|-----|---|------------|-----|--|------------|-----|---|------------|------|
| | Unirradiated | Irradiated | ΔT | Unirradiated | Irradiated | ΔT | Unirradiated | Irradiated | ΔT | Unirradiated | Irradiated | ΔE |
| Plate B5012-1 (longitudinal) | 5 | 90 | 85 | 35 | 105 | 70 | 35 | 125 | 90 | 140 | 125 | - 15 |
| Plate B5012-1 (transverse) | 0 | 85 | 85 | 50 | 115 | 65 | 75 | 135 | 60 | 101 | 94 | - 7 |
| Weld Metal | - 5 | 170 | 175 | 0 | 185 | 185 | 20 | 210 | 190 | 112 | 72 | - 40 |
| HAZ Metal | - 50 | 85 | 135 | - 15 | 105 | 120 | - 5 | 120 | 125 | 118 | 83 | - 35 |

(a) "Average" is defined as the value read from the curve fit through the data points of the Charpy tests (see Figures 5-1 through 5-4)

| TABLE 5-10 | | | | | | |
|--|---------|---|--|------------------|---------------------------------|-----------------|
| Comparison of the McGuire Unit 1 Surveillance Material 30 ft-lb Transition Temperature Shifts and Upper Shelf Energy Decreases with Regulatory Guide 1.99 Revision 2 Predictions | | | | | | |
| Material | Capsule | Fluence n/cm ² (E > 1.0 MeV) | 30 ft-lb Transition Temperature Shift | | Upper Shelf Energy Decrease | |
| | | | Predicted ^(a) (°F) | Measured (°F) | Predicted ^(a) (%) | Measured (%) |
| Intermediate Shell Plate B-5012-1 (longitudinal) | U | 4.712 x 10 ¹⁸ | 59 | 45 | 18 | 5 |
| | X | 1.409 x 10 ¹⁹ | 81 | 45 | 22 | 5 |
| | V | 2.186 x 10 ¹⁹ | 90 | 85 | 24 | 11 |
| Intermediate Shell Plate B-5012-1 (transverse) | U | 4.712 x 10 ¹⁸ | 59 | 50 | 18 | 1 |
| | X | 1.409 x 10 ¹⁹ | 81 | 65 | 22 | 0 |
| | V | 2.186 x 10 ¹⁹ | 90 | 85 | 24 | 7 |
| Weld Metal | U | 4.712 x 10 ¹⁸ | 168 | 160 | 31 | 33 |
| | X | 1.409 x 10 ¹⁹ | 233 | 165 | 38 | 26 |
| | V | 2.186 x 10 ¹⁹ | 258 | 175 | 42 | 36 |
| HAZ Metal | U | 4.712 x 10 ¹⁸ | - | 90 | - | 8 |
| | X | 1.409 x 10 ¹⁹ | - | 115 | - | 19 |
| | V | 2.186 x 10 ¹⁹ | - | 135 | - | 30 |

(a) Based on Regulatory Guide 1.99, Revision 2 methodology using Mean wt. % values of Cu and Ni.

TABLE 5-11

Tensile Properties of the McGuire Unit 1 Reactor Vessel Surveillance Materials Irradiated at 550°F to $2.186 \times 10^{19} \text{ n/cm}^2$ ($E > 1.0 \text{ MeV}$)

| Material | Sample Number | Test Temp. (°F) | 0.2% Yield Strength (ksi) | Ultimate Strength (ksi) | Fracture Load (kip) | Fracture Stress (ksi) | Fracture Strength (ksi) | Uniform Elongation (%) | Total Elongation (%) | Reduction in Area (%) |
|------------------------------|---------------|-----------------|---------------------------|-------------------------|---------------------|-----------------------|-------------------------|------------------------|----------------------|-----------------------|
| Plate B5012-1 (longitudinal) | DL4 | 135 | 74.9 | 93.7 | 2.90 | 164.1 | 59.1 | 12.0 | 26.6 | 64 |
| Plate B5012-1 (longitudinal) | DL5 | 300 | 70.3 | 88.6 | 3.00 | 169.8 | 61.1 | 11.5 | 21.9 | 64 |
| Plate B5012-1 (Longitudinal) | DL6 | 550 | 67.5 | 91.2 | 3.15 | 166.9 | 64.2 | 10.8 | 23.3 | 62 |
| Plate B5012-1 (transverse) | DT4 | 115 | 73.8 | 92.7 | 3.45 | 152.8 | 70.3 | 12.0 | 23.3 | 54 |
| Plate B5012-1 (transverse) | DT5 | 250 | 69.3 | 86.6 | 2.95 | 158.1 | 60.1 | 11.1 | 22.1 | 62 |
| Plate B5012-1 (transverse) | DT6 | 550 | 67.2 | 88.6 | 3.10 | 143.5 | 63.2 | 9.9 | 19.8 | 56 |
| Weld Metal | DW4 | 160 | 86.3 | 97.8 | 3.45 | 152.8 | 70.3 | 11.5 | 22.6 | 54 |
| Weld Metal | DW5 | 250 | 83.0 | 95.7 | 3.55 | 190.3 | 72.3 | 11.1 | 21.5 | 62 |
| Weld Metal | DW6 | 550 | 78.4 | 94.7 | 3.40 | 157.4 | 69.3 | 9.3 | 19.7 | 56 |

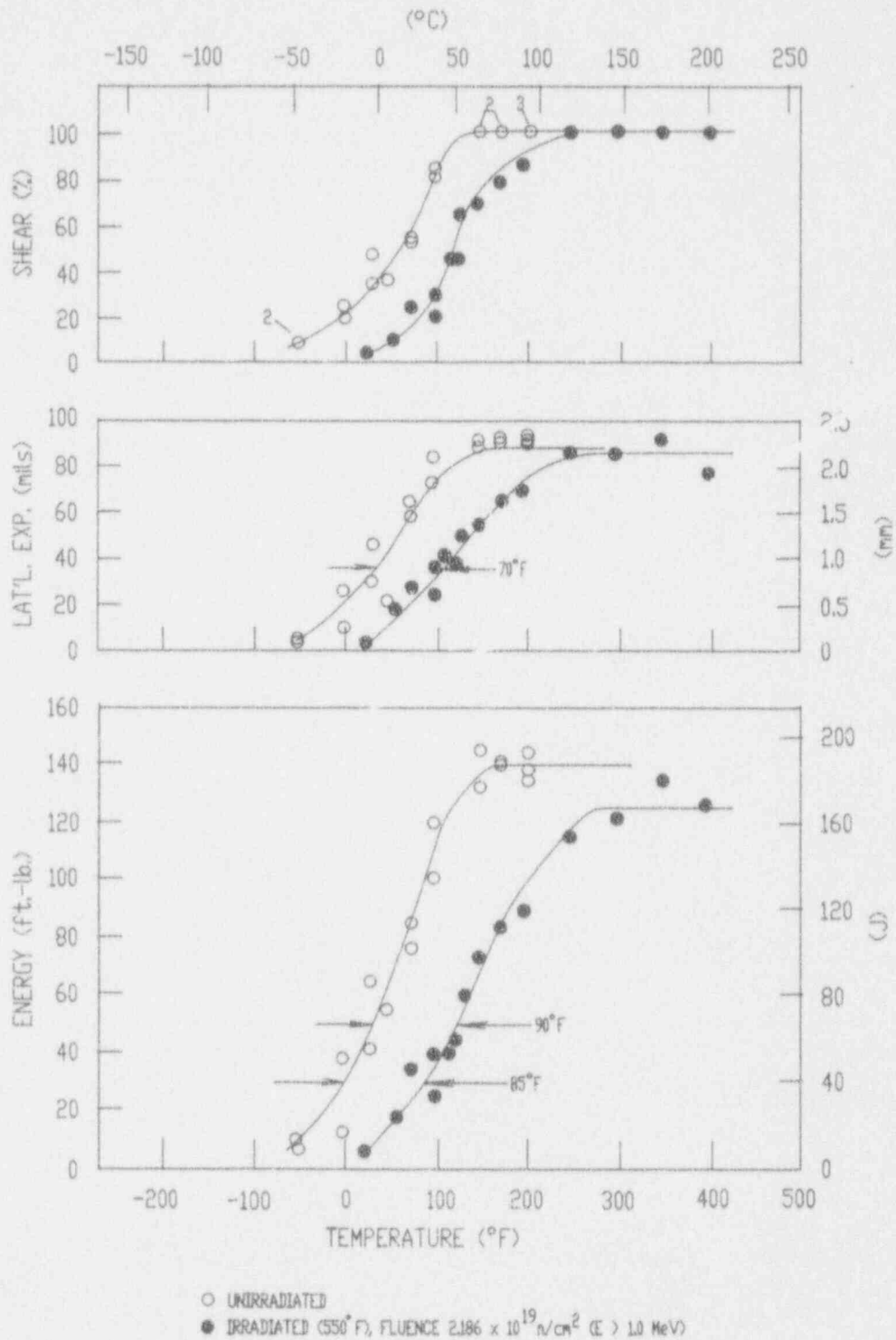


Figure 5-1 Charpy V-Notch Impact Properties for McGuire Unit 1 Reactor Vessel Intermediate Shell Plate B5012-1 (Longitudinal Orientation)

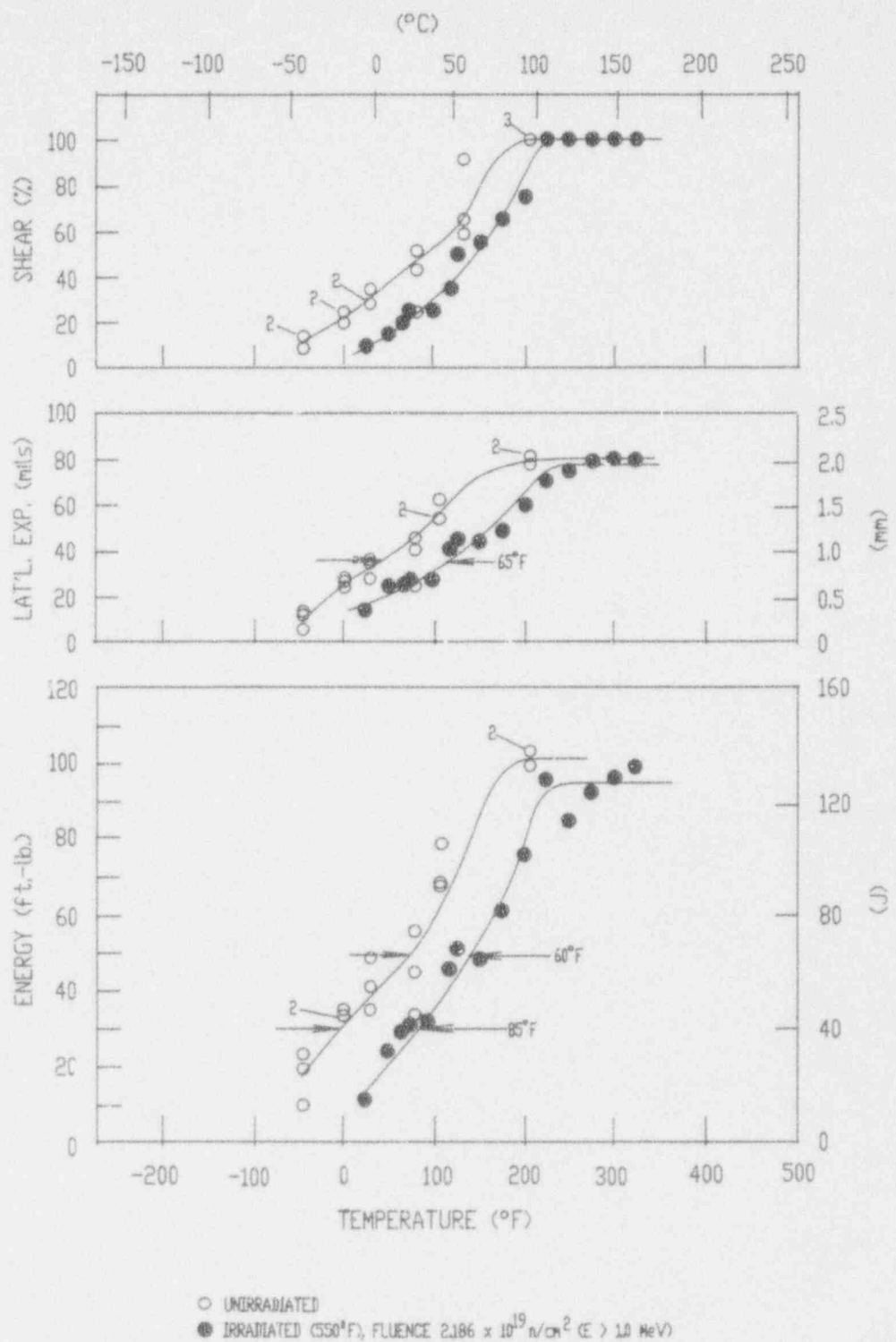


Figure 5-2 Charpy V-Notch Impact Properties for McGuire Unit 1 Reactor Vessel Intermediate Shell Plate B5012-1 (Transverse Orientation)

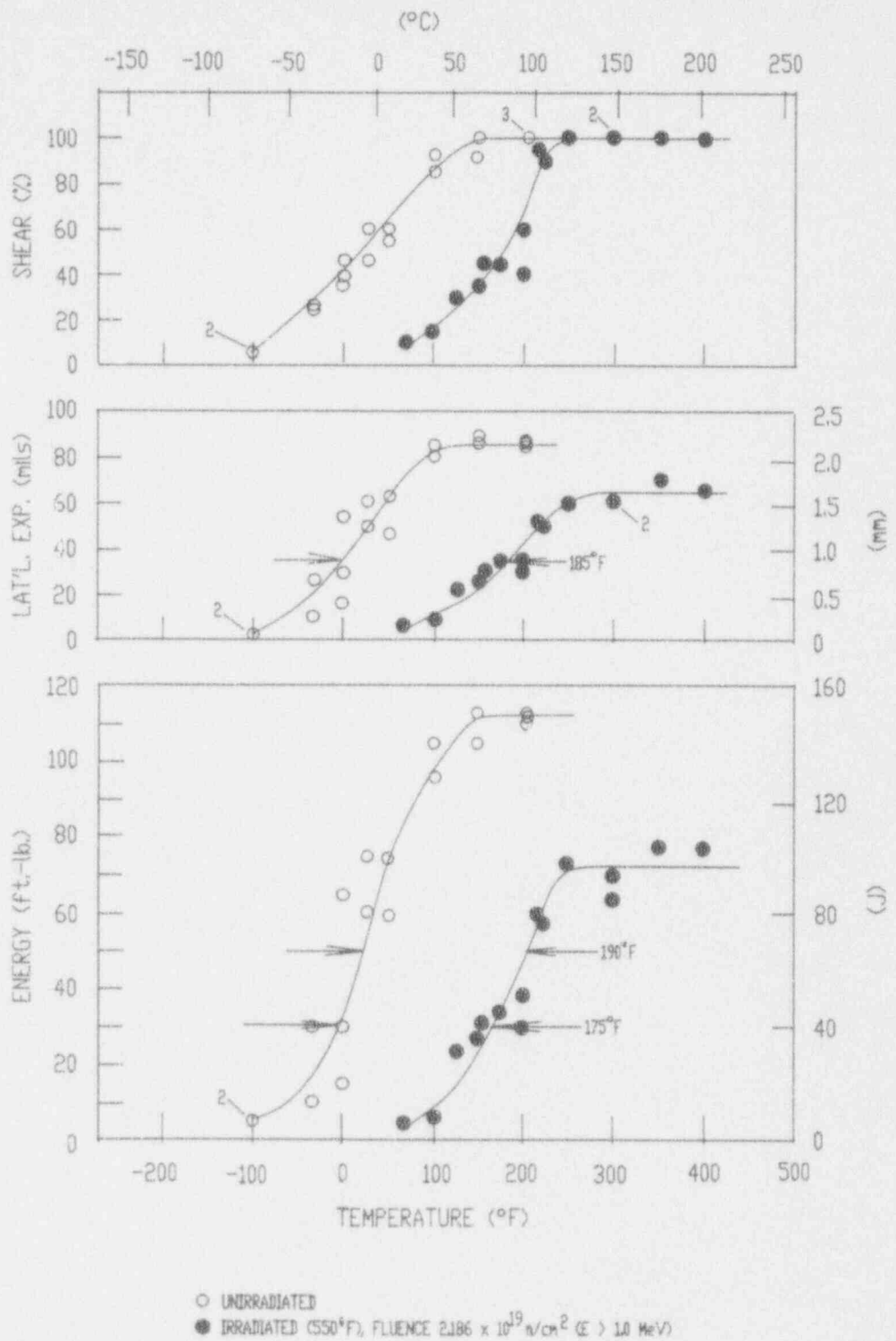


Figure 5-3 Charpy V-Notch Impact Properties for McGuire Unit 1 Reactor Vessel Surveillance Weld Metal

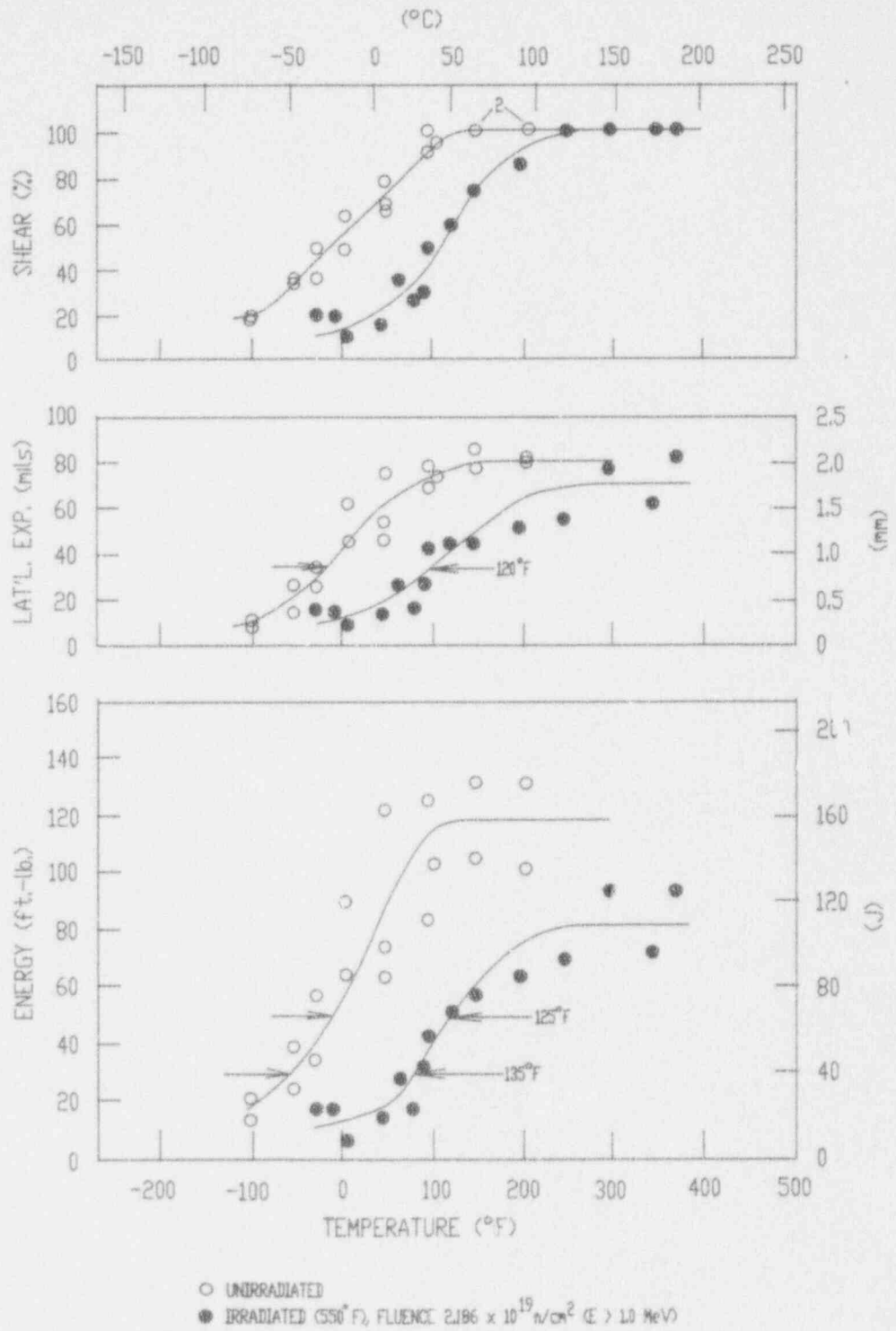


Figure 5-4 Charpy V-Notch Impact Properties for McGuire Unit 1 Reactor Vessel Weld Heat-Affected-Zone Metal

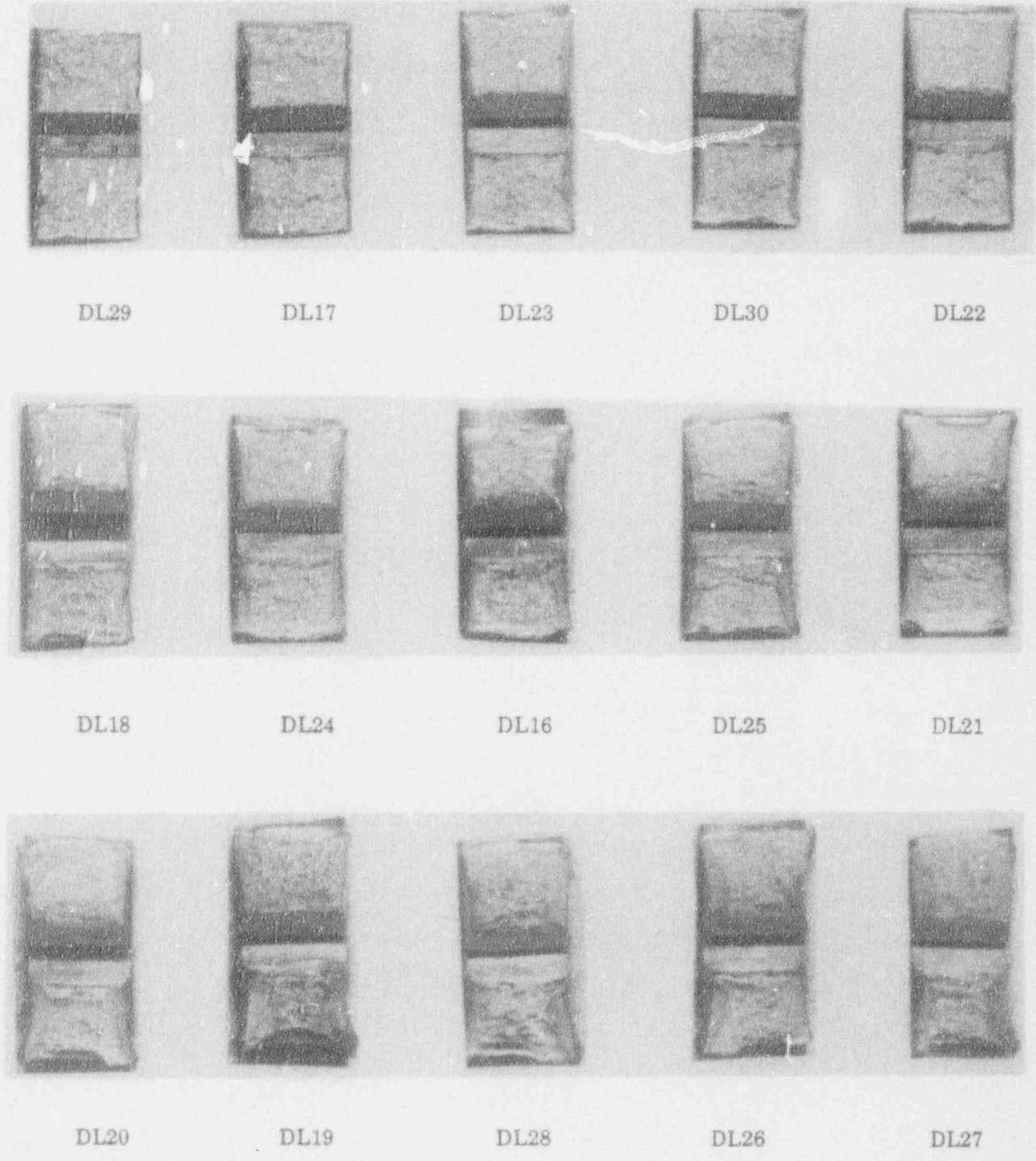


Figure 5-5 Charpy Impact Specimen Fracture Surfaces for McGuire Unit 1 Reactor Vessel Intermediate Shell Plate B5012-1 (Longitudinal Orientation)

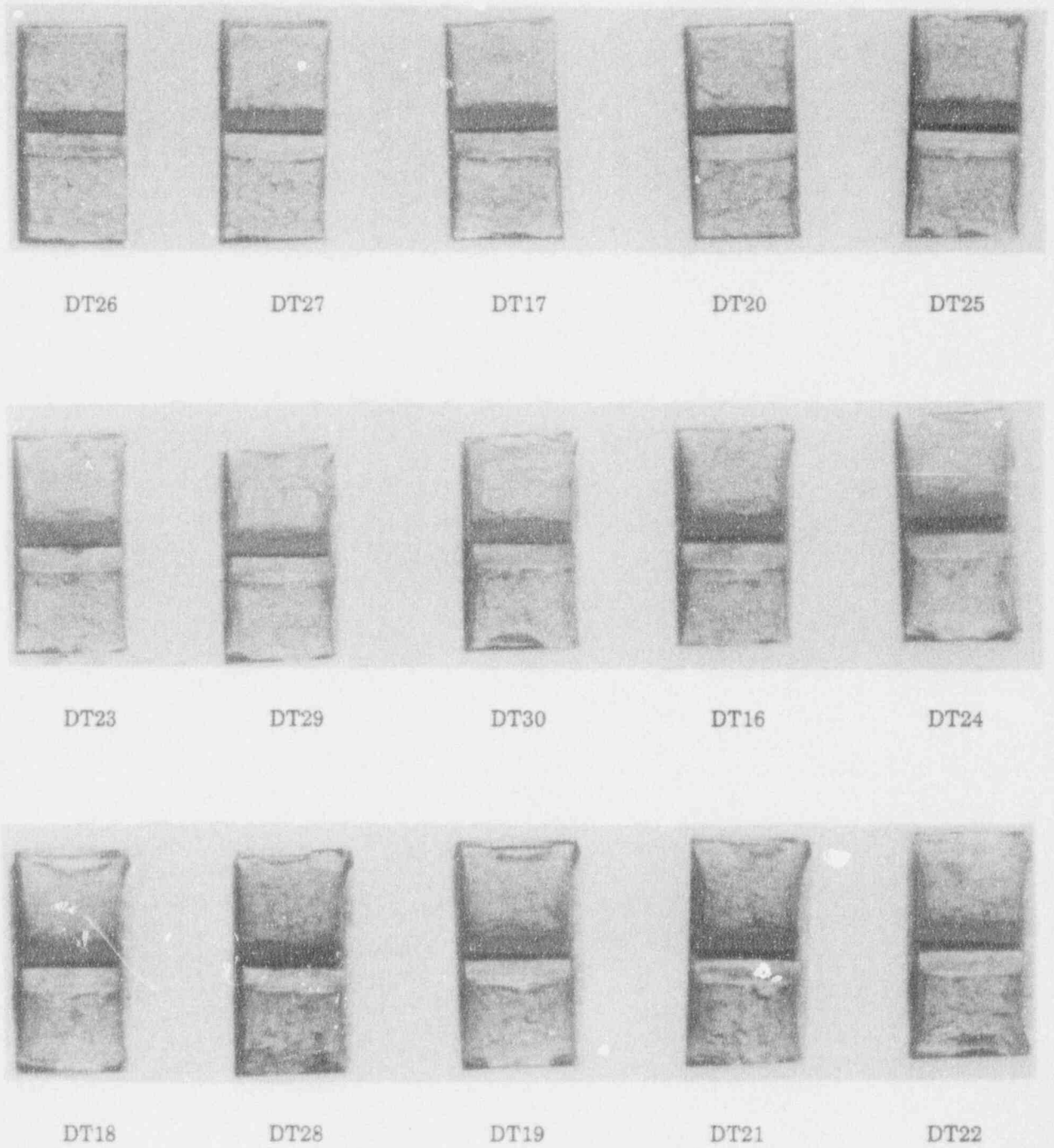
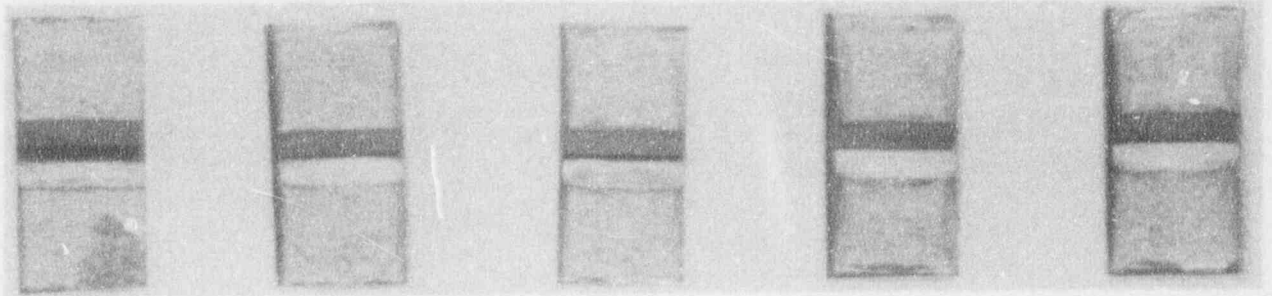


Figure 5-6 Charpy Impact Specimen Fracture Surfaces for McGuire Unit 1 Reactor Vessel Intermediate Shell Plate B5012-1 (Transverse Orientation)



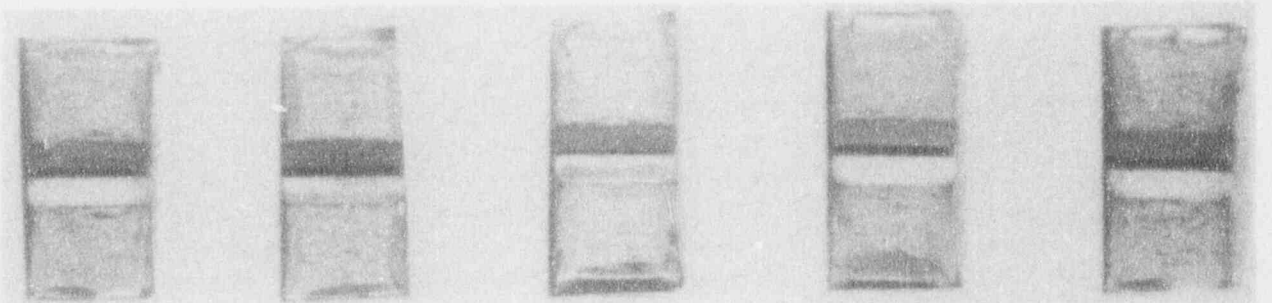
DW21

DW17

DW27

DW22

DW26



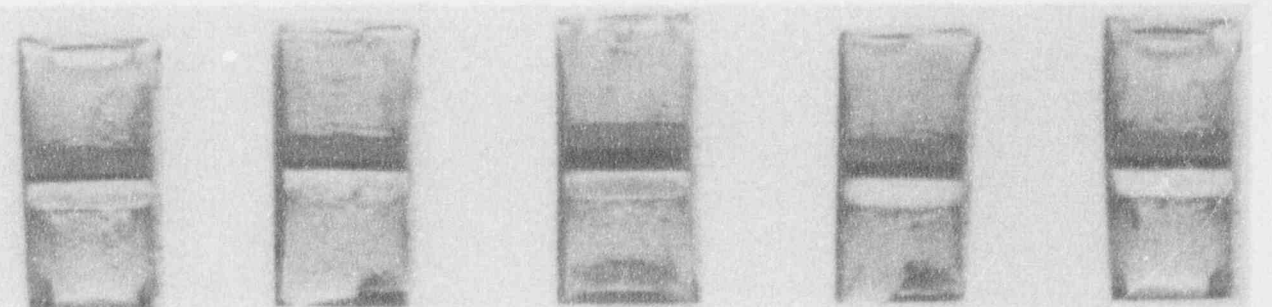
DW24

DW16

DW25

DW19

DW29



DW28

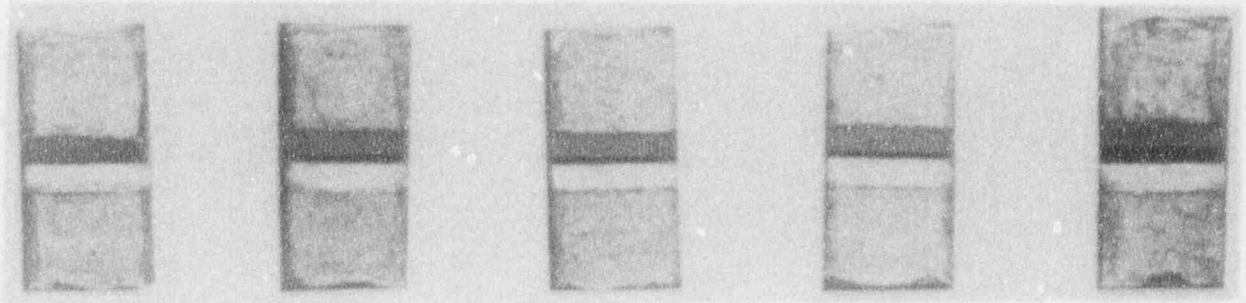
DW18

DW30

DW23

DW20

Figure 5-7 Charpy Impact Specimen Fracture Surfaces for McGuire Unit 1 Reactor Vessel Surveillance Weld Metal



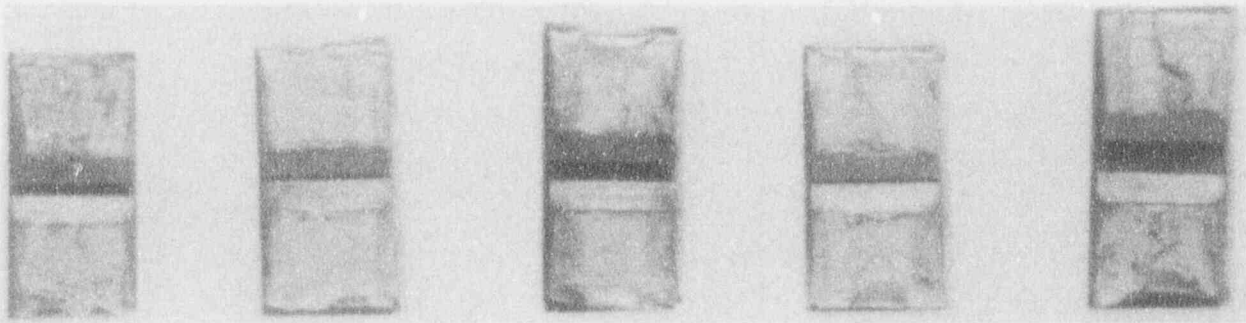
DH21

DH22

DH18

DH19

DH27



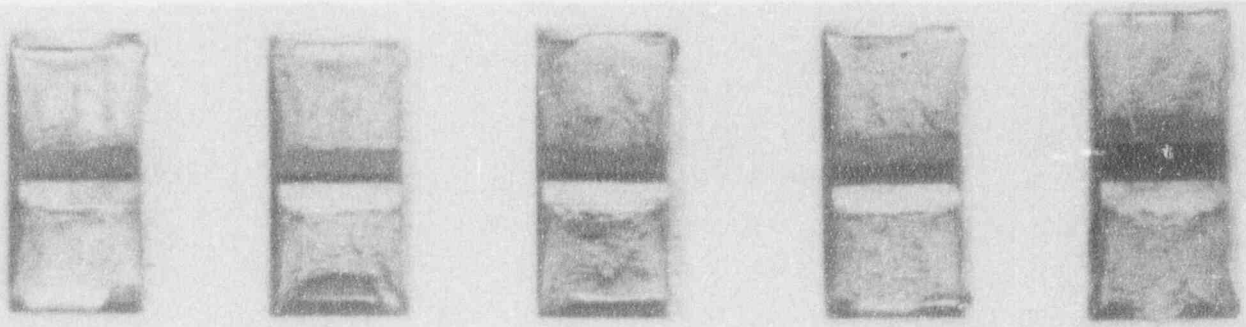
DH24

DH25

DH26

DH16

DH28



DH23

DH30

DH17

DH20

DH29

Figure 5-8 Charpy Impact Specimen Fracture Surfaces for McGuire Unit 1 Reactor Vessel Heat-Affected-Zone Metal

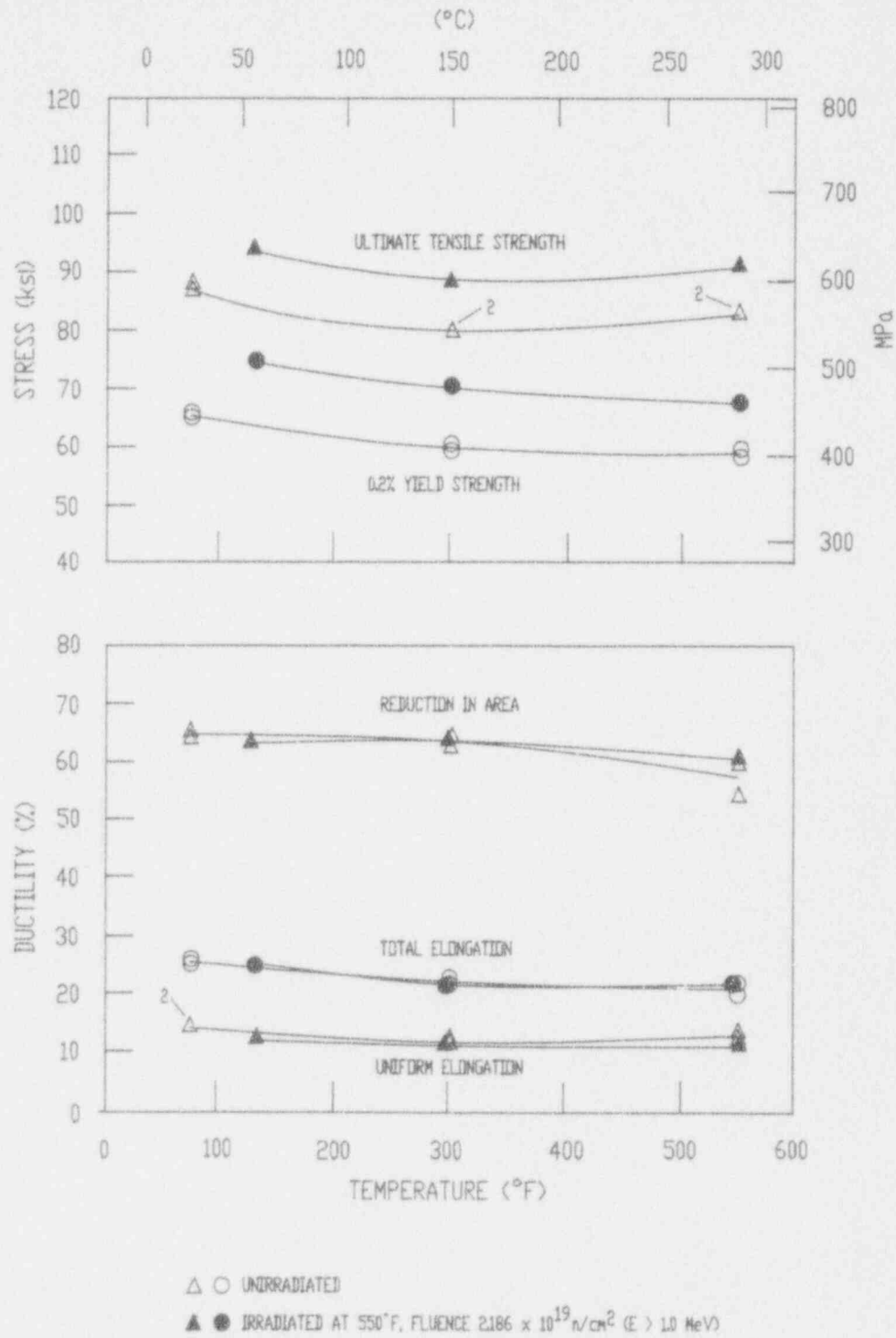


Figure 5-9 Tensile Properties for McGuire Unit 1 Reactor Vessel Intermediate Shell Plate B5012-1 (Longitudinal Orientation)

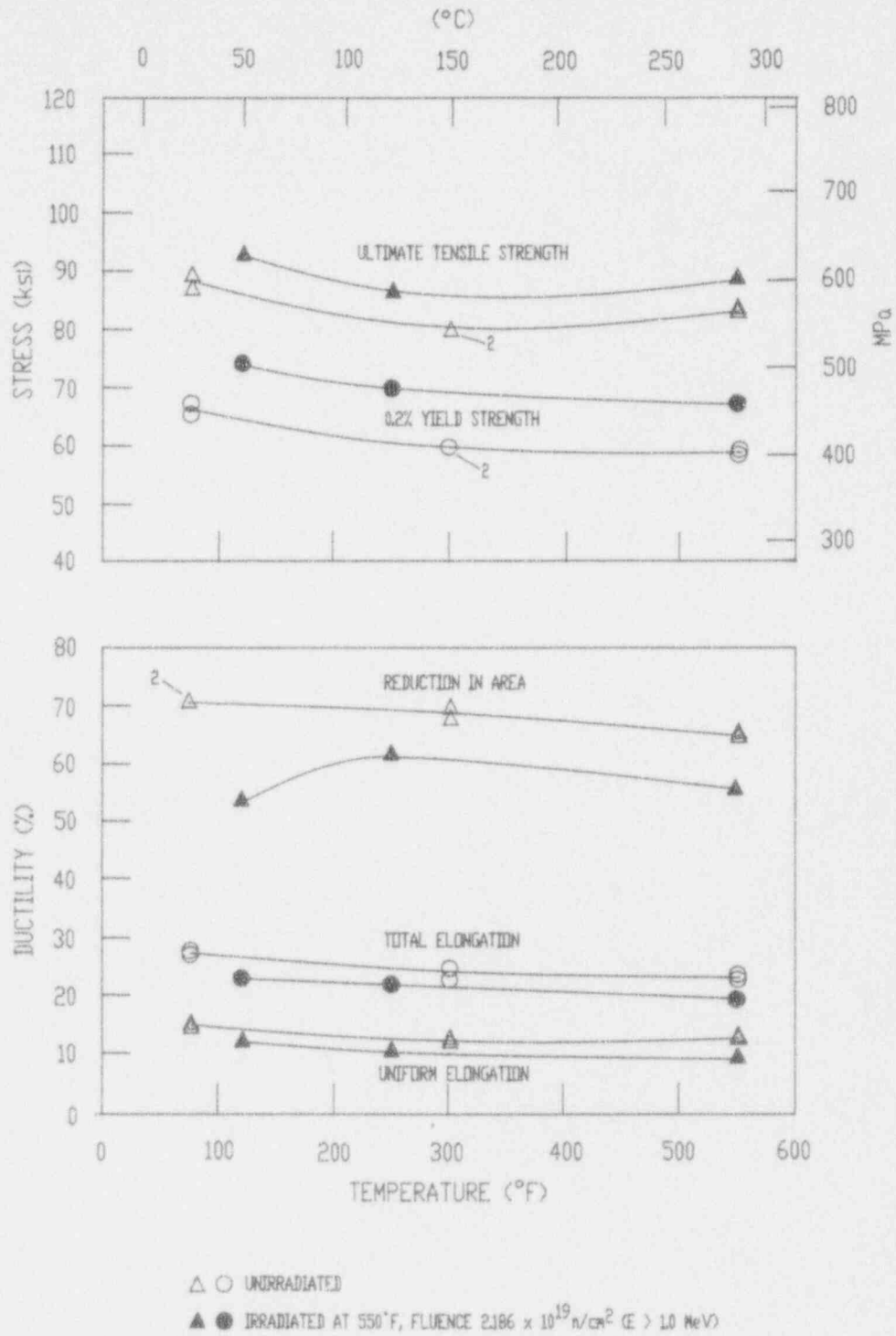
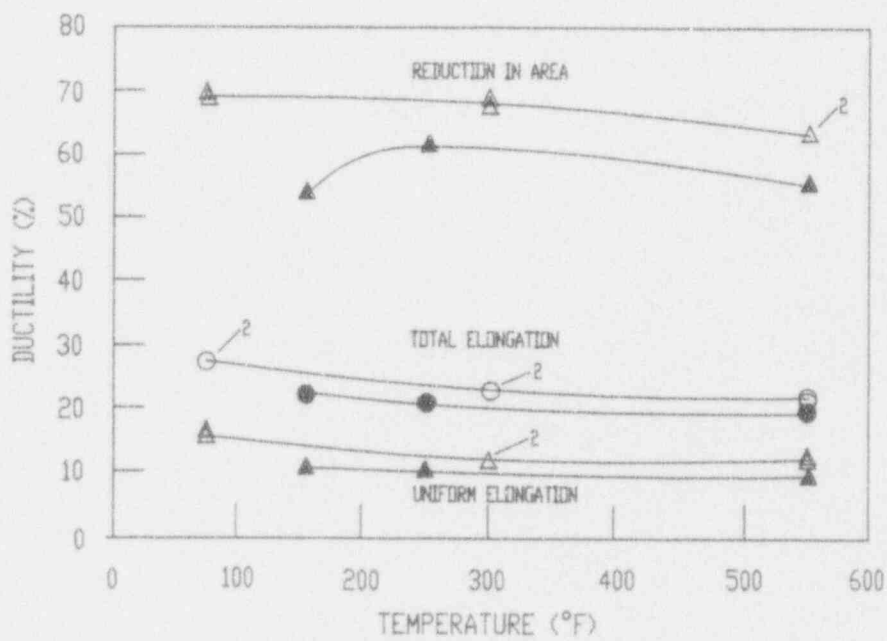
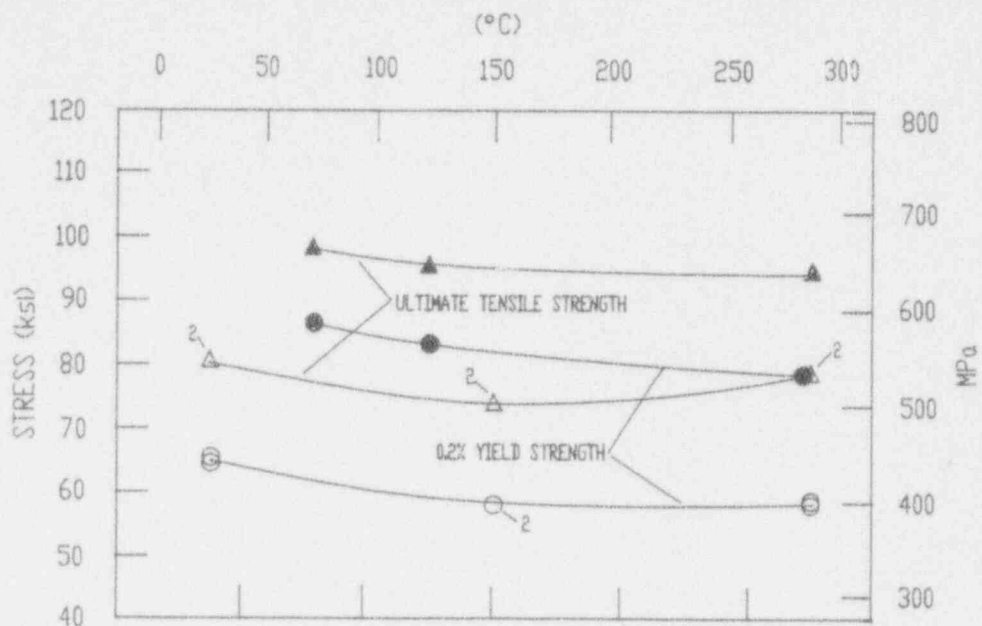
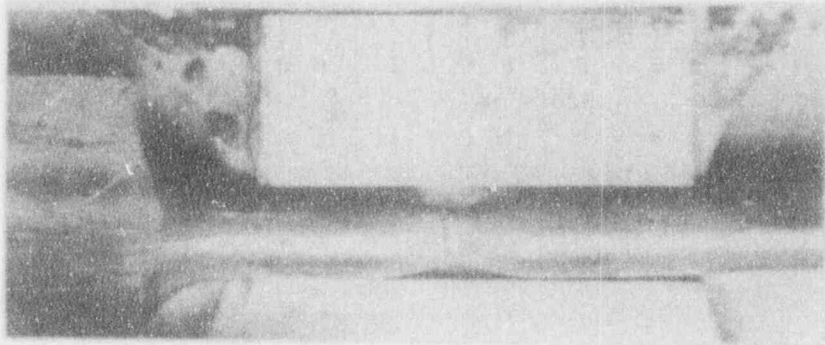


Figure 5-10 Tensile Properties for McGuire Unit 1 Reactor Vessel Intermediate Shell Plate B5012-1 (Transverse Orientation)



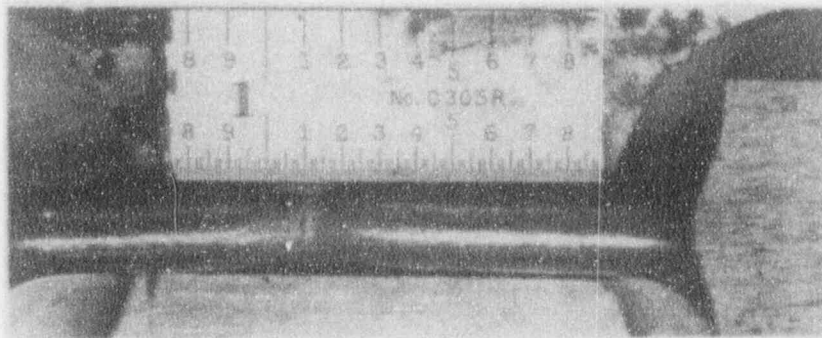
△ ○ UNIRRADIATED
 ▲ ● IRRADIATED AT 550°F, FLUENCE 2.186×10^{19} n/cm² (E > 1.0 MeV)

Figure 5-11 Tensile Properties for McGuire Unit 1 Reactor Vessel Surveillance Weld Metal



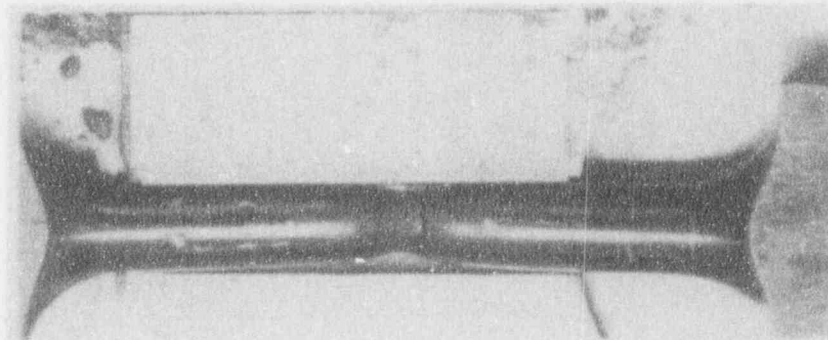
Specimen DL4

115° F



Specimen DL5

250° F



Specimen DL6

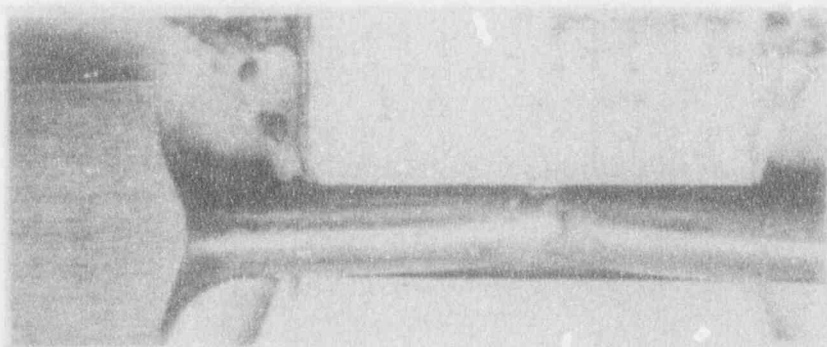
550° F

Figure 5-12 Fractured Tensile Specimens from McGuire Unit 1 Reactor Vessel Intermediate Shell Plate B5012-1 (Longitudinal Orientation)



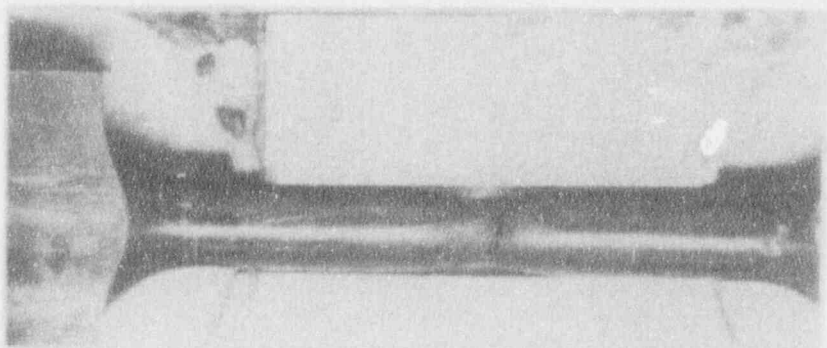
Specimen DT4

135°F



Specimen DT5

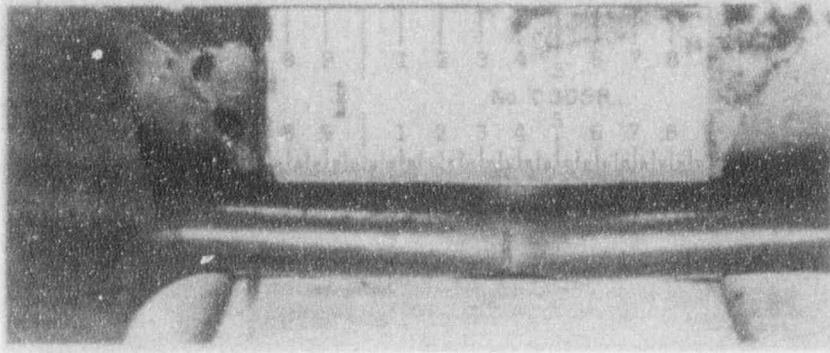
300°F



Specimen DT6

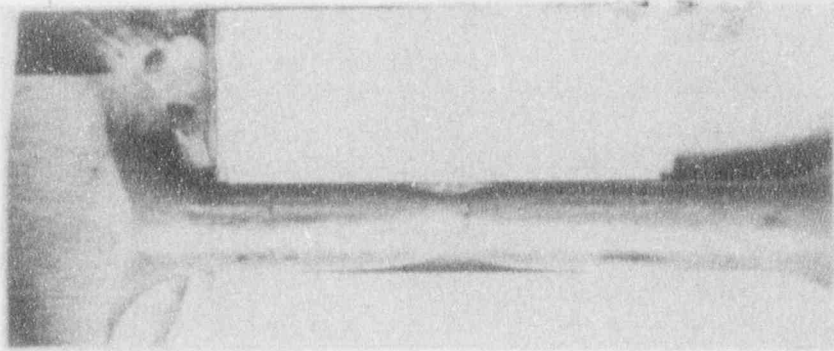
550°F

Figure 5-13 Fractured Tensile Specimens from McGuire Unit 1 Reactor Vessel Intermediate Shell Plate B5012-1 (Transverse Orientation)



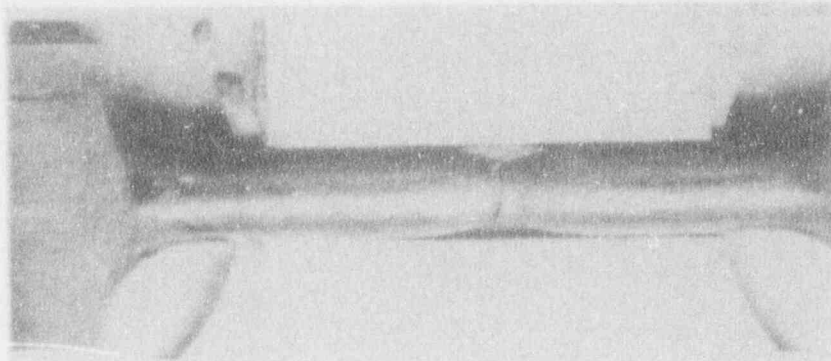
Specimen DW4

160°F



Specimen DW5

250°F



Specimen DW6

550°F

Figure 5-14 Fractured Tensile Specimens from McGuire Unit 1 Reactor Vessel Surveillance Weld Metal

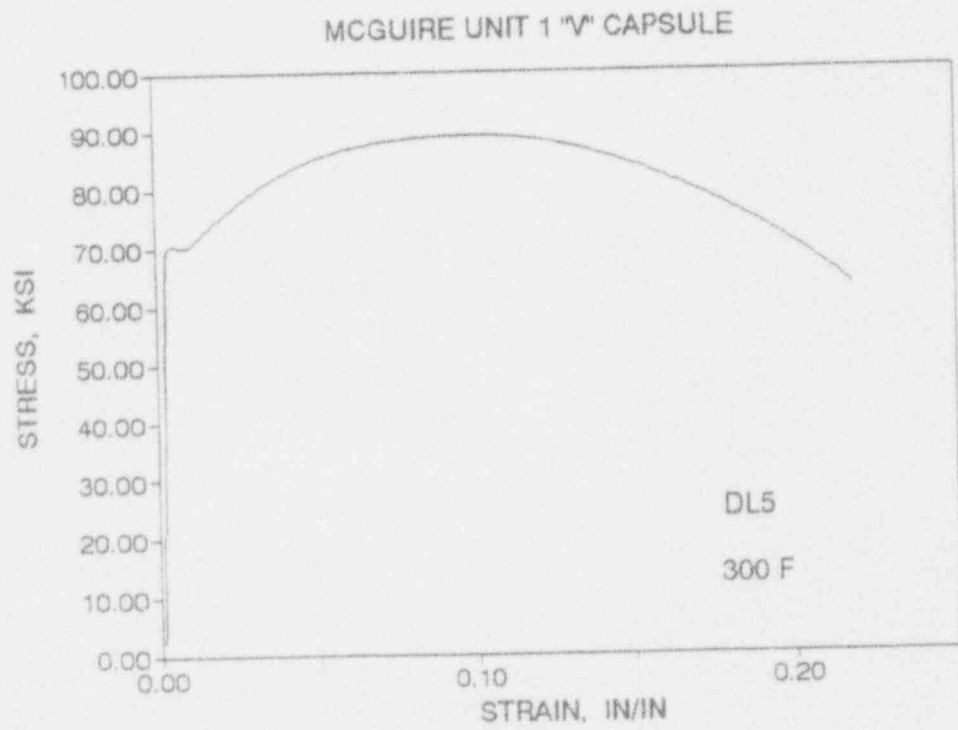
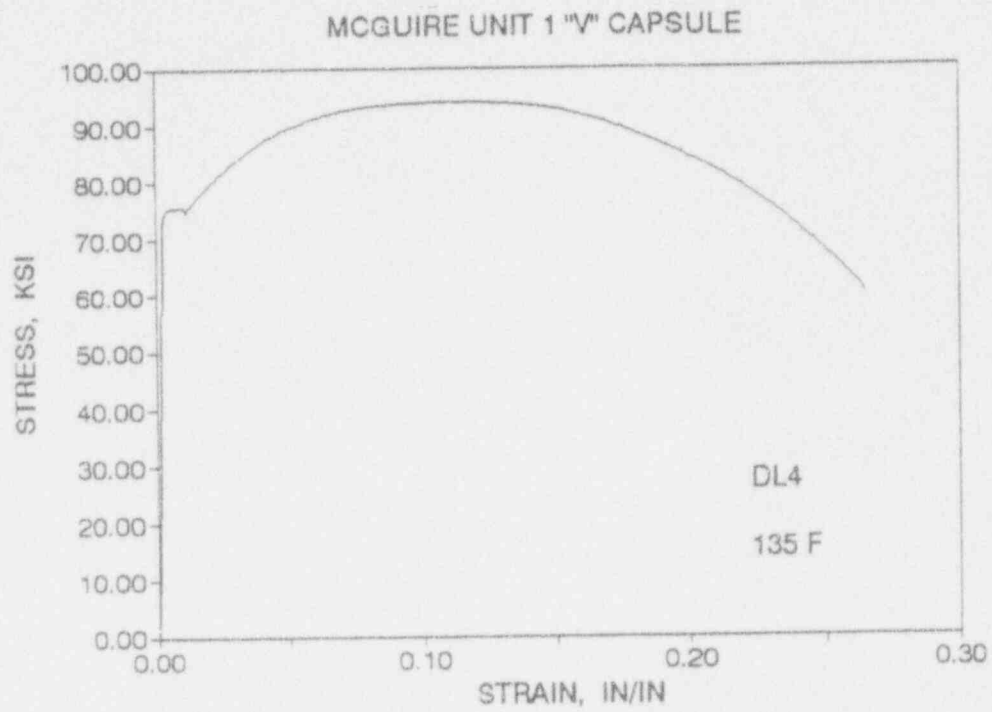


Figure 5-15 Engineering Stress-Strain Curves for Intermediate Shell Plate B5012-1 Tensile Specimens DL4 and DL5 (Longitudinal Orientation)

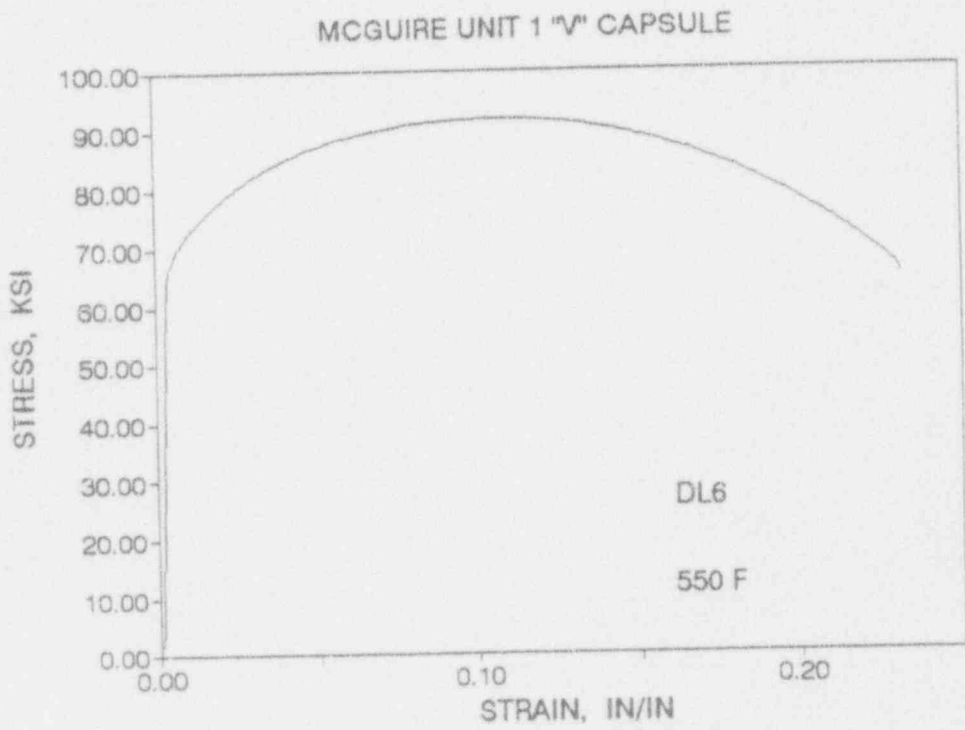


Figure 5-16 Engineering Stress-Strain Curve for Intermediate Shell Plate B5012-1 Tensile Specimen DL6 (Longitudinal Orientation)

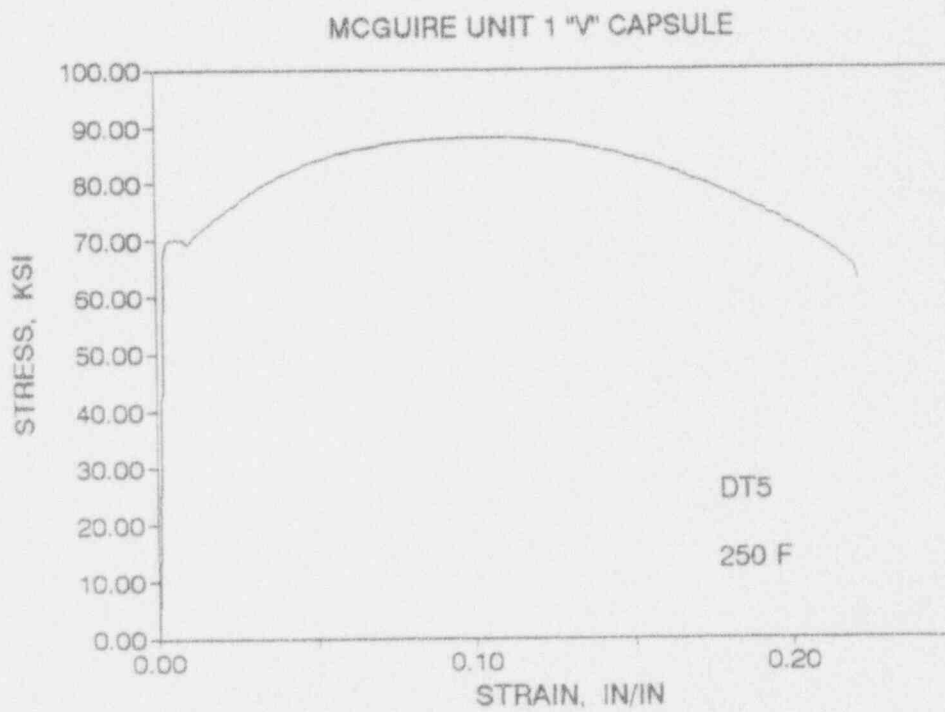
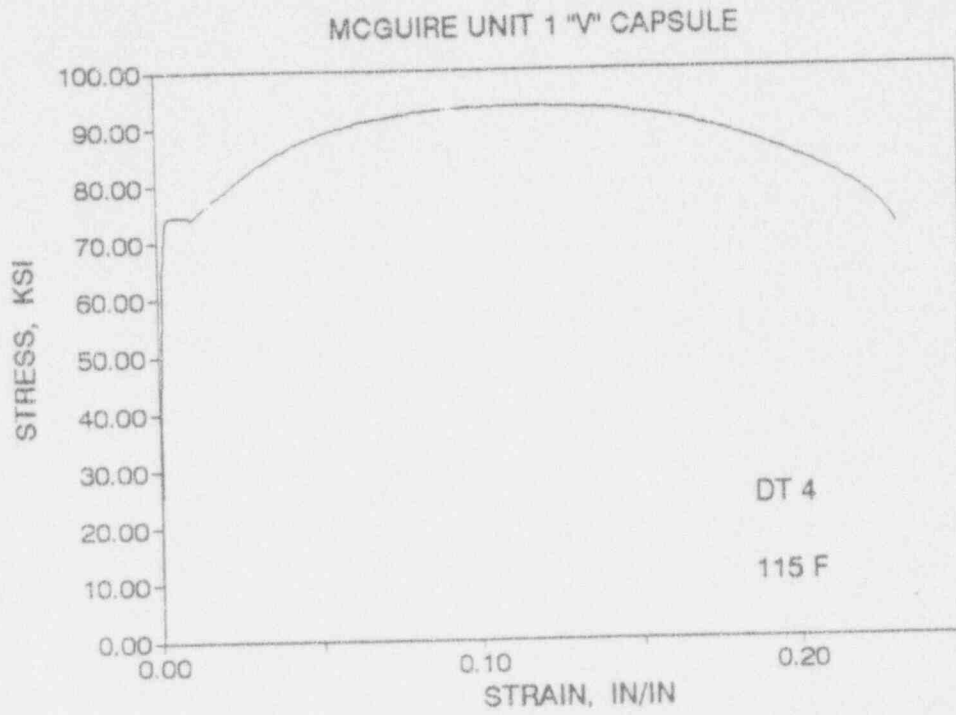


Figure 5-17 Engineering Stress-Strain Curves for Intermediate Shell Plate B5012-1 Tensile Specimens DT4 and DT5 (Transverse Orientation)

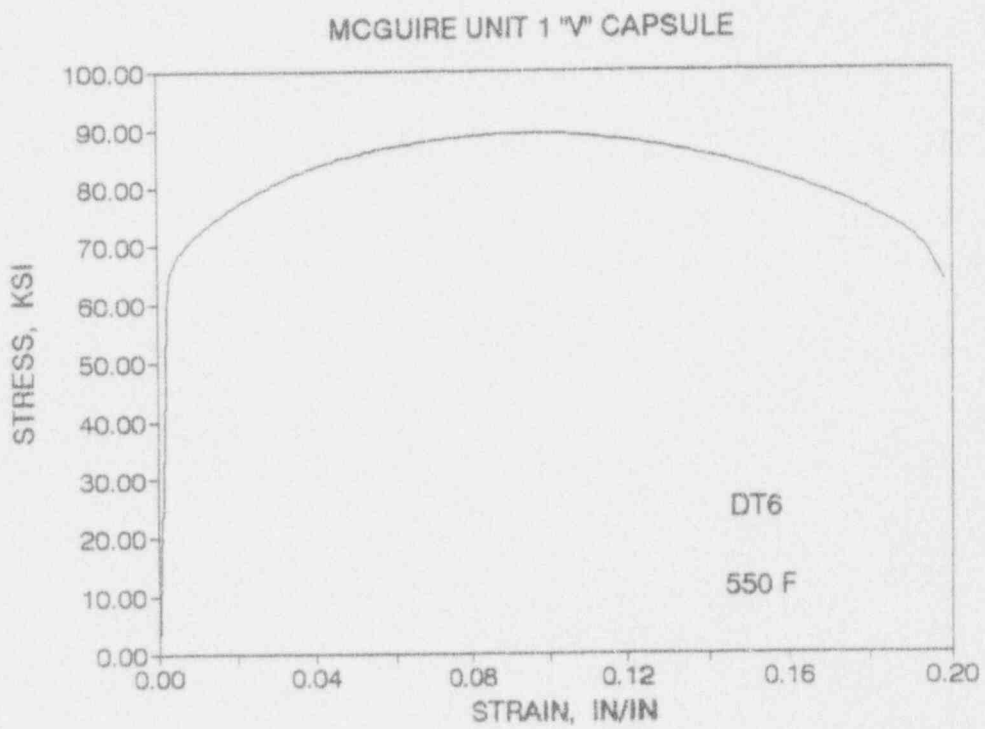


Figure 5-18 Engineering Stress-Strain Curve for Intermediate Shell Plate B5012-1
Tensile Specimen DT6 (Transverse Orientation)

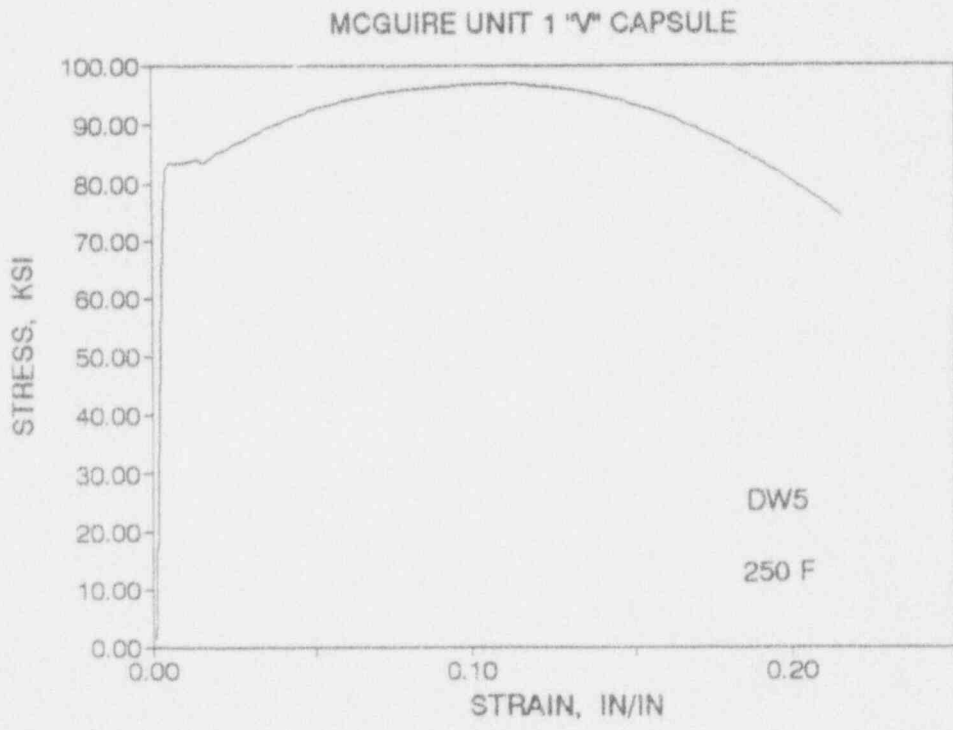
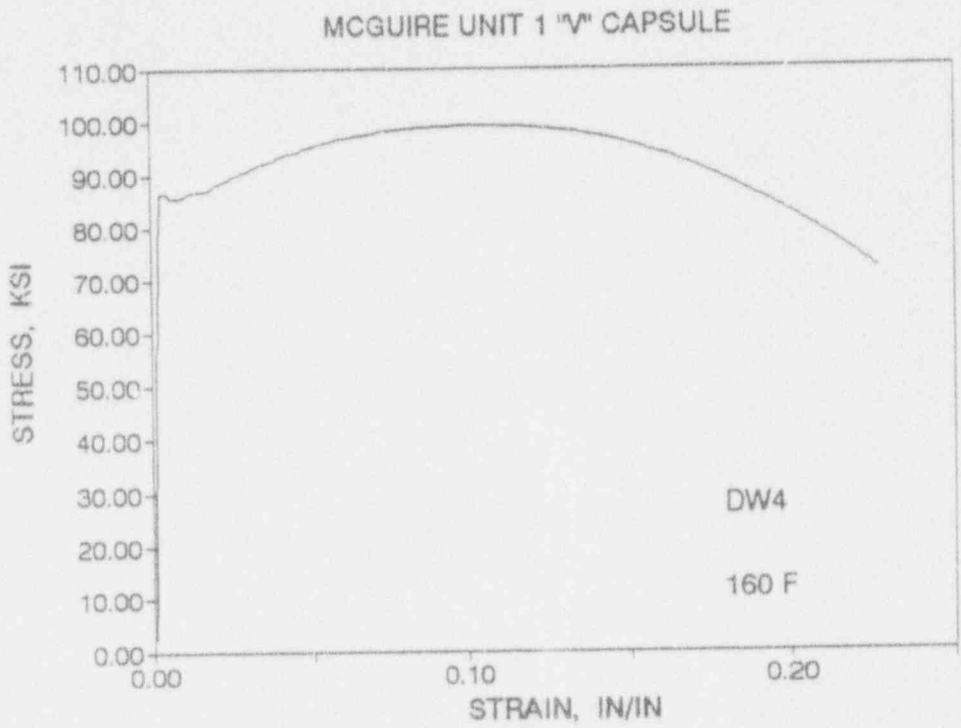


Figure 5-19 Engineering Stress-Strain Curves for Weld Metal Tensile Specimens DW4 and DW5

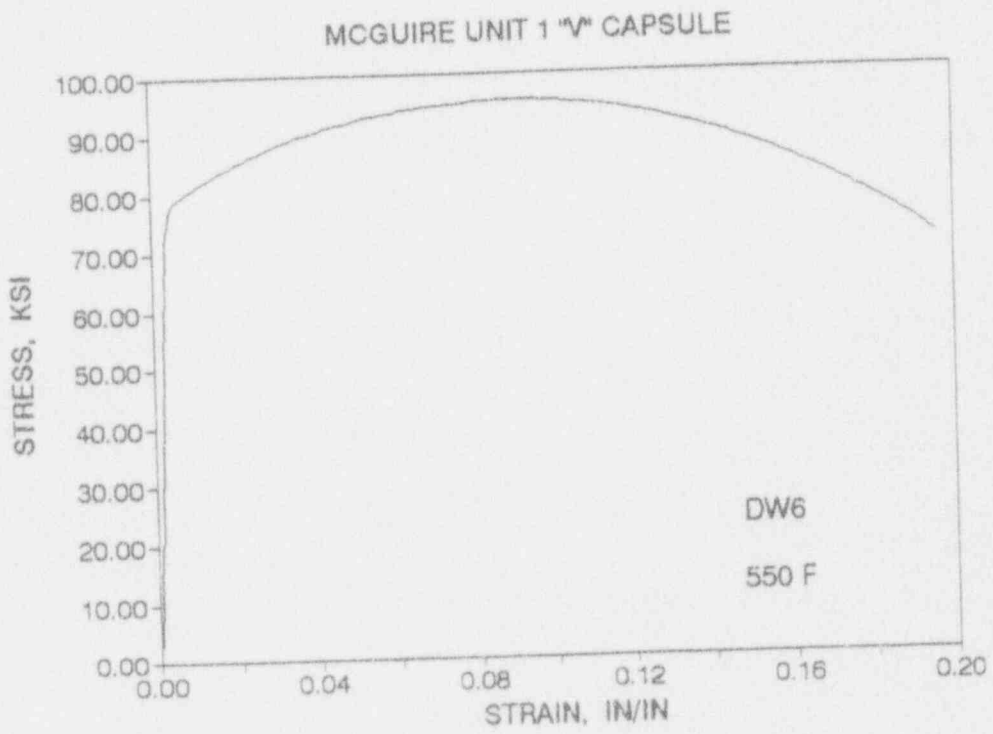


Figure 5-20 Engineering Stress-Strain Curve for Weld Metal Tensile Specimen DW6

SECTION 6.0 RADIATION ANALYSIS AND NEUTRON DOSIMETRY

6.1 Introduction

Knowledge of the neutron environment within the reactor pressure vessel and surveillance capsule geometry is required as an integral part of LWR reactor pressure vessel surveillance programs for two reasons. First, in order to interpret the neutron radiation induced material property changes observed in the test specimens, the neutron environment (energy spectrum, flux, fluence) to which the test specimens were exposed must be known. Second, in order to relate the changes observed in the test specimens to the present and future condition of the reactor vessel, a relationship must be established between the neutron environment at various positions within the pressure vessel and that experienced by the test specimens. The former requirement is normally met by employing a combination of rigorous analytical techniques and measurements obtained with passive neutron flux monitors contained in each of the surveillance capsules. The latter information is generally derived solely from analysis

The use of fast neutron fluence ($E > 1.0$ MeV) to correlate measured material property changes to the neutron exposure of the material has traditionally been accepted for development of damage trend curves as well as for the implementation of trend curve data to assess vessel condition. In recent years, however, it has been suggested that an exposure model that accounts for differences in neutron energy spectra between surveillance capsule locations and positions within the vessel wall could lead to an improvement in the uncertainties associated with damage trend curves as well as to a more accurate evaluation of damage gradients through the pressure vessel wall.

Because of this potential shift away from a threshold fluence toward an energy dependent damage function for data correlation, ASTM Standard Practice E853, "Analysis and Interpretation of Light Water Reactor Surveillance Results," recommends reporting displacements per iron atom (dpa) along with fluence ($E > 1.0$ MeV) to provide a data base for future reference. The energy dependent dpa function to be used for this evaluation is specified in ASTM Standard Practice E693, "Characterizing Neutron Exposures in Ferritic Steels in Terms of Displacements per Atom." The application of the dpa parameter to the assessment of embrittlement gradients through the thickness of the pressure vessel wall has already been promulgated in Revision 2 to Regulatory Guide 1.99, "Radiation Damage to Reactor Vessel Materials."

This section provides the results of the neutron dosimetry evaluations performed in conjunction with the analysis of test specimens contained in surveillance capsules V and Z, withdrawn at the end of the eighth fuel cycle. Also included is an updated evaluation of the dosimetry contained in capsules U and X, withdrawn at the conclusion of cycles one and five, respectively. This update is based on current state-of-the-art methodology and nuclear data; and, together with the capsule V and Z results, provides a consistent up to date data base for use in evaluating the material properties of the McGuire Unit 1 reactor vessel.

In each of the dosimetry evaluations, fast neutron exposure parameters in terms of neutron fluence ($E > 1.0$ MeV), neutron fluence ($E > 0.1$ MeV), and iron atom displacements (dpa) are established for the capsule irradiation history. The analytical formalism relating the measured capsule exposure to the exposure of the vessel wall is described and used to project the integrated exposure of the vessel wall. Also, uncertainties associated with the derived exposure parameters at the surveillance capsules and with the projected exposure of the pressure vessel are provided.

6.2 Discrete Ordinates Analysis

A plan view of the reactor geometry at the core midplane is shown in Figure 4-1. Six irradiation capsules attached to the thermal shield are included in the reactor design to constitute the reactor vessel surveillance program. The capsules are located at azimuthal angles of 56° , 58.5° , 124° , 236° , 238.5° , and 304° relative to the core cardinal axis as shown in Figure 4-1. A plan view of a dual surveillance capsule holder attached to the neutron pad is shown in Figure 6-1. The stainless steel specimen containers are 1.182 by 1-inch and approximately 56 inches in height. The containers are positioned axially such that the test specimens are centered on the core midplane, thus spanning the central 5 feet of the 12 foot high reactor core.

From a neutronic standpoint, the surveillance capsules and associated support structures are significant. The presence of these materials has a marked effect on both the spatial distribution of neutron flux and the neutron energy spectrum in the water annulus between the thermal shield and the reactor vessel. In order to determine the neutron environment at the test specimen location, the capsules themselves must be included in the analytical model.

In performing the fast neutron exposure evaluations for the surveillance capsules and reactor vessel, two distinct sets of transport calculations were carried out. The first, a single computation in the conventional forward mode, was used primarily to obtain relative neutron energy distributions throughout the reactor geometry as well as to establish relative radial distributions of exposure parameters ($\phi(E > 1.0 \text{ MeV})$, $\phi(E > 0.1 \text{ MeV})$, and dpa/sec) through the vessel wall. The neutron spectral information was required for the interpretation of neutron dosimetry withdrawn from the surveillance capsules as well as for the determination of exposure parameter ratios; i.e., $[\text{dpa/sec}]/[\phi(E > 1.0 \text{ MeV})]$, within the pressure vessel geometry. The relative radial gradient information was required to permit the projection of measured exposure parameters to locations interior to the pressure vessel wall; i.e., the 1/4T, 1/2T, and 3/4T locations.

The second set of calculations consisted of a series of adjoint analyses relating the fast neutron flux, $\phi(E > 1.0 \text{ MeV})$, at surveillance capsule positions and at several azimuthal locations on the pressure vessel inner radius to neutron source distributions within the reactor core. The source importance functions generated from these adjoint analyses provided the basis for all absolute exposure calculations and comparison with measurement. These importance functions, when combined with fuel cycle specific neutron source distributions, yielded absolute predictions of neutron exposure at the locations of interest for each cycle of irradiation. They also established the means to perform similar predictions and dosimetry evaluations for all subsequent fuel cycles. It is important to note that the cycle specific neutron source distributions utilized in these analyses included not only spatial variations of fission rates within the reactor core but also accounted for the effects of varying neutron yield per fission and fission spectrum introduced by the build-up of plutonium as the burnup of individual fuel assemblies increased.

The absolute cycle specific data from the adjoint evaluations together with the relative neutron energy spectra and radial distribution information from the reference forward calculation provided the means to:

- 1 - Evaluate neutron dosimetry obtained from surveillance capsules.
- 2 - Extrapolate dosimetry results to key locations at the inner radius and through the thickness of the pressure vessel wall.
- 3 - Enable a direct comparison of analytical prediction with measurement.
- 4 - Establish a mechanism for projection of pressure vessel exposure as the design of each new fuel cycle evolves.

The forward transport calculation for the reactor model summarized in Figures 4-1 and 6-1 was carried out in R,θ geometry using the DOT two-dimensional discrete ordinates code^[14] and the SAILOR cross-section library^[15]. The SAILOR library is a 47 energy group ENDF/B-IV based data set produced specifically for light water reactor applications. In these analyses anisotropic scattering was treated with a P_3 expansion of the scattering cross-sections and the angular discretization was modeled with an S_8 order of angular quadrature.

The core power distribution utilized in the reference forward transport calculation was derived from statistical studies of long-term operation of Westinghouse 4-loop plants. Inherent in the development of this reference core power distribution is the use of an out-in fuel management strategy; i.e., fresh fuel on the core periphery. Furthermore, for the peripheral fuel assemblies, the neutron source was increased by a 2σ margin derived from the statistical evaluation of plant to plant and cycle to cycle variations in peripheral power. Since it is unlikely that any single reactor would exhibit power levels on the core periphery at the nominal $+2\sigma$ value for a large number of fuel cycles, the use of this reference distribution is expected to yield somewhat conservative results.

All adjoint calculations were also carried out using an S_8 order of angular quadrature and the P_3 cross-section approximation from the SAILOR library. Adjoint source locations were chosen at several azimuthal locations along the pressure vessel inner radius as well as at the geometric center of each surveillance capsule. Again, these calculations were run in R,θ geometry to provide neutron source distribution importance functions for the exposure parameter of interest, in this case $\phi(E > 1.0 \text{ MeV})$.

Having the importance functions and appropriate core source distributions, the response of interest could be calculated as:

$$R(r,\theta) = \int_r \int_\theta \int_E I(r,\theta,E) S(r,\theta,E) r dr d\theta dE$$

where: $R(r,\theta) = \phi(E > 1.0 \text{ MeV})$ at radius r and azimuthal angle θ .

$I(r,\theta,E) =$ Adjoint source importance function at radius r , azimuthal angle θ , and neutron source energy E .

$S(r,\theta,E) =$ Neutron source strength at core location r,θ and energy E .

Although the adjoint importance functions used in this analysis were based on a response function defined by the threshold neutron flux $\phi(E > 1.0 \text{ MeV})$, prior calculations^[15] have shown that, while the

implementation of low leakage loading patterns significantly impacts both the magnitude and spatial distribution of the neutron field, changes in the relative neutron energy spectrum are of second order. Thus, for a given location the ratio of $[dpa/sec]/[\phi(E > 1.0 \text{ MeV})]$ is insensitive to changing core source distributions. In the application of these adjoint importance functions to the McGuire Unit 1 reactor, therefore, the iron atom displacement rates (dpa/sec) and the neutron flux $\phi(E > 0.1 \text{ MeV})$ were computed on a cycle specific basis by using $[dpa/sec]/[\phi(E > 1.0 \text{ MeV})]$ and $[\phi(E > 0.1 \text{ MeV})]/[\phi(E > 1.0 \text{ MeV})]$ ratios from the forward analysis in conjunction with the cycle specific $\phi(E > 1.0 \text{ MeV})$ solutions from the individual adjoint evaluations.

The reactor core power distributions used in the plant specific adjoint calculations were taken from the fuel cycle design reports for the first eight operating cycles of McGuire Unit 1 [17 through 24].

Selected results from the neutron transport analyses are provided in Tables 6-1 through 6-5. The data listed in these tables establish the means for absolute comparisons of analysis and measurement for the capsule irradiation periods and provide the means to correlate dosimetry results with the corresponding exposure of the pressure vessel wall.

In Table 6-1, the calculated exposure parameters [$\phi(E > 1.0 \text{ MeV})$, $\phi(E > 0.1 \text{ MeV})$, and dpa/sec] are given at the geometric center of the two surveillance capsule positions for both the reference and the plant specific core power distributions. The plant specific data, based on the adjoint transport analysis, are meant to establish the absolute comparison of measurement with analysis. The reference data derived from the forward calculation are provided as a conservative exposure evaluation against which plant specific fluence calculations can be compared. Similar data are given in Table 6-2 for the pressure vessel inner radius. Again, the three pertinent exposure parameters are listed for the reference and the cycle one through eight plant specific power distributions. It is important to note that the data for the vessel inner radius were taken at the clad/base metal interface; and, thus, represent the maximum predicted exposure levels of the vessel wall itself.

Radial gradient information applicable to $\phi(E > 1.0 \text{ MeV})$, $\phi(E > 0.1 \text{ MeV})$, and dpa/sec is given in Tables 6-3, 6-4, and 6-5, respectively. The data, obtained from the reference forward neutron transport calculation, are presented on a relative basis for each exposure parameter at several azimuthal locations. Exposure distributions through the vessel wall may be obtained by normalizing the calculated or projected exposure at the vessel inner radius to the gradient data listed in Tables 6-3 through 6-5.

For example, the neutron flux $\phi(E > 1.0 \text{ MeV})$ at the 1/4T depth in the pressure vessel wall along the 45° azimuth is given by:

$$\phi_{1/4T}(45^\circ) = \phi(220.27, 45^\circ) F(225.75, 45^\circ)$$

where: $\phi_{1/4T}(45^\circ)$ = Projected neutron flux at the 1/4T position on the 45° azimuth.

$\phi(220.27, 45^\circ)$ = Projected or calculated neutron flux at the vessel inner radius on the 45° azimuth.

$F(225.75, 45^\circ)$ = Ratio of the neutron flux at the 1/4T position to the flux at the vessel inner radius for the 45° azimuth. This data is obtained from Table 6-3

Similar expressions apply for exposure parameters expressed in terms of $\phi(E > 0.1 \text{ MeV})$ and dpa/sec where the attenuation function: F is obtained from Tables 6-4 and 6-5, respectively.

6.3 Neutron Dosimetry

The passive neutron sensors included in the McGuire Unit 1 surveillance program are listed in Table 6-6. Also given in Table 6-6 are the primary nuclear reactions and associated nuclear constants that were used in the evaluation of the neutron energy spectrum within the surveillance capsules and in the subsequent determination of the various exposure parameters of interest [$\phi(E > 1.0 \text{ MeV})$, $\phi(E > 0.1 \text{ MeV})$, dpa/sec]. The relative locations of the neutron sensors within the capsules are shown in Figure 4-2. The iron, nickel, copper, and cobalt-aluminum monitors, in wire form, were placed in holes drilled in spacers at several axial levels within the capsules. The cadmium shielded uranium and neptunium fission monitors were accommodated within the dosimeter block located near the center of the capsule.

The use of passive monitors such as those listed in Table 6-6 does not yield a direct measure of the energy dependent neutron flux at the point of interest. Rather, the activation or fission process is a measure of the integrated effect that the time and energy dependent neutron flux has on the target material over the course of the irradiation period. An accurate assessment of the average neutron flux level incident on the various monitors may be derived from the activation measurements only if the irradiation parameters are well known. In particular, the following variables are of interest:

- The measured specific activity of each monitor.
- The physical characteristics of each monitor.

- The operating history of the reactor.
- The energy response of each monitor.
- The neutron energy spectrum at the monitor location.

The specific activity of each of the neutron monitors was determined using established ASTM procedures^[25 through 38]. Following sample preparation and weighing, the activity of each monitor was determined by means of a lithium-drifted germanium, Ge(Li), gamma spectrometer. The irradiation history of the McGuire Unit 1 reactor during cycles one through eight was supplied by NUREG-0020, "Licensed Operating Reactors Status Summary Report," for the applicable period. The irradiation history applicable to capsules U, X, V and Z is given in Table 6-7.

Having the measured specific activities, the physical characteristics of the sensors, and the operating history of the reactor, reaction rates referenced to full power operation were determined from the following equation:

$$R = \frac{A}{N_0 F Y \sum \frac{P_j}{P_{ref}} C_j [1 - e^{-\lambda t_j}] [e^{-\lambda t_d}]}$$

where:

- R = Reaction rate averaged over the irradiation period and referenced to operation at a core power level of P_{ref} (rps/nucleus).
- A = Measured specific activity (dps/gm).
- N_0 = Number of target element atoms per gram of sensor.
- F = Weight fraction of the target isotope in the sensor material.
- Y = Number of product atoms produced per reaction.
- P_j = Average core power level during irradiation period j (MW).
- P_{ref} = Maximum or reference power level of the reactor (MW).
- C_j = Calculated ratio of $\phi(E > 1.0 \text{ MeV})$ during irradiation period j to the time weighted average $\phi(E > 1.0 \text{ MeV})$ over the entire irradiation period.
- λ = Decay constant of the product isotope (1/sec).
- t_j = Length of irradiation period j (sec).
- t_d = Decay time following irradiation period j (sec).

and the summation is carried out over the total number of monthly intervals comprising the irradiation period.

In the equation describing the reaction rate calculation, the ratio $[P_j]/[P_{ref}]$ accounts for month by month variation of reactor core power level within any given fuel cycle as well as over multiple fuel cycles. The ratio C_j , which can be calculated for each fuel cycle using the adjoint transport technology discussed in Section 6.2, accounts for the change in sensor reaction rates caused by variations in flux level induced by changes in core spatial power distributions from fuel cycle to fuel cycle. For a single cycle irradiation C_j is normally taken to be 1.0. However, for multiple cycle irradiations, particularly those employing low leakage fuel management, the additional C_j term should be employed. The impact of changing flux levels for constant power operation can be quite significant for sensor sets that have been irradiated for many cycles in a reactor that has transitioned from non-low leakage to low leakage fuel management or for sensor sets contained in surveillance capsules that have been moved from one capsule location to another.

For the irradiation history of capsules U, X, V, and Z, the flux level term in the reaction rate calculations was developed from the plant specific analysis provided in Table 6-1. Measured and saturated reaction product specific activities as well as the derived full power reaction rates are listed in Tables 6-8 through 6-11 for capsules U, X, V, and Z, respectively.

Values of key fast neutron exposure parameters were derived from the measured reaction rates using the FERRET least squares adjustment code^[39]. The FERRET approach used the measured reaction rate data, sensor reaction cross-sections, and a calculated trial spectrum as input and proceeded to adjust the group fluxes from the trial spectrum to produce a best fit (in a least squares sense) to the measured reaction rate data. The "measured" exposure parameters along with the associated uncertainties were then obtained from the adjusted spectrum.

In the FERRET evaluations, a log-normal least squares algorithm weights both the a priori values and the measured data in accordance with the assigned uncertainties and correlations. In general, the measured values f are linearly related to the flux ϕ by some response matrix A :

$$f_i^{(s,\alpha)} = \sum_g A_{ig}^{(s)} \phi_g^{(\alpha)}$$

where i indexes the measured values belonging to a single data set s , g designates the energy group, and α delineates spectra that may be simultaneously adjusted. For example,

$$R_i = \sum_g \sigma_{ig} \phi_g$$

relates a set of measured reaction rates R_i to a single spectrum ϕ_g by the multigroup reaction cross-section σ_{ig} . The log-normal approach automatically accounts for the physical constraint of positive fluxes, even with large assigned uncertainties.

In the least squares adjustment, the continuous quantities (i.e., neutron spectra and cross-sections) were approximated in a multi-group format consisting of 53 energy groups. The trial input spectrum was converted to the FERRET 53 group structure using the SAND-II code^[40]. This procedure was carried out by first expanding the 47 group calculated spectrum into the SAND-II 620 group structure using a SPLINE interpolation procedure in regions where group boundaries do not coincide. The 620 point spectrum was then re-collapsed into the group structure used in FERRET.

The sensor set reaction cross-sections, obtained from the ENDF/B-V dosimetry file, were also collapsed into the 53 energy group structure using the SAND-II code. In this instance, the trial spectrum, as expanded to 620 groups, was employed as a weighting function in the cross-section collapsing procedure. Reaction cross-section uncertainties in the form of a 53 x 53 covariance matrix for each sensor reaction were also constructed from the information contained on the ENDF/B-V data files. These matrices included energy group to energy group uncertainty correlations for each of the individual reactions. However, correlations between cross-sections for different sensor reactions were not included. The omission of this additional uncertainty information does not significantly impact the results of the adjustment.

Due to the importance of providing a trial spectrum that exhibits a relative energy distribution close to the actual spectrum at the sensor set locations, the neutron spectrum input to the FERRET evaluation was taken from the center of the surveillance capsule modeled in the reference forward transport calculation. While the 53 x 53 group covariance matrices applicable to the sensor reaction cross-sections were developed from the ENDF/B-V data files, the covariance matrix for the input trial spectrum was constructed from the following relation:

$$M_{gg'} = R_n^2 + R_g R_{g'} P_{gg'}$$

where R_n specifies an overall fractional normalization uncertainty (i.e., complete correlation) for the set of values. The fractional uncertainties R_g specify additional random uncertainties for group g that are correlated with a correlation matrix given by:

$$P_{gg'} = [1-\theta] \delta_{gg'} + \theta e^{-H}$$

where:

$$H = \frac{(g-g')^2}{2 \gamma^2}$$

The first term in the correlation matrix equation specifies purely random uncertainties, while the second term describes short range correlations over a group range γ (θ specifies the strength of the latter term). The value of δ is 1 when $g = g'$ and 0 otherwise. For the trial spectrum used in the current evaluations, a short range correlation of $\gamma = 6$ groups was used. This choice implies that neighboring groups are strongly correlated when θ is close to 1. Strong long range correlations (or anti-correlations) were justified based on information presented by R. E. Maerker⁴¹¹. Maerker's results are closely duplicated when $\gamma = 6$.

The uncertainties associated with the measured reaction rates included both statistical (counting) and systematic components. The systematic component of the overall uncertainty accounts for counter efficiency, counter calibrations, irradiation history corrections, and corrections for competing reactions in the individual sensors.

Results of the FERRET evaluations of the capsules U, X, V, and Z dosimetry are given in Tables 6-12 and 6-13. The data summarized in these tables include fast neutron exposure evaluations in terms of $\Phi(E > 1.0 \text{ MeV})$, $\Phi(E > 0.1 \text{ MeV})$, and dpa. In general good results were achieved in the fits of the adjusted spectra to the individual measured reaction rates. The adjusted spectra from the least squares evaluations are given in Tables 6-14 and 6-15 in the FERRET 53 energy group structure. The results for capsules V and Z are consistent with results obtained from similar evaluations of dosimetry from other Westinghouse reactors.

6.4 Projections of Pressure Vessel Exposure

Neutron exposure projections at key locations on the pressure vessel inner radius are given in Table 6-17. Along with the current (7.241 EFPY) exposure, projections are also provided for exposure periods of 16 EFPY and 32 EFPY. In computing these vessel exposures, the calculated values from Table 6-2 were scaled by the average measurement/calculation ratios (M/C) observed from the evaluations of dosimetry from capsules U, X, V, and Z for each fast neutron exposure parameter. This procedure resulted in bias factors of 1.23, 1.23, and 1.18 being applied to the calculated values of $\Phi(E > 1.0 \text{ MeV})$, $\Phi(E > 0.1 \text{ MeV})$, and dpa, respectively. Projections for future operation were based on the

assumption that the average exposure rates characteristic of the cycle one through eight irradiation would continue to be applicable throughout plant life.

For McGuire Unit 1, the uncertainty in each individual capsule derived fluence is estimated to consist of a 9% random component and a 5 % systematic component, and the extrapolation uncertainty is estimated to be 5%. A statistical combination of these uncertainties for the two capsules produces an overall uncertainty estimate in the exposure of the pressure vessel wall in the beltline region of 8% (1σ) for fluence above 1 MeV.

In the calculation of exposure gradients for use in the development of heatup and cooldown curves for the McGuire Unit 1 reactor coolant system, exposure projections to 16 EFPY and 32 EFPY were also employed. Data based on both a $\Phi(E > 1.0 \text{ MeV})$ slope and a plant specific dpa slope through the vessel wall are provided in Table 6-14.

In order to access RT_{NDT} vs fluence curves, dpa equivalent fast neutron fluence levels for the 1/4T and 3/4T positions were defined by the relations:

$$\phi(1/4T) = \phi(0T) \frac{dpa(1/4T)}{dpa(0T)}$$

and

$$\phi(3/4T) = \phi(0T) \frac{dpa(3/4T)}{dpa(0T)}$$

Using this approach results in the dpa equivalent fluence values listed in Table 6-18. In Table 6-19 updated lead factors are listed for each of the McGuire Unit 1 surveillance capsules. Lead factor data based on the accumulated fluence through cycle eight are provided for each remaining capsule.

FIGURE 6-1

PLAN VIEW OF A DUAL REACTOR VESSEL SURVEILLANCE CAPSULE

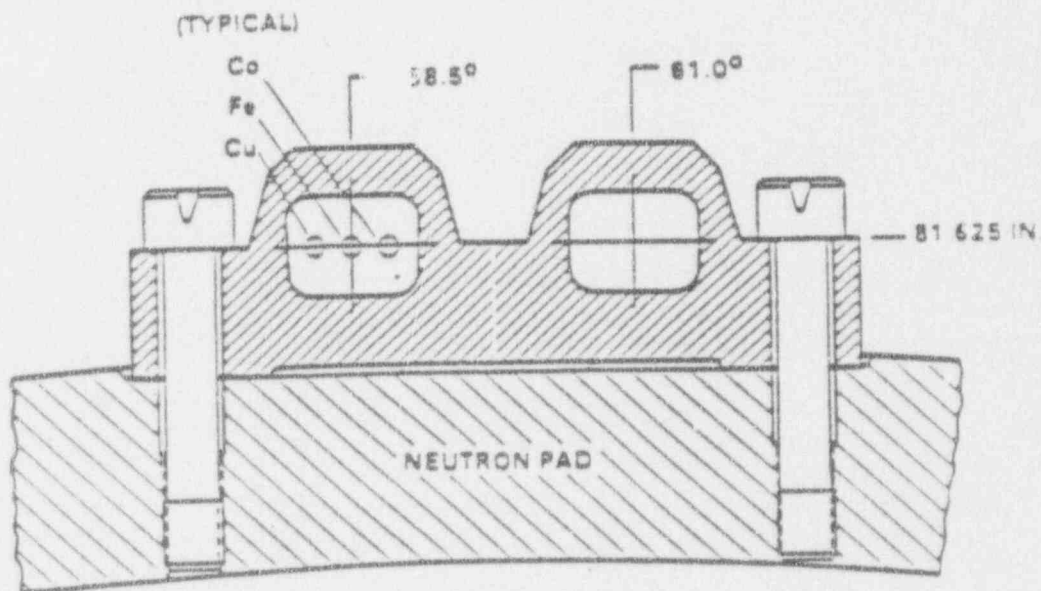


FIGURE 6-2

AXIAL DISTRIBUTION OF NEUTRON FLUENCE ($E > 1.0$ MEV)
ALONG THE 45 DEGREE AZIMUTH

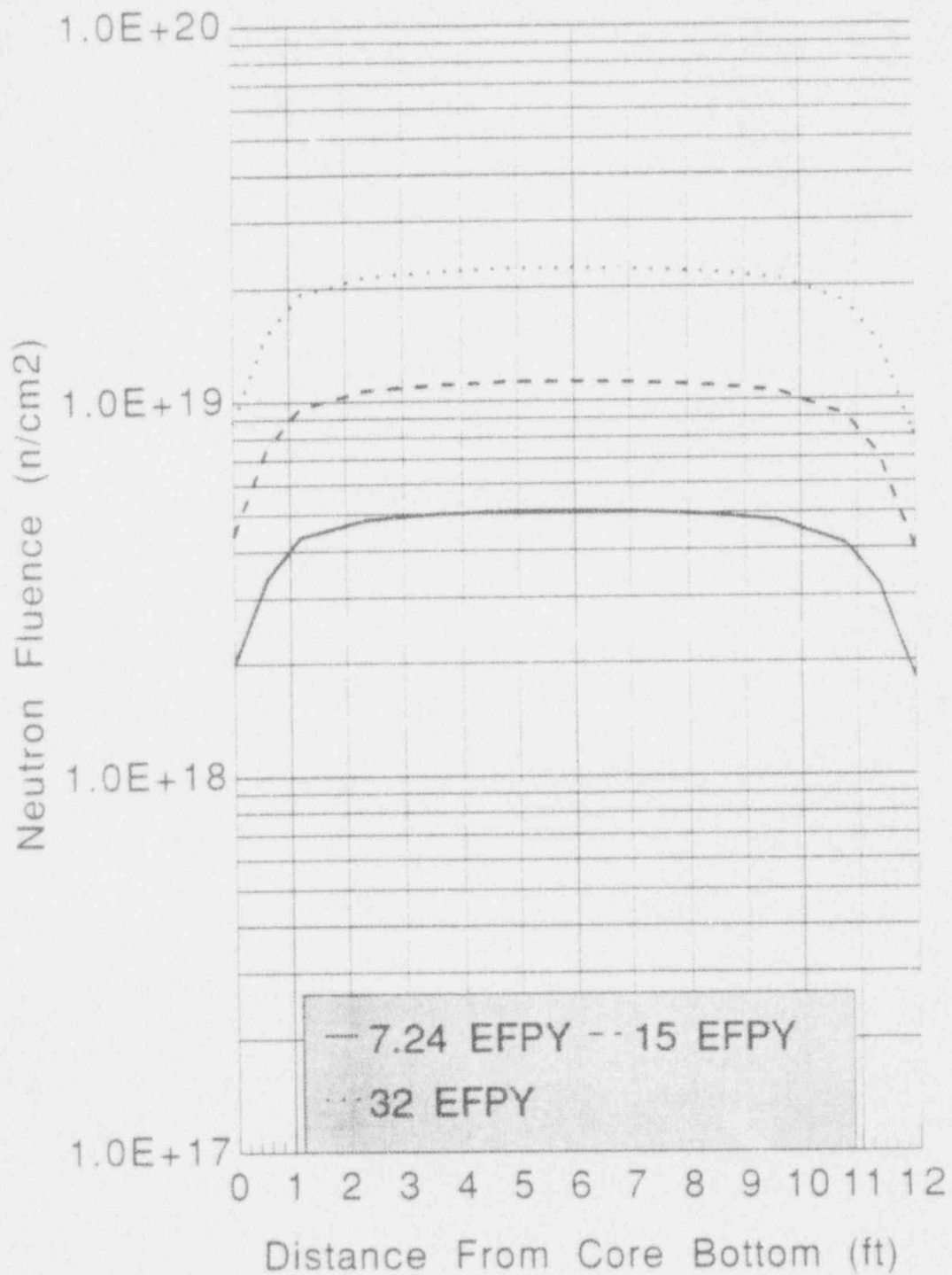


TABLE 6-1

CALCULATED FAST NEUTRON EXPOSURE RATES AT
THE SURVEILLANCE CAPSULE CENTERCALCULATED FLUX $\phi(E > 1.0 \text{ MeV})$ [n/cm²-sec] AT THE SURVEILLANCE CAPSULES

| | CAPSULE LOCATION | |
|---------|------------------|--------------|
| | <u>31.5°</u> | <u>34.0°</u> |
| CYCLE 1 | 8.5777E+10 | 9.8957E+10 |
| CYCLE 2 | 1.0586E+11 | 1.2074E+11 |
| CYCLE 3 | 7.6650E+10 | 8.6146E+10 |
| CYCLE 4 | 7.0165E+10 | 7.9365E+10 |
| CYCLE 5 | 6.6807E+10 | 7.4018E+10 |
| CYCLE 6 | 7.1250E+10 | 7.9446E+10 |
| CYCLE 7 | 6.9907E+10 | 7.8699E+10 |
| CYCLE 8 | 6.9324E+10 | 7.7147E+10 |

CALCULATED FLUX $\phi(E > 0.1 \text{ MeV})$ [n/cm²-sec] AT THE SURVEILLANCE CAPSULES

| | CAPSULE LOCATION | |
|---------|------------------|--------------|
| | <u>31.5°</u> | <u>34.0°</u> |
| CYCLE 1 | 3.8042E+11 | 4.4699E+11 |
| CYCLE 2 | 4.6949E+11 | 5.4538E+11 |
| CYCLE 3 | 3.3994E+11 | 3.8912E+11 |
| CYCLE 4 | 3.1118E+11 | 3.5849E+11 |
| CYCLE 5 | 2.9629E+11 | 3.3434E+11 |
| CYCLE 6 | 3.1599E+11 | 3.5886E+11 |
| CYCLE 7 | 3.1004E+11 | 3.5548E+11 |
| CYCLE 8 | 3.0745E+11 | 3.4847E+11 |

CALCULATED Iron Displacement Rate [dpa/sec] AT THE SURVEILLANCE CAPSULES

| | CAPSULE LOCATION | |
|---------|------------------|--------------|
| | <u>31.5°</u> | <u>34.0°</u> |
| CYCLE 1 | 1.7052E-10 | 1.9861E-10 |
| CYCLE 2 | 2.1045E-10 | 2.4233E-10 |
| CYCLE 3 | 1.5238E-10 | 1.7290E-10 |
| CYCLE 4 | 1.3949E-10 | 1.5929E-10 |
| CYCLE 5 | 1.3281E-10 | 1.4855E-10 |
| CYCLE 6 | 1.4165E-10 | 1.5945E-10 |
| CYCLE 7 | 1.3898E-10 | 1.5795E-10 |
| CYCLE 8 | 1.3782E-10 | 1.5483E-10 |

TABLE 6-2

CALCULATED AZIMUTHAL VARIATION OF FAST NEUTRON EXPOSURE RATES
AT THE PRESSURE VESSEL CLAD/BASE METAL INTERFACE

| | <u>$\phi(E > 1.0 \text{ MeV})$ [n/cm²-sec]</u> | | | |
|---------|---|------------|------------|------------|
| | 0 DEG | 15 DEG | 30 DEG | 45 DEG |
| CYCLE 1 | 1.0932E+10 | 1.6394E+10 | 1.3024E+10 | 1.8845E+10 |
| CYCLE 2 | 1.4170E+10 | 2.1316E+10 | 1.6230E+10 | 2.2679E+10 |
| CYCLE 3 | 1.0672E+10 | 1.5620E+10 | 1.1687E+10 | 1.6069E+10 |
| CYCLE 4 | 1.0200E+10 | 1.5141E+10 | 1.0913E+10 | 1.5155E+10 |
| CYCLE 5 | 1.0791E+10 | 1.5222E+10 | 1.0304E+10 | 1.3717E+10 |
| CYCLE 6 | 1.0161E+10 | 1.5184E+10 | 1.0971E+10 | 1.4801E+10 |
| CYCLE 7 | 9.4351E+09 | 1.3867E+10 | 1.0624E+10 | 1.4737E+10 |
| CYCLE 8 | 1.0125E+10 | 1.5096E+10 | 1.0738E+10 | 1.4410E+10 |

| | <u>$\phi(E > 0.1 \text{ MeV})$ [n/cm²-sec]</u> | | | |
|---------|---|------------|------------|------------|
| | 0 DEG | 15 DEG | 30 DEG | 45 DEG |
| CYCLE 1 | 2.2769E+10 | 3.4456E+10 | 3.3513E+10 | 4.7190E+10 |
| CYCLE 2 | 2.9513E+10 | 4.4801E+10 | 4.1763E+10 | 5.6790E+10 |
| CYCLE 3 | 2.2227E+10 | 3.2830E+10 | 3.0073E+10 | 4.0238E+10 |
| CYCLE 4 | 2.1244E+10 | 3.1823E+10 | 2.8081E+10 | 3.7950E+10 |
| CYCLE 5 | 2.2475E+10 | 3.1993E+10 | 2.6514E+10 | 3.4349E+10 |
| CYCLE 6 | 2.1163E+10 | 3.1913E+10 | 2.8230E+10 | 3.7063E+10 |
| CYCLE 7 | 1.9651E+10 | 2.9145E+10 | 2.7337E+10 | 3.6903E+10 |
| CYCLE 8 | 2.1088E+10 | 3.1728E+10 | 2.7631E+10 | 3.6084E+10 |

| | <u>Iron Displacement Rate [dpa/sec]</u> | | | |
|---------|---|------------|------------|------------|
| | 0 DEG | 15 DEG | 30 DEG | 45 DEG |
| CYCLE 1 | 1.6963E-11 | 2.5244E-11 | 2.1204E-11 | 2.9967E-11 |
| CYCLE 2 | 2.1988E-11 | 3.2823E-11 | 2.6423E-11 | 3.6063E-11 |
| CYCLE 3 | 1.6560E-11 | 2.4052E-11 | 1.9027E-11 | 2.5552E-11 |
| CYCLE 4 | 1.5828E-11 | 2.3314E-11 | 1.7767E-11 | 2.4099E-11 |
| CYCLE 5 | 1.6745E-11 | 2.3439E-11 | 1.6775E-11 | 2.1812E-11 |
| CYCLE 6 | 1.5767E-11 | 2.3381E-11 | 1.7861E-11 | 2.3536E-11 |
| CYCLE 7 | 1.4641E-11 | 2.1353E-11 | 1.7296E-11 | 2.3434E-11 |
| CYCLE 8 | 1.5711E-11 | 2.3245E-11 | 1.7482E-11 | 2.2914E-11 |

TABLE 6-3

RELATIVE RADIAL DISTRIBUTION OF $\phi(E > 1.0 \text{ MeV})$
WITHIN THE PRESSURE VESSEL WALL

| Radius (cm) | <u>0.0°</u> | <u>15.0°</u> | <u>25.0°</u> | <u>35.0°</u> | <u>45.0°</u> |
|-----------------------|-------------|--------------|--------------|--------------|--------------|
| 220.27 ⁽¹⁾ | 1.00 | 1.00 | 1.00 | 1.00 | 1.00 |
| 220.64 | 0.976 | 0.979 | 0.980 | 0.977 | 0.979 |
| 221.66 | 0.888 | 0.891 | 0.893 | 0.891 | 0.889 |
| 222.99 | 0.768 | 0.770 | 0.772 | 0.770 | 0.766 |
| 224.31 | 0.653 | 0.653 | 0.657 | 0.655 | 0.648 |
| 225.63 | 0.551 | 0.550 | 0.554 | 0.552 | 0.543 |
| 226.95 | 0.462 | 0.460 | 0.465 | 0.463 | 0.452 |
| 228.28 | 0.386 | 0.384 | 0.388 | 0.386 | 0.375 |
| 229.60 | 0.321 | 0.319 | 0.324 | 0.321 | 0.311 |
| 230.92 | 0.267 | 0.263 | 0.275 | 0.267 | 0.257 |
| 232.25 | 0.221 | 0.219 | 0.225 | 0.221 | 0.211 |
| 233.57 | 0.183 | 0.181 | 0.185 | 0.183 | 0.174 |
| 234.89 | 0.151 | 0.149 | 0.153 | 0.151 | 0.142 |
| 236.22 | 0.124 | 0.122 | 0.126 | 0.124 | 0.116 |
| 237.54 | 0.102 | 0.100 | 0.104 | 0.102 | 0.0945 |
| 238.86 | 0.0828 | 0.0817 | 0.0846 | .0835 | 0.0762 |
| 240.19 | 0.0671 | 0.0660 | 0.0689 | .0679 | 0.0608 |
| 241.51 | 0.0538 | 0.0522 | 0.0550 | 0.0545 | 0.0471 |
| 242.17 ⁽²⁾ | 0.0506 | 0.0488 | 0.0518 | 0.0521 | 0.0438 |

NOTES: 1) Base Metal Inner Radius
2) Base Metal Outer Radius

TABLE 6-4

RELATIVE RADIAL DISTRIBUTION OF $\phi(E > 0.1 \text{ MeV})$
WITHIN THE PRESSURE VESSEL WALL

| Radius (cm) | <u>0.0°</u> | <u>15.0°</u> | <u>25.0°</u> | <u>35.0°</u> | <u>45.0°</u> |
|-----------------------|-------------|--------------|--------------|--------------|--------------|
| 220.27 ⁽¹⁾ | 1.00 | 1.00 | 1.00 | 1.00 | 1.00 |
| 220.64 | 1.00 | 1.00 | 1.00 | 1.00 | 1.00 |
| 221.66 | 1.00 | 1.00 | 1.00 | 0.999 | 0.995 |
| 222.99 | 0.974 | 0.969 | 0.974 | 0.959 | 0.956 |
| 224.31 | 0.927 | 0.920 | 0.927 | 0.907 | 0.901 |
| 225.63 | 0.874 | 0.865 | 0.874 | 0.850 | 0.842 |
| 226.95 | 0.818 | 0.808 | 0.818 | 0.792 | 0.782 |
| 228.28 | 0.761 | 0.750 | 0.716 | 0.734 | 0.721 |
| 229.60 | 0.705 | 0.693 | 0.704 | 0.677 | 0.662 |
| 230.92 | 0.649 | 0.637 | 0.649 | 0.621 | 0.605 |
| 232.25 | 0.594 | 0.582 | 0.594 | 0.567 | 0.549 |
| 233.57 | 0.540 | 0.529 | 0.542 | 0.515 | 0.495 |
| 234.89 | 0.487 | 0.478 | 0.490 | 0.465 | 0.443 |
| 236.22 | 0.436 | 0.428 | 0.440 | 0.416 | 0.392 |
| 237.54 | 0.386 | 0.380 | 0.392 | 0.369 | 0.343 |
| 238.86 | 0.337 | 0.333 | 0.344 | 0.324 | 0.295 |
| 240.19 | 0.289 | 0.287 | 0.298 | 0.279 | 0.248 |
| 241.51 | 0.244 | 0.238 | 0.249 | 0.233 | 0.201 |
| 242.17 ⁽²⁾ | 0.233 | 0.226 | 0.237 | 0.223 | 0.188 |

NOTES: 1) Base Metal Inner Radius
2) Base Metal Outer Radius

TABLE 6-5

RELATIVE RADIAL DISTRIBUTION OF dpa/sec
WITHIN THE PRESSURE VESSEL WALL

| Radius (cm) | <u>0.0°</u> | <u>15.0°</u> | <u>25.0°</u> | <u>35.0°</u> | <u>45.0°</u> |
|-----------------------|-------------|--------------|--------------|--------------|--------------|
| 220.27 ⁽¹⁾ | 1.00 | 1.00 | 1.00 | 1.00 | 1.00 |
| 220.64 | 0.984 | 0.981 | 0.984 | 0.983 | 0.984 |
| 221.66 | 0.912 | 0.909 | 0.917 | 0.921 | 0.915 |
| 222.99 | 0.815 | 0.812 | 0.826 | 0.833 | 0.821 |
| 224.31 | 0.722 | 0.719 | 0.737 | 0.747 | 0.730 |
| 225.63 | 0.638 | 0.634 | 0.656 | 0.668 | 0.647 |
| 226.95 | 0.563 | 0.559 | 0.584 | 0.597 | 0.572 |
| 228.28 | 0.497 | 0.493 | 0.519 | 0.533 | 0.506 |
| 229.60 | 0.439 | 0.435 | 0.462 | 0.475 | 0.447 |
| 230.92 | 0.387 | 0.383 | 0.410 | 0.423 | 0.394 |
| 232.25 | 0.341 | 0.338 | 0.364 | 0.376 | 0.347 |
| 233.57 | 0.300 | 0.297 | 0.322 | 0.334 | 0.305 |
| 234.89 | 0.263 | 0.261 | 0.285 | 0.295 | 0.266 |
| 236.22 | 0.230 | 0.228 | 0.250 | 0.260 | 0.231 |
| 237.54 | 0.199 | 0.198 | 0.218 | 0.227 | 0.199 |
| 238.86 | 0.171 | 0.170 | 0.189 | 0.196 | 0.169 |
| 240.19 | 0.145 | 0.144 | 0.161 | 0.167 | 0.140 |
| 241.51 | 0.121 | 0.119 | 0.135 | 0.139 | 0.113 |
| 242.17 ⁽²⁾ | 0.116 | 0.113 | 0.128 | 0.134 | 0.106 |

NOTES: 1) Base Metal Inner Radius
2) Base Metal Outer Radius

TABLE 6-6

NUCLEAR PARAMETERS USED IN THE EVALUATION OF NEUTRON SENSORS

| <u>Monitor Material</u> | <u>Reaction of Interest</u> | <u>Target Weight Fraction</u> | <u>Response Range</u> | <u>Product Half-Life</u> | <u>Fission Yield (%)</u> |
|-------------------------|---|-------------------------------|--|--------------------------|--------------------------|
| Copper | $\text{Cu}^{63}(\text{n},\alpha)\text{Co}^{60}$ | 0.6917 | $E > 4.7 \text{ MeV}$ | 5.271 yrs | |
| Iron | $\text{Fe}^{54}(\text{n},\text{p})\text{Mn}^{54}$ | 0.0580 | $E > 1.0 \text{ MeV}$ | 312.5 days | |
| Nickel | $\text{Ni}^{58}(\text{n},\text{p})\text{Co}^{58}$ | 0.6827 | $E > 1.0 \text{ MeV}$ | 70.78 days | |
| Uranium-238* | $\text{U}^{238}(\text{n},\text{f})\text{Cs}^{137}$ | 1.0 | $E > 0.4 \text{ MeV}$ | 30.17 yrs | 6.00 |
| Neptunium-237* | $\text{Np}^{237}(\text{n},\text{f})\text{Cs}^{137}$ | 1.0 | $E > 0.08 \text{ MeV}$ | 30.17 yrs | 6.27 |
| Cobalt-Aluminum* | $\text{Co}^{59}(\text{n},\gamma)\text{Co}^{60}$ | 0.0015 | $0.4\text{eV} > E > 0.015 \text{ MeV}$ | 5.271 yrs | |
| Cobalt-Aluminum | $\text{Co}^{59}(\text{n},\gamma)\text{Co}^{60}$ | 0.0015 | $E > 0.015 \text{ MeV}$ | 5.271 yrs | |

*Denotes that monitor is cadmium shielded.

TABLE 6-7

MONTHLY THERMAL GENERATION DURING THE FIRST EIGHT FUEL CYCLES
OF THE MCGUIRE UNIT 1 REACTOR

| Thermal Generation | | | Thermal Generation | | |
|--------------------|-------|-----------|--------------------|-------|-----------|
| Year | Month | (MW-hr) | Year | Month | (MW-hr) |
| 1981 | 10 | 222,129 | | 7 | 2,534,622 |
| | 11 | 781,796 | | 8 | 1,847,703 |
| | 12 | 84,955 | | 9 | 221,936 |
| 1982 | 1 | 1,273,713 | | 10 | 0 |
| | 2 | 1,054,504 | | 11 | 1,101,430 |
| | 3 | 530,357 | 1988 | 12 | 2,251,637 |
| | 4 | 1,192,627 | | 1 | 2,379,899 |
| | 5 | 1,484,279 | | 2 | 2,314,778 |
| | 6 | 1,266,005 | | 3 | 2,380,942 |
| | 7 | 561,572 | | 4 | 2,314,604 |
| | 8 | 1,467,549 | | 5 | 2,528,964 |
| | 9 | 1,454,192 | | 6 | 2,281,133 |
| | 10 | 1,338,949 | | 7 | 2,485,619 |
| | 11 | 527,736 | | 8 | 3,522,007 |
| | 12 | 1,265,980 | | 9 | 2,437,962 |
| 1983 | 1 | 857,172 | | 10 | 898,152 |
| | 2 | 0 | | 11 | 0 |
| | 3 | 0 | | 12 | 9,881 |
| | 4 | 0 | 1989 | 1 | 2,245,259 |
| | 5 | 167,441 | | 2 | 2,286,701 |
| | 6 | 1,953,836 | | 3 | 569,136 |
| | 7 | 1,975,352 | | 4 | 0 |
| | 8 | 1,139,545 | | 5 | 1,664,673 |
| | 9 | 2,260,850 | | 6 | 2,412,733 |
| | 10 | 1,935,163 | | 7 | 2,368,074 |
| | 11 | 1,623,905 | | 8 | 2,300,333 |
| | 12 | 2,011,387 | | 9 | 2,425,699 |
| 1984 | 1 | 2,222,932 | | 10 | 2,518,039 |
| | 2 | 1,889,758 | | 11 | 2,456,058 |
| | 3 | 0 | | 12 | 2,530,503 |
| | 4 | 0 | 1990 | 1 | 608,302 |
| | 5 | 1,994,565 | | 2 | 0 |
| | 6 | 2,266,395 | | 3 | 0 |
| | 7 | 2,319,518 | | 4 | 0 |
| | 8 | 2,370,549 | | 5 | 521,935 |
| | 9 | 2,480,184 | | 6 | 2,156,153 |
| | 10 | 2,042,345 | | 7 | 2,494,895 |
| | 11 | 1,553,094 | | 8 | 2,124,989 |
| | 12 | 226,629 | | 9 | 2,200,794 |
| 1985 | 1 | 2,356,943 | | 10 | 1,063,172 |
| | 2 | 2,088,791 | | 11 | 1,146,029 |
| | 3 | 1,694,129 | 1991 | 12 | 2,518,560 |
| | 4 | 596,719 | | 1 | 2,519,888 |
| | 5 | 0 | | 2 | 1,818,751 |
| | 6 | 117,945 | | 3 | 2,521,731 |
| | 7 | 2,344,677 | | 4 | 1,993,480 |
| | 8 | 2,533,610 | | 5 | 1,274,443 |
| | 9 | 2,329,794 | | 6 | 2,446,944 |
| | 10 | 2,533,965 | | 7 | 2,516,832 |
| | 11 | 1,540,353 | | 8 | 2,534,664 |
| | 12 | 2,425,449 | | 9 | 1,557,266 |
| 1986 | 1 | 2,471,899 | | 10 | 0 |
| | 2 | 2,022,499 | | 11 | 0 |
| | 3 | 2,089,263 | 1992 | 12 | 1,566,100 |
| | 4 | 2,204,598 | | 1 | 1,277,016 |
| | 5 | 1,001,197 | | 2 | 752,634 |
| | 6 | 0 | | 3 | 2,438,606 |
| | 7 | 0 | | 4 | 2,390,345 |
| | 8 | 0 | | 5 | 305,612 |
| | 9 | 944,223 | | 6 | 880,274 |
| | 10 | 2,393,046 | | 7 | 2,285,861 |
| | 11 | 44,556 | | 8 | 2,514,974 |
| | 12 | 2,516,554 | | 9 | 2,450,774 |
| 1987 | 1 | 2,534,776 | | 10 | 2,514,483 |
| | 2 | 1,861,001 | | 11 | 2,451,002 |
| | 3 | 2,537,575 | 1993 | 12 | 2,526,799 |
| | 4 | 2,287,291 | | 1 | 2,543,424 |
| | 5 | 2,498,567 | | 2 | 2,288,198 |
| | 6 | 2,441,831 | | 3 | 904,384 |

TABLE 6-8

MEASURED SENSOR ACTIVITIES AND REACTION RATES
SURVEILLANCE CAPSULE U
SATURATED ACTIVITIES AND DERIVED FAST NEUTRON FLUX

| <u>MONITOR AND AXIAL LOCATION</u> | <u>MEASURED ACTIVITY (dis/sec-gm)</u> | <u>SATURATED ACTIVITY (dis/sec-gm)</u> | <u>REACTION RATE (rps/nucleus)</u> |
|--|---|--|--|
| <u>Cu-63 (n,α) Co-60</u> | | | |
| 84-2731 TOP | 4.510E+04 | 3.873E+05 | |
| 84-2737 MID | 4.740E+04 | 4.070E+05 | |
| 84-2743 BOT | 4.530E+04 | 3.890E+05 | |
| AVERAGES | 4.593E+04 | 3.945E+05 | 6.018E-17 |
| <u>Fe-54 (n,p) Mn-54</u> | | | |
| 84-2730 TOP | 1.100E+06 | 3.935E+06 | |
| 84-2736 MID | 1.130E+06 | 4.042E+06 | |
| 84-2742 BOT | 1.150E+06 | 4.114E+06 | |
| AVERAGES | 1.127E+06 | 4.030E+06 | 6.444E-15 |
| <u>Ni-58 (n,p) Co-58</u> | | | |
| 84-2734 TOP | 4.950E+06 | 6.149E+07 | |
| 84-2740 MID | 5.160E+06 | 6.409E+07 | |
| 84-2746 BOT | 5.340E+06 | 6.633E+07 | |
| AVERAGES | 5.150E+06 | 6.397E+07 | 9.134E-15 |
| <u>Co-59 (n,γ) Co-60</u> | | | |
| 84-2732 TOP | 1.310E+07 | 1.125E+08 | |
| 84-2738 MID | 1.170E+07 | 1.005E+08 | |
| 84-2744 BOT | 9.270E+06 | 7.961E+07 | |
| 84-2735 TOP | 1.250E+07 | 1.073E+08 | |
| 84-2741 MID | 9.780E+06 | 8.399E+07 | |
| 84-2747 BOT | 1.210E+07 | 1.039E+08 | |
| AVERAGES | 1.141E+07 | 9.797E+07 | 6.392E-12 |
| <u>Co-59 (n,γ) Co-60</u> | | | |
| 84-2733 TOP | 6.440E+06 | 5.530E+07 | |
| 84-2739 MID | 6.360E+06 | 5.462E+07 | |
| 84-2745 BOT | 6.470E+06 | 5.556E+07 | |
| AVERAGES | 6.423E+06 | 5.516E+07 | 3.599E-12 |
| <u>U-238 (n,f) Cs-137</u> | | | |
| 84-2729 MID | 1.800E+05 | 7.464E+06 | 4.919E-14 |
| <u>Np-237 (n,f) Cs-137</u> | | | |
| 84-2728 MID | 1.650E+06 | 6.842E+07 | 4.295E-13 |

TABLE 6-9

MEASURED SENSOR ACTIVITIES AND REACTION RATES
SURVEILLANCE CAPSULE X
SATURATED ACTIVITIES AND DERIVED FAST NEUTRON FLUX

| <u>MONITOR AND AXIAL LOCATION</u> | <u>MEASURED ACTIVITY (dis/sec-gm)</u> | <u>SATURATED ACTIVITY (dis/sec-gm)</u> | <u>REACTION RATE (rps/nucleus)</u> |
|--|---|--|--|
| <u>Cu-63 (n,α) Co-60</u> | | | |
| 89-336 TOP | 1.260E+05 | 3.479E+05 | |
| 89-342 MID | 1.250E+05 | 3.451E+05 | |
| 89-348 BOT | 1.290E+05 | 3.561E+05 | |
| AVERAGES | 1.267E+05 | 3.497E+05 | 5.335E-17 |
| <u>Fe-54 (n,p) Mn-54</u> | | | |
| 89-337 TOP | 1.650E+06 | 3.292E+06 | |
| 89-343 MID | 1.640E+06 | 3.272E+06 | |
| 89-349 BOT | 1.730E+06 | 3.451E+06 | |
| AVERAGES | 1.673E+06 | 3.338E+06 | 5.338E-15 |
| <u>Ni-58 (n,p) Co-58</u> | | | |
| 89-338 TOP | 1.100E+07 | 5.284E+07 | |
| 89-344 MID | 1.070E+07 | 5.140E+07 | |
| 89-350 BOT | 1.120E+07 | 5.380E+07 | |
| AVERAGES | 1.097E+07 | 5.268E+07 | 7.522E-15 |
| <u>Co-59 (n,γ) Co-60</u> | | | |
| 89-333 TOP | 2.760E+07 | 7.620E+07 | |
| 89-339 MID | 2.950E+07 | 8.144E+07 | |
| 89-345 BOT | 2.490E+07 | 6.874E+07 | |
| 89-334 TOP | 3.140E+07 | 8.669E+07 | |
| 89-340 MID | 3.350E+07 | 9.249E+07 | |
| 89-346 BOT | 3.000E+07 | 8.282E+07 | |
| AVERAGES | 2.948E+07 | 8.140E+07 | 5.311E-12 |
| <u>Co-59 (n,γ) Co-60</u> | | | |
| 89-335 TOP | 1.680E+07 | 4.638E+07 | |
| 89-341 MID | 1.680E+07 | 4.638E+07 | |
| 89-347 BOT | 1.550E+07 | 4.279E+07 | |
| AVERAGES | 1.637E+07 | 4.519E+07 | 2.948E-12 |
| <u>U-238 (n,f) Cs-137</u> | | | |
| 89-331 MID | 6.270E+05 | 6.889E+06 | 4.540E-14 |
| <u>Np-237 (n,f) Cs-137</u> | | | |
| 89-332 MID | 3.910E+06 | 4.296E+07 | 2.697E-13 |

TABLE 6-10

MEASURED SENSOR ACTIVITIES AND REACTION RATES
SURVEILLANCE CAPSULE V
SATURATED ACTIVITIES AND DERIVED FAST NEUTRON FLUX

| <u>MONITOR AND AXIAL LOCATION</u> | <u>MEASURED ACTIVITY (dis/sec-gm)</u> | <u>SATURATED ACTIVITY (dis/sec-gm)</u> | <u>REACTION RATE (rps/nucleus)</u> |
|--|---|--|--|
| <u>Cu-63 (n,α) Co-60</u> | | | |
| 93-4158 TOP | 1.470E+05 | 3.169E+05 | |
| 93-4163 MID | 1.610E+05 | 3.470E+05 | |
| 93-4169 BOT | 1.450E+05 | 3.126E+05 | |
| AVERAGES | 1.510E+05 | 3.255E+05 | 4.965E-17 |
| <u>Fe-54 (n,p) Mn-54</u> | | | |
| 93-4160 TOP | 1.280E+06 | 2.938E+06 | |
| 93-4165 MID | 1.280E+06 | 2.938E+06 | |
| 93-4171 BOT | 1.200E+06 | 2.755E+06 | |
| AVERAGES | 1.253E+06 | 2.877E+06 | 4.600E-15 |
| <u>Ni-58 (n,p) Co-58</u> | | | |
| 93-4159 TOP | 4.730E+06 | 4.487E+07 | |
| 93-4164 MID | 4.810E+06 | 4.563E+07 | |
| 93-4170 BOT | 4.740E+06 | 4.497E+07 | |
| AVERAGES | 4.760E+06 | 4.516E+07 | 6.448E-15 |
| <u>Co-59 (n,γ) Co-60</u> | | | |
| 93-4155 TOP | 2.740E+07 | 5.906E+07 | |
| 93-4161 MID | 2.940E+07 | 6.337E+07 | |
| 93-4166 BOT | 2.600E+07 | 5.604E+07 | |
| 93-4156 TOP | 3.220E+07 | 6.941E+07 | |
| 93-4162 MID | 2.430E+07 | 5.238E+07 | |
| 93-4167 BOT | 2.970E+07 | 6.402E+07 | |
| AVERAGES | 6.071E+07 | 6.071E+07 | 3.961E-12 |
| <u>Co-59 (n,γ) Co-60</u> | | | |
| 93-4157 TOP | 1.690E+07 | 3.643E+07 | |
| 93-4162 MID | 1.620E+07 | 3.492E+07 | |
| 93-4168 BOT | 1.630E+07 | 3.514E+07 | |
| AVERAGES | 1.647E+07 | 3.549E+07 | 2.316E-12 |
| <u>U-238 (n,f) Cs-137</u> | | | |
| 93-4153 MID | 8.380E+05 | 5.785E+06 | 3.812E-14 |
| <u>Np-237 (n,f) Cs-137</u> | | | |
| 93-4154 MID | 3.110E+06 | 2.147E+07 | 1.348E-13 |

TABLE 6-11

MEASURED SENSOR ACTIVITIES AND REACTION RATES
SURVEILLANCE CAPSULE Z
SATURATED ACTIVITIES AND DERIVED FAST NEUTRON FLUX

| <u>MONITOR AND AXIAL LOCATION</u> | <u>MEASURED ACTIVITY (dis/sec-gm)</u> | <u>SATURATED ACTIVITY (dis/sec-gm)</u> | <u>REACTION RATE (rps/nucleus)</u> |
|--|---|--|--|
| <u>Cu-63 (n,α) Co-60</u> | | | |
| 93-4176 TOP | 1.530E+05 | 3.311E+05 | |
| 93-4183 MID | 1.610E+05 | 3.484E+05 | |
| 93-4189 BOT | 1.570E+05 | 3.398E+05 | |
| AVERAGES | 1.570E+05 | 3.398E+05 | 5.184E-17 |
| <u>Fe-54 (n,p) Mn-54</u> | | | |
| 93-4178 TOP | 1.290E+06 | 2.994E+06 | |
| 93-4185 MID | 1.350E+06 | 3.133E+06 | |
| 93-4191 BOT | 1.310E+06 | 3.041E+06 | |
| AVERAGES | 1.317E+06 | 3.056E+06 | 4.886E-15 |
| <u>Ni-58 (n,p) Co-58</u> | | | |
| 93-4177 TOP | 5.090E+06 | 4.896E+07 | |
| 93-4184 MID | 5.220E+06 | 5.021E+07 | |
| 93-4190 BOT | 5.110E+06 | 4.915E+07 | |
| AVERAGES | 5.140E+06 | 4.944E+07 | 7.059E-15 |
| <u>Co-59 (n,γ) Co-60</u> | | | |
| 93-4179 TOP | 2.800E+07 | 6.060E+07 | |
| 93-4180 MID | 3.010E+07 | 6.514E+07 | |
| 93-4186 BOT | 3.030E+07 | 6.558E+07 | |
| 93-4174 TOP | 3.430E+07 | 7.423E+07 | |
| 93-4181 MID | 3.350E+07 | 7.250E+07 | |
| 93-4187 BOT | 3.540E+07 | 7.661E+07 | |
| AVERAGES | 6.911E+07 | 6.911E+07 | 4.509E-12 |
| <u>Co-59 (n,γ) Co-60</u> | | | |
| 93-4175 TOP | 1.820E+07 | 3.939E+07 | |
| 93-4182 MID | 1.780E+07 | 3.852E+07 | |
| 93-4188 BOT | 1.890E+07 | 4.090E+07 | |
| AVERAGES | 1.830E+07 | 3.961E+07 | 2.584E-12 |
| <u>U-238 (n,f) Cs-137</u> | | | |
| 93-4172 MID | 9.570E+05 | 6.611E+06 | 4.357E-14 |
| <u>Np-237 (n,f) Cs-137</u> | | | |
| 93-4173 MID | 6.80E+06 | 4.546E+07 | 2.854E-13 |

TABLE 6-12

SUMMARY OF NEUTRON DOSIMETRY RESULTS
SURVEILLANCE CAPSULES U, X, V, AND Z

| Calculation of Measured Fluence for Capsule U | Flux | Time | Fluence | Uncertainty |
|--|-----------|-----------|-----------|-------------|
| Meas Fluence < 0.414 ev = (Meas Flux < 0.414) * (EFPS) | 1.146E+11 | 3.437E+07 | 3.939E+18 | 22 |
| Meas Fluence > 0.1 Mev = (Meas Flux > .1) * (EFPS) | 6.348E+11 | 3.437E+07 | 2.182E+19 | 18 |
| Meas Fluence > 1.0 Mev = (Meas Flux > 1) * (EFPS) | 1.371E+11 | 3.437E+07 | 4.712E+18 | 9 |
| dpa | 2.678E-10 | 3.437E+07 | 9.204E-03 | 13 |
| Calculation of Measured Fluence for Capsule X | Flux | Time | Fluence | Uncertainty |
| Meas Fluence < 0.414 ev = (Meas Flux < 0.414) * (EFPS) | 9.608E+10 | 1.358E+08 | 1.304E+19 | 22 |
| Meas Fluence > 0.1 Mev = (Meas Flux > .1) * (EFPS) | 4.308E+11 | 1.358E+08 | 5.848E+19 | 15 |
| Meas Fluence > 1.0 Mev = (Meas Flux > 1) * (EFPS) | 1.038E+11 | 1.358E+08 | 1.409E+19 | 8 |
| dpa | 1.908E-10 | 1.358E+08 | 2.590E-02 | 11 |
| Calculation of Measured Fluence for Capsule V | Flux | Time | Fluence | Uncertainty |
| Meas Fluence < 0.414 ev = (Meas Flux < 0.414) * (EFPS) | 6.830E+10 | 2.285E+08 | 1.561E+19 | 23 |
| Meas Fluence > 0.1 Mev = (Meas Flux > .1) * (EFPS) | 4.480E+11 | 2.285E+08 | 1.024E+20 | 21 |
| Meas Fluence > 1.0 Mev = (Meas Flux > 1) * (EFPS) | 9.565E+10 | 2.285E+08 | 2.186E+19 | 10 |
| dpa | 1.885E-10 | 2.285E+08 | 4.308E-02 | 16 |
| Calculation of Measured Fluence for Capsule Z | Flux | Time | Fluence | Uncertainty |
| Meas Fluence < 0.414 ev = (Meas Flux < 0.414) * (EFPS) | 7.958E+10 | 2.285E+08 | 1.819E+19 | 23 |
| Meas Fluence > 0.1 Mev = (Meas Flux > .1) * (EFPS) | 4.397E+11 | 2.285E+08 | 1.005E+20 | 15 |
| Meas Fluence > 1.0 Mev = (Meas Flux > 1) * (EFPS) | 1.000E+11 | 2.285E+08 | 2.285E+19 | 8 |
| dpa | 1.899E-10 | 2.285E+08 | 4.340E-02 | 11 |

TABLE 6-13

COMPARISON OF MEASURED AND FERRET CALCULATED
REACTION RATES AT THE SURVEILLANCE CAPSULE CENTER
SURVEILLANCE CAPSULES U, X, V, and Z

| <u>REACTION</u> | <u>MEASURED</u> | <u>ADJUSTED CALCULATION</u> | <u>C/M</u> |
|-------------------------------|-----------------|---------------------------------|------------|
| CAPSULE U WITHDRAWN EOC 1 | | | |
| Cu63 (n, α) Co60 | 6.02E-17 | 6.12E-17 | 1.02 |
| Fe54 (n,p) Mn54 | 6.44E-15 | 6.48E-15 | 1.01 |
| Ni58 (n,p) Co58 | 9.13E-15 | 9.07E-15 | 0.99 |
| Co59 (n, γ) Co60 | 6.39E-12 | 6.34E-12 | 0.99 |
| Co59 (n, γ) Co60 (Cd) | 3.60E-12 | 3.62E-12 | 1.00 |
| U238 (n,f) Cs137 (Cd) | 4.28E-14 | 4.05E-14 | 0.94 |
| Np237 (n,f) Cs137 (Cd) | 4.29E-13 | 4.46E-13 | 1.04 |
| CAPSULE X WITHDRAWN EOC 5 | | | |
| Cu63 (n, α) Co60 | 5.33E-17 | 5.40E-17 | 1.01 |
| Fe54 (n,p) Mn54 | 5.34E-15 | 5.41E-15 | 1.01 |
| Ni58 (n,p) Co58 | 7.52E-15 | 7.50E-15 | 1.00 |
| Co59 (n, γ) Co60 | 5.31E-12 | 5.26E-12 | 0.99 |
| Co59 (n, γ) Co60 (Cd) | 2.95E-12 | 2.96E-12 | 1.00 |
| U238 (n,f) Cs137 (Cd) | 3.80E-14 | 3.25E-14 | 0.86 |
| Np237 (n,f) Cs137 (Cd) | 2.70E-13 | 2.97E-13 | 1.10 |
| CAPSULE V WITHDRAWN EOC 8 | | | |
| Cu63 (n, α) Co60 | 4.96E-17 | 4.98E-17 | 1.00 |
| Fe54 (n,p) Mn54 | 4.60E-15 | 4.68E-15 | 1.02 |
| Ni58 (n,p) Co58 | 6.45E-15 | 6.46E-15 | 1.00 |
| Co59 (n, γ) Co60 | 3.96E-12 | 3.93E-12 | 0.99 |
| Co59 (n, γ) Co60 (Cd) | 2.32E-12 | 2.33E-12 | 1.01 |
| U238 (n,f) Cs137 (Cd) | 3.12E-14 | 2.86E-14 | 0.92 |
| CAPSULE Z WITHDRAWN EOC 8 | | | |
| Cu63 (n, α) Co60 | 5.18E-17 | 5.21E-17 | 1.00 |
| Fe54 (n,p) Mn54 | 4.89E-15 | 5.01E-15 | 1.03 |
| Ni58 (n,p) Co58 | 7.06E-15 | 7.02E-15 | 1.00 |
| Co59 (n, γ) Co60 | 4.51E-12 | 4.47E-12 | 0.99 |
| Co59 (n, γ) Co60 (Cd) | 2.58E-12 | 2.60E-12 | 1.00 |
| U238 (n,f) Cs137 (Cd) | 3.53E-14 | 3.07E-14 | 0.87 |
| Np237 (n,f) Cs137 (Cd) | 2.85E-13 | 3.03E-13 | 1.06 |

TABLE 6-14

ADJUSTED NEUTRON ENERGY SPECTRUM AT THE
CENTER OF SURVEILLANCE CAPSULE V

| <u>GROUP</u> | <u>ENERGY</u> <u>(MeV)</u> | <u>ADJUSTED FLUX</u> <u>(n/cm²-sec)</u> | <u>GROUP</u> | <u>ENERGY</u> <u>(MeV)</u> | <u>ADJUSTED FLUX</u> <u>(n/cm²-sec)</u> |
|--------------|-------------------------------|---|--------------|-------------------------------|---|
| 1 | 1.733E+01 | 7.385E+06 | 27 | 1.503E-02 | 1.533E+10 |
| 2 | 1.492E+01 | 1.634E+07 | 28 | 9.119E-03 | 1.876E+10 |
| 3 | 1.350E+01 | 6.144E+07 | 29 | 5.531E-03 | 2.196E+10 |
| 4 | 1.162E+01 | 1.370E+08 | 30 | 3.355E-03 | 6.909E+09 |
| 5 | 1.000E+01 | 2.980E+08 | 31 | 2.839E-03 | 6.653E+09 |
| 6 | 8.607E+00 | 5.023E+08 | 32 | 2.404E-03 | 6.499E+09 |
| 7 | 7.408E+00 | 1.144E+09 | 33 | 2.035E-03 | 1.916E+10 |
| 8 | 6.065E+00 | 1.633E+09 | 34 | 1.234E-03 | 1.840E+10 |
| 9 | 4.966E+00 | 3.430E+09 | 35 | 7.485E-04 | 1.628E+10 |
| 10 | 3.679E+00 | 4.629E+09 | 36 | 4.540E-04 | 1.400E+10 |
| 11 | 2.865E+00 | 9.975E+09 | 37 | 2.754E-04 | 1.628E+10 |
| 12 | 2.231E+00 | 1.427E+10 | 38 | 1.670E-04 | 1.731E+10 |
| 13 | 1.738E+00 | 2.058E+10 | 39 | 1.013E-04 | 1.771E+10 |
| 14 | 1.353E+00 | 2.358E+10 | 40 | 6.144E-05 | 1.776E+10 |
| 15 | 1.108E+00 | 4.505E+10 | 41 | 3.727E-05 | 1.745E+10 |
| 16 | 8.208E-01 | 5.104E+10 | 42 | 2.260E-05 | 1.692E+10 |
| 17 | 6.393E-01 | 5.556E+10 | 43 | 1.371E-05 | 1.629E+10 |
| 18 | 4.979E-01 | 3.837E+10 | 44 | 8.315E-06 | 1.546E+10 |
| 19 | 3.877E-01 | 5.484E+10 | 45 | 5.043E-06 | 1.442E+10 |
| 20 | 3.020E-01 | 5.929E+10 | 46 | 3.059E-06 | 1.337E+10 |
| 21 | 1.832E-01 | 5.487E+10 | 47 | 1.855E-06 | 1.201E+10 |
| 22 | 1.111E-01 | 4.125E+10 | 48 | 1.125E-06 | 9.178E+09 |
| 23 | 6.738E-02 | 3.196E+10 | 49 | 6.826E-07 | 1.104E+10 |
| 24 | 4.087E-02 | 1.566E+10 | 50 | 4.140E-07 | 1.331E+10 |
| 25 | 2.554E-02 | 2.160E+10 | 51 | 2.511E-07 | 1.264E+10 |
| 26 | 1.989E-02 | 1.036E+10 | 52 | 1.523E-07 | 1.149E+10 |
| | | | 53 | 9.237E-08 | 3.085E+10 |

Note: Tabulated energy levels represent the upper energy in each group.

TABLE 6-15

ADJUSTED NEUTRON ENERGY SPECTRUM AT THE
CENTER OF SURVEILLANCE CAPSULE Z

| <u>GROUP</u> | <u>ENERGY</u> (MeV) | <u>ADJUSTED FLUX</u> (n/cm ² -sec) | <u>GROUP</u> | <u>ENERGY</u> (MeV) | <u>ADJUSTED FLUX</u> (n/cm ² -sec) |
|--------------|------------------------|--|--------------|------------------------|--|
| 1 | 1.733E+01 | 7.283E+06 | 27 | 1.503E-02 | 1.582E+10 |
| 2 | 1.492E+01 | 1.626E+07 | 28 | 9.119E-03 | 1.965E+10 |
| 3 | 1.350E+01 | 6.198E+07 | 29 | 5.531E-03 | 2.318E+10 |
| 4 | 1.162E+01 | 1.405E+08 | 30 | 3.355E-03 | 7.367E+09 |
| 5 | 1.000E+01 | 3.091E+08 | 31 | 2.839E-03 | 7.146E+09 |
| 6 | 8.607E+00 | 5.288E+08 | 32 | 2.404E-03 | 7.020E+09 |
| 7 | 7.408E+00 | 1.216E+09 | 33 | 2.035E-03 | 2.071E+10 |
| 8 | 6.065E+00 | 1.748E+09 | 34 | 1.234E-03 | 1.991E+10 |
| 9 | 4.966E+00 | 3.727E+09 | 35 | 7.485E-04 | 1.773E+10 |
| 10 | 3.679E+00 | 5.068E+09 | 36 | 4.540E-04 | 1.536E+10 |
| 11 | 2.865E+00 | 1.083E+10 | 37 | 2.754E-04 | 1.769E+10 |
| 12 | 2.231E+00 | 1.531E+10 | 38 | 1.670E-04 | 1.939E+10 |
| 13 | 1.738E+00 | 2.168E+10 | 39 | 1.013E-04 | 1.946E+10 |
| 14 | 1.353E+00 | 2.405E+10 | 40 | 6.144E-05 | 1.930E+10 |
| 15 | 1.108E+00 | 4.488E+10 | 41 | 3.727E-05 | 1.899E+10 |
| 16 | 8.208E-01 | 4.994E+10 | 42 | 2.260E-05 | 1.844E+10 |
| 17 | 6.393E-01 | 5.368E+10 | 43 | 1.371E-05 | 1.778E+10 |
| 18 | 4.979E-01 | 3.675E+10 | 44 | 8.315E-06 | 1.691E+10 |
| 19 | 3.877E-01 | 5.229E+10 | 45 | 5.043E-06 | 1.577E+10 |
| 20 | 3.020E-01 | 5.648E+10 | 46 | 3.059E-06 | 1.467E+10 |
| 21 | 1.832E-01 | 5.259E+10 | 47 | 1.855E-06 | 1.324E+10 |
| 22 | 1.111E-01 | 3.996E+10 | 48 | 1.125E-06 | 1.013E+10 |
| 23 | 6.738E-02 | 3.135E+10 | 49 | 6.826E-07 | 1.231E+10 |
| 24 | 4.087E-02 | 1.565E+10 | 50 | 4.140E-07 | 1.501E+10 |
| 25 | 2.554E-02 | 2.186E+10 | 51 | 2.511E-07 | 1.444E+10 |
| 26 | 1.989E-02 | 1.053E+10 | 52 | 1.523E-07 | 1.327E+10 |
| | | | 53 | 9.237E-08 | 3.687E+10 |

Note: Tabulated energy levels represent the upper energy in each group.

TABLE 6-16

COMPARISON OF CALCULATED AND MEASURED NEUTRON EXPOSURE LEVELS FOR McGUIRE UNIT 1 SURVEILLANCE CAPSULES U, X, V, AND Z

Comparison of Calculated and Measured INTEGRATED Neutron EXPOSURE Rate for Capsule U

| | Calculated | Measured | C / M | 1 / C/M |
|-----------------------------------|------------|------------|-------|---------|
| Fluence (E > 1.0 Mev) [n/cm2-sec] | 3.4012E+18 | 4.7119E+18 | 0.722 | 1.385 |
| Fluence (E > 0.1 Mev) [n/cm2-sec] | 1.5363E+19 | 2.1817E+19 | 0.704 | 1.420 |
| dpa | 6.8262E-03 | 9.2038E-03 | 0.742 | 1.348 |

Comparison of Calculated and Measured INTEGRATED Neutron EXPOSURE Rate for Capsule X

| | Calculated | Measured | C / M | 1 / C/M |
|-----------------------------------|------------|------------|-------|---------|
| Fluence (E > 1.0 Mev) [n/cm2-sec] | 1.2430E+19 | 1.4091E+19 | 0.882 | 1.134 |
| Fluence (E > 0.1 Mev) [n/cm2-sec] | 5.6146E+19 | 5.8483E+19 | 0.960 | 1.042 |
| dpa | 2.4947E-02 | 2.5902E-02 | 0.963 | 1.038 |

Comparison of Calculated and Measured INTEGRATED Neutron EXPOSURE Rate for Capsule V

| | Calculated | Measured | C / M | 1 / C/M |
|-----------------------------------|------------|------------|-------|---------|
| Fluence (E > 1.0 Mev) [n/cm2-sec] | 1.7461E+19 | 2.1858E+19 | 0.799 | 1.252 |
| Fluence (E > 0.1 Mev) [n/cm2-sec] | 7.7440E+19 | 1.0238E+20 | 0.756 | 1.322 |
| dpa | 3.4712E-02 | 4.3076E-02 | 0.806 | 1.241 |

Comparison of Calculated and Measured INTEGRATED Neutron EXPOSURE Rate for Capsule Z

| | Calculated | Measured | C / M | 1 / C/M |
|-----------------------------------|------------|------------|-------|---------|
| Fluence (E > 1.0 Mev) [n/cm2-sec] | 1.9701E+19 | 2.2852E+19 | 0.862 | 1.160 |
| Fluence (E > 0.1 Mev) [n/cm2-sec] | 8.8989E+19 | 1.0048E+20 | 0.886 | 1.129 |
| dpa | 3.9540E-02 | 4.3396E-02 | 0.911 | 1.098 |

TABLE 6-17

NEUTRON EXPOSURE PROJECTIONS AT KEY LOCATIONS
ON THE PRESSURE VESSEL CLAD/BASE METAL INTERFACE

BEST ESTIMATE EXPOSURE (7.241 EFPY) AT THE PRESSURE VESSEL INNER RADIUS

| | 0 DEG | 15 DEG | 30 DEG | 45 DEG |
|---------|-----------|-----------|-----------|-----------|
| E > 1.0 | 3.015E+18 | 4.457E+18 | 3.301E+18 | 4.562E+18 |
| E > 0.1 | 6.257E+18 | 9.333E+18 | 8.464E+18 | 1.138E+19 |
| dpa | 4.483E-03 | 6.576E-03 | 5.151E-03 | 6.951E-03 |

BEST ESTIMATE EXTRAPOLATION FLUX AT THE PRESSURE VESSEL INNER RADIUS

| | 0 DEG | 15 DEG | 30 DEG | 45 DEG |
|---------|-----------|-----------|-----------|-----------|
| E > 1.0 | 1.319E+10 | 1.950E+10 | 1.445E+10 | 1.996E+10 |
| E > 0.1 | 2.738E+10 | 4.084E+10 | 3.704E+10 | 4.980E+10 |
| dpa | 1.962E-11 | 2.878E-11 | 2.254E-11 | 3.042E-11 |

ESTIMATE EXPOSURE (16.0 EFPY) AT THE PRESSURE VESSEL INNER RADIUS

| | 0 DEG | 15 DEG | 30 DEG | 45 DEG |
|---------|-----------|-----------|-----------|-----------|
| E > 1.0 | 6.662E+18 | 9.847E+18 | 7.295E+18 | 1.008E+19 |
| E > 0.1 | 1.382E+19 | 2.062E+19 | 1.870E+19 | 2.515E+19 |
| dpa | 9.906E-03 | 1.453E-02 | 1.138E-02 | 1.536E-02 |

ESTIMATE EXPOSURE (32.0 EFPY) AT THE PRESSURE VESSEL INNER RADIUS

| | 0 DEG | 15 DEG | 30 DEG | 45 DEG |
|---------|-----------|-----------|-----------|-----------|
| E > 1.0 | 1.332E+19 | 1.969E+19 | 1.459E+19 | 2.016E+19 |
| E > 0.1 | 2.765E+19 | 4.124E+19 | 3.740E+19 | 5.029E+19 |
| dpa | 1.981E-02 | 2.906E-02 | 2.276E-02 | 3.072E-02 |

TABLE 6-18

NEUTRON EXPOSURE VALUES

FLUENCE BASED ON E > 1.0 MeV SLOPE

| | 0 DEG | 15 DEG | 30 DEG | 45 DEG |
|-----------------|-----------|-----------|-----------|-----------|
| 16 EFPY FLUENCE | | | | |
| SURFACE | 6.662E+18 | 9.847E+18 | 7.295E+18 | 1.008E+19 |
| 1/4T | 3.617E+18 | 5.327E+18 | 3.983E+18 | 5.503E+18 |
| 3/4T | 7.727E+17 | 1.123E+18 | 8.608E+17 | 1.179E+18 |
| 32 EFPY FLUENCE | | | | |
| SURFACE | 1.332E+19 | 1.969E+19 | 1.459E+19 | 2.016E+19 |
| 1/4T | 7.234E+18 | 1.065E+19 | 7.966E+18 | 1.101E+19 |
| 3/4T | 1.545E+18 | 2.245E+18 | 1.722E+18 | 2.359E+18 |

FLUENCE BASED ON dpa SLOPE

| | 0 DEG | 15 DEG | 30 DEG | 45 DEG |
|-----------------|-----------|-----------|-----------|-----------|
| 16 EFPY FLUENCE | | | | |
| SURFACE | 6.662E+18 | 9.847E+18 | 7.295E+18 | 1.008E+19 |
| 1/4T | 4.203E+18 | 6.164E+18 | 4.741E+18 | 6.693E+18 |
| 3/4T | 1.459E+18 | 2.137E+18 | 1.743E+18 | 2.510E+18 |
| 32 EFPY FLUENCE | | | | |
| SURFACE | 1.332E+19 | 1.969E+19 | 1.459E+19 | 2.016E+19 |
| 1/4T | 8.407E+18 | 1.233E+19 | 9.483E+18 | 1.339E+19 |
| 3/4T | 2.918E+18 | 4.274E+18 | 3.487E+18 | 5.019E+18 |

TABLE 6-19

UPDATED LEAD FACTORS FOR BYRON UNIT 1
SURVEILLANCE CAPSULES

| <u>CAPSULE</u> | <u>LEAD FACTOR</u> |
|----------------|--------------------|
| U | 5.25 |
| V | 4.72* |
| X | 5.31 |
| W | 5.32 |
| Y | 4.72 |
| Z | 5.32* |

* WITHDRAWN EOC 8, BASIS FOR THIS ANALYSIS

SECTION 7.0
SURVEILLANCE CAPSULE REMOVAL SCHEDULE

The following surveillance capsule removal schedule meets the requirements of ASTM E185-82 and is recommended for future capsules to be removed from the McGuire Unit 1 reactor vessel:

| <u>TABLE 7-1</u> | | | | |
|--|----------|-------------|------------------------------------|---|
| McGuire Unit 1 Reactor Vessel Surveillance Capsule Withdrawal Schedule | | | | |
| Capsule | Location | Lead Factor | Removal Time (EFPY) ^(a) | Fluence (n/cm ²) ^(d) |
| U | 56° | 5.25 | 1.06 | 4.712×10^{18} ^(b) |
| X | 236° | 5.31 | 4.33 | 1.409×10^{19} ^(b) |
| V | 58.5° | 4.72 | 7.24 | 2.186×10^{19} ^(b) |
| Z | 304° | 5.32 | 7.24 ^(c) | 2.285×10^{19} ^(b) |
| Y | 238.5° | 4.72 | 10 | 2.97×10^{19} |
| W | 124° | 5.32 | Stand-By | - - |

- (a) Effective Full Power Years (EFPY) from plant startup.
- (b) Actual measured neutron fluence
- (c) Capsule Z was removed and disassembled. The specimens were placed in storage and the dosimeters analyzed.
- (d) E > 1.0 MeV

SECTION 8.0
REFERENCES

1. Davidson, J.A. and Yanichko, S.E., *Duke Power Company William B. McGuire Unit No. 1 Reactor Vessel Radiation Surveillance Program*, WCAP-9195, November 1977.
2. Section III of the ASME Boiler and Pressure Vessel Code, Appendix G, *Protection Against Nonductile Failure*.
3. ASTM E208, *Standard Test Method for Conducting Drop-Weight Test to Determine Nil-Ductility Transition Temperature of Ferritic Steels*, in ASTM Standards, Section 3, American Society for Testing and Materials, Philadelphia, PA.
4. Yanichko, S.E., Congedo, T.V., Kaiser W.T., *Analysis of Capsule U from the Duke Power Company McGuire Unit 1 Reactor Vessel Radiation Surveillance Program*, WCAP-10786, February 1985.
5. Yanichko, S.E., Anderson, S.L., Albertin, L., Ray, N.K., *Analysis of Capsule X from the Duke Power Company McGuire Unit 1 Reactor Vessel Radiation Surveillance Program*, WCAP-12354, August 1989.
6. Code of Federal Regulations, 10CFR50, Appendix G, *Fracture Toughness Requirements*, and Appendix H, *Reactor Vessel Material Surveillance Program Requirements*, U.S. Nuclear Regulatory Commission, Washington, D.C.
7. ASTM E185-82, *Standard Practice for Conducting Surveillance Tests for Light-Water Cooled Nuclear Power Reactor Vessels, E706 (IF)*, in ASTM Standards, Section 3, American Society for Testing and Materials, Philadelphia, PA, 1993.
8. ASTM E23-92, *Standard Test Methods for Notched Bar Impact Testing of Metallic Materials*, in ASTM Standards, Section 3, American Society for Testing and Materials, Philadelphia, PA, 1992.
9. ASTM A370-92, *Standard Test Methods and Definitions for Mechanical Testing of Steel Products*, in ASTM Standards, Section 3, American Society for Testing and Materials, Philadelphia, PA, 1992.

10. ASTM E8-91, *Standard Test Methods of Tension Testing of Metallic Materials*, in ASTM Standards, Section 3, American Society for Testing and Materials, Philadelphia, PA, 1992.
11. ASTM E21-79(1988), *Standard Practice for Elevated Temperature Tension Tests of Metallic Materials*, in ASTM Standards, Section 3, American Society for Testing and Materials, Philadelphia, PA, 1991.
12. ASTM E83-93, *Standard Practice for Verification and Classification of Extensometers*, in ASTM Standards, Section 3, American Society for Testing and Materials, Philadelphia, PA, 1993.
13. Regulatory Guide 1.99, Revision 2, *Radiation Embrittlement of Reactor Vessel Materials*, U.S. Nuclear Regulatory Commission, May, 1988.
14. R. G. Soltesz, R. K. Disney, J. Jedruch, and S. L. Ziegler, *Nuclear Rocket Shielding Methods, Modification, Updating and Input Data Preparation. Vol. 5--Two-Dimensional Discrete Ordinates Transport Technique*, WANL-PR(LL)-034, Vol. 5, August 1970.
15. *ORNL RSCI Data Library Collection DLC-76 SAILOR Coupled Self-Shielded, 47 Neutron, 20 Gamma-Ray, P3, Cross Section Library for Light Water Reactors.*
16. R. E. Maerker, et al, *Accounting for Changing Source Distributions in Light Water Reactor Surveillance Dosimetry Analysis*, Nuclear Science and Engineering, Volume 94, Pages 291-308, 1986.
17. A. Saeed, D. R. Gibson, M. A. Kotun, "The Nuclear Design and Core Physics Characteristics of the W. B. McGuire Unit 1 Nuclear Power Plant, Cycle 1," WCAP-9323-R1, August, 11, 1978.
18. J. R. Lesko, C. R. Savage, R.W. Miller, L. R. Rios, R. M. Turcovski, "The Nuclear Design of the W. B. McGuire Unit 1 Nuclear Power Plant, Cycle 2," WCAP-10463, January, 1984.
19. J. R. Lesko, R.W. Miller, L. R. Rios, Et. Al., "The Nuclear Design of the W. B. McGuire Unit 1 Nuclear Power Plant, Cycle 3," WCAP-10782, February, 1985.

20. J. R. Lesko, L. R. Rios, D. A. Johnson, Et. Al., "*The Nuclear Design of the W. B. McGuire Unit 1 Nuclear Power Plant, Cycle 4,*" WCAP-11141, May, 1986.
21. J. R. Lesko, P. D. Banning, M. A Kotun, Et. Al., "*The Nuclear Design of the W. B. McGuire Unit 1 Nuclear Power Plant, Cycle 5,*" WCAP-11589, October, 1987.
22. J. R. Lesko, R.W. Miller, M. A Kotun, "*The Nuclear Design of the W. B. McGuire Unit 1 Nuclear Power Plant, Cycle 6,*" WCAP-112044, November, 1988.
23. J. R. Lesko, M. A Kotun, "*The Nuclear Design of the W. B. McGuire Unit 1 Nuclear Power Plant, Cycle 7,*" WCAP-12544, April, 1990.
24. Tonya M. Hall, "McGuire 1 Cycle 8 Final Fuel Cycle Design, Revision 3," Design engineering, Duke Power Company, October, 1991.
25. ASTM Designation E482-89, *Standard Guide for Application of Neutron Transport Methods for Reactor Vessel Surveillance*, in ASTM Standards, Section 12, American Society for Testing and Materials, Philadelphia, PA, 1993.
26. ASTM Designation E560-84, *Standard Recommended Practice for Extrapolating Reactor Vessel Surveillance Dosimetry Results*, in ASTM Standards, Section 12, American Society for Testing and Materials, Philadelphia, PA, 1993.
27. ASTM Designation E693-79, *Standard Practice for Characterizing Neutron Exposures in Ferritic Steels in Terms of Displacements per Atom (dpa)*, in ASTM Standards, Section 12, American Society for Testing and Materials, Philadelphia, PA, 1993.
28. ASTM Designation E706-87, *Standard Master Matrix for Light-Water Reactor Pressure Vessel Surveillance Standard*, in ASTM Standards, Section 12, American Society for Testing and Materials, Philadelphia, PA, 1993.
29. ASTM Designation E853-87, *Standard Practice for Analysis and Interpretation of Light-Water Reactor Surveillance Results*, in ASTM Standards, Section 12, American Society for Testing and Materials, Philadelphia, PA, 1993.

30. ASTM Designation E261-90, *Standard Method for Determining Neutron Flux, Fluence, and Spectra by Radioactivation Techniques*, in ASTM Standards, Section 12, American Society for Testing and Materials, Philadelphia, PA, 1993.
31. ASTM Designation E262-86, *Standard Method for Measuring Thermal Neutron Flux by Radioactivation Techniques*, in ASTM Standards, Section 12, American Society for Testing and Materials, Philadelphia, PA, 1993.
32. ASTM Designation E263-88, *Standard Method for Determining Fast-Neutron Flux Density by Radioactivation of Iron*, in ASTM Standards, Section 12, American Society for Testing and Materials, Philadelphia, PA, 1993.
33. ASTM Designation E264-92, *Standard Method for Determining Fast-Neutron Flux Density by Radioactivation of Nickel*, in ASTM Standards, Section 12, American Society for Testing and Materials, Philadelphia, PA, 1993.
34. ASTM Designation E481-92, *Standard Method for Measuring Neutron-Flux Density by Radioactivation of Cobalt and Silver*, in ASTM Standards, Section 12, American Society for Testing and Materials, Philadelphia, PA, 1993.
35. ASTM Designation E523-87, *Standard Method for Determining Fast-Neutron Flux Density by Radioactivation of Copper*, in ASTM Standards, Section 12, American Society for Testing and Materials, Philadelphia, PA, 1993.
36. ASTM Designation E704-90, *Standard Method for Measuring Reaction Rates by Radioactivation of Uranium-238*, in ASTM Standards, Section 12, American Society for Testing and Materials, Philadelphia, PA, 1993.
37. ASTM Designation E705-90, *Standard Method for Measuring Fast-Neutron Flux Density by Radioactivation of Neptunium-237*, in ASTM Standards, Section 12, American Society for Testing and Materials, Philadelphia, PA, 1993.
38. ASTM Designation E1005-84, *Standard Method for Application and Analysis of Radiometric Monitors for Reactor Vessel Surveillance*, in ASTM Standards, Section 12, American Society for Testing and Materials, Philadelphia, PA, 1993.

39. F. A. Schmittroth, *FERRET Data Analysis Core*, HEDL-TME 79-40, Hanford Engineering Development Laboratory, Richland, WA, September 1979.
40. W. N. McElroy, S. Berg and T. Crocket, *A Computer-Automated Iterative Method of Neutron Flux Spectra Determined by Foil Activation*, AFWL-TR-7-41, Vol. I-IV, Air Force Weapons Laboratory, Kirkland AFB, NM, July 1967.
41. R. E. Maerker, et al., *Development and Demonstration of an Advanced Methodology for LWR Dosimetry Applications*, EPRI-NP-2188, 1981.

APPENDIX A

Load-Time Records for Charpy Specimen Tests

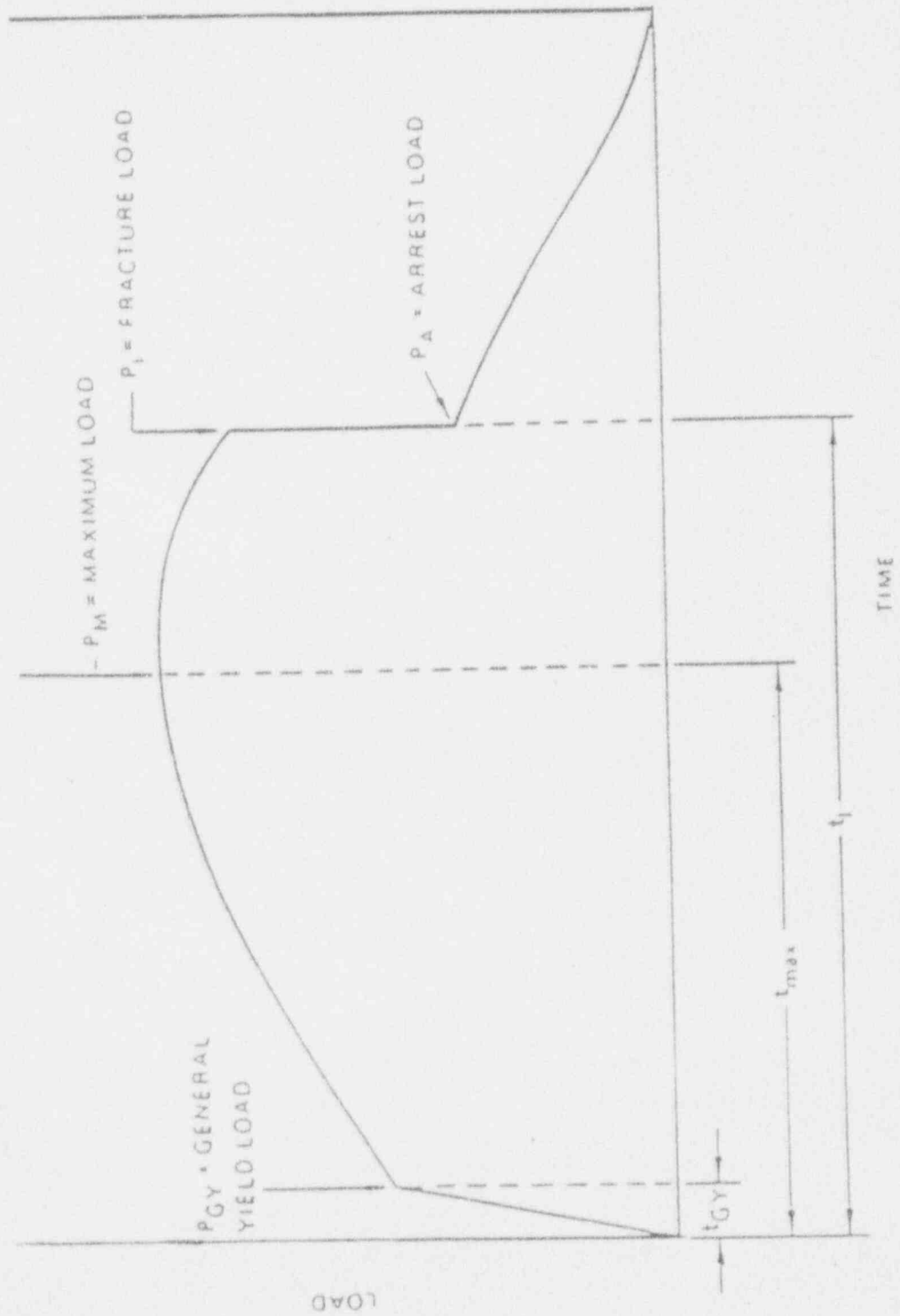


Figure A-1. Idealized load-time record

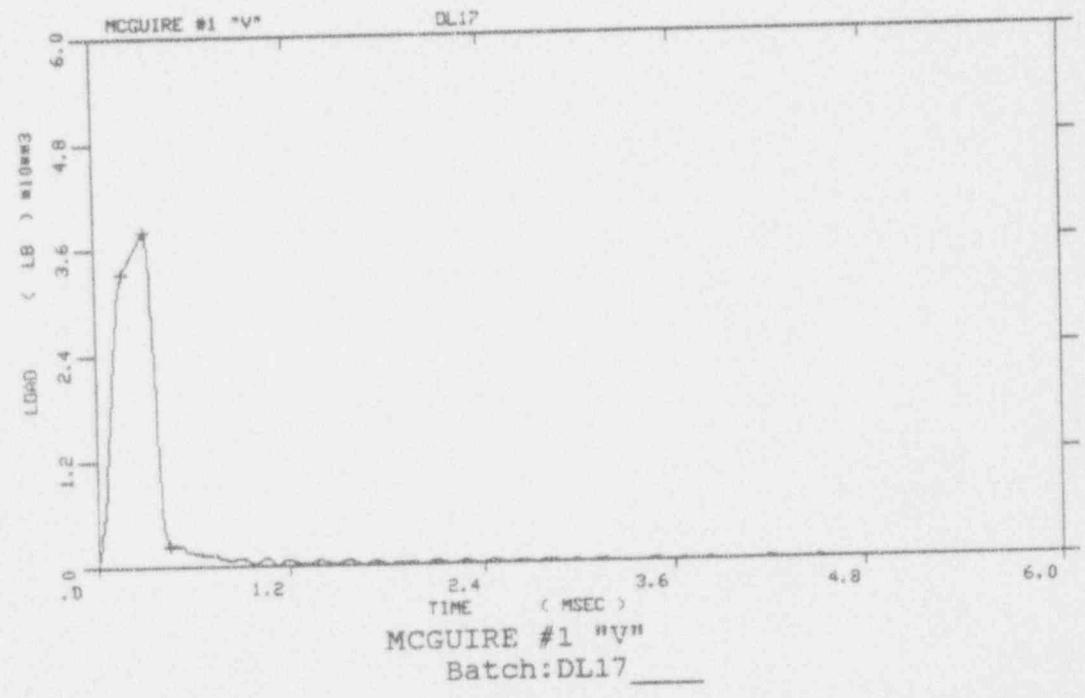
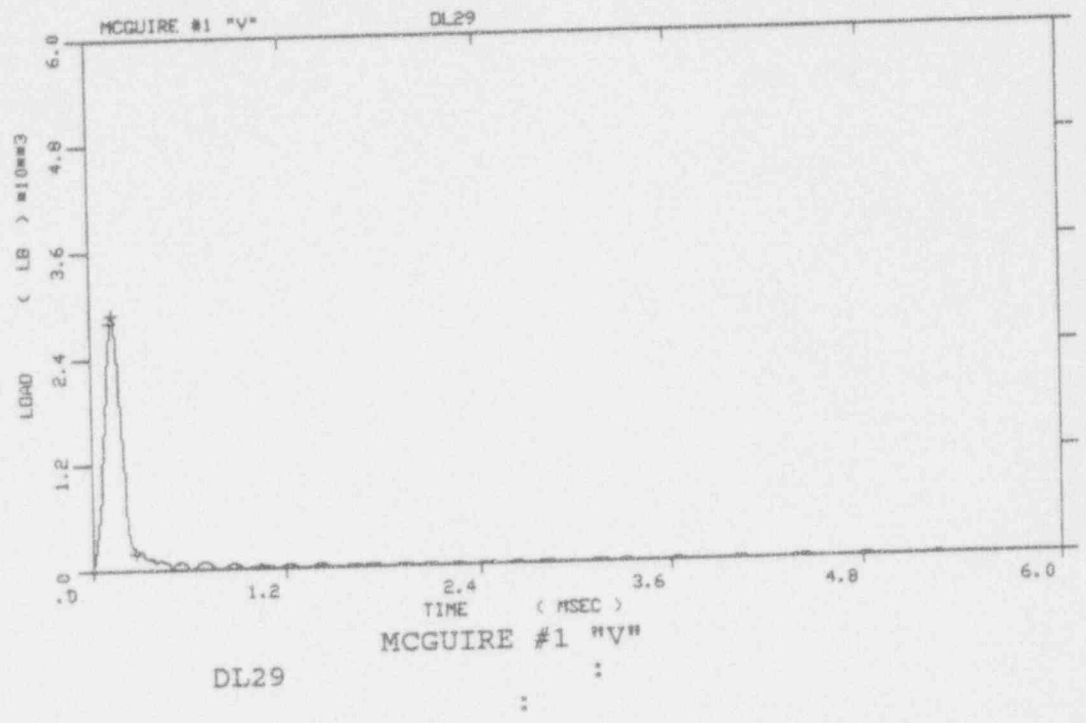
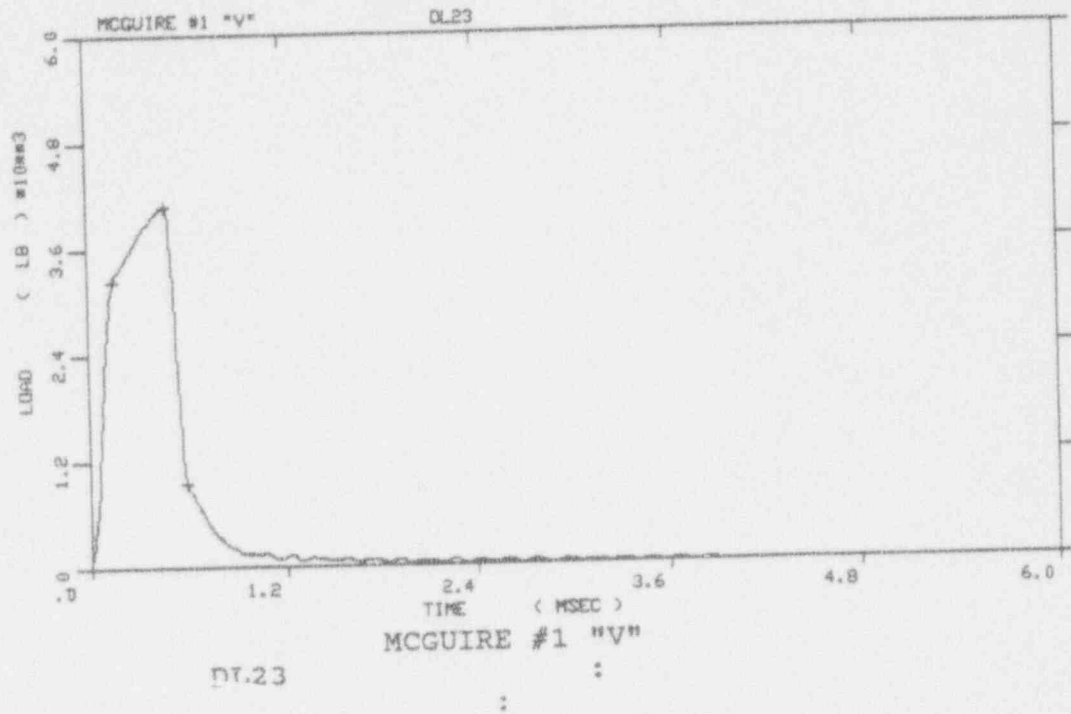


Figure A-2. Load-time records for Specimens DL29 and DL17



The load-time record
 for Specimen DL30 is not available
 because of computer system malfunction

Figure A-3. Load-time records for Specimens DL23 and DL30

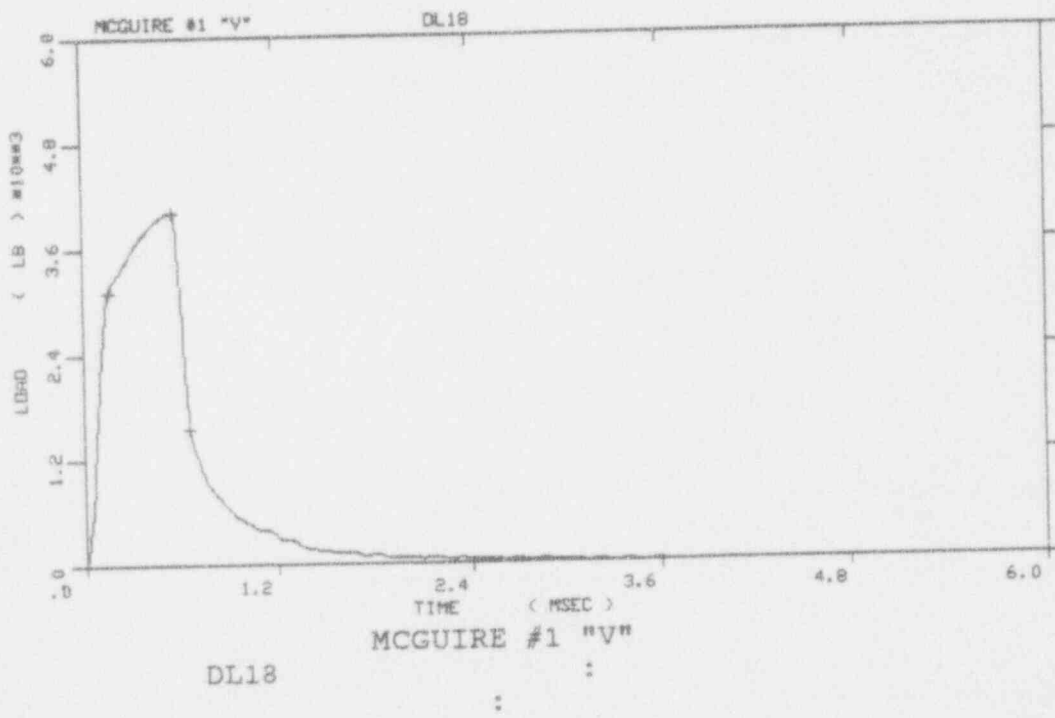
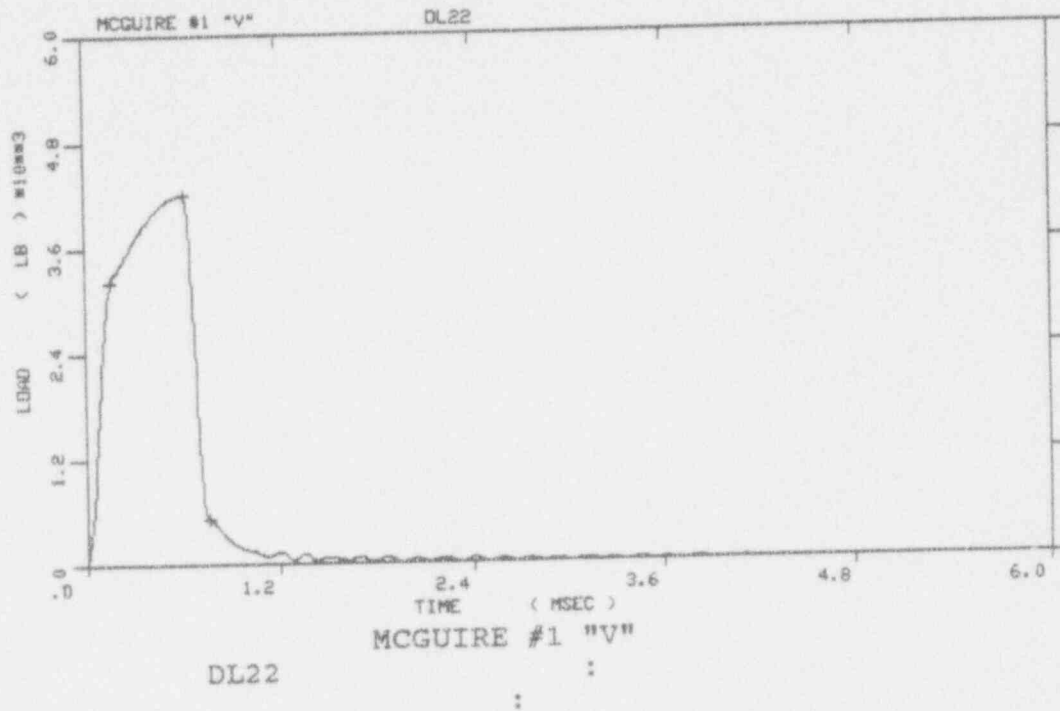


Figure A-4. Load-time records for Specimens DL22 and DL18

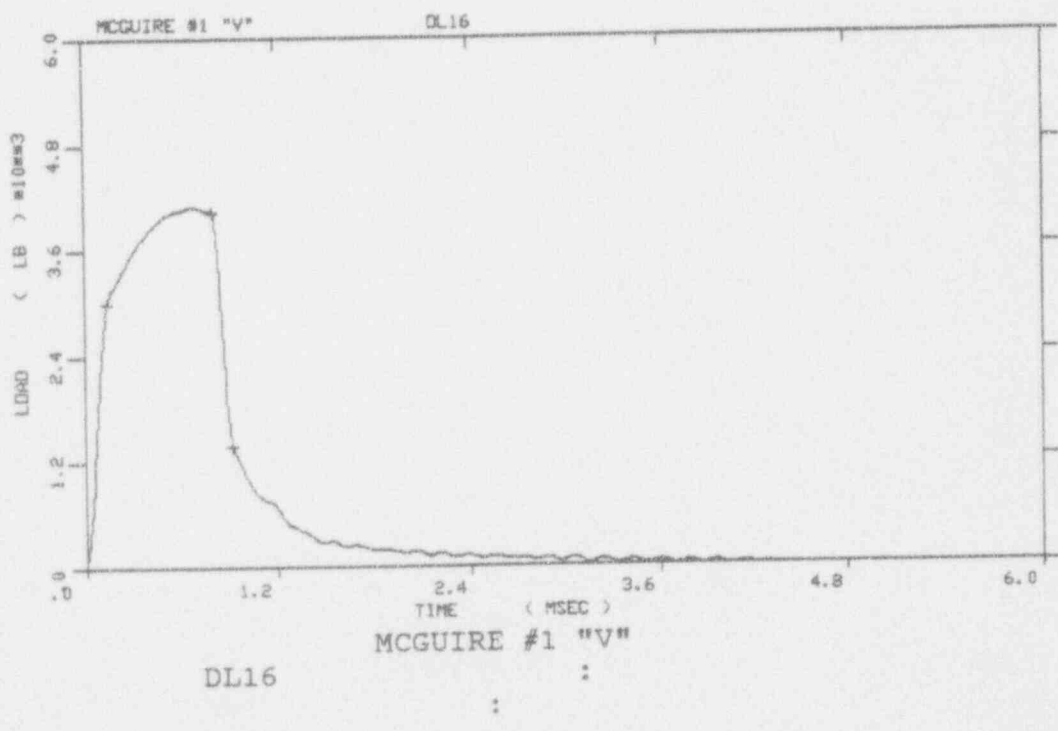
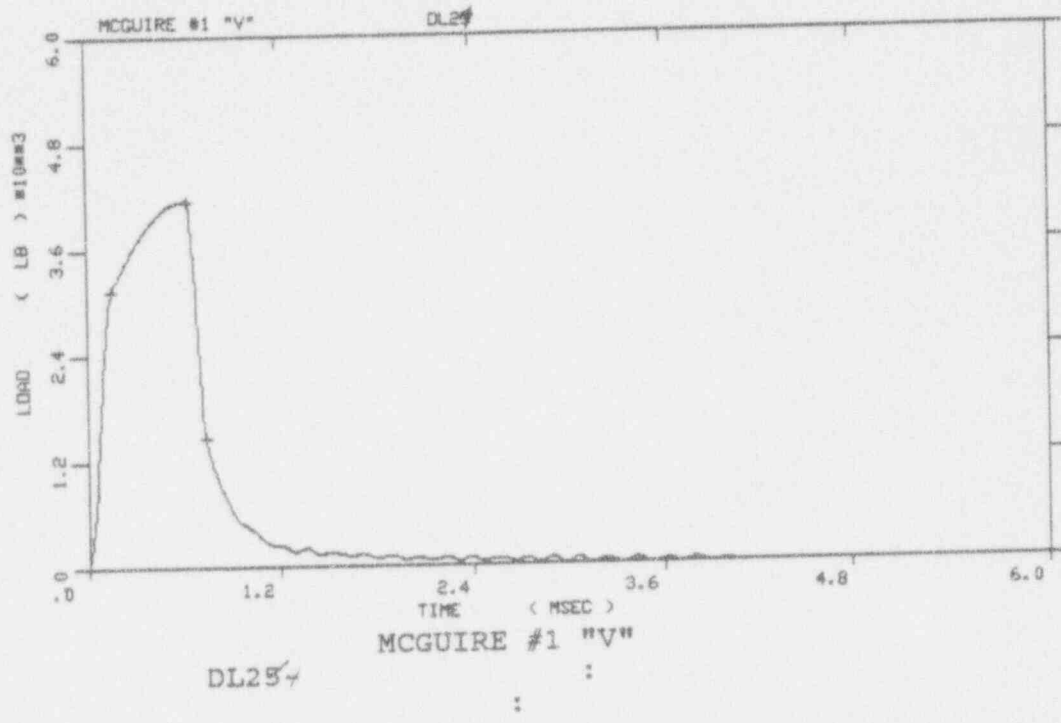


Figure A-5. Load-time records for Specimens DL24 and DL16

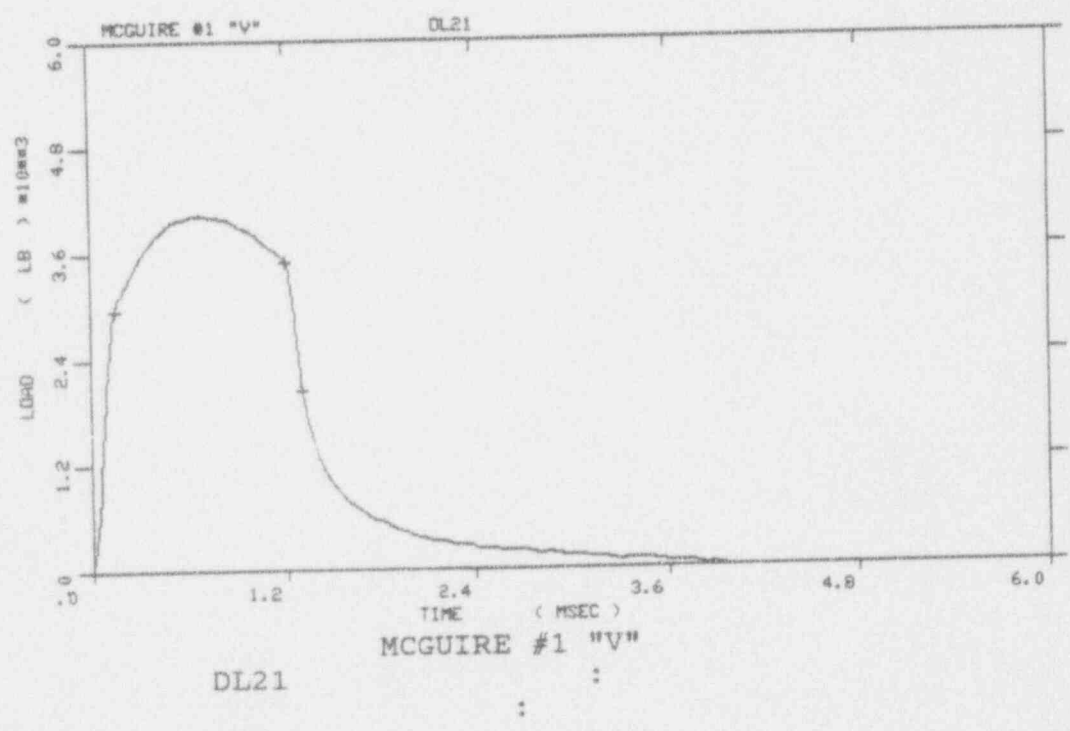
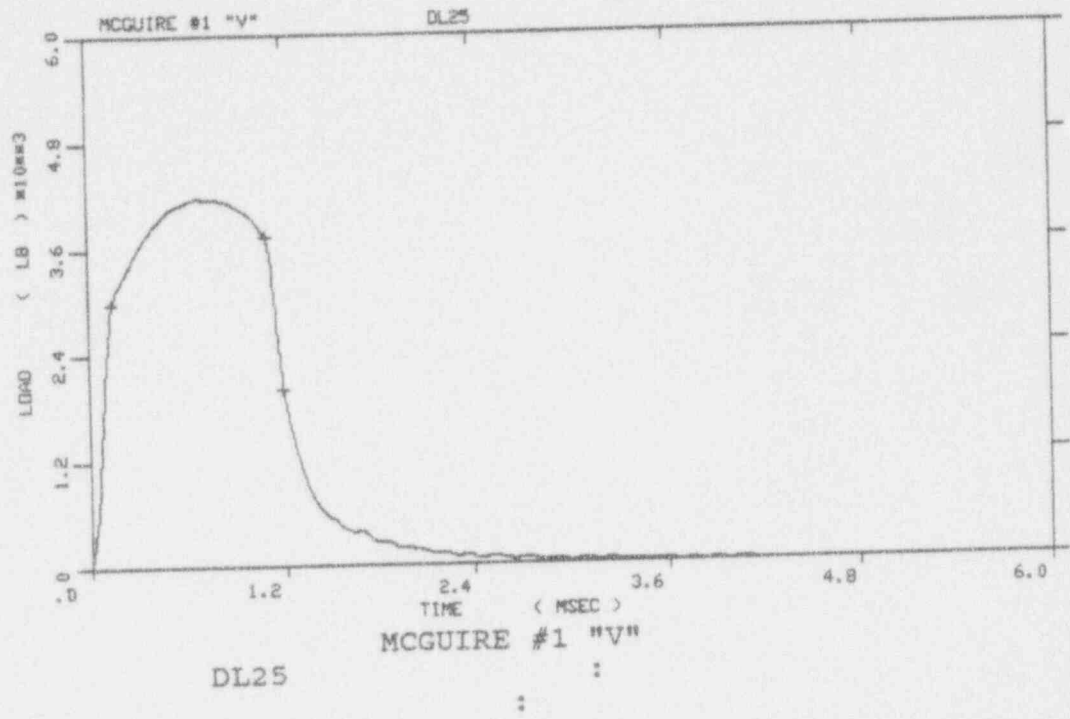
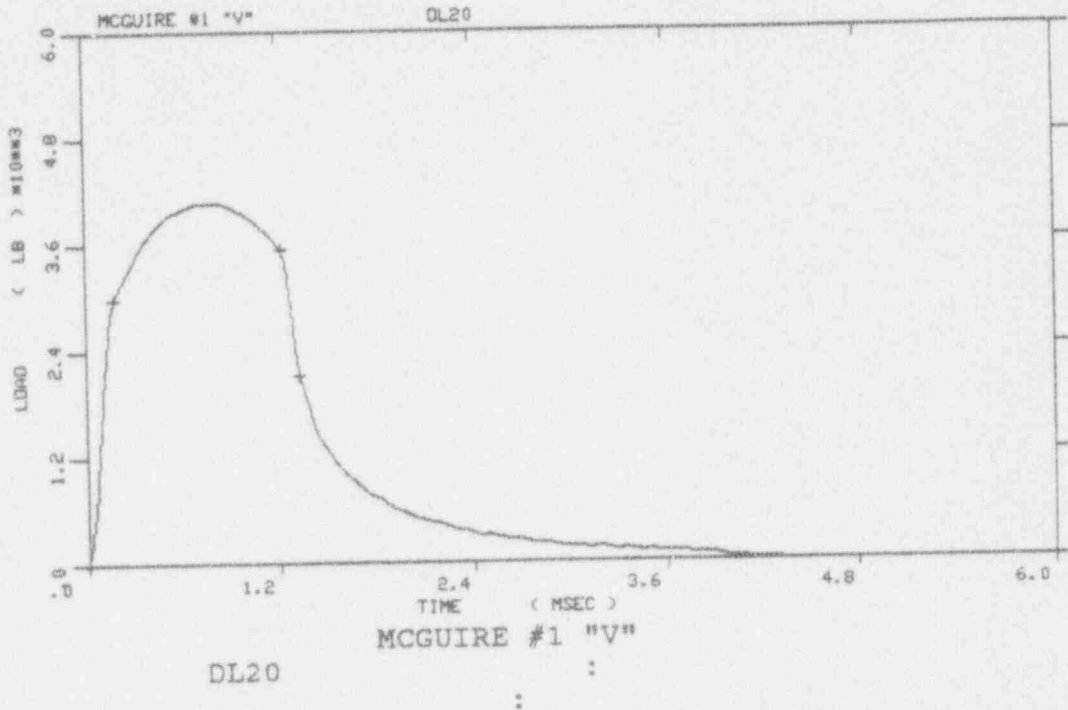


Figure A-6. Load-time records for Specimens DL25 and DL21



The load-time record
 for Specimen DL19 is not available
 because of computer system malfunction

Figure A-7. Load-time records for Specimens DL20 and DL19

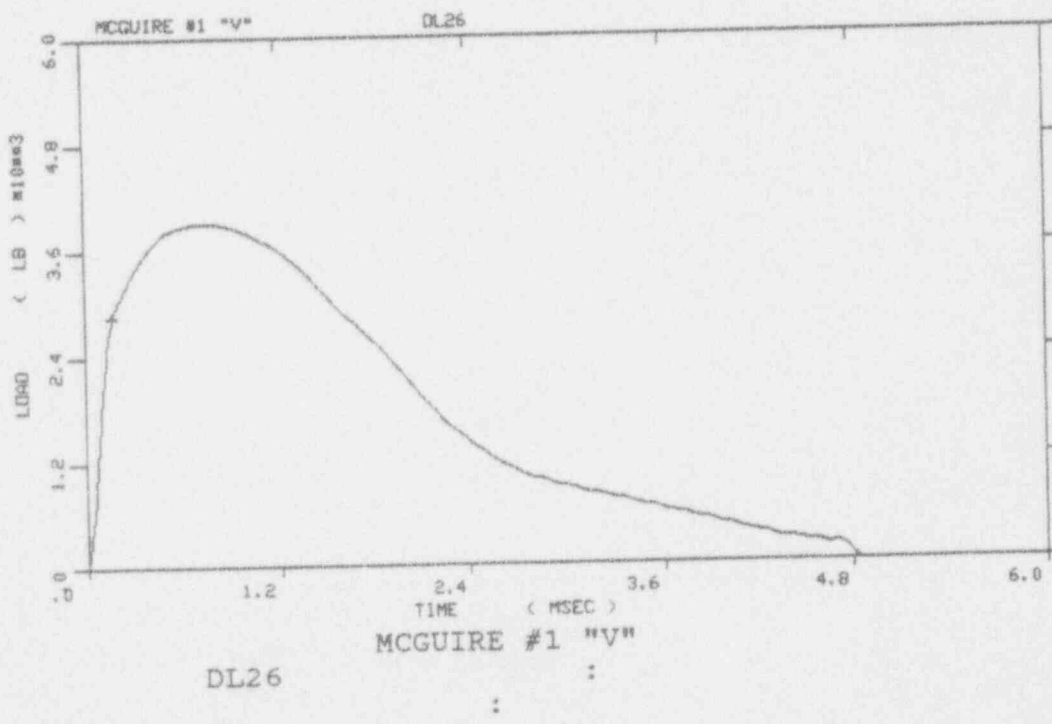
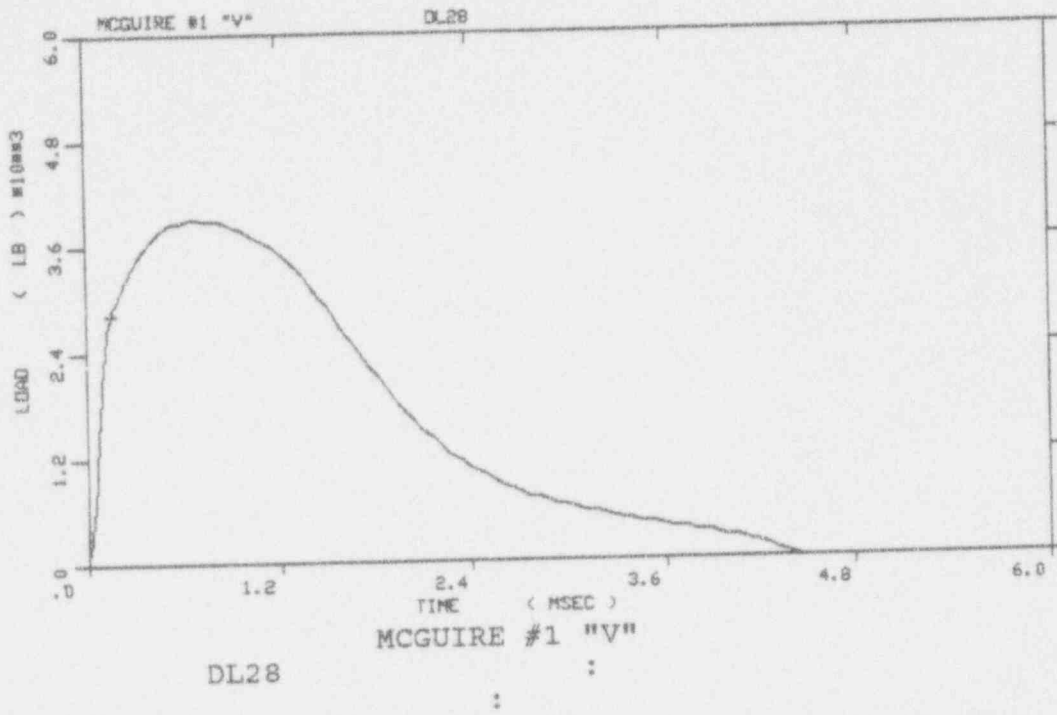


Figure A-8. Load-time records for Specimens DL28 and DL26

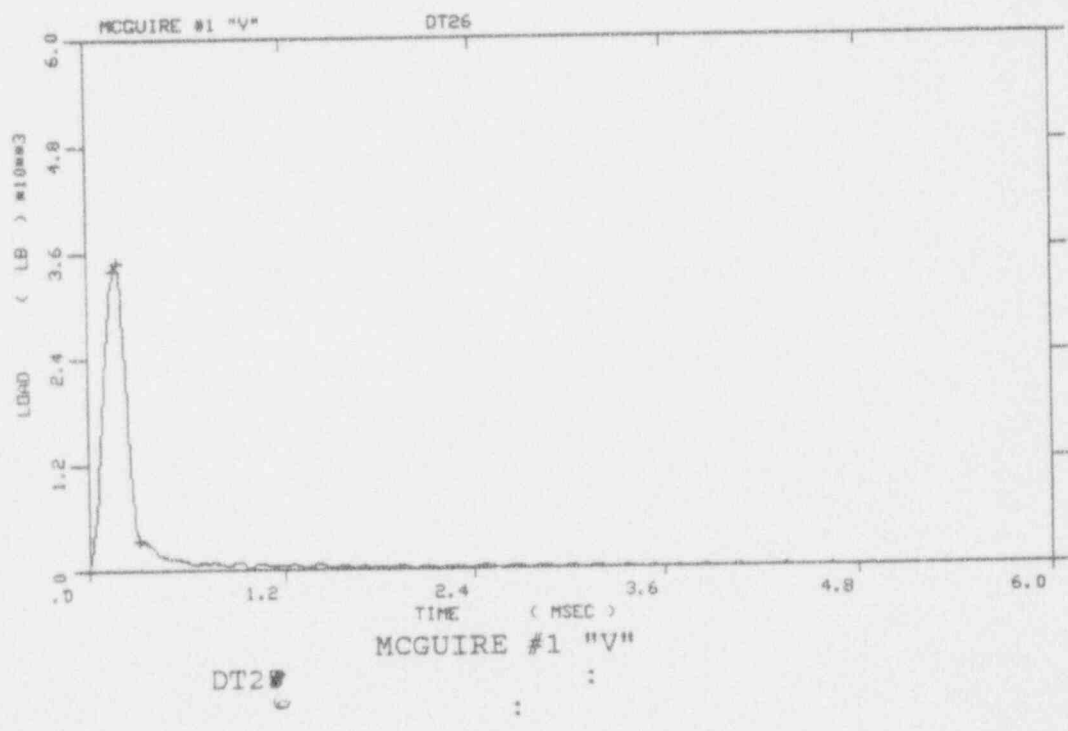
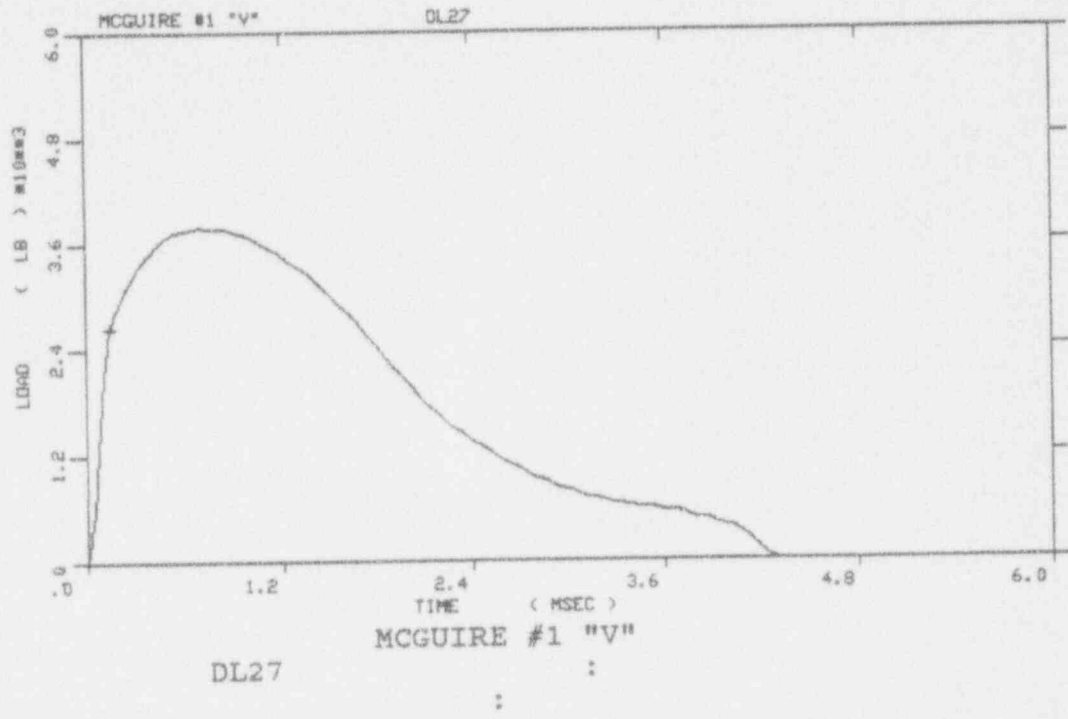


Figure A-9. Load-time records for Specimens DL27 and DT26

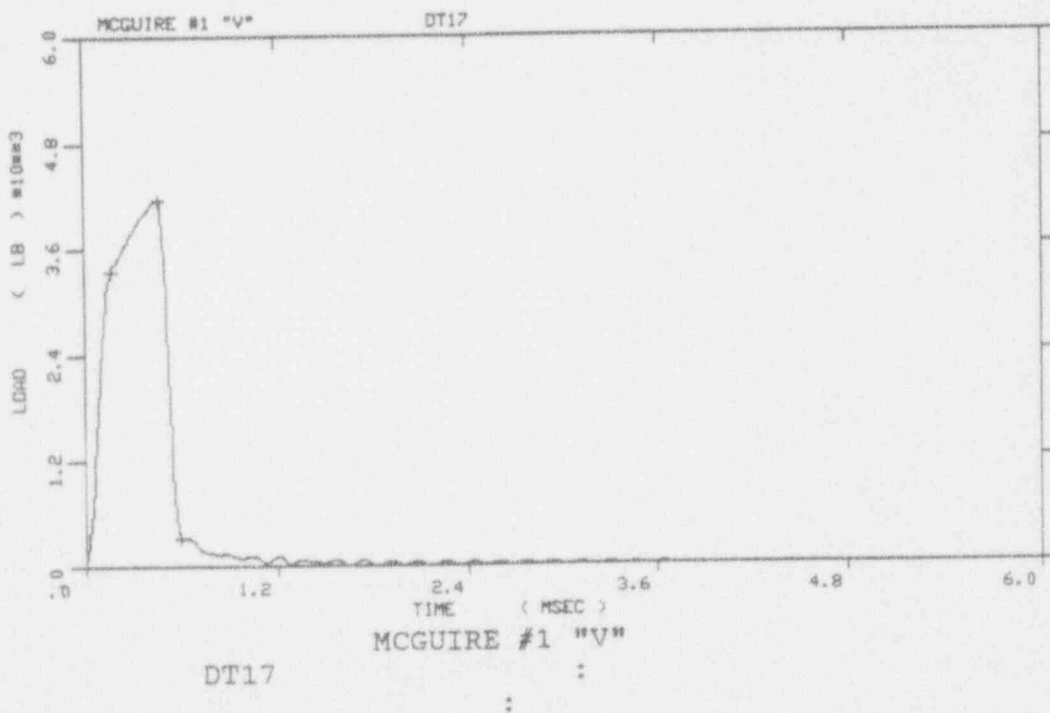
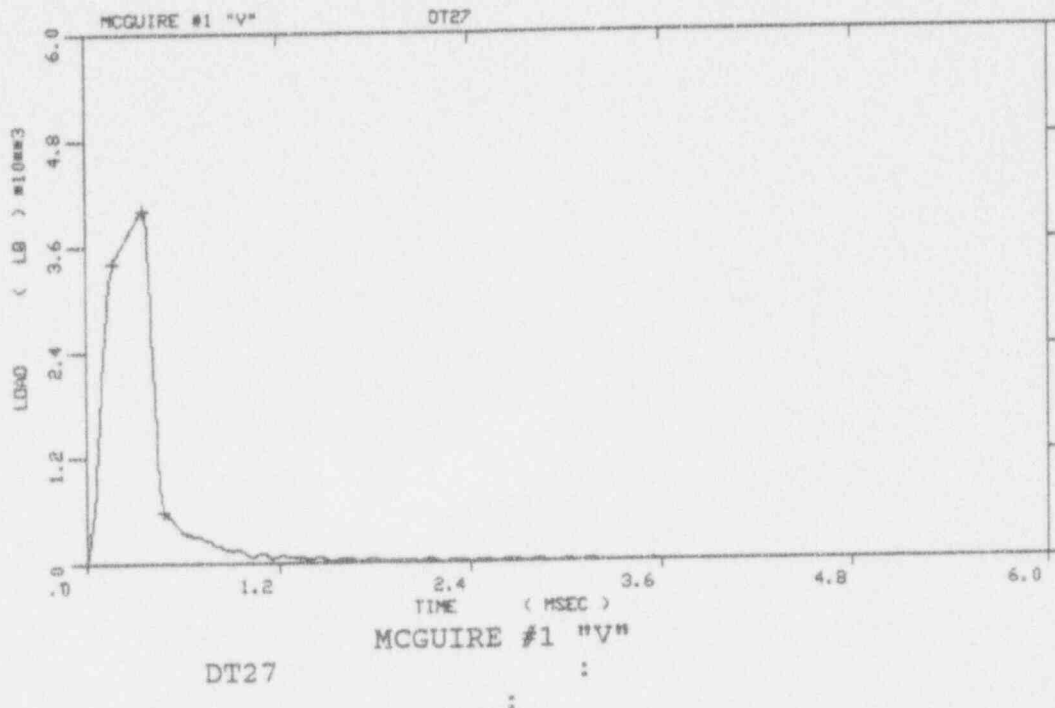


Figure A-10. Load-time records for Specimens DT27 and DT17

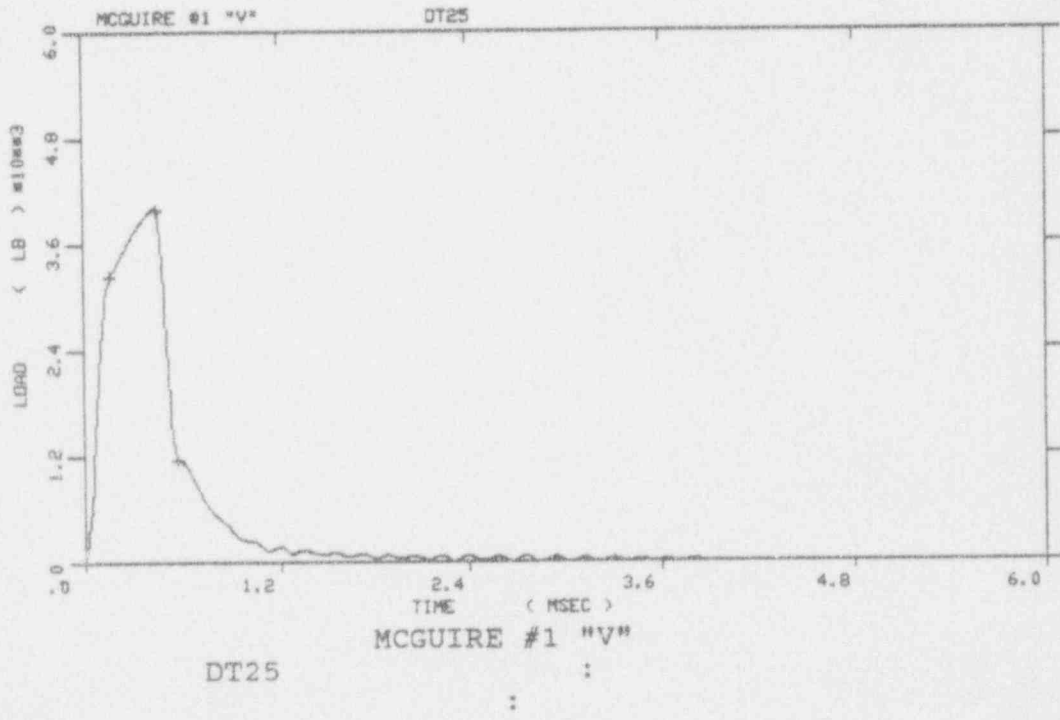
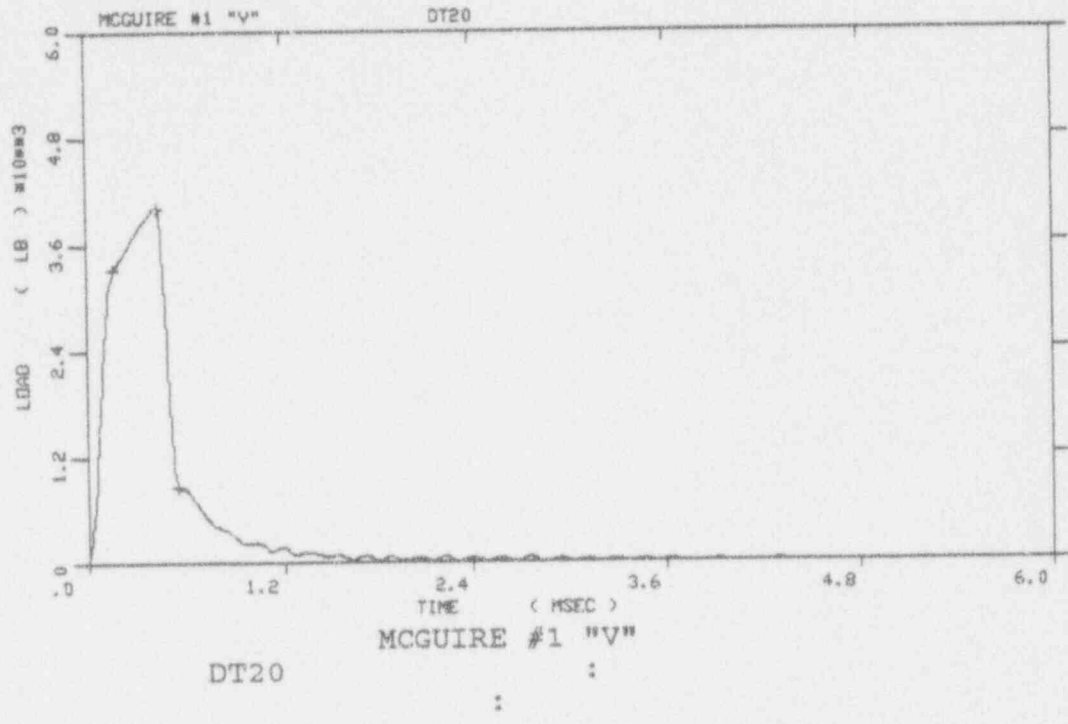


Figure A-11. Load-time records for Specimens DT20 and DT25

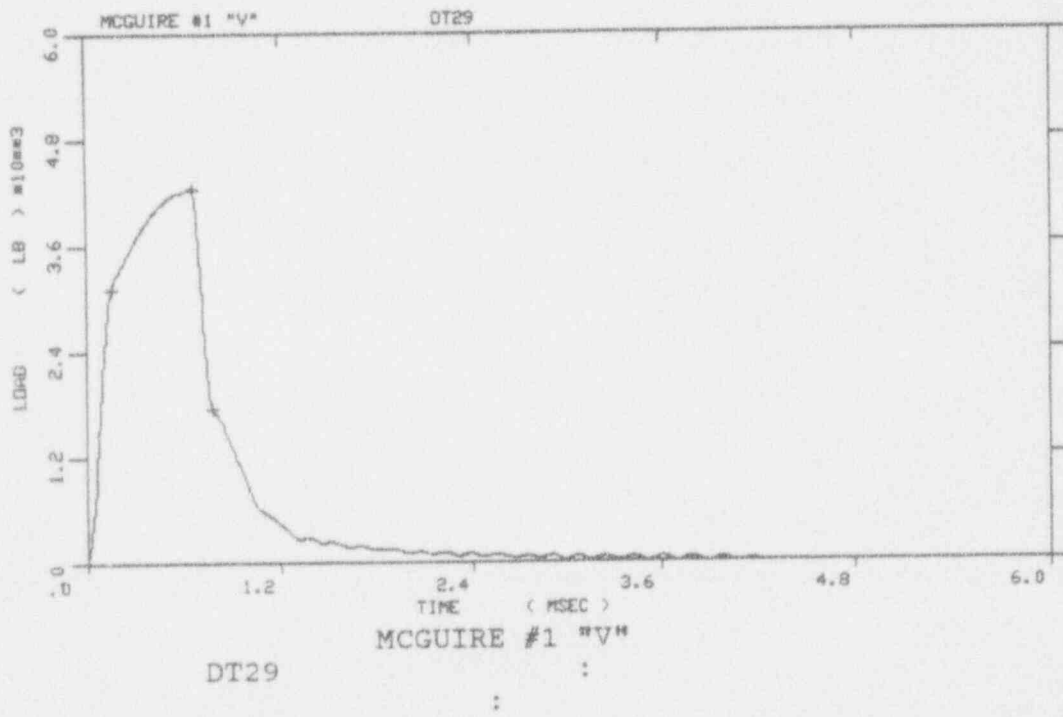
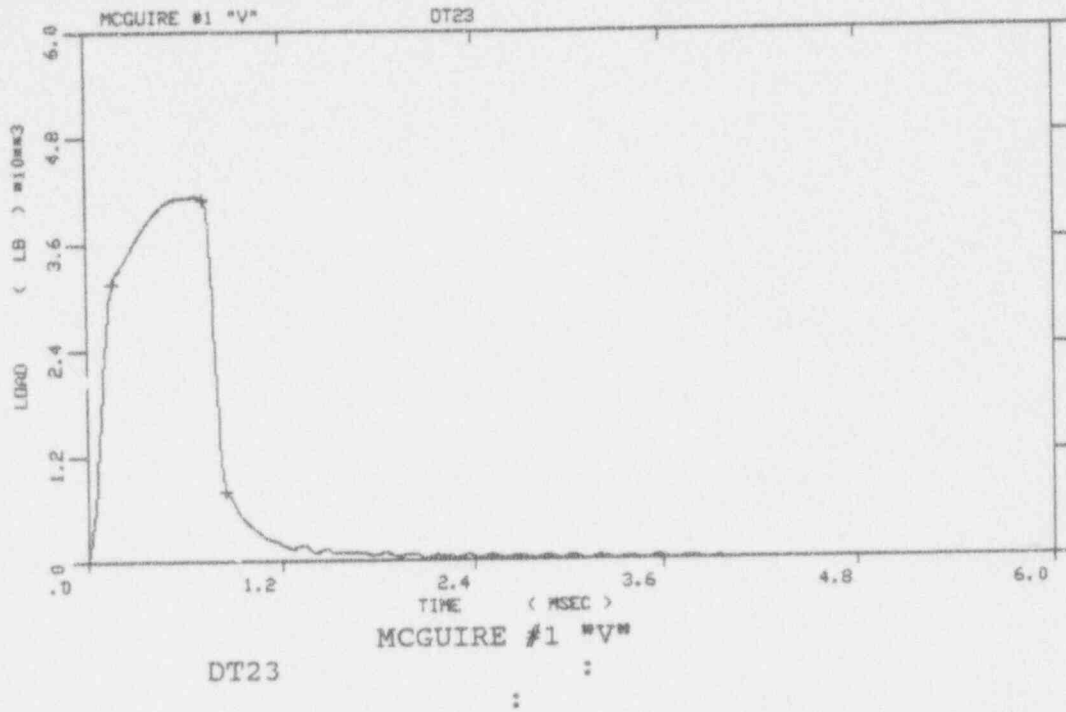


Figure A-12. Load-time records for Specimens DT23 and DT29

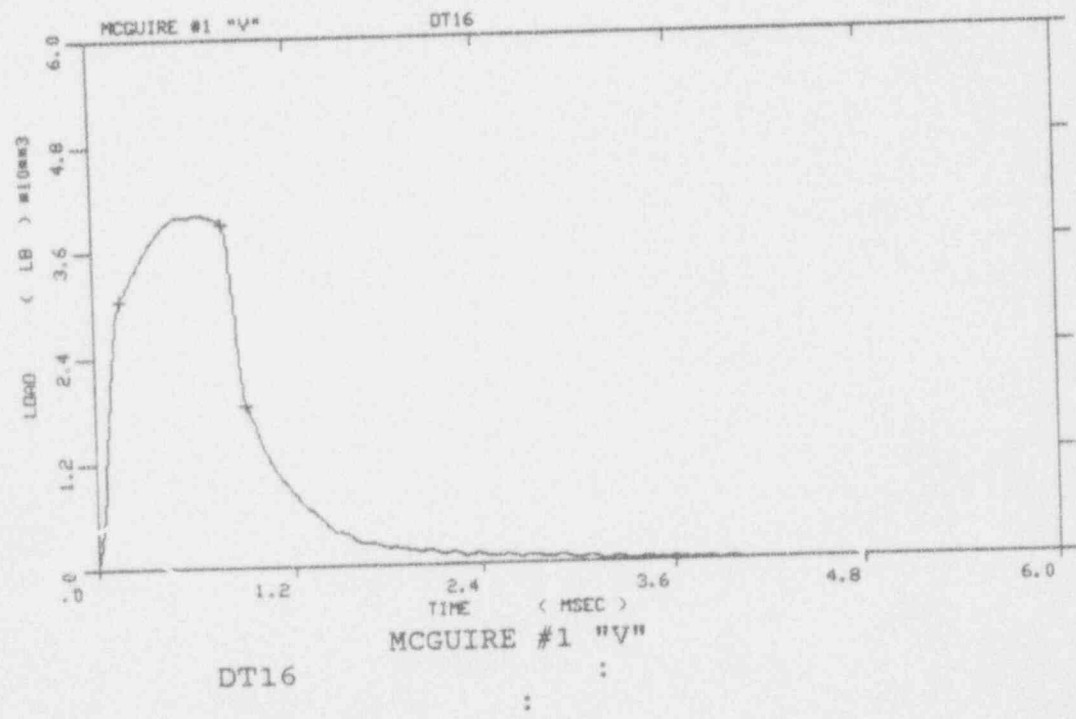
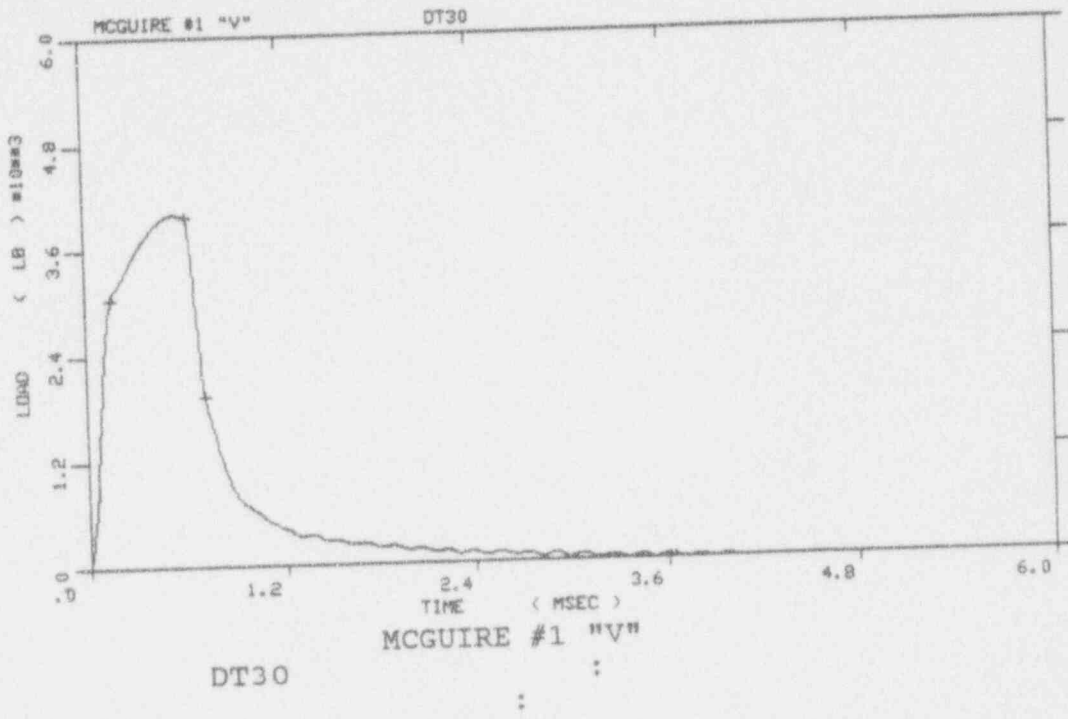


Figure A-13. Load-time records for Specimens DT30 and DT16

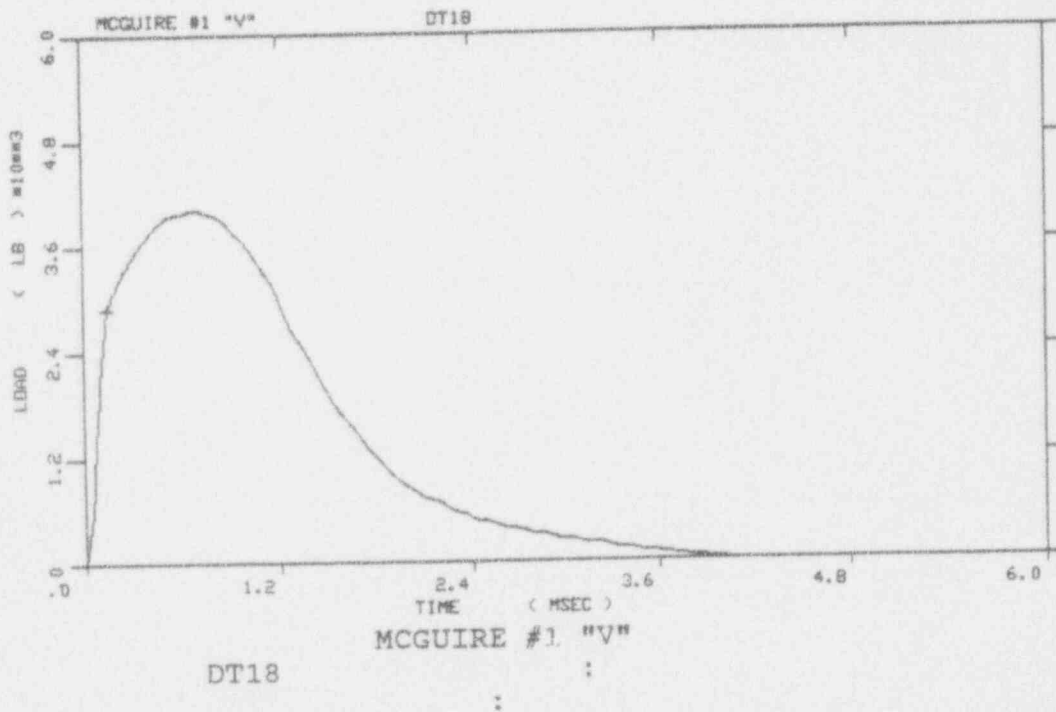
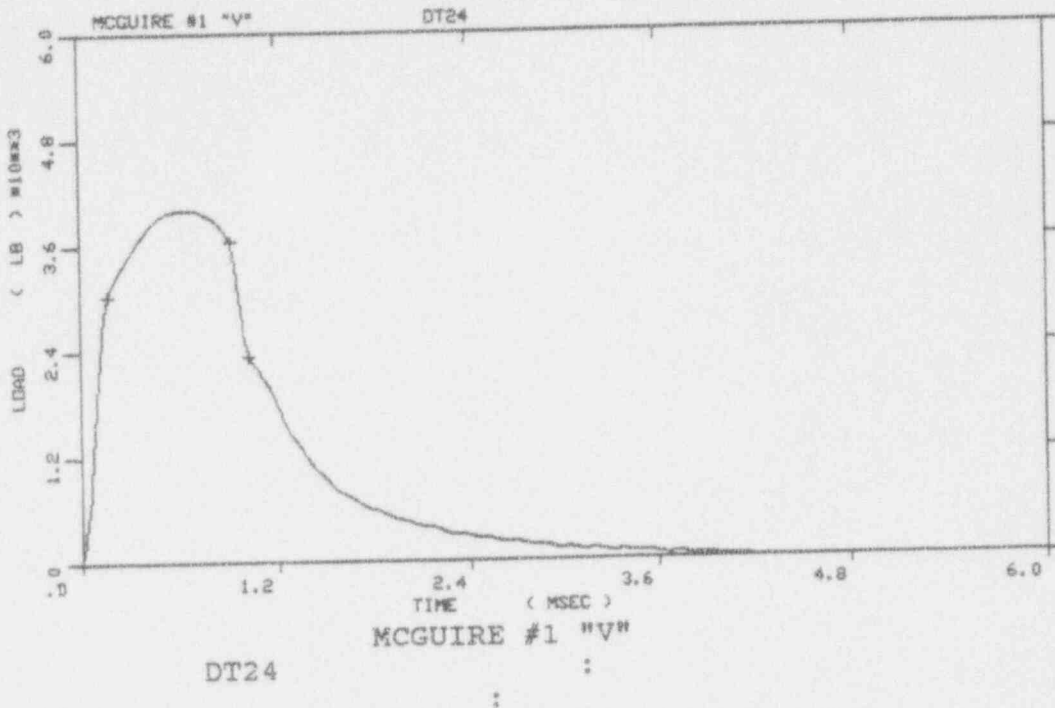


Figure A-14. Load-time records for Specimens DT24 and DT18

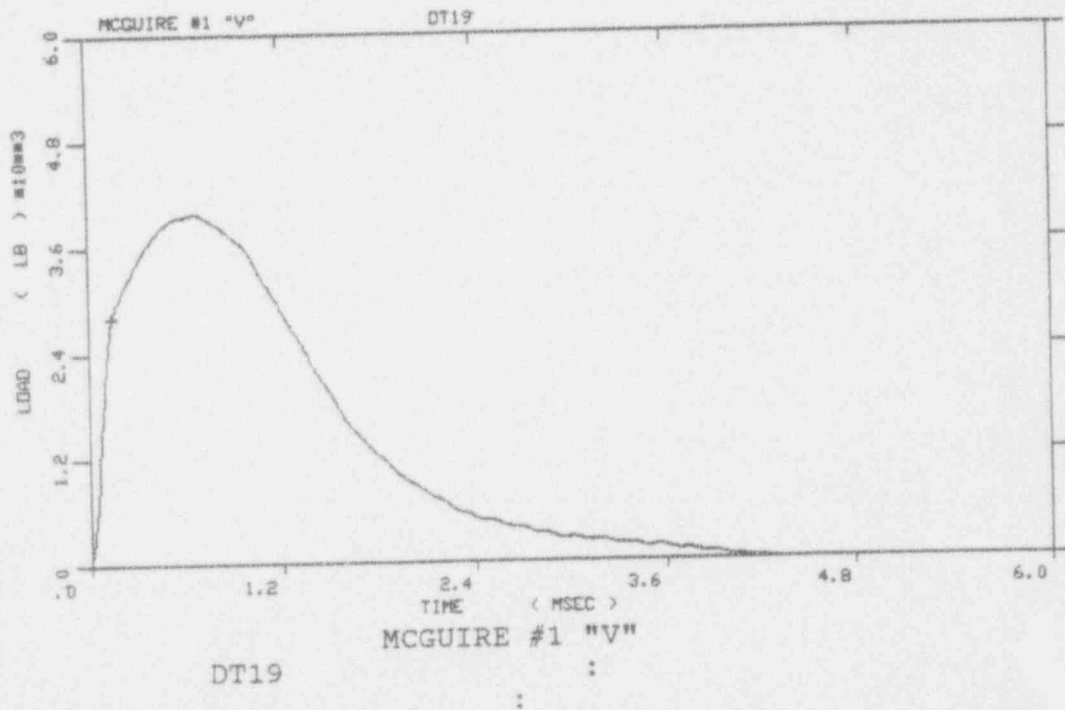
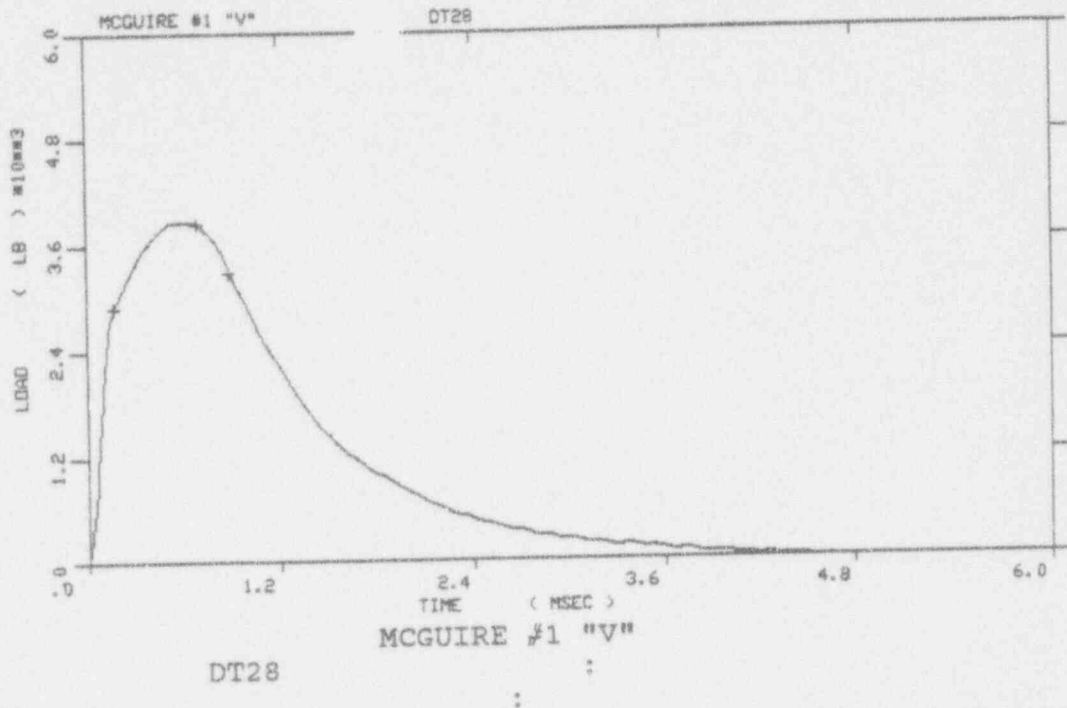


Figure A-15. Load-time records for Specimens DT28 and DT19

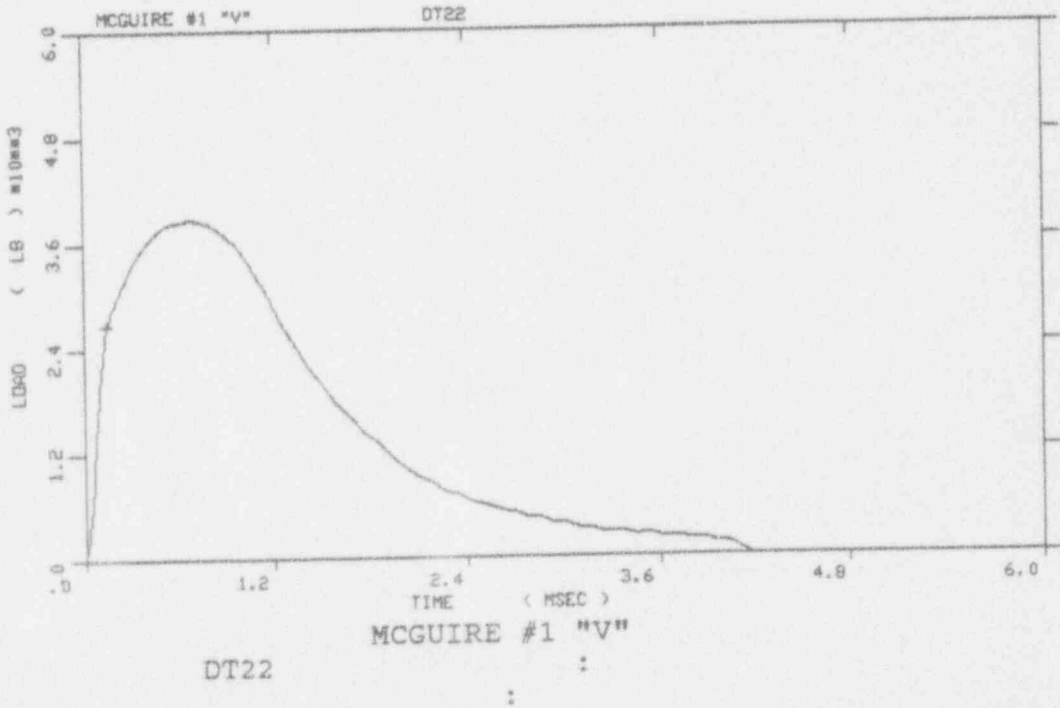
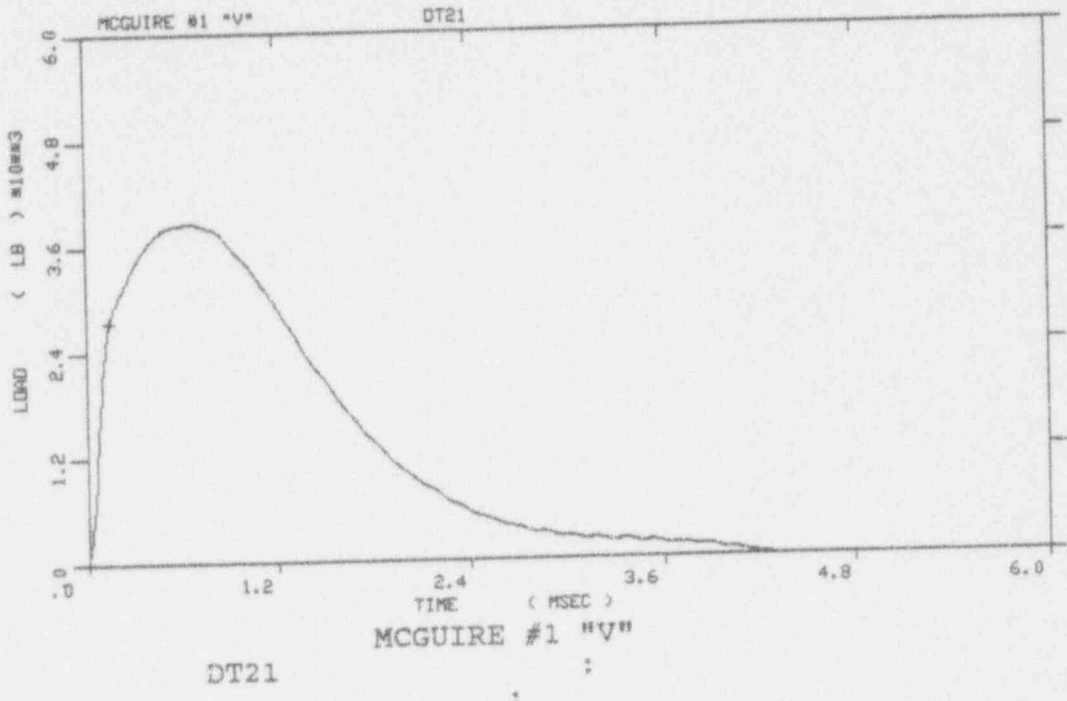


Figure A-16. Load-time records for Specimens DT21 and DT22

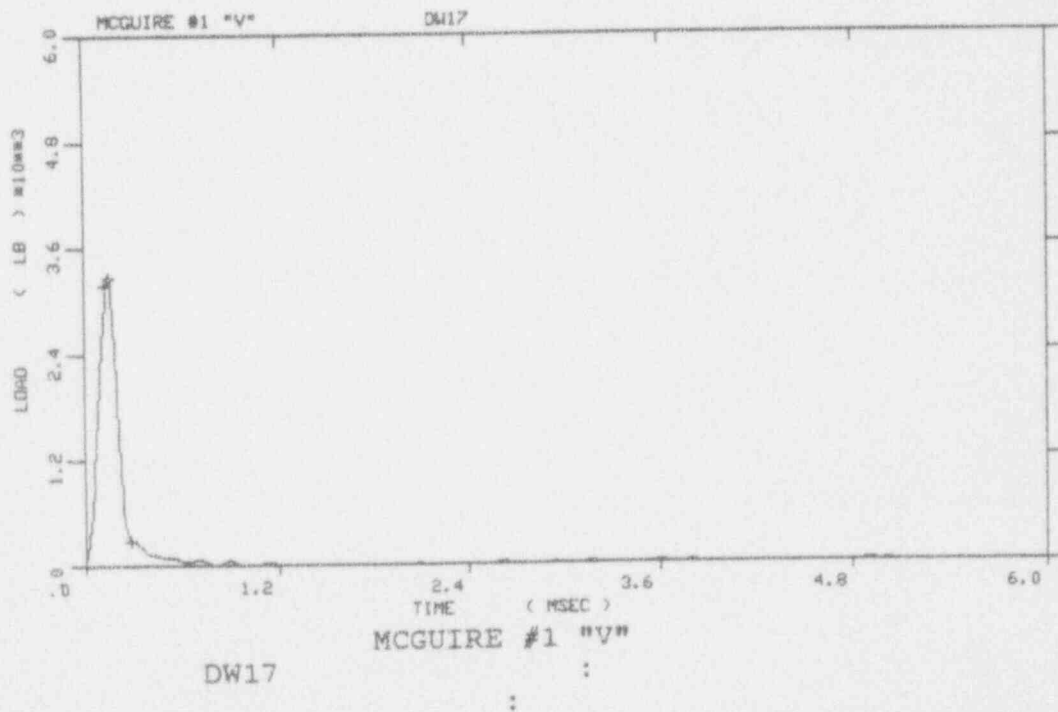
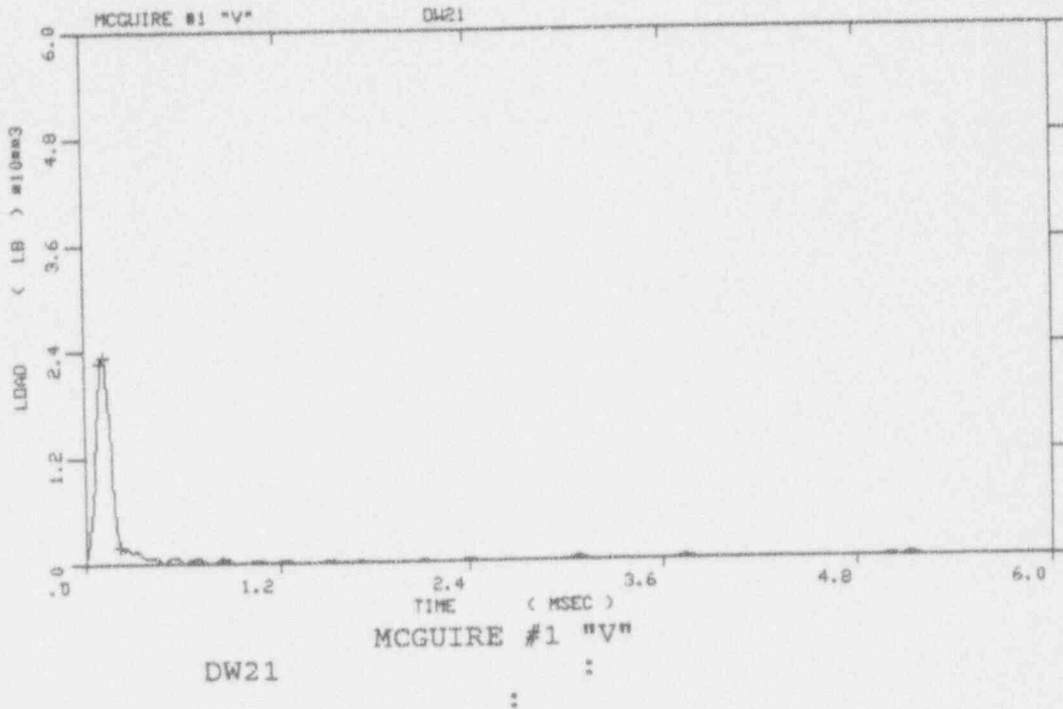


Figure A-17. Load-time records for Specimens DW21 and DW17

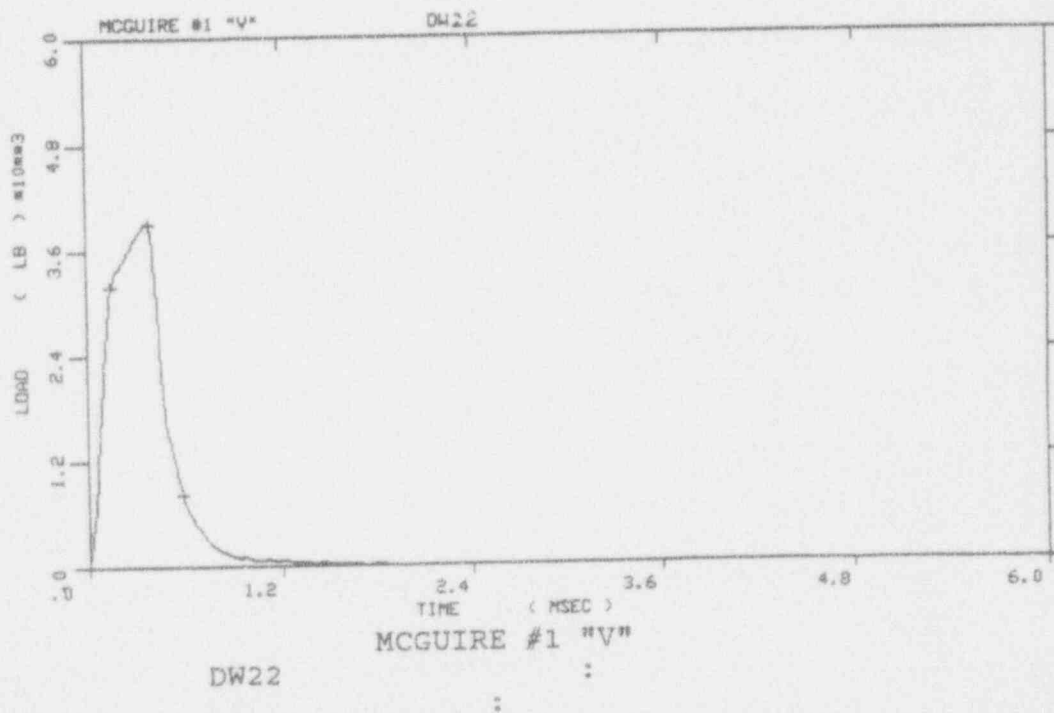
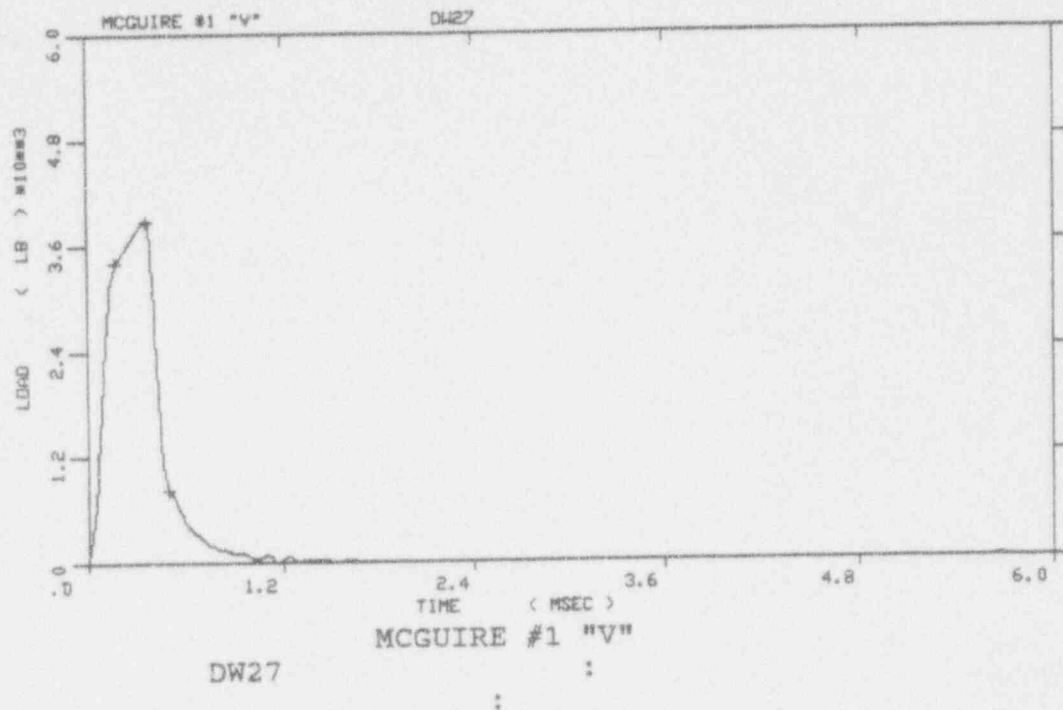


Figure A-18. Load-time records for Specimens DW27 and DW22

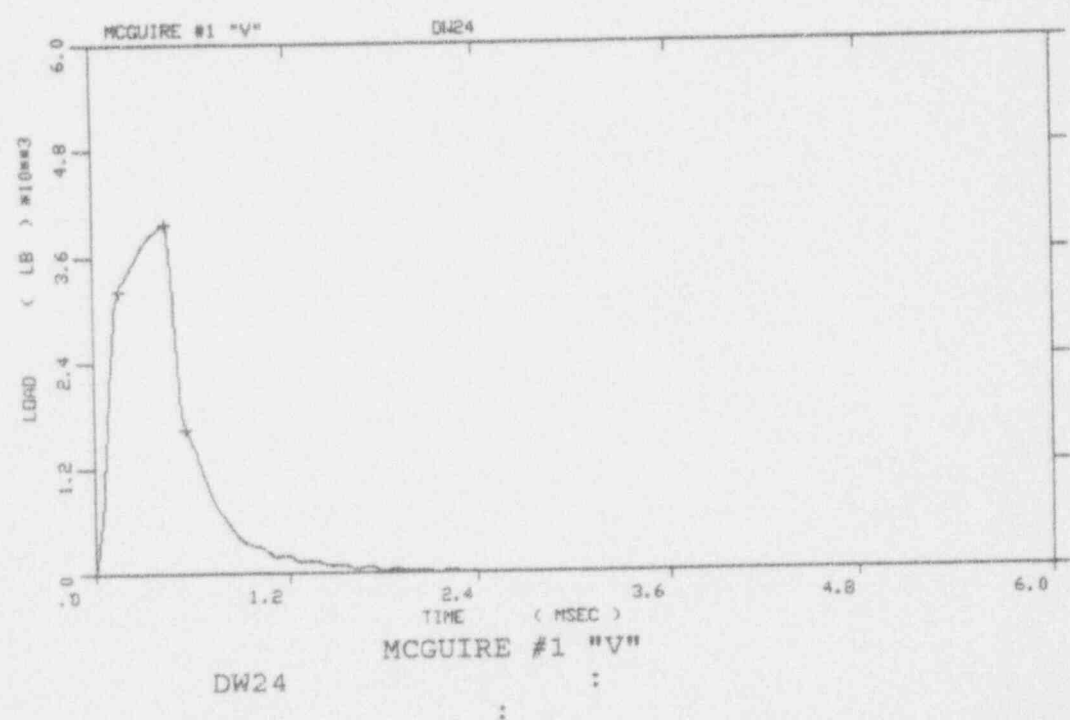
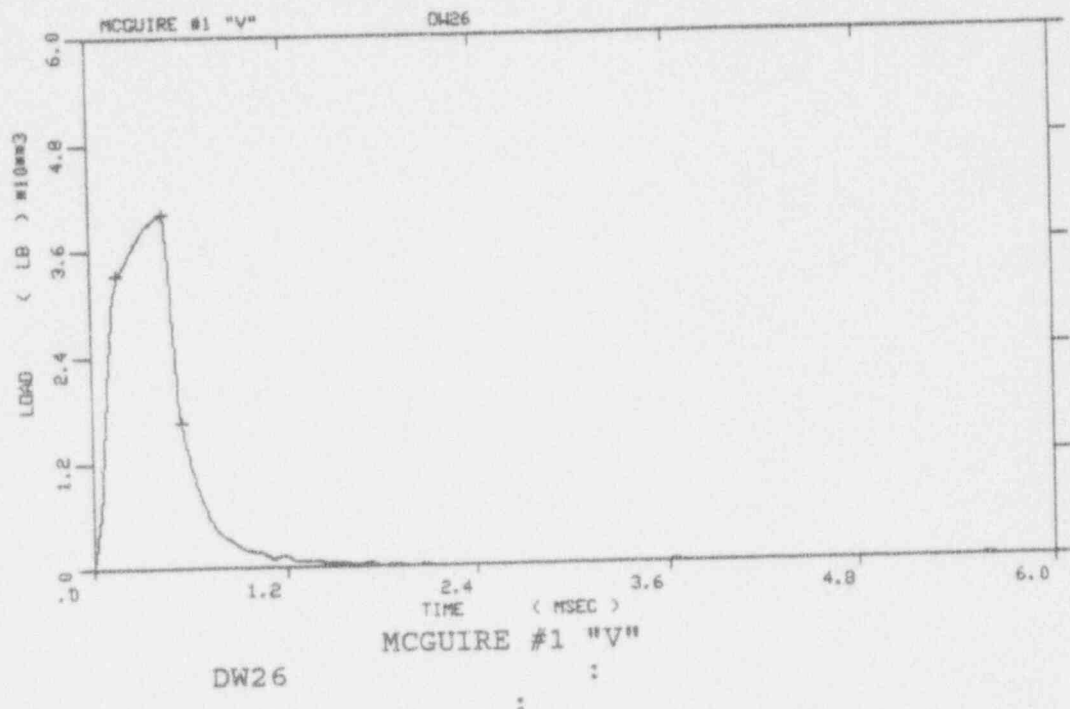


Figure A-19. Load-time records for Specimens DW26 and DW24

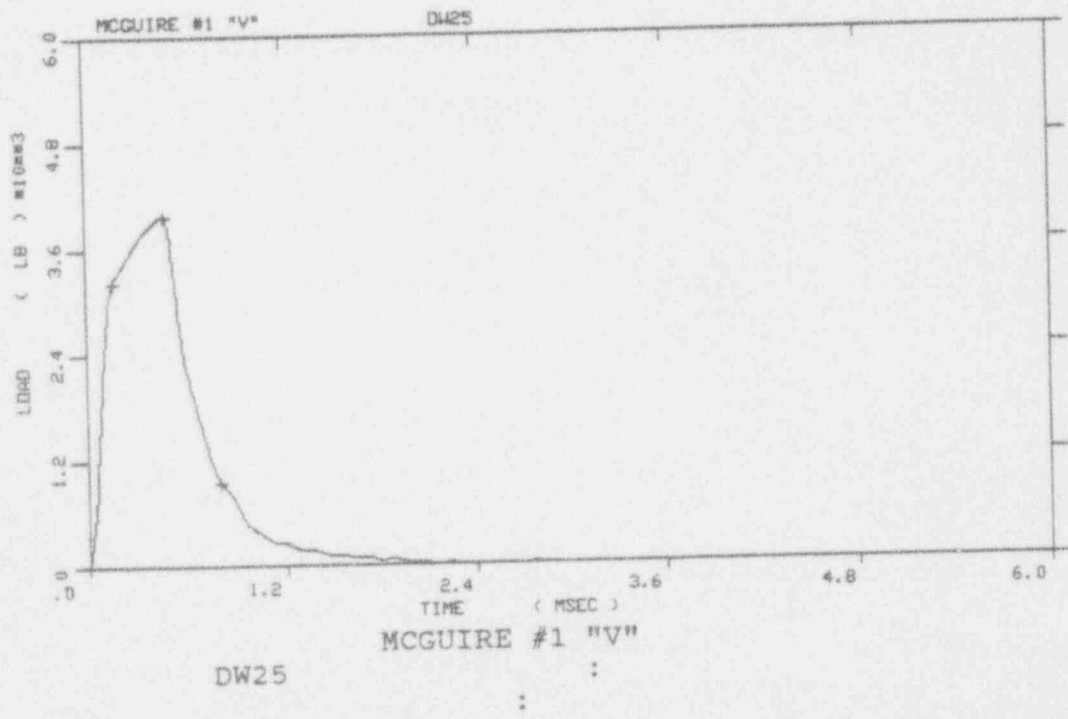
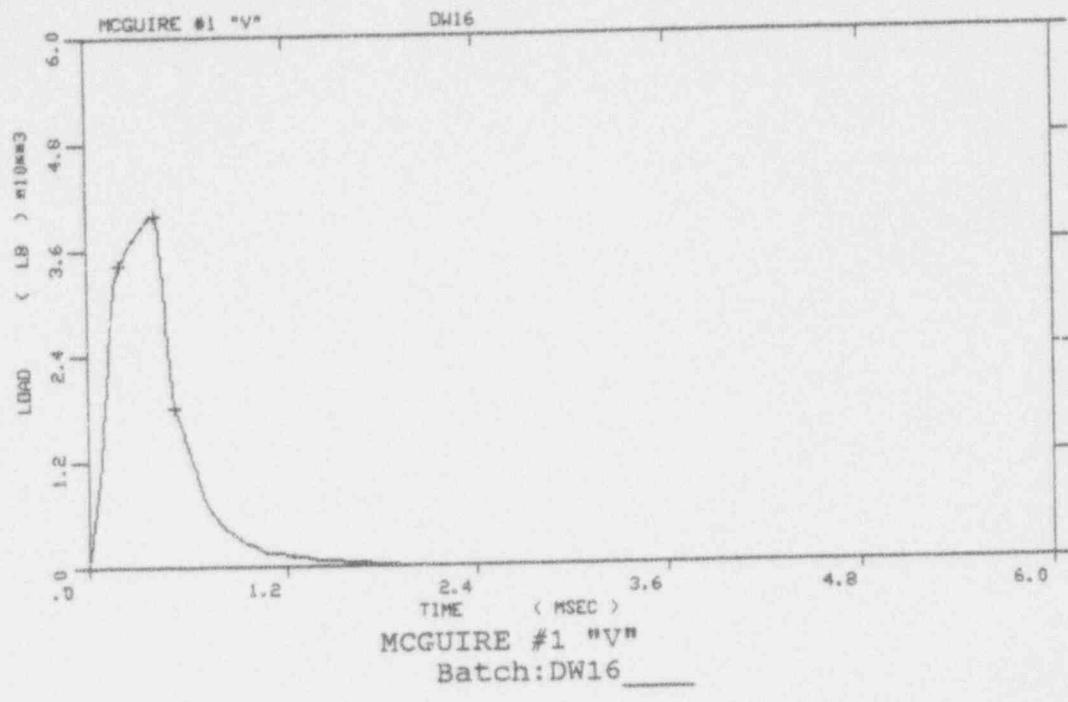


Figure A-20. Load-time records for Specimens DW16 and DW25

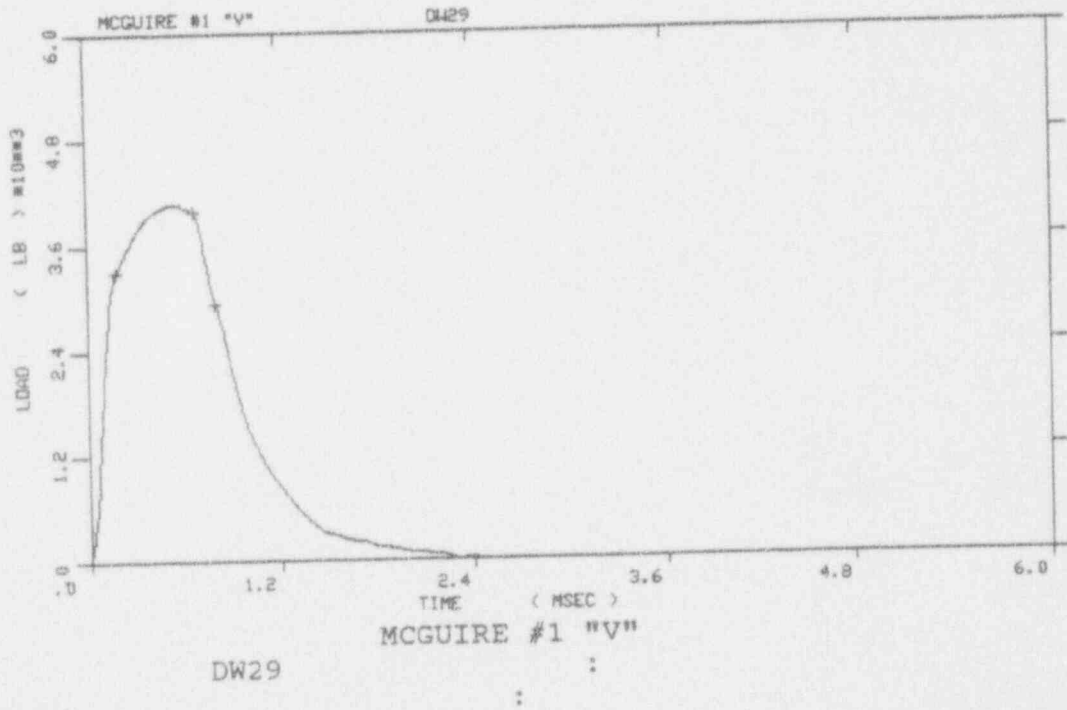
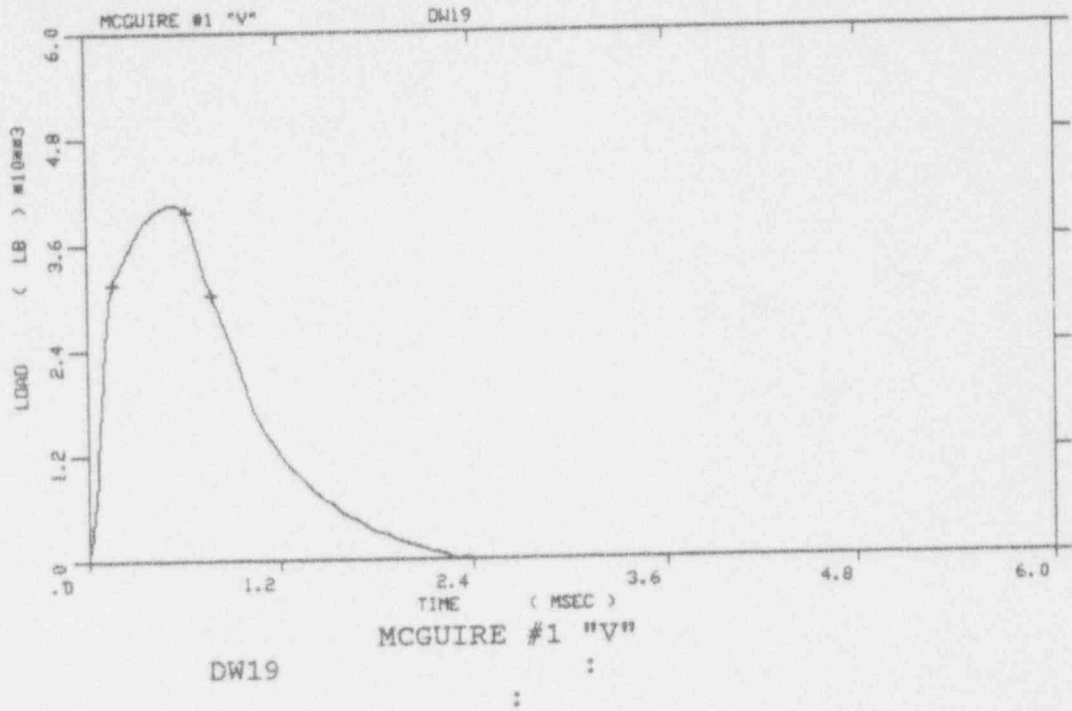


Figure A-21. Load-time records for Specimens DW19 and DW29

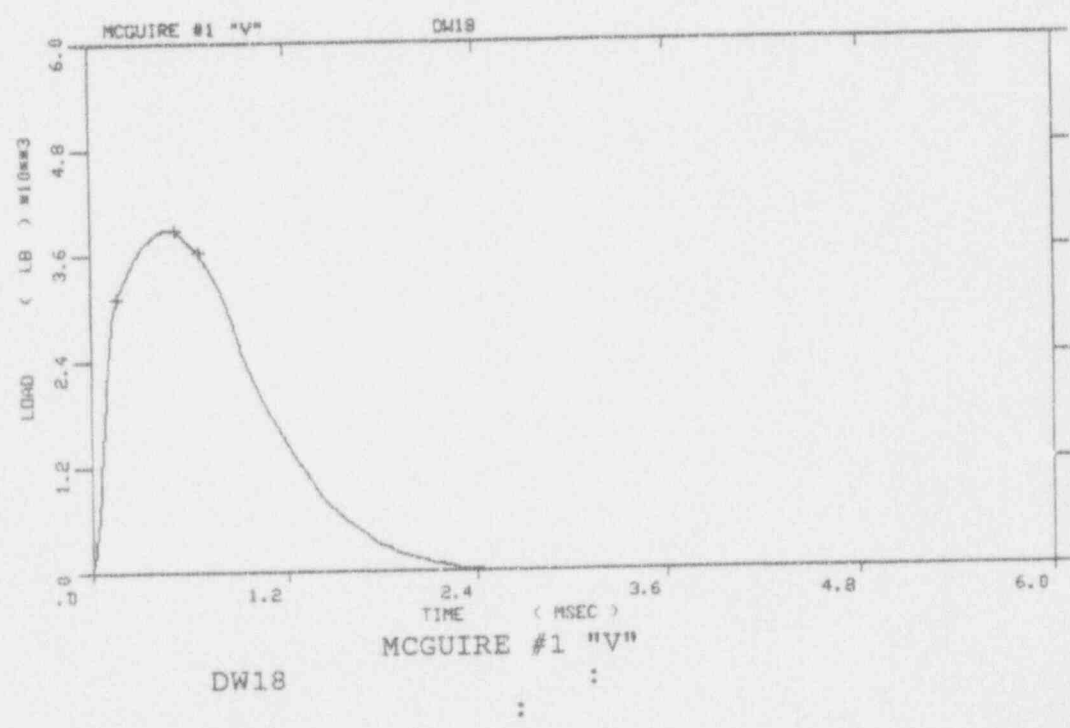
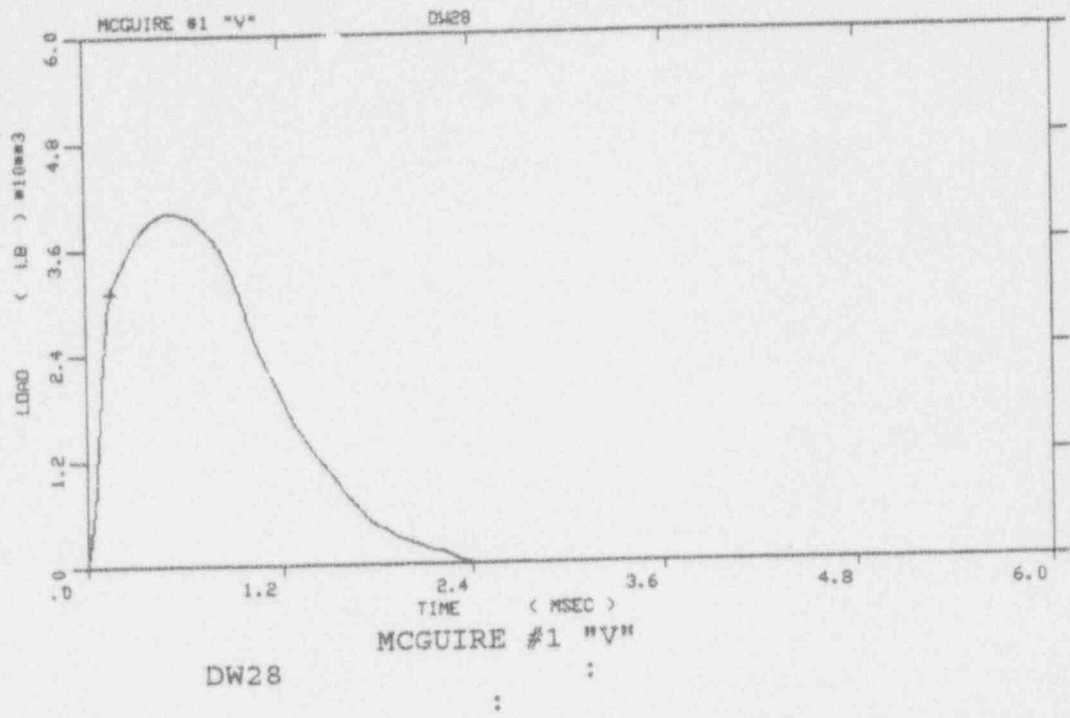


Figure A-22. Load-time records for Specimens DW28 and DW18

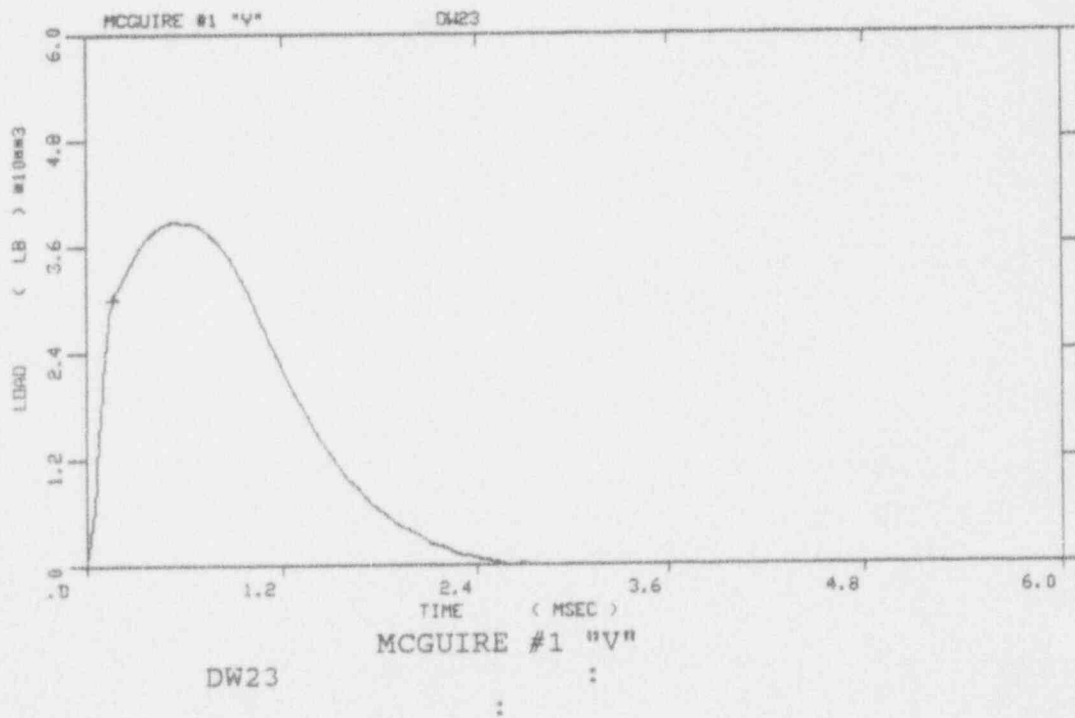
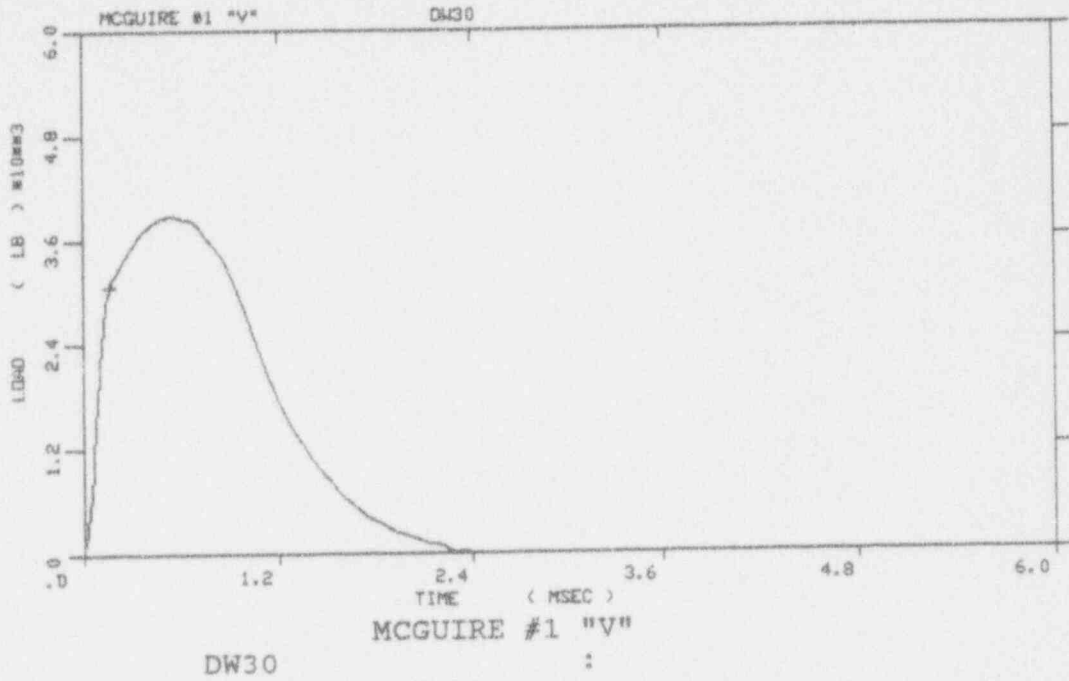


Figure A-23. Load-time records for Specimens DW30 and DW23

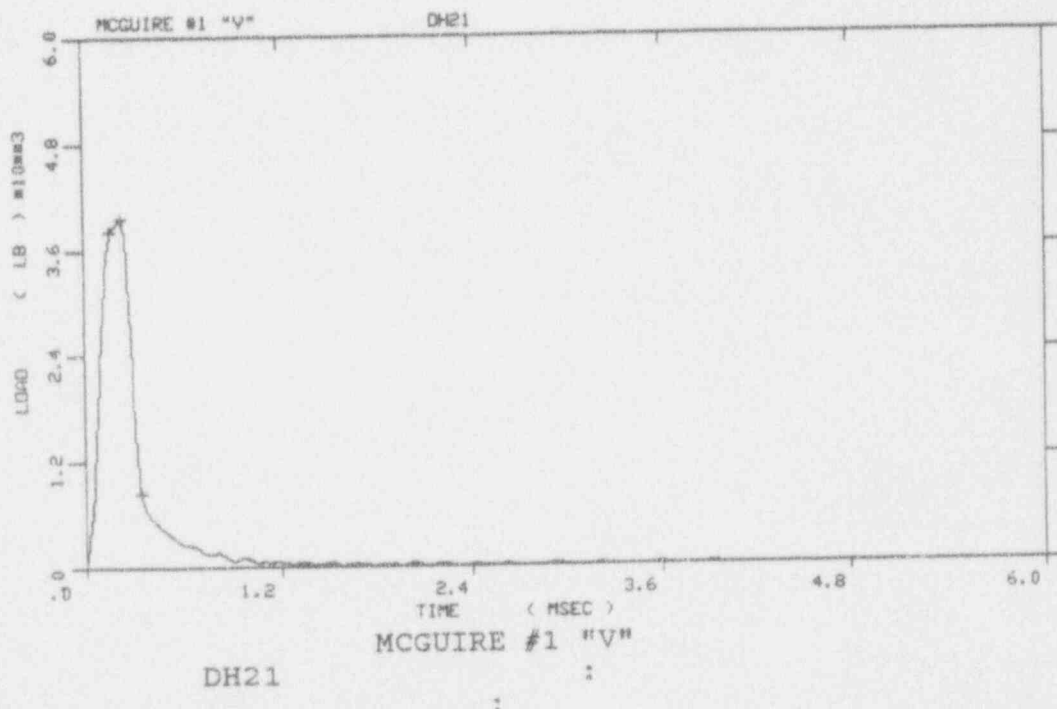
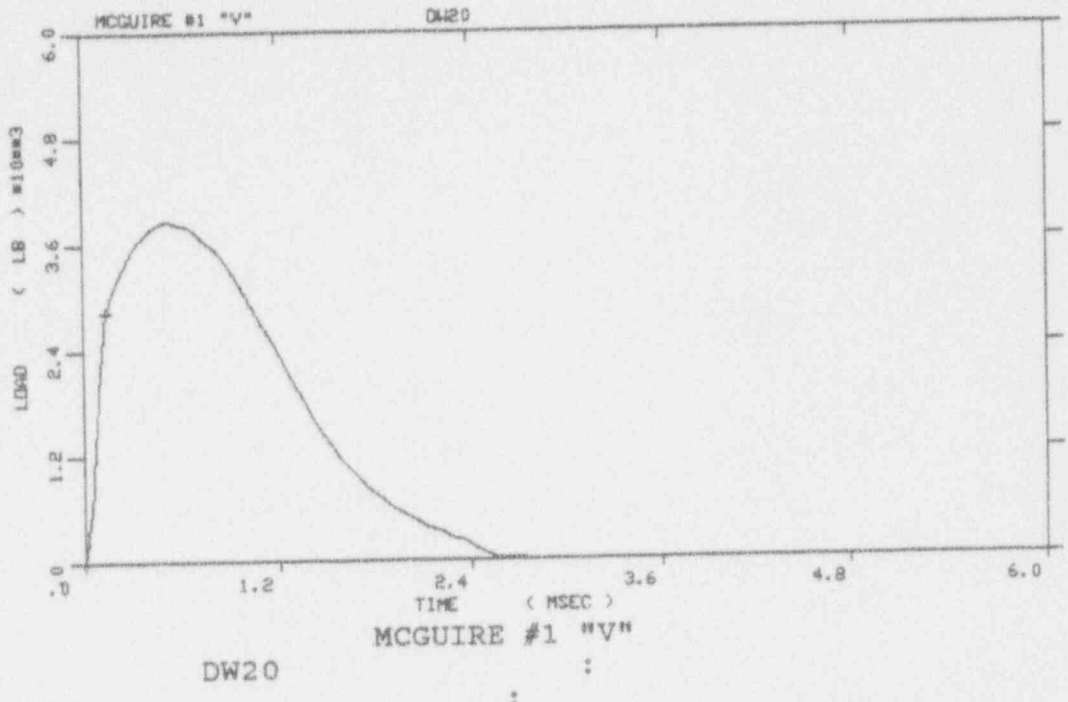


Figure A-24. Load-time records for Specimens DW20 and DH21

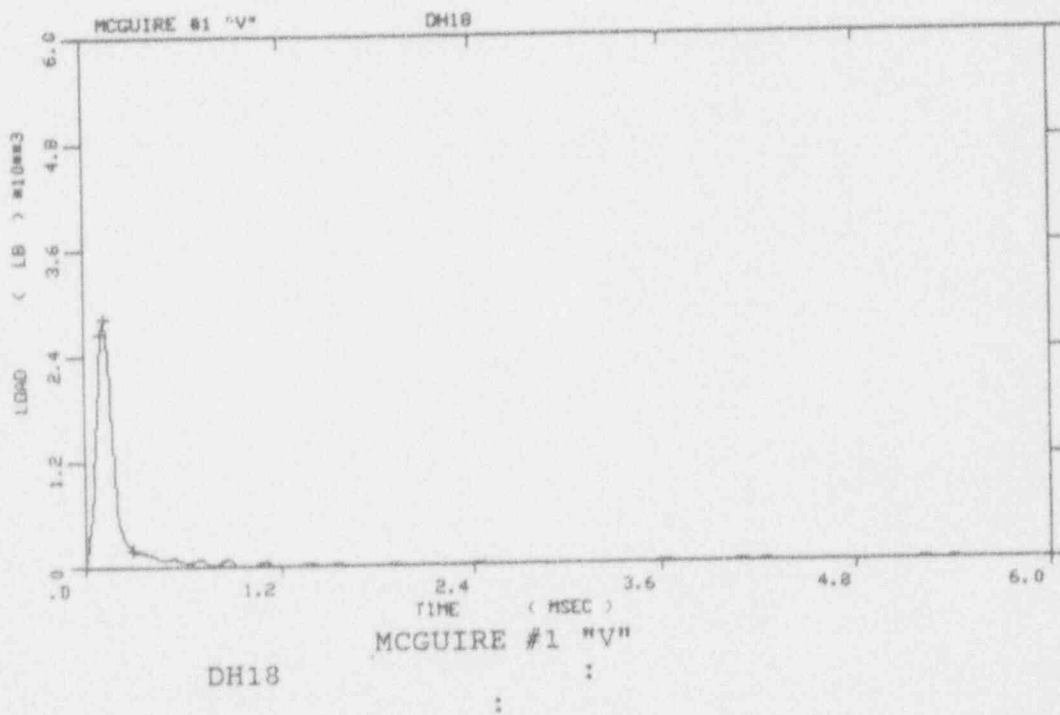
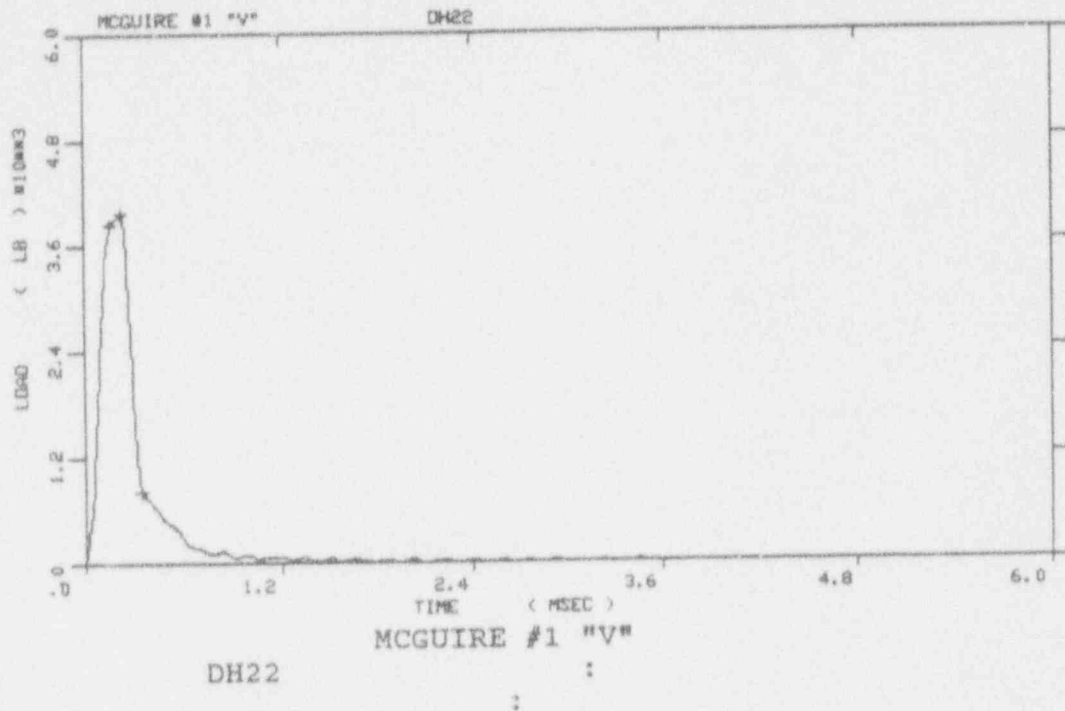


Figure A-25. Load-time records for Specimens DH22 and DH18

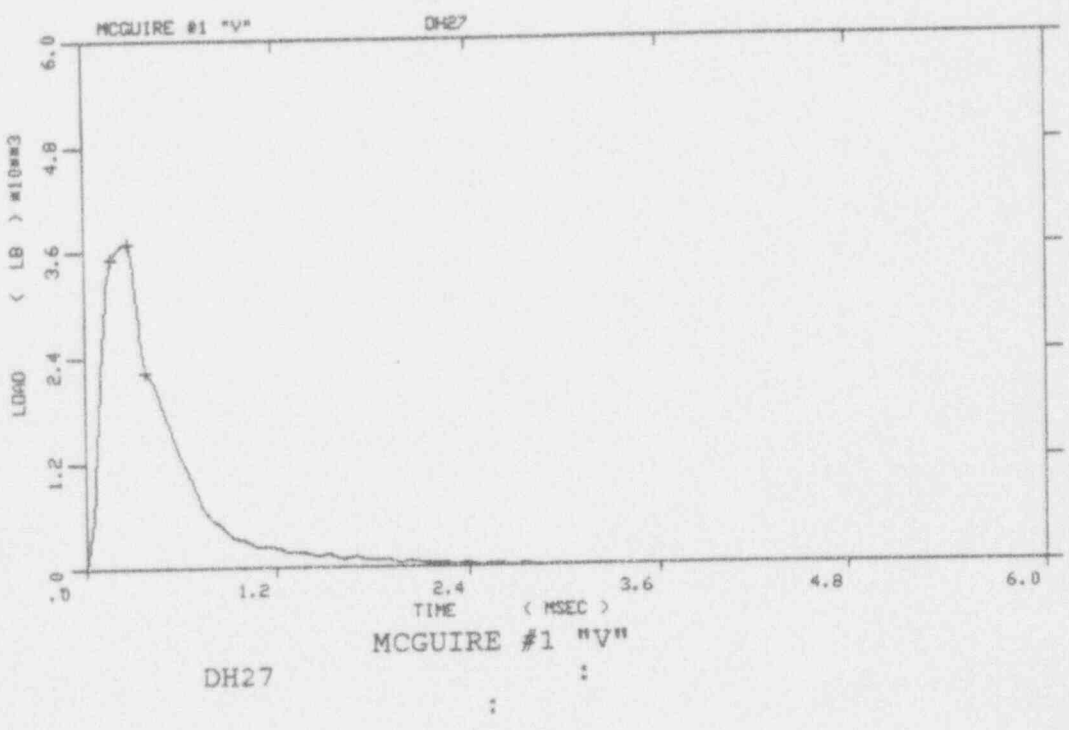
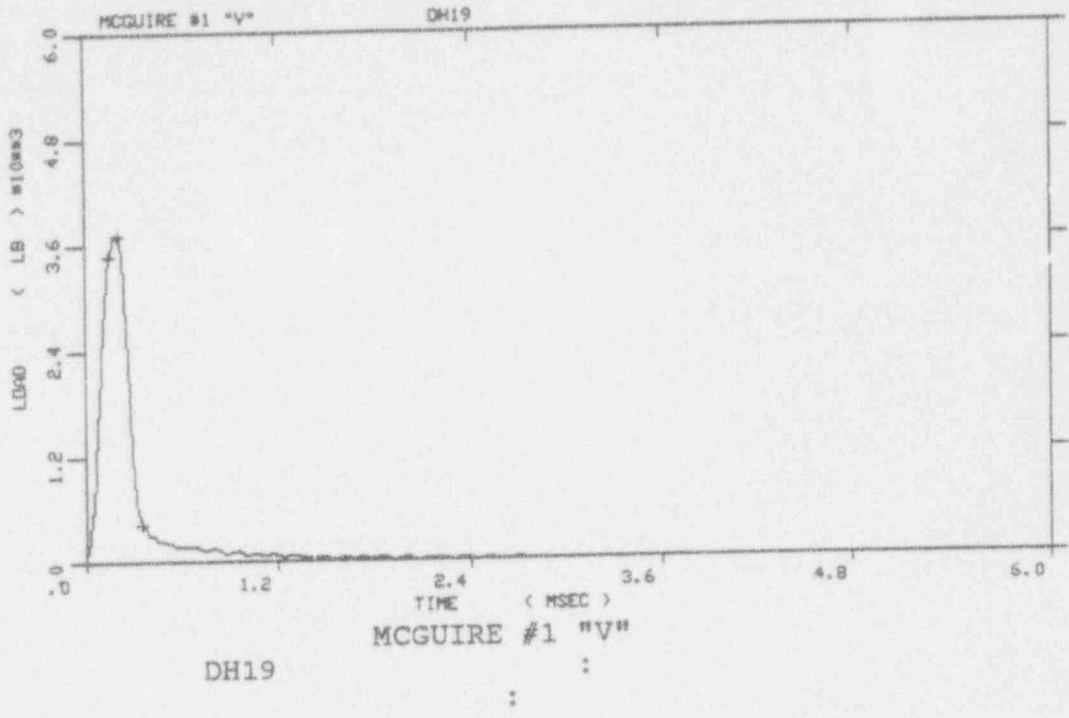


Figure A-26. Load-time records for Specimens DH19 and DH27

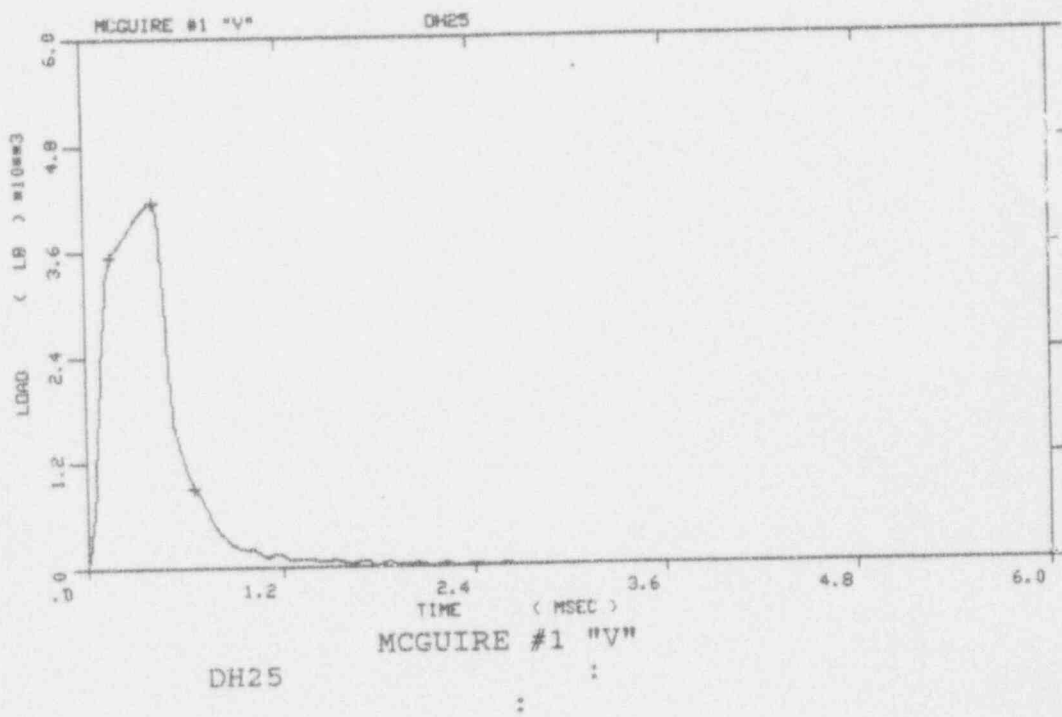
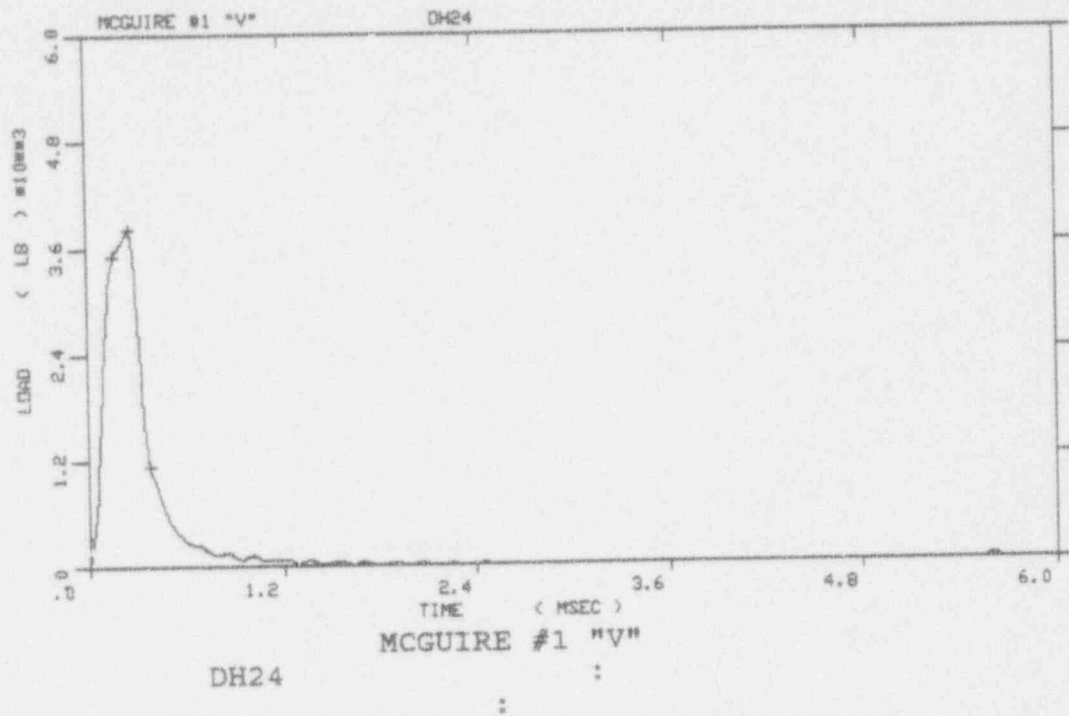


Figure A-27. Load-time records for Specimens DH24 and DH25

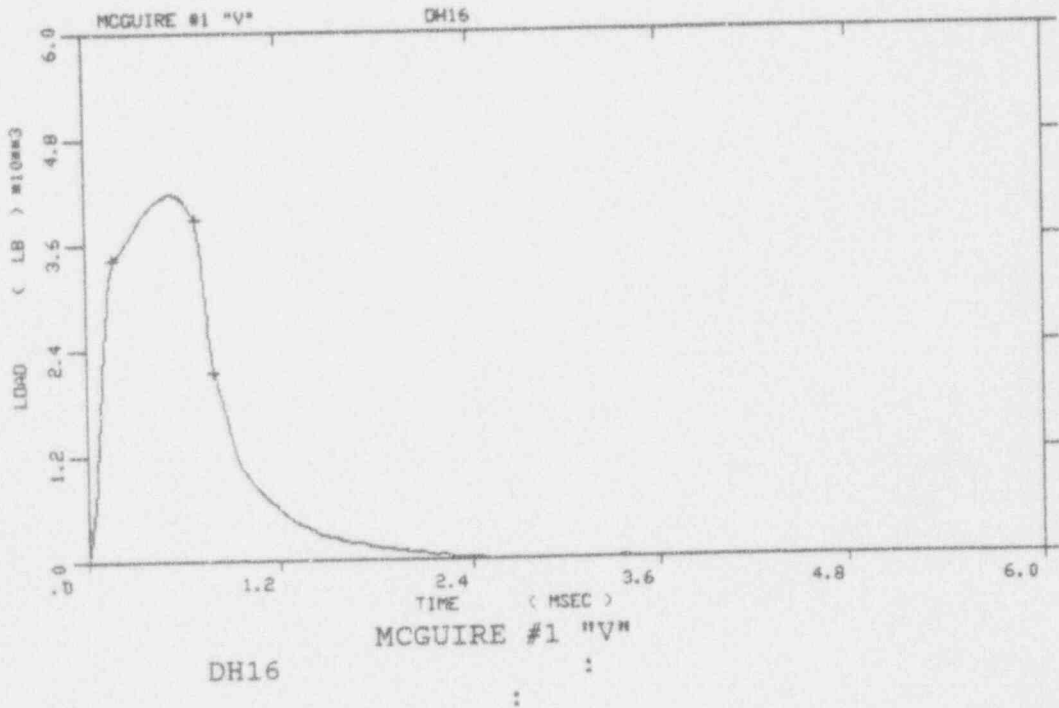
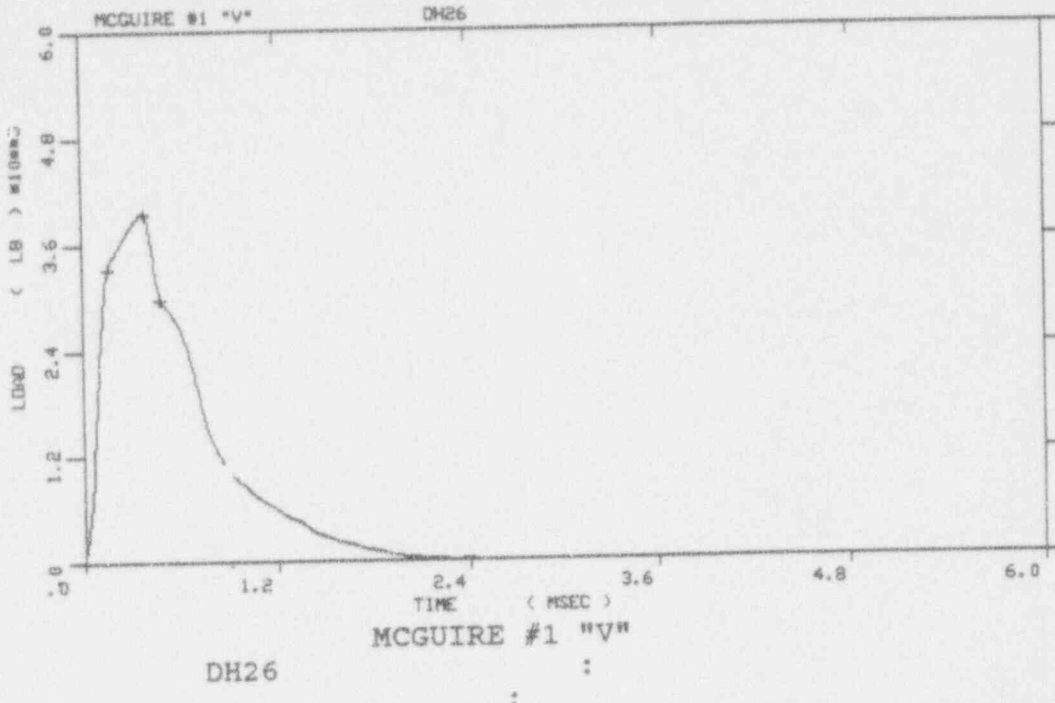


Figure A-28. Load-time records for Specimens DH26 and DH16

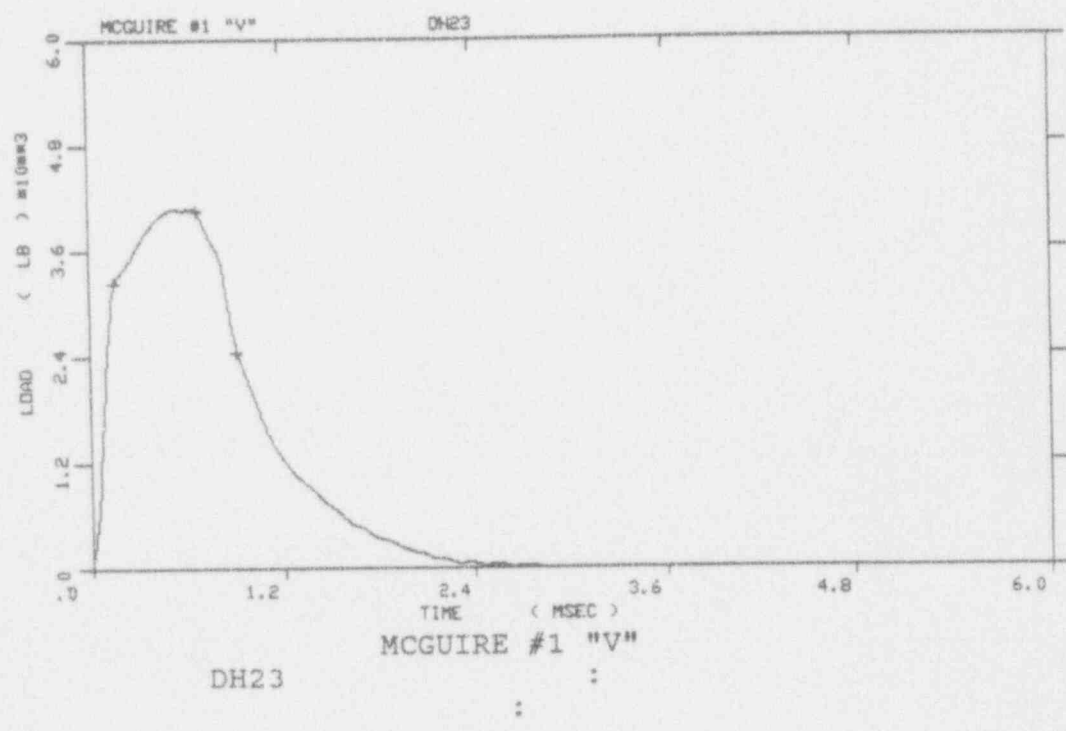
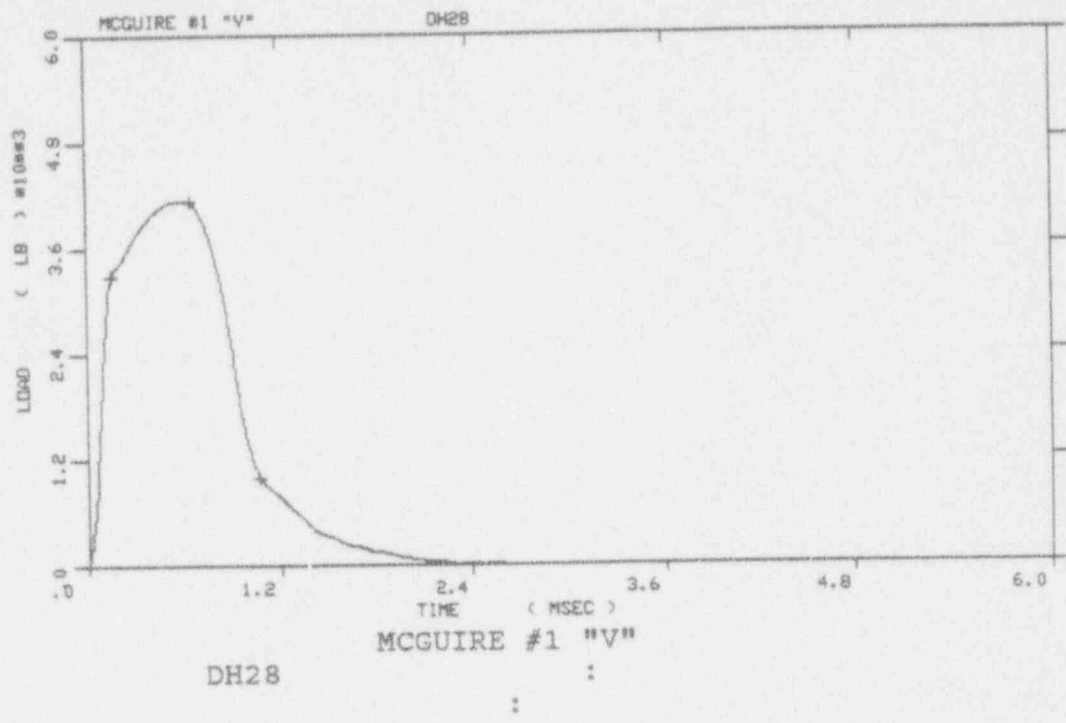


Figure A-29. Load-time records for Specimens DH28 and DH23

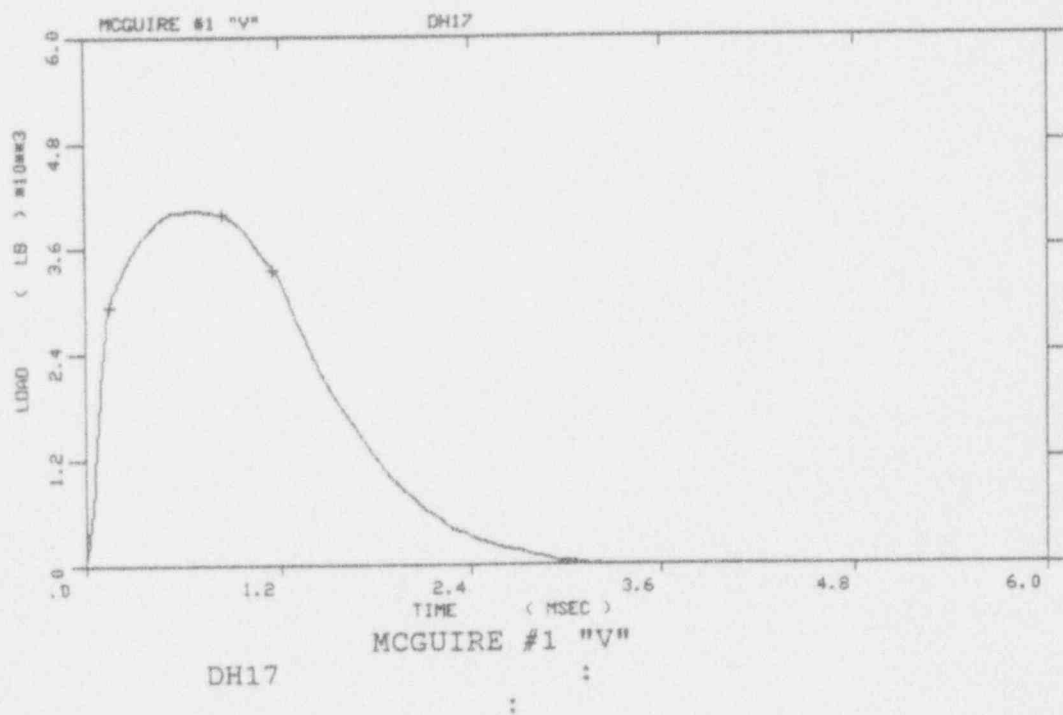
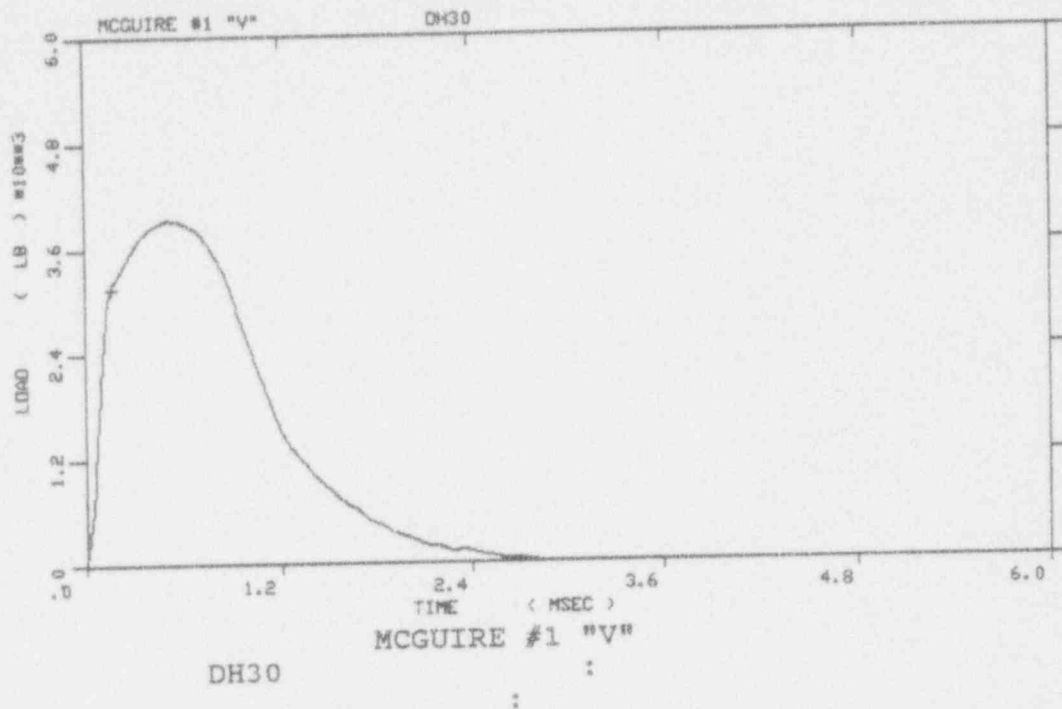


Figure A-30. Load-time records for Specimens DH30 and DH17

The load-time record
for Specimen DH20 is not available
because of computer system malfunction

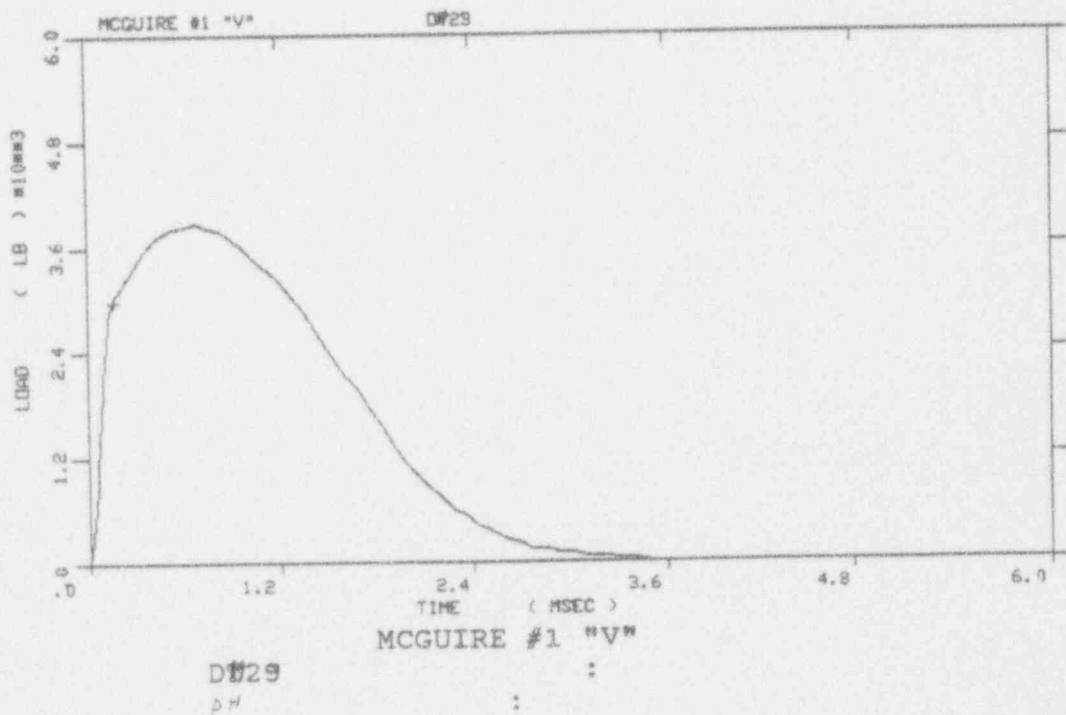


Figure A-31. Load-time records for Specimens DH20 and DH29

APPENDIX B

Heatup and Cooldown Limit Curves for Normal Operation

TABLE OF CONTENTS

| <u>Section</u> | <u>Title</u> | <u>Page</u> |
|----------------|--|-------------|
| | LIST OF ILLUSTRATIONS | B-2 |
| | LIST OF TABLES | B-2 |
| B-1 | INTRODUCTION | B-3 |
| B-2 | FRACTURE TOUGHNESS PROPERTIES | B-3 |
| B-3 | CRITERIA FOR ALLOWABLE PRESSURE-TEMPERATURE RELATIONSHIPS | B-4 |
| B-4 | HEATUP AND COOLDOWN PRESSURE-TEMPERATURE LIMIT CURVES | B-7 |
| B-5 | CALCULATION OF ADJUSTED REFERENCE TEMPERATURE | B-9 |
| B-6 | REFERENCES | B-21 |
| ATTACHMENT B1 | DATA POINTS FOR HEATUP AND COOLDOWN CURVES (WITHOUT MARGINS FOR INSTRUMENTATION ERRORS) | B-24 |
| ATTACHMENT B2 | HEATUP AND COOLDOWN CURVES AND DATA POINTS (WITH MARGINS OF 12°F AND 30 PSIG FOR INSTRUMENTATION ERRORS) | B-26 |

LIST OF ILLUSTRATIONS

| <u>Figure</u> | <u>Title</u> | <u>Page</u> |
|---------------|---|-------------|
| B-1 | McGuire Unit 1 Reactor Coolant System Heatup Limitations (Heatup Rate of 60°F/hr) Applicable for the First 16 EFPY (Without Margins for Instrumentation Errors) | B-19 |
| B-2 | McGuire Unit 1 Reactor Coolant System Cooldown Limitations (Cooldown Rates up to 100°F/hr) Applicable for the First 16 EFPY (Without Margins for Instrumentation Errors) | B-20 |
| B-3 | McGuire Unit 1 Reactor Coolant System Heatup Limitations (Heatup Rate of 60°F/hr) Applicable for the First 16 EFPY (With Margins of 12°F and 30 psig for Instrumentation Errors) | B-27 |
| B-4 | McGuire Unit 1 Reactor Coolant System Cooldown Limitations (Cooldown Rates up to 100°F/hr) Applicable for the First 16 EFPY (With Margins of 12°F and 30 psig for Instrumentation Errors) | B-28 |

LIST OF TABLES

| <u>Table</u> | <u>Title</u> | <u>Page</u> |
|--------------|--|-------------|
| B-1 | Calculation of Average Cu and Ni Weight Percent for McGuire Unit 1 | B-11 |
| B-2 | McGuire Unit 1 Reactor Vessel Toughness Table (Unirradiated) | B-15 |
| B-3 | Calculation of Chemistry Factors Using Surveillance Capsule Data | B-16 |
| B-4 | Summary of Adjusted Reference Temperatures (ART's) at 1/4-t and 3/4-t Locations for 16 EFPY | B-17 |
| B-5 | Calculation of Adjusted Reference Temperatures at 16 EFPY for the Limiting McGuire Unit 1 Reactor Vessel Materials - Lower Shell Longitudinal Welds 3-442A & C and Lower Shell Plate B5013-2 | B-18 |

B-1. INTRODUCTION

Heatup and cooldown limit curves are calculated using the most limiting value of RT_{NDT} (reference nil-ductility temperature) corresponding to the limiting beltline region material for the reactor vessel. The most limiting RT_{NDT} of the material in the core region of the reactor vessel is determined by using the unirradiated reactor vessel material fracture toughness properties and estimating the radiation-induced ΔRT_{NDT} . The unirradiated RT_{NDT} is designated as the higher of either the drop weight nil-ductility transition temperature (NDTT) or the temperature at which the material exhibits at least 50 ft-lb of impact energy and 35-mil lateral expansion (normal to the major working direction) minus 60°F.

RT_{NDT} increases as the material is exposed to fast-neutron radiation. Therefore, to find the most limiting RT_{NDT} at any time period in the reactor's life, ΔRT_{NDT} due to the radiation exposure associated with that time period must be added to the original unirradiated RT_{NDT} . The extent of the shift in RT_{NDT} is enhanced by certain chemical elements (such as copper and nickel) present in reactor vessel steels. The Nuclear Regulatory Commission (NRC) has published a method for predicting radiation embrittlement in Regulatory Guide 1.99, Revision 2 (Radiation Embrittlement of Reactor Vessel Materials)^(B1). Regulatory Guide 1.99, Revision 2 is used for the calculation of Adjusted Reference Temperature values (irradiated RT_{NDT} with margins for uncertainties) at 1/4-t and 3/4-t locations. "t" is the thickness of the vessel at the beltline region measured from the clad/base metal interface.

The pressure-temperature limit curves in Figures B-1 and B-2 of this report do not include margins for instrumentation errors or for pressure differences between the wide-range pressure transmitter and the limiting reactor vessel beltline region. The pressure-temperature limit curves in Attachment B2 of this report only include instrumentation error margins of 12°F and 30 psig; no margins are included for pressure differences between the wide-range pressure transmitter and the limiting reactor vessel beltline region.

B-2. FRACTURE TOUGHNESS PROPERTIES

The fracture-toughness properties of the ferritic material in the reactor coolant pressure boundary are determined in accordance with the NRC Regulatory Standard Review Plan^(B2). The pre-irradiation fracture-toughness properties of the McGuire Unit 1 reactor vessel are presented in Table B-1. The post-irradiation fracture toughness properties of the reactor vessel beltline material were obtained

directly from the McGuire Unit 1 and Diablo Canyon Unit 2 Reactor Vessel Radiation Surveillance Programs. Credible surveillance data is available for three capsules (Capsules U, X and V) for McGuire Unit 1 and two capsules (Capsules U and X) for Diablo Canyon Unit 2.

B-3. CRITERIA FOR ALLOWABLE PRESSURE-TEMPERATURE RELATIONSHIPS

The ASME approach for calculating the allowable limit curves for various heatup and cooldown rates specifies that the total stress intensity factor, K_t , for the combined thermal and pressure stresses at any time during heatup or cooldown cannot be greater than the reference stress intensity factor, K_{Ia} , for the metal temperature at that time. K_{Ia} is obtained from the reference fracture toughness curve, defined in Appendix G of the ASME Code^[B3]. The K_{Ia} curve is given by the following equation:

$$K_{Ia} = 26.78 + 1.223 * e^{[0.0145 (T - RT_{NDT} + 160)]} \quad (1)$$

where,

K_{Ia} = reference stress intensity factor as a function of the metal temperature T and the metal reference nil-ductility temperature RT_{NDT}

Therefore, the governing equation for the heatup-cooldown analysis is defined in Appendix G of the ASME Code^[B3] as follows:

$$C * K_{IM} + K_{IT} \leq K_{Ia} \quad (2)$$

where,

K_{IM} = stress intensity factor caused by membrane (pressure) stress

K_{IT} = stress intensity factor caused by the thermal gradient

K_{Ia} = reference stress intensity factor as a function of temperature relative to the RT_{NDT} of the material

C = 2.0 for Level A and Level B service limits

$C = 1.5$ for hydrostatic and leak test conditions during which the reactor core is not critical

At any time during the heatup or cooldown transient, K_{Ia} is determined by the metal temperature at the tip of the postulated flaw, the appropriate value for RT_{NDT} , and the reference fracture toughness curve. The thermal stresses resulting from the temperature gradients through the vessel wall are calculated and then the corresponding (thermal) stress intensity factors, K_{IT} , for the reference flaw are computed. From Equation 2, the pressure stress intensity factors are obtained and, from these, the allowable pressures are calculated.

For the calculation of the allowable pressure versus coolant temperature during cooldown, the reference flaw of Appendix G to the ASME Code is assumed to exist at the inside of the vessel wall. During cooldown, the controlling location of the flaw is always at the inside of the wall because the thermal gradients produce tensile stresses at the inside, which increase with increasing cooldown rates. Allowable pressure-temperature relations are generated for both steady-state and finite cooldown rate situations. From these relations, composite limit curves are constructed for each cooldown rate of interest.

The use of the composite curve in the cooldown analysis is necessary because control of the cooldown procedure is based on the measurement of reactor coolant temperature, whereas the limiting pressure is actually dependent on the material temperature at the tip of the assumed flaw. During cooldown, the 1/4-t vessel location is at a higher temperature than the fluid adjacent to the vessel inner diameter. This condition, of course, is not true for the steady-state situation. It follows that, at any given reactor coolant temperature, the ΔT developed during cooldown results in a higher value of K_{Ia} at the 1/4-t location for finite cooldown rates than for steady-state operation. Furthermore, if conditions exist so that the increase in K_{Ia} exceeds K_{IT} , the calculated allowable pressure during cooldown will be greater than the steady-state value.

The above procedures are needed because there is no direct control on temperature at the 1/4-t location and, therefore, allowable pressures may unknowingly be violated if the rate of cooling is decreased at various intervals along a cooldown ramp. The use of the composite curve eliminates this problem and ensures conservative operation of the system for the entire cooldown period.

Three separate calculations are required to determine the limit curves for finite heatup rates. As is done in the cooldown analysis, allowable pressure-temperature relationships are developed for steady-state conditions as well as finite heatup rate conditions assuming the presence of a 1/4-t defect at the inside of the wall. The heatup results in compressive stresses at the inside surface that alleviate the tensile stresses produced by internal pressure. The metal temperature at the crack tip lags the coolant temperature; therefore, the K_{Ic} for the 1/4-t crack during heatup is lower than the K_{Ic} for the 1/4-t crack during steady-state conditions at the same coolant temperature. During heatup, especially at the end of the transient, conditions may exist so that the effects of compressive thermal stresses and lower K_{Ic} 's do not offset each other, and the pressure-temperature curve based on steady-state conditions no longer represents a lower bound of all similar curves for finite heatup rates when the 1/4-t flaw is considered. Therefore, both cases have to be analyzed in order to ensure that at any coolant temperature the lower value of the allowable pressure calculated for steady-state and finite heatup rates is obtained.

The second portion of the heatup analysis concerns the calculation of the pressure-temperature limitations for the case in which a 1/4-t deep outside surface flaw is assumed. Unlike the situation at the vessel inside surface, the thermal gradients established at the outside surface during heatup produce stresses which are tensile in nature and therefore tend to reinforce any pressure stresses present. These thermal stresses are dependent on both the rate of heatup and the time (or coolant temperature) along the heatup ramp. Since the thermal stresses at the outside are tensile and increase with increasing heatup rates, each heatup rate must be analyzed on an individual basis.

Following the generation of pressure-temperature curves for both the steady state and finite heatup rate situations, the final limit curves are produced by constructing a composite curve based on a point-by-point comparison of the steady-state and finite heatup rate data. At any given temperature, the allowable pressure is taken to be the lesser of the three values taken from the curves under consideration. The use of the composite curve is necessary to set conservative heatup limitations because it is possible for conditions to exist wherein, over the course of the heatup ramp, the controlling condition switches from the inside to the outside, and the pressure limit must at all times be based on analysis of the most critical criterion.

Finally, the 1982 Amendment to 10CFR50^(B4) has a rule which addresses the metal temperature of the closure head flange and vessel flange regions. This rule states that the metal temperature of the closure flange regions must exceed the material unirradiated RT_{NDT} by at least 120°F for normal

operation when the pressure exceeds 20 percent of the preservice hydrostatic test pressure (621 psig for McGuire Unit 1).

Table B-2 indicates that the limiting unirradiated RT_{NDT} of 40°F occurs in the closure head flange of the McGuire Unit 1 reactor vessel, so the minimum allowable temperature of this region is 160 F at pressures greater than 621 psig. This limit is shown in Figures B-1 and B-2 whenever applicable. Figures B-3 and B-4 in Attachment B2 contain margins of 12°F and 30 psig for instrumentation errors; for these curves the minimum allowable temperature is 172°F at pressures greater than 591 psig.

B-4. HEATUP AND COOLDOWN PRESSURE-TEMPERATURE LIMIT CURVES

Pressure-temperature limit curves for normal heatup and cooldown of the primary reactor coolant system have been calculated for the pressure and temperature in the reactor vessel beltline region using the methods discussed in Section B-3^(B32) of this report.

The time and position dependent temperature solution utilized in both the heatup and cooldown analyses was based on the one-dimensional transient heat conduction equation:

$$\rho C \frac{\partial^2 T}{\partial t} = K \left[\frac{\partial^2 T}{\partial r^2} + \frac{1}{r} \frac{\partial T}{\partial r} \right]$$

With the following boundary conditions applied at the inner and outer radii of the pressure vessel:

$$\text{At } r = r_i, \quad -K \frac{\partial T}{\partial r} = h (T - T_c)$$

$$\text{At } r = r_o, \quad \frac{\partial T}{\partial r} = 0$$

where h = heat transfer coefficient between the coolant and the vessel wall,

a conservative value of 7000 (Btu/hr-ft²-°F) was used

ρ = density (@ 70°F = 490.9 lbm/ft³, @ 550°F = 484.7 lbm/ft³)

C = specific heat (@ 70°F = 0.104 Btu/lbm-°F, @ 550°F = 0.130 Btu/lbm-°F)

K = conductivity (@ 70°F = 26.42 Btu/hr-ft-°F, @ 550°F = 23.90 Btu/hr-ft-°F)

T = wall temperature variable

r = radius variable

t = time variable

The above is solved numerically to obtain the results of the heat transfer analysis as input; position and time dependent temperature distributions of hoop thermal stress were calculated for each heatup and cooldown rate^[B32].

Since indication of reactor vessel beltline pressure is not available on the plant, the pressure difference between the wide-range pressure transmitter and the limiting beltline region must be accounted for when using pressure-temperature limit curves presented in Figures B-1 through B-4. The limit curves presented in Figures B-3 and B-4 include only instrumentation error margins.

Figure B-1 presents the heatup curve without margins for instrumentation errors and pressure differences using a heatup rate of 60°F/hr applicable for the first 16 EFPY. Figure B-2 presents the cooldown curves without margins using cooldown rates up to 100°F/hr applicable for the first 16 EFPY. Margins of 12°F and 30 psig for possible instrumentation errors are included in the development of heatup and cooldown curves found in Attachment B2. Allowable combinations of temperature and pressure for specific temperature change rates are below and to the right of the limit lines shown in Figures B-1 through B-4. This is in addition to other criteria which must be met before the reactor is made critical.

The reactor must not be made critical until pressure-temperature combinations are to the right of the criticality limit line shown in Figures B-1 and B-3. The straight-line portion of the criticality limit is at the minimum permissible temperature for the 2485 psig inservice hydrostatic test as required by Appendix G to 10CFR Part 50. The governing equation for the hydrostatic test is defined in Appendix G to Section XI of the ASME Code as follows:

$$1.5 K_{IM} \leq K_{Lr}$$

where,

K_{IM} is the stress intensity factor covered by membrane (pressure) stress,

$$K_{Lr} = 26.78 + 1.233 e^{[0.0145 (T - RTNDT + 160)]}$$

T is the minimum permissible metal temperature, and

RTNDT is the metal reference nil-ductility temperature.

The criticality limit curves shown in Figures B-1 and B-3 specify pressure-temperature limits for core operation to provide additional margin during actual power production as specified in Reference B4. The pressure-temperature limits for core operation (except for low power physics tests) are that the

reactor vessel must be at a temperature equal to or higher than the minimum temperature required for the inservice hydrostatic test, and at least 40°F higher than the minimum permissible temperature in the corresponding pressure-temperature curve for heatup and cooldown calculated as described in Section B-3. The minimum temperature for the inservice hydrostatic leak test (without margins for instrumentation errors) for the McGuire Unit 1 reactor vessel at 16 EFPY is 282°F. A vertical line drawn from these points on the pressure-temperature curve, intersecting a curve 40°F higher than the pressure-temperature limit curve, constitutes the limit for core operation for the reactor vessel. Additionally, the minimum temperature for the inservice hydrostatic leak test (with instrumentation error margins of 12°F and 30 psig) for the McGuire Unit 1 reactor vessel at 16 EFPY is 295°F. This is shown in Figure B-3.

Figures B-1 through B-4 define limits for ensuring prevention of nonductile failure for the McGuire Unit 1 reactor vessel. The data points used to develop the heatup and cooldown pressure-temperature limit curves shown in Figures B-1 through B-4 are presented in Attachments B1 and B2.

B-5. CALCULATION OF ADJUSTED REFERENCE TEMPERATURE

From Regulatory Guide 1.99, Revision 2^(B1) the adjusted reference temperature (ART) for each material in the beltline is given by the following expression:

$$\text{ART} = \text{Initial RT}_{\text{NDT}} + \Delta\text{RT}_{\text{NDT}} + \text{Margin} \quad (3)$$

Initial RT_{NDT} is the reference temperature for the unirradiated material as defined in paragraph NB-2331 of Section III of the ASME Boiler and Pressure Vessel Code. If measured values of initial RT_{NDT} for the material in question are not available, generic mean values for that class of material may be used if there are sufficient test results to establish a mean and standard deviation for the class.

$\Delta\text{RT}_{\text{NDT}}$ is the mean value of the adjustment in reference temperature caused by irradiation and should be calculated as follows:

$$\Delta\text{RT}_{\text{NDT}} = \text{CF} * f^{(0.25 - 0.10 \log D)} \quad (4)$$

To calculate $\Delta\text{RT}_{\text{NDT}}$ at any depth (e.g., at 1/4-t or 3/4-t), the following formula must first be used to attenuate the fluence at the specific depth.

$$f_{(\text{depth } x)} = f_{\text{surface}} * e^{(-0.24x)} \quad (5)$$

where x (in inches) is the depth into the vessel wall measured from the vessel clad/base metal interface. The resultant fluence is then put into equation (4) to calculate ΔRT_{NDT} at the specific depth. The calculated surface fluence for McGuire Unit 1 intermediate and lower shells and circumferential weld at 16 EFPY is $1.008 \times 10^{19} \text{ n/cm}^2$ ^[B33]. The calculated surface fluences for McGuire Unit 1 longitudinal welds at 16 EFPY at the 0° and 30° azimuthal angles is $6.662 \times 10^8 \text{ n/cm}^2$ and $7.295 \times 10^{18} \text{ n/cm}^2$, respectively^[B33].

Material property values were obtained from material test certifications from the original fabrication as well as the additional material chemistry tests performed as part of the surveillance capsule testing program^[B5]. In addition, pertinent chemistry test results were also obtained from other plants with similar weld materials. Specifically, Diablo Canyon Unit 2 surveillance data was used to calculate a chemistry factor for the lower shell longitudinal welds. Justification for the use of this data can be found in Appendix D of this report. The average copper and nickel values were calculated for each of the beltline region materials using all of the available material chemistry information as shown in Table B-1.

CF (°F) is the chemistry factor, obtained from Tables in Reference B1, using the average values of the copper and nickel content calculated in Table B-1 and reported in Table B-2. The chemistry factors were also calculated using the surveillance capsule data in Table B-3. All materials in the beltline region of McGuire Unit 1 reactor vessel were considered in determining the limiting material. The results of the ART's at 1/4-t and 3/4-t are summarized in Table B-4. From Table B-4, it can be seen that the limiting materials are the Lower Shell Longitudinal Welds 3-442A & C and Lower Shell Plate B5013-2 for heatup and cooldown curves applicable up to 16 EFPY. Sample calculations to determine the ART values for the lower shell longitudinal welds and lower shell plate at 16 EFPY are shown in Table B-5.

Table B-1
Calculation of Average Cu and Ni Weight Percent for McGuire Unit 1

Intermediate Shell Longitudinal Weld Seams, 2-442A, B & C
(Ht. 20291 & 12008, Linde 1092, Flux Lot No. 3854)

| Reference | wt. % Cu | wt. % Ni |
|-----------|-------------|-------------|
| B5 | 0.21 | 0.88 |
| B6 | 0.20 | 0.91 |
| B31 | 0.195 | 0.87 |
| B31 | 0.191 | 0.848 |
| B31 | 0.193 | 0.863 |
| Average | 0.20 | 0.87 |

Intermediate to Lower Shell Circumferential Weld, 9-442
(Ht. 83640, Linde 0091, Flux Lot No. 3490)

| Reference | wt. % Cu | wt. % Ni |
|-----------|-------------|-------------|
| B7 | 0.050 | --- |
| B8 | 0.050 | 0.120 |
| Average | 0.050 | 0.120 |

Table B-1 (Continued)

Lower Shell Longitudinal Weld Seams, 3-442A, B & C
 (Ht. 21935 & 12008, Linde 1092, Flux Lot No. 3889)

| Reference | wt. % Cu | wt. % Ni |
|-----------|-------------|-------------|
| B9 | 0.220 | --- |
| B10 | 0.200 | --- |
| B11 | 0.22 | 0.83 |
| B12 | 0.23 | 0.90 |
| | 0.21 | 0.76 |
| | 0.22 | 0.90 |
| B13 | 0.219 | 0.86 |
| | 0.212 | 0.88 |
| | 0.213 | 0.90 |
| B14 | 0.225 | 0.875 |
| | 0.213 | 0.856 |
| | 0.225 | 0.877 |
| Average | 0.22 | 0.86 |

Lower Shell Longitudinal Weld Seams, 3-442A (Root Weld)*
 (Ht. 305424, Linde 1092, Flux Lot No. 3889)

| Reference | wt. % Cu | wt. % Ni |
|-----------|-------------|-------------|
| B15 | 0.300 | 0.640 |
| B16 | 0.260 | 0.620 |
| B34 | 0.230 | 0.637 |
| Average | 0.263 | 0.632 |

* The lower shell longitudinal welds also contained a different weld wire heat in the double U root area of the weld. Since the root weld chemistry is not more limiting than the above weld data, it was not utilized in the evaluations.

Table B-1 (Continued)

Lower Shell Longitudinal Weld Seams, 3-442B & C (Root Weld)*
 (Ht. 21935, Linde 1092, Flux Lot No. 5889)

| Reference | wt. % Cu | wt. % Ni |
|-----------|-------------|-------------|
| B17 | 0.200 | --- |
| B12 | 0.21 | 0.68 |
| | --- | 0.71 |
| Average | 0.21 | 0.70 |

Intermediate Shell Plate, B5012-1 (Ht. C4387-2)

| Reference | wt. % Cu | wt. % Ni |
|-----------|-------------|-------------|
| B18, B19 | 0.13 | 0.60 |
| B5 | 0.087 | --- |
| B20 | --- | 0.58 |
| B31 | 0.117 | 0.643 |
| Average | 0.11 | 0.61 |

Intermediate Shell Plate, B5012-2 (Ht. C4417-3)

| Reference | wt. % Cu | wt. % Ni |
|-----------|-------------|-------------|
| B18, B21 | 0.14 | 0.62 |
| B22 | --- | 0.60 |
| Average | 0.14 | 0.61 |

- * The lower shell longitudinal welds also contained a different weld wire heat in the double U root area of the weld. Since the root weld chemistry is not more limiting than the above weld data, it was not utilized in the evaluations.

Table B-1 (Continued)

Intermediate Shell Plate, B5012-3 (Ht. C4377-2)

| Reference | wt. % Cu | wt. % Ni |
|-----------|-------------|-------------|
| B18, B23 | 0.11 | 0.66 |
| B20 | --- | 0.65 |
| Average | 0.11 | 0.66 |

Lower Shell Plate, B5013-1 (Ht. C4315-1)

| Reference | wt. % Cu | wt. % Ni |
|-----------|-------------|-------------|
| B18, B24 | 0.14 | 0.56 |
| B25 | --- | 0.59 |
| Average | 0.14 | 0.58 |

Lower Shell Plate, B5013-2 (Ht. C4374-2)

| Reference | wt. % Cu | wt. % Ni |
|-----------|-------------|-------------|
| B18, B26 | 0.10 | 0.52 |
| B27 | --- | 0.50 |
| Average | 0.10 | 0.51 |

Lower Shell Plate, B5013-3 (Ht. C4371-2)

| Reference | wt. % Cu | wt. % Ni |
|-----------|-------------|-------------|
| B18, B28 | 0.10 | 0.55 |
| B29 | --- | 0.54 |
| Average | 0.10 | 0.55 |

Table B-2
McGuire Unit 1 Reactor Vessel Toughness Table (Unirradiated)

| Material Description | Cu (%) * | Ni (%) * | I (°F) ^(B30) (a) |
|--|----------|----------|-----------------------------|
| Intermediate Shell Plate, B5012-1 | 0.11 | 0.61 | 34 |
| Intermediate Shell Plate, B5012-2 | 0.14 | 0.61 | 0 |
| Intermediate Shell Plate, B5012-3 | 0.11 | 0.66 | -13 |
| Lower Shell Plate, B5013-1 | 0.14 | 0.58 | 0 |
| Lower Shell Plate, B5013-2 | 0.10 | 0.51 | 30 |
| Lower Shell Plate, B5013-3 | 0.10 | 0.55 | 15 |
| Inter. Shell Longitudinal Welds, 2-442A, B & C | 0.20 | 0.87 | -50 |
| Lower Shell Longitudinal Welds, 3-442A, B & C | 0.22 | 0.86 | -50** |
| Circumferential Weld, 9-442 | 0.05 | 0.12 | -70 |

(a) Initial RT_{NDT} values were estimated per U.S. NRC Standard Review Plan. The initial RT_{NDT} values for the plates and welds are measured values, except for the lower shell longitudinal welds (which are generic values).

* Average values of copper and nickel as indicated in Table B-1.

** Diablo Canyon Unit 2 initial RT_{NDT} value. Justification can be found in Appendix D of this report.

Table B-3
Calculation of Chemistry Factors Using Surveillance Capsule Data

| Material | Capsule | Fluence | FF | ΔRT_{NDT} | $FF * \Delta RT_{NDT}$ | FF^2 |
|--|---|-------------------------|-------|-------------------|------------------------|--------|
| Inter. Shell Plate, B5012-1 (Longitudinal) | U | 4.719×10^{18} | 0.790 | 45 | 35.550 | 0.624 |
| | X | 1.4091×10^{19} | 1.095 | 45 | 49.275 | 1.199 |
| | V | 2.1858×10^{19} | 1.212 | 85 | 103.020 | 1.469 |
| Inter. Shell Plate, B5012-1 (Transverse) | U | 4.719×10^{18} | 0.790 | 50 | 39.500 | 0.624 |
| | X | 1.4091×10^{19} | 1.095 | 65 | 71.175 | 1.199 |
| | V | 2.1858×10^{19} | 1.212 | 85 | 103.020 | 1.469 |
| | Sum: | | | | 401.54 | 6.584 |
| | Chemistry Factor = $401.54 \div 6.584 = 61.0 \approx 61$ | | | | | |
| Intermediate Shell Longitudinal Welds, 2-442A, B & C | U | 4.719×10^{18} | 0.790 | 160 | 126.400 | 0.624 |
| | X | 1.4091×10^{19} | 1.095 | 165 | 180.675 | 1.199 |
| | V | 2.1858×10^{19} | 1.212 | 175 | 212.100 | 1.469 |
| | Sum: | | | | 519.175 | 3.292 |
| | Chemistry Factor = $519.175 \div 3.292 = 157.7 \approx 158$ | | | | | |

Using Diablo Canyon Unit 2 Surveillance Data

| Material | Capsule | Fluence | FF | ΔRT_{NDT} | $FF * \Delta RT_{NDT}$ | FF^2 |
|---|---------|-----------------------|-------|-------------------|------------------------|--------|
| Lower Shell Longitudinal Welds 3-442A, B, C | U | 3.51×10^{18} | 0.711 | 174 | 123.7 | 0.506 |
| | X | 8.87×10^{18} | 0.966 | 204.2 | 197.3 | 0.933 |
| | Sum: | | | | 321.0 | 1.439 |
| Chemistry Factor = $321.0 \div 1.439 = 223.1$ | | | | | | |

Justification for the use of this data can be found in Appendix D of this report.

Table B-4

Summary of Adjusted Reference Temperatures (ART's) at 1/4-t and 3/4-t Locations for 16 EFPY

| Component | 16 EFPY RT _{NDT} | |
|---|---------------------------|------------|
| | 1/4-t (°F) | 3/4-t (°F) |
| Intermediate Shell Plate, B5012-1 | 131.61 | 111.41 |
| Using Surveillance Capsule Data** | 103.30 | 86.69 |
| Intermediate Shell Plate, B5012-2 | 119.95 | 92.65 |
| Intermediate Shell Plate, B5012-3 | 85.21 | 64.82 |
| Lower Shell Plate, B5013-1 | 118.96 | 91.98 |
| Lower Shell Plate, B5013-2 | 119.73 | 102.03* |
| Lower Shell Plate, B5013-3 | 104.73 | 87.03 |
| Inter. Shell Longitudinal Weld, 2-442A | 157.93 | 105.89 |
| Using Surveillance Capsule Data** | 95.56 | 55.29 |
| Inter. Shell Longitudinal Welds, 2-442B & C | 162.92 | 110.02 |
| Using Surveillance Capsule Data** | 99.42 | 58.48 |
| Lower Shell Longitudinal Weld, 3-442B | 165.45 | 112.03 |
| Using Surveillance Capsule Data*** | 143.99 | 87.13 |
| Lower Shell Longitudinal Welds 3-442A & C | 170.57 | 116.27 |
| Using Surveillance Capsule Data*** | 149.45* | 91.65 |
| Circumferential Weld, 9-442 | -1.76 | -23.43 |

* These ART numbers were used to generate heatup and cooldown curves.

** Numbers were calculated using a chemistry factor (CF) based on McGuire Unit 1 surveillance capsule data.

*** Numbers were calculated using a chemistry factor (CF) based on Diablo Canyon Unit 2 surveillance capsule data. Justification for the use of this data can be found in Appendix D of this report.

Table B-5
 Calculation of Adjusted Reference Temperatures at 16 EFPY for the Limiting McGuire Unit 1
 Reactor Vessel Materials - Lower Shell Longitudinal Welds 3-442A & C
 and Lower Shell Plate B5013-2

| Parameter | Values | |
|---|--|------------------------------|
| Operating Time | 16 EFPY | |
| Material | Lower Shell Longitudinal Welds, 3-442A&C | Lower Shell Plate B5013-2 |
| Location | 1/4-t | 3/4-t |
| Chemistry Factor, CF (°F) | 223.1 | 65.0 |
| Fluence, f (10 ¹⁹ n/cm ²) ^(a) | 0.4348 | 0.2134 |
| Fluence Factor, ff | 0.768 | 0.585 |
| $\Delta RT_{NDT} = CF \times ff$ (°F) | 171.448 | 38.028 |
| Initial RT _{NDT} , I (°F) | -50 | 30 |
| Margin, M (°F) ^(b) | 28 | 34 |
| Adjusted Reference Temperature, (°F) per Regulatory Guide 1.99, Revision 2 | 149.45 | 102.03 |

(a) Fluence, f, is based upon f_{surf} (10¹⁹ n/cm², E>1 MeV) = 0.7295 at 16 EFPY for the lower shell longitudinal welds. Fluence, f, is based upon f_{surf} (10¹⁹ n/cm², E>1 MeV) = 1.008 at 16 EFPY for the lower shell plate. The McGuire Unit 1 reactor vessel wall thickness is 8.625 inches at the beltline region.

(b) Margin is calculated as, $M = 2 \sqrt{\sigma_I^2 + \sigma_\Delta^2}$.

σ_I = standard deviation for the initial RT_{NDT}: $\sigma_I = 0$ when I is a measured value
 $\sigma_I = 17$ when I is a generic value

For plates and forgings: $\sigma_\Delta = 17$ when surveillance capsule data is not used
 $\sigma_\Delta = 8.5$ when surveillance capsule data is used

For welds: $\sigma_\Delta = 28$ when surveillance capsule data is not used
 $\sigma_\Delta = 14$ when surveillance capsule data is used

σ_Δ not to exceed 0.5* ΔRT_{NDT} per Regulatory Guide 1.99, Revision 2.

MATERIAL PROPERTY BASIS

LIMITING MATERIALS: LOWER SHELL LONGITUDINAL WELDS 3-442A & C AND
LOWER SHELL PLATE B5013-2

LIMITING ART AT 16 EFPY: 1/4-t, 149.5°F
3/4-t, 102.0°F

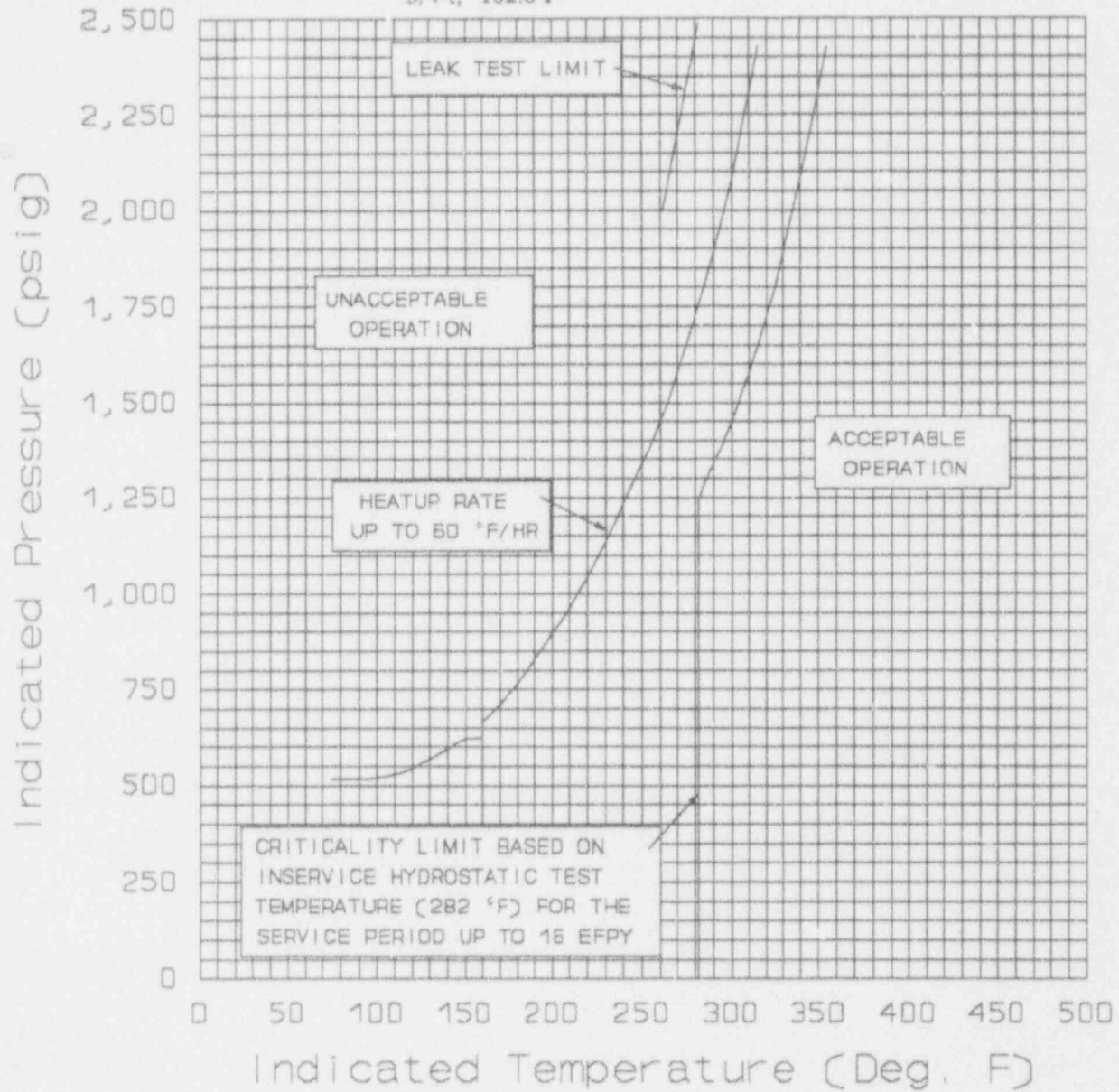


Figure B-1

McGuire Unit 1 Reactor Coolant System Heatup Limitations (Heatup Rate of 60°F/hr) Applicable for the First 16 EFPY (Without Margins for Instrumentation Errors)

MATERIAL PROPERTY BASIS

LIMITING MATERIALS: LOWER SHELL LONGITUDINAL WELDS 3-442A & C AND
LOWER SHELL PLATE B5013-2

LIMITING ART AT 16 EFY: 1/4-t, 149.5°F
3/4-t, 102.0°F

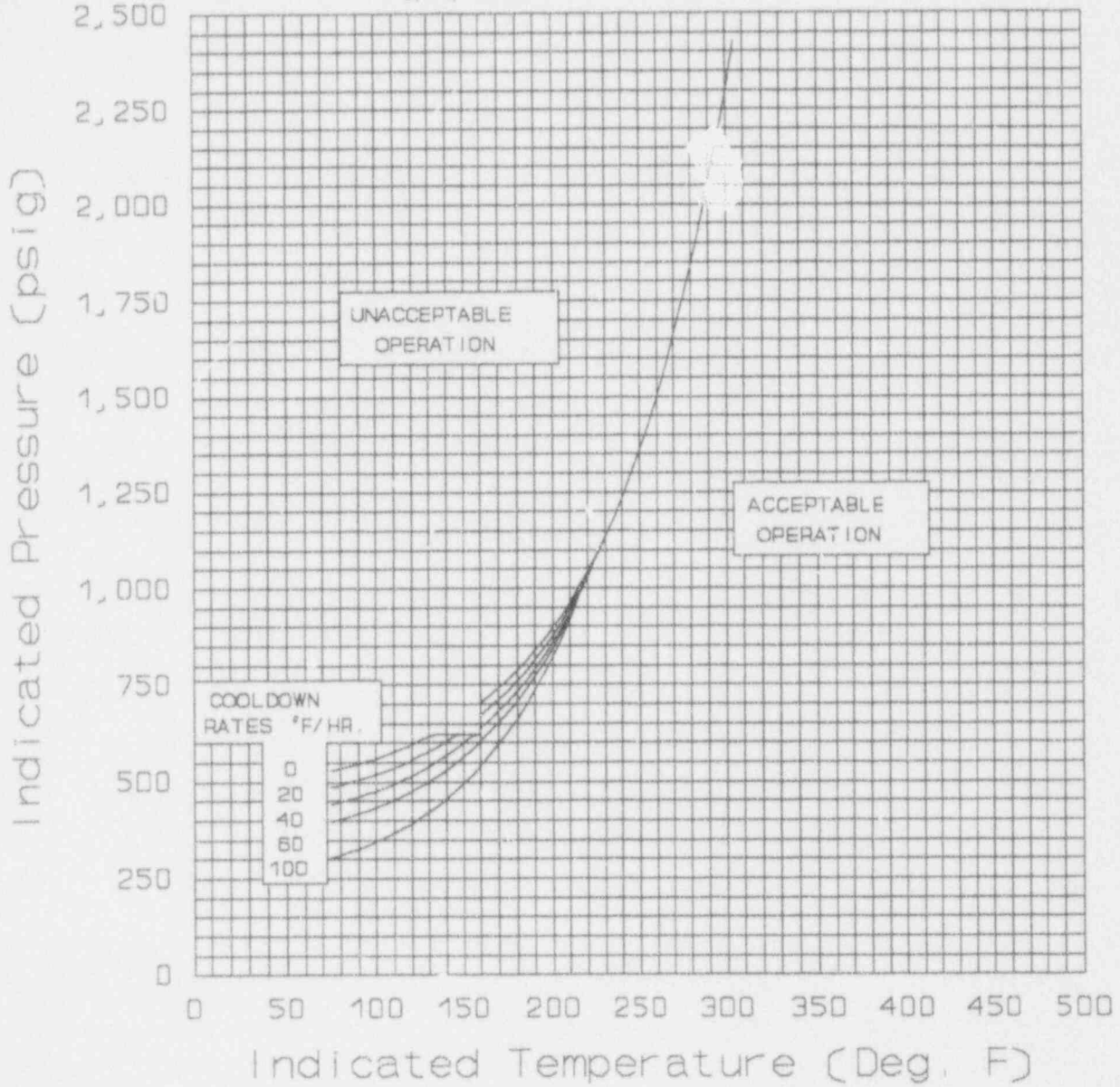


Figure B-2

McGuire Unit 1 Reactor Coolant System Cooldown Limitations (Cooldown Rates up to 100°F/hr) Applicable for the First 16 EFY (Without Margins for Instrumentation Errors)

B-6. REFERENCES

- [B1] Regulatory Guide 1.99, Revision 2, "Radiation Embrittlement of Reactor Vessel Materials", U.S. Nuclear Regulatory Commission, May, 1988.
- [B2] "Fracture Toughness Requirements", Branch Technical Position MTEB 5-2, Chapter 5.3.2 in Standard Review Plan for the Review of Safety Analysis Reports for Nuclear Power Plants, LWR Edition, NUREG-0800, 1981.
- [B3] ASME Boiler and Pressure Vessel Code, Section XI, Division 1 - Appendixes, "Rules for Inservice Instruction of Nuclear Power Plant Components, Appendix G, Fracture Toughness Criteria for Protection Against Failure", pp. 401-411, 1989 Edition, American Society of Mechanical Engineers, New York, 1989.
- [B4] Code of Federal Regulations, 10CFR50, Appendix G, "Fracture Toughness Requirements", U.S. Nuclear Regulatory Commission, Washington, D.C., Federal Register, Vol. 48 No. 104, May 27, 1983.
- [B5] WCAP-9195, "Duke Power Company William B. McGuire Unit No. 1 Reactor Vessel Radiation Surveillance Program", J. A. Davidson and S. E. Yanichko, November 1977.
- [B6] WCAP-10786, "Analysis of Capsule U from the Duke Power Company McGuire Unit 1 Reactor Vessel Radiation Surveillance Program", S. E. Yanichko, et al., February 1985.
- [B7] Combustion Engineering, Inc., Metallurgical Research & Development, "Chemical Analysis of Wire-Flux Test Coupon", Job Number D32255, 8-15-72.
- [B8] WCAP-8819, "Central Nuclear de Almaraz, Almaraz Unit No. 1 Reactor Vessel Radiation Surveillance Program", R. A. Smith, et al., December 1976.
- [B9] Combustion Engineering, Inc., Welding Material Certification and Release for Section III, "Chemical Analysis of Test Weld Sample", August 12, 1969.
- [B10] Combustion Engineering, Inc., Metallurgical Research & Development, "Chemical Analysis of Wire-Flux Test Coupon", Job Number X-32255, 10-14-69.
- [B11] WCAP-8783, "Pacific Gas and Electric Company Diablo Canyon Unit No. 2 Reactor Vessel Radiation Surveillance Program", J. A. Davidson and S. E. Yanichko, December 1976.
- [B12] WCAP-10472, "Evaluation of Diablo Canyon Units 1 and 2 Reactor Vessel Beltline Weld Chemistry", S. E. Yanichko and M. K. Kunka, September 1983. (Proprietary)
- [B13] WCAP-11851, "Analysis of Capsule U from the Pacific Gas and Electric Company Diablo Canyon Unit 2 Reactor Vessel Radiation Surveillance Program", S. E. Yanichko, et al., May 1988.

- [B14] WCAP-12811, "Analysis of Capsule X from the Pacific Gas and Electric Company Diablo Canyon Unit 2 Reactor Vessel Radiation Surveillance Program", E. Terek, et al., December 1990.
- [B15] Combustion Engineering, Inc., Metallurgical Research & Development, "Chemical Analysis of Wire-Flux Test Coupon", 2-10-70.
- [B16] WCAP-8457, "Duquesne Light Company Beaver Valley Unit No. 1 Reactor Vessel Radiation Surveillance Program", J. A. Davidson, et al., October 1974.
- [B17] Combustion Engineering, Inc., Welding Material Certification and Release for Section III, "Chemical Analysis of Test Weld Sample", Sample No. D-7279, August 12, 1969.
- [B18] Lukens Steel Company Letter from John A. Soltesz to S. E. Yanichko dated December 6, 1973, Ladle Copper Analysis for Lukens Vessel Materials.
- [B19] Combustion Engineering, Inc., Metallurgical Research & Development Department, "Materials Certification Report", Job No. V-70333-001, March 5, 1969.
- [B20] Lukens Steel Company, "Test Certificate", Mill Order No. 20241-2, corrected copy dated 7-23-68.
- [B21] Combustion Engineering, Inc., Metallurgical Research & Development Department, "Materials Certification Report", Job No. V-70333-004, corrected copy dated 5/4/70.
- [B22] Lukens Steel Company, "Test Certificate", Mill Order No. 20241-2, dated 7-24-68.
- [B23] Combustion Engineering, Inc., Metallurgical Research & Development Department, "Materials Certification Report", Job No. V-70333-007, corrected copy dated 3/31/70.
- [B24] Combustion Engineering, Inc., Metallurgical Research & Development Department, "Materials Certification Report", Job No. V-70334-001, September 4, 1969.
- [B25] Lukens Steel Company, "Test Certificate", Mill Order No. 20241-3, dated 5-25-68.
- [B26] Combustion Engineering, Inc., Metallurgical Research & Development Department, "Materials Certification Report", Job No. V-70334-005, September 4, 1969.
- [B27] Lukens Steel Company, "Test Certificate", Mill Order No. 20241-3, dated 7-10-68.
- [B28] Combustion Engineering, Inc., Metallurgical Research & Development Department, "Materials Certification Report", Job No. V-70334-009, September 4, 1969.
- [B29] Lukens Steel Company, "Test Certificate", Mill Order No. 20241-3, dated 6-24-68.
- [B30] WCAP-12354, "Analysis of Capsule X from the Duke Power Company McGuire Unit 1 Reactor Vessel Radiation Surveillance Programs", S.E. Yanichko, et al., August 1989.
- [B31] Westinghouse Electric Corporation Nuclear Service Division CMT - Analytical Laboratory, Waltz Mill Site, Analytical Request #15211, Alloy Analysis - Steel, Duke Power Company McGuire Nuclear Plant Unit 1, Lawrence Kardos, November 15, 1993.

- [B32] WCAP-7924-A, "Basis for Heatup and Cooldown Limit Curves", W. S. Hazelton, et al., April 1975.
- [B33] Fluence data given in Section 6.0 of this report.
- [B34] WCAP-10867, "Analysis of Capsule U from the Duquesne Light Company Beaver Valley Unit 1 Reactor Vessel Radiation Surveillance Program", R. S. Boggs, et al., September 1985.

ATTACHMENT B1

DATA POINTS FOR HEATUP AND COOLDOWN CURVES
(WITHOUT MARGINS FOR INSTRUMENTATION ERRORS)

McGuire Unit 1 Heatup and Cooldown Data Without Margins at 16 EFPY

Cooldown Curves

| Steady State | | 20 DEG CD | | 40 DEG CD | | 60 DEG CD | | 100 DEG CD | |
|--------------|---------|-----------|---------|-----------|---------|-----------|---------|------------|---------|
| T | P | T | P | T | P | T | P | T | P |
| 75 | 529.22 | 75 | 486.15 | 75 | 442.18 | 75 | 397.27 | 75 | 304.39 |
| 80 | 534.63 | 80 | 491.75 | 80 | 447.94 | 80 | 403.36 | 80 | 311.12 |
| 85 | 540.46 | 85 | 497.81 | 85 | 454.26 | 85 | 409.98 | 85 | 318.48 |
| 90 | 546.61 | 90 | 504.23 | 90 | 461.06 | 90 | 417.06 | 90 | 326.42 |
| 95 | 553.35 | 95 | 511.27 | 95 | 468.44 | 95 | 424.83 | 95 | 335.13 |
| 100 | 560.58 | 100 | 518.83 | 100 | 476.38 | 100 | 433.20 | 100 | 344.55 |
| 105 | 568.37 | 105 | 527.00 | 105 | 484.99 | 105 | 442.29 | 105 | 354.83 |
| 110 | 576.73 | 110 | 535.78 | 110 | 494.25 | 110 | 452.02 | 110 | 365.93 |
| 115 | 585.73 | 115 | 545.16 | 115 | 504.17 | 115 | 462.64 | 115 | 377.96 |
| 120 | 595.27 | 120 | 555.35 | 120 | 514.95 | 120 | 474.09 | 120 | 391.01 |
| 125 | 605.67 | 125 | 566.34 | 125 | 526.61 | 125 | 486.49 | 125 | 405.19 |
| 130 | 616.85 | 130 | 578.16 | 130 | 539.15 | 130 | 499.76 | 130 | 420.44 |
| 135 | 621.00 | 135 | 590.89 | 135 | 552.60 | 135 | 514.21 | 135 | 437.05 |
| 140 | 621.00 | 140 | 604.48 | 140 | 567.18 | 140 | 529.78 | 140 | 454.90 |
| 145 | 621.00 | 145 | 619.25 | 145 | 582.92 | 145 | 546.50 | 145 | 474.32 |
| 150 | 621.00 | 150 | 621.00 | 150 | 599.74 | 150 | 564.63 | 150 | 495.28 |
| 155 | 621.00 | 155 | 621.00 | 155 | 618.02 | 155 | 584.22 | 155 | 517.88 |
| 160 | 621.00 | 160 | 621.00 | 160 | 621.00 | 160 | 605.18 | 160 | 542.36 |
| 160 | 703.60 | 160 | 670.48 | 160 | 637.67 | 165 | 627.96 | 165 | 568.72 |
| 165 | 722.15 | 165 | 690.27 | 165 | 658.75 | 170 | 652.33 | 170 | 597.14 |
| 170 | 741.90 | 170 | 711.43 | 170 | 681.56 | 175 | 678.79 | 175 | 627.99 |
| 175 | 763.35 | 175 | 734.34 | 175 | 706.02 | 180 | 707.11 | 180 | 661.10 |
| 180 | 786.34 | 180 | 758.85 | 180 | 732.46 | 185 | 737.79 | 185 | 696.86 |
| 185 | 810.96 | 185 | 785.35 | 185 | 760.83 | 190 | 770.73 | 190 | 735.54 |
| 190 | 837.35 | 190 | 813.75 | 190 | 791.31 | 195 | 806.18 | 195 | 777.17 |
| 195 | 865.95 | 195 | 844.24 | 195 | 824.34 | 200 | 844.33 | 200 | 821.98 |
| 200 | 896.48 | 200 | 877.21 | 200 | 859.71 | 205 | 885.44 | 205 | 870.33 |
| 205 | 929.45 | 205 | 912.55 | 205 | 897.76 | 210 | 929.85 | 210 | 922.33 |
| 210 | 964.76 | 210 | 950.51 | 210 | 938.66 | 215 | 977.52 | 215 | 978.40 |
| 215 | 1002.71 | 215 | 991.32 | 215 | 982.71 | 220 | 1028.57 | 220 | 1038.64 |
| 220 | 1043.42 | 220 | 1035.18 | 220 | 1030.07 | 225 | 1083.78 | | |
| 225 | 1087.17 | 225 | 1082.36 | 225 | 1081.05 | | | | |
| 230 | 1134.18 | 230 | 1133.06 | | | | | | |
| 235 | 1184.70 | | | | | | | | |
| 240 | 1238.98 | | | | | | | | |
| 245 | 1297.13 | | | | | | | | |
| 250 | 1359.59 | | | | | | | | |
| 255 | 1426.60 | | | | | | | | |
| 260 | 1498.41 | | | | | | | | |
| 265 | 1575.51 | | | | | | | | |
| 270 | 1658.07 | | | | | | | | |
| 275 | 1746.46 | | | | | | | | |
| 280 | 1841.27 | | | | | | | | |
| 285 | 1942.98 | | | | | | | | |
| 290 | 2051.60 | | | | | | | | |
| 295 | 2167.68 | | | | | | | | |
| 300 | 2291.83 | | | | | | | | |
| 305 | 2424.34 | | | | | | | | |

Heatup Curve

| 60 DEG HU | | Criticality Limit | |
|-----------|---------|-------------------|---------|
| T | P | T | P |
| 75 | 517.92 | 282 | 0.00 |
| 80 | 517.92 | 282 | 525.46 |
| 85 | 517.92 | 282 | 520.40 |
| 90 | 517.92 | 282 | 517.92 |
| 95 | 517.96 | 282 | 517.96 |
| 100 | 519.92 | 282 | 519.92 |
| 105 | 523.85 | 282 | 523.85 |
| 110 | 529.37 | 282 | 529.37 |
| 115 | 536.56 | 282 | 536.56 |
| 120 | 545.06 | 282 | 545.06 |
| 125 | 555.17 | 282 | 555.17 |
| 130 | 566.65 | 282 | 566.65 |
| 135 | 579.58 | 282 | 579.58 |
| 140 | 593.78 | 282 | 593.78 |
| 145 | 609.59 | 282 | 609.59 |
| 150 | 621.00 | 282 | 626.88 |
| 155 | 621.00 | 282 | 645.61 |
| 160 | 621.00 | 282 | 621.00 |
| 160 | 666.10 | 282 | 666.10 |
| 165 | 688.30 | 282 | 688.30 |
| 170 | 712.19 | 282 | 712.19 |
| 175 | 738.12 | 282 | 738.12 |
| 180 | 765.99 | 282 | 765.99 |
| 185 | 795.97 | 282 | 795.97 |
| 190 | 828.44 | 282 | 828.44 |
| 195 | 863.26 | 282 | 863.26 |
| 200 | 896.48 | 282 | 896.48 |
| 205 | 929.45 | 282 | 929.45 |
| 210 | 964.76 | 282 | 964.76 |
| 215 | 1002.71 | 282 | 1002.71 |
| 220 | 1043.42 | 282 | 1043.42 |
| 225 | 1087.17 | 282 | 1087.17 |
| 230 | 1134.18 | 282 | 1134.18 |
| 235 | 1184.70 | 282 | 1184.70 |
| 240 | 1238.98 | 282 | 1238.98 |
| 245 | 1287.52 | 285 | 1287.52 |
| 250 | 1337.80 | 290 | 1337.80 |
| 255 | 1391.53 | 295 | 1391.53 |
| 260 | 1449.24 | 300 | 1449.24 |
| 265 | 1510.82 | 305 | 1510.82 |
| 270 | 1577.19 | 310 | 1577.19 |
| 275 | 1647.73 | 315 | 1647.73 |
| 280 | 1723.83 | 320 | 1723.83 |
| 285 | 1805.03 | 325 | 1805.03 |
| 290 | 1891.36 | 330 | 1891.36 |
| 295 | 1984.71 | 335 | 1984.71 |
| 300 | 2084.23 | 340 | 2084.23 |
| 305 | 2190.26 | 345 | 2190.26 |
| 310 | 2303.62 | 350 | 2303.62 |
| 315 | 2424.65 | 355 | 2424.65 |

Leak Test Data

| T | P |
|-----|------|
| 261 | 2000 |
| 282 | 2435 |

B-25

ATTACHMENT B2

HEATUP AND COOLDOWN CURVES AND DATA POINTS

(WITH MARGINS OF 12°F AND 30 PSIG FOR INSTRUMENTATION ERRORS)

MATERIAL PROPERTY BASIS

LIMITING MATERIALS: LOWER SHELL LONGITUDINAL WELDS 3-442A & C AND
LOWER SHELL PLATE B5013-2

LIMITING ART AT 16 EFPY: 1/4-t, 149.5°F
3/4-t, 102.0°F

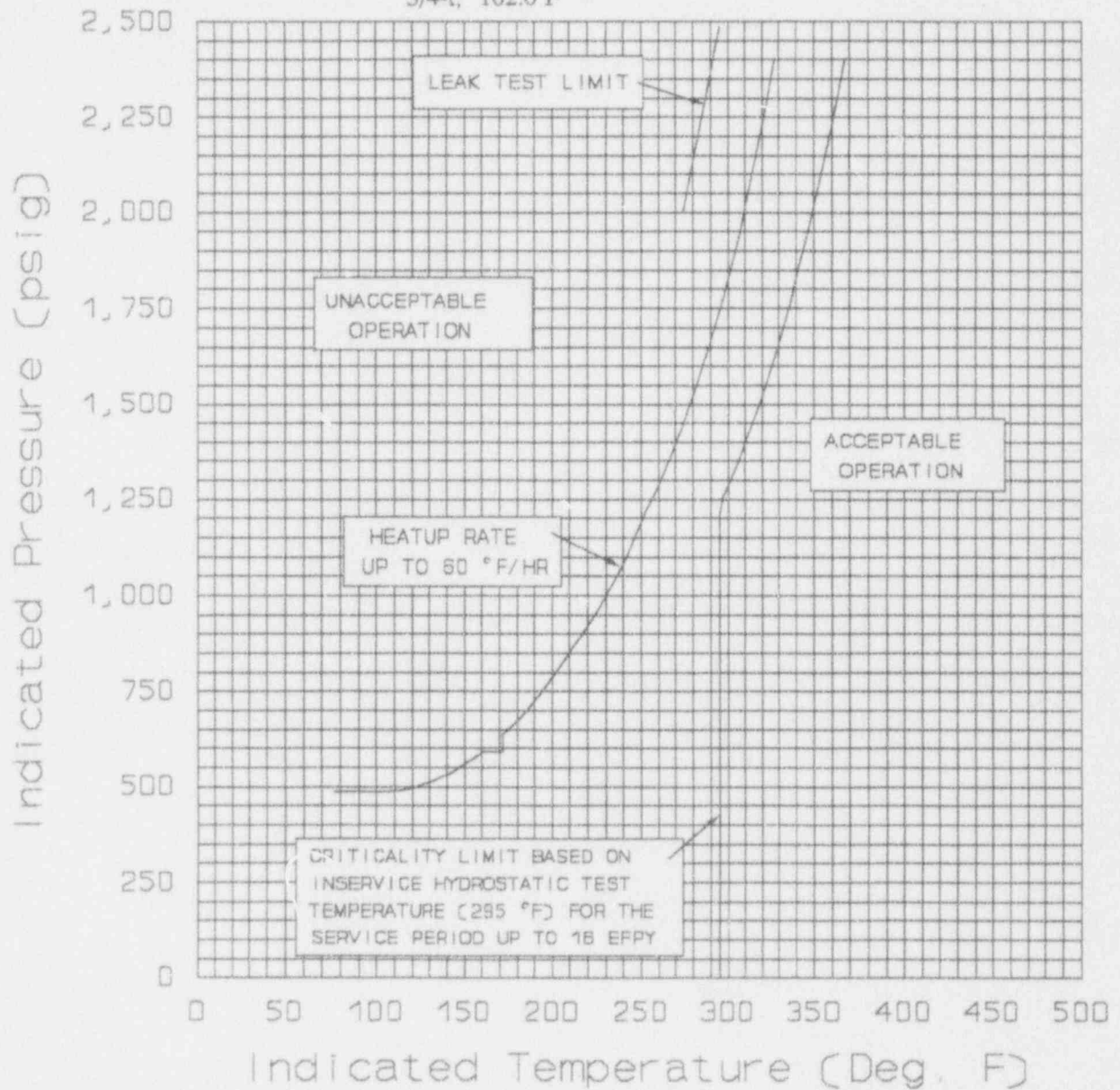


Figure B-3 McGuire Unit 1 Reactor Coolant System Heatup Limitations (Heatup Rate of 60°F/hr) Applicable for the First 16 EFPY (With Margins of 12°F and 30 psig for Instrumentation Errors)

MATERIAL PROPERTY BASIS

LIMITING MATERIALS: LOWER SHELL LONGITUDINAL WELDS 3-442A & C AND LOWER SHELL PLATE B5013-2

LIMITING ART AT 16 EFPY: 1/4-t, 149.5°F
3/4-t, 102.0°F

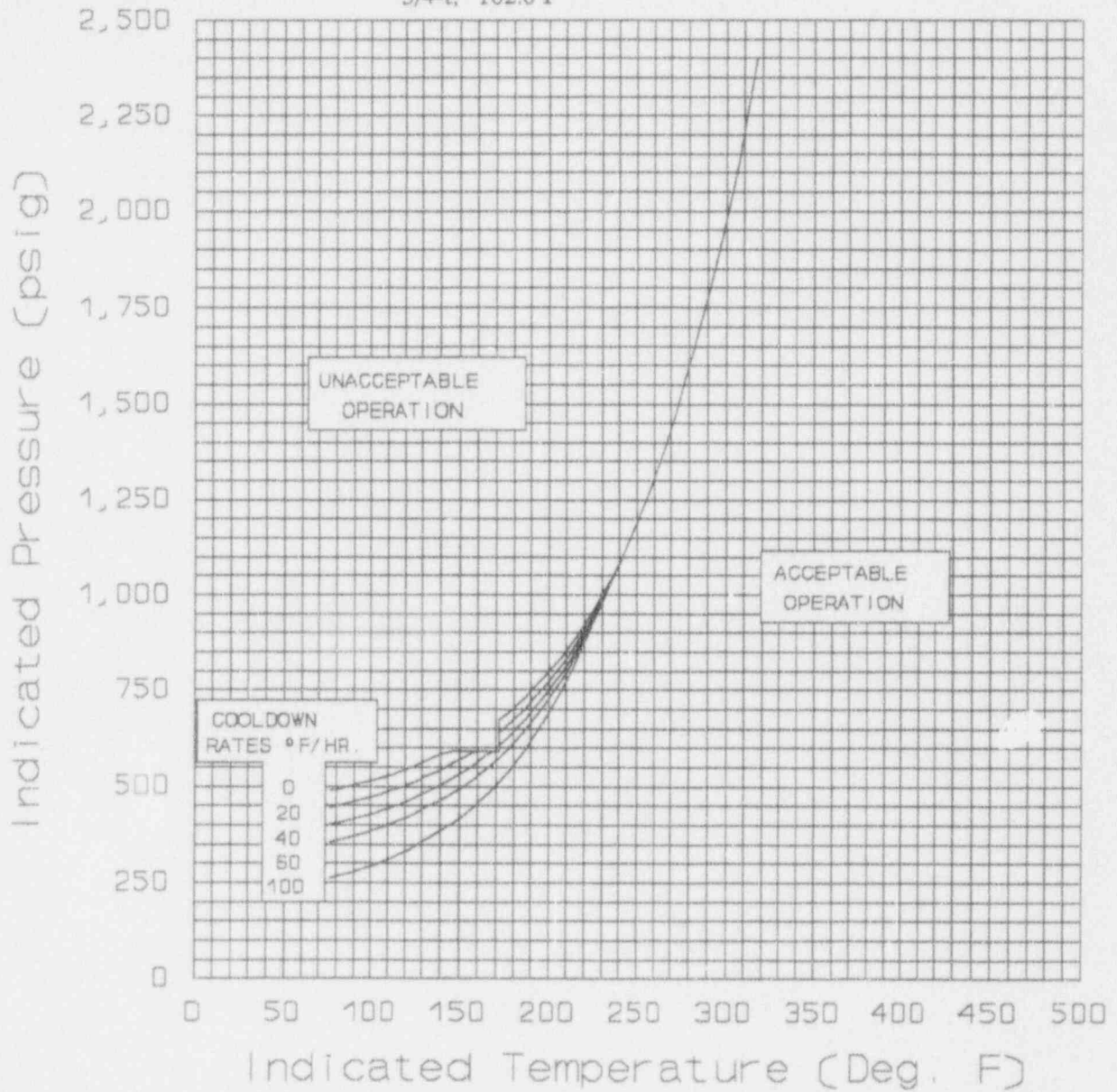


Figure B-4

McGuire Unit 1 Reactor Coolant System Cooldown Limitations (Cooldown Rates up to 100°F/hr) Applicable for the First 16 EFPY (With Margins of 12°F and 30 psig for Instrumentation Errors)

McGuire Unit 1 Heatup and Cooldown Data With Margins at 16 EFPY

Cooldown Curves

Heatup Curve

Leak Test Data

| Steady State | | 20 DEG CD | | 40 DEG CD | | 60 DEG CD | | 100 DFG CD | | 60 DEG HU | | Criticality Limit | | T | P |
|--------------|---------|-----------|---------|-----------|---------|-----------|---------|------------|---------|-----------|---------|-------------------|---------|-----|------|
| T | P | T | P | T | P | T | P | T | P | T | P | T | P | T | P |
| 77 | 489.49 | 77 | 446.12 | 77 | 401.80 | 77 | 356.47 | 77 | 262.54 | 77 | 487.92 | 295 | 0.00 | 274 | 2000 |
| 82 | 494.18 | 82 | 450.93 | 82 | 406.77 | 82 | 361.64 | 82 | 268.19 | 82 | 487.92 | 295 | 494.18 | 295 | 2485 |
| 87 | 499.22 | 87 | 456.15 | 87 | 412.18 | 87 | 367.27 | 87 | 274.39 | 87 | 487.92 | 295 | 499.22 | | |
| 92 | 504.63 | 92 | 461.75 | 92 | 417.94 | 92 | 373.36 | 92 | 281.12 | 92 | 487.92 | 295 | 495.46 | | |
| 97 | 510.46 | 97 | 467.81 | 97 | 424.26 | 97 | 379.98 | 97 | 288.48 | 97 | 487.92 | 295 | 490.40 | | |
| 102 | 516.61 | 102 | 474.23 | 102 | 431.06 | 102 | 387.06 | 102 | 296.42 | 102 | 487.92 | 295 | 487.92 | | |
| 107 | 523.35 | 107 | 481.27 | 107 | 438.44 | 107 | 394.83 | 107 | 305.13 | 107 | 487.96 | 295 | 487.96 | | |
| 112 | 530.58 | 112 | 488.83 | 112 | 446.38 | 112 | 403.20 | 112 | 314.55 | 112 | 489.92 | 295 | 489.92 | | |
| 117 | 538.37 | 117 | 497.00 | 117 | 454.99 | 117 | 412.29 | 117 | 324.83 | 117 | 493.85 | 295 | 493.85 | | |
| 122 | 546.73 | 122 | 505.78 | 122 | 464.25 | 122 | 422.02 | 122 | 335.93 | 122 | 499.37 | 295 | 499.37 | | |
| 127 | 555.73 | 127 | 515.16 | 127 | 474.17 | 127 | 432.64 | 127 | 347.96 | 127 | 506.56 | 295 | 506.56 | | |
| 132 | 565.27 | 132 | 525.35 | 132 | 484.95 | 132 | 444.09 | 132 | 361.01 | 132 | 515.06 | 295 | 515.06 | | |
| 137 | 575.67 | 137 | 536.34 | 137 | 496.61 | 137 | 456.49 | 137 | 375.19 | 137 | 525.17 | 295 | 525.17 | | |
| 142 | 586.85 | 142 | 548.16 | 142 | 509.15 | 142 | 469.76 | 142 | 390.44 | 142 | 536.65 | 295 | 536.65 | | |
| 147 | 591.00 | 147 | 560.89 | 147 | 522.60 | 147 | 484.21 | 147 | 407.05 | 147 | 549.58 | 295 | 549.58 | | |
| 152 | 591.00 | 152 | 574.48 | 152 | 537.18 | 152 | 499.78 | 152 | 424.90 | 152 | 563.78 | 295 | 563.78 | | |
| 157 | 591.00 | 157 | 589.25 | 157 | 552.92 | 157 | 516.50 | 157 | 444.32 | 157 | 579.59 | 295 | 579.59 | | |
| 162 | 591.00 | 162 | 591.00 | 162 | 569.74 | 162 | 534.63 | 162 | 465.28 | 162 | 591.00 | 295 | 596.88 | | |
| 167 | 591.00 | 167 | 591.00 | 167 | 588.02 | 167 | 554.22 | 167 | 487.88 | 167 | 591.00 | 295 | 615.61 | | |
| 172 | 591.00 | 172 | 591.00 | 172 | 591.00 | 172 | 575.18 | 172 | 512.36 | 172 | 591.00 | 295 | 591.00 | | |
| 172 | 673.60 | 172 | 640.48 | 172 | 607.67 | 177 | 597.96 | 177 | 538.72 | 172 | 636.10 | 295 | 636.10 | | |
| 177 | 692.15 | 177 | 660.27 | 177 | 628.75 | 182 | 622.33 | 182 | 567.14 | 177 | 658.30 | 295 | 658.30 | | |
| 182 | 711.90 | 182 | 681.43 | 182 | 651.56 | 187 | 648.79 | 187 | 597.99 | 182 | 682.19 | 295 | 682.19 | | |
| 187 | 733.35 | 187 | 704.34 | 187 | 676.02 | 192 | 677.11 | 192 | 631.10 | 187 | 708.12 | 295 | 708.12 | | |
| 192 | 756.34 | 192 | 728.85 | 192 | 702.46 | 197 | 707.79 | 197 | 666.86 | 192 | 735.99 | 295 | 735.99 | | |
| 197 | 780.96 | 197 | 755.35 | 197 | 730.83 | 202 | 740.73 | 202 | 705.54 | 197 | 765.97 | 295 | 765.97 | | |
| 202 | 807.35 | 202 | 783.75 | 202 | 761.31 | 207 | 776.18 | 207 | 747.17 | 202 | 798.44 | 295 | 798.44 | | |
| 207 | 835.95 | 207 | 814.24 | 207 | 794.34 | 212 | 814.33 | 212 | 791.98 | 207 | 833.26 | 295 | 833.26 | | |
| 212 | 866.48 | 212 | 847.21 | 212 | 829.71 | 217 | 855.44 | 217 | 840.33 | 212 | 866.48 | 295 | 866.48 | | |
| 217 | 899.45 | 217 | 882.55 | 217 | 867.76 | 222 | 899.85 | 222 | 892.33 | 217 | 899.45 | 295 | 899.45 | | |
| 222 | 934.76 | 222 | 920.51 | 222 | 908.66 | 227 | 947.52 | 227 | 948.40 | 222 | 934.76 | 295 | 934.76 | | |
| 227 | 972.71 | 227 | 961.32 | 227 | 952.71 | 232 | 998.57 | 232 | 1008.64 | 227 | 972.71 | 295 | 972.71 | | |
| 232 | 1013.42 | 232 | 1005.18 | 232 | 1000.07 | 237 | 1053.78 | | | 232 | 1013.42 | 295 | 1013.42 | | |
| 237 | 1057.17 | 237 | 1052.36 | 237 | 1051.05 | | | | | 237 | 1057.17 | 295 | 1057.17 | | |
| 242 | 1104.18 | 242 | 1103.06 | | | | | | | 242 | 1104.18 | 295 | 1104.18 | | |
| 247 | 1154.70 | | | | | | | | | 247 | 1154.70 | 295 | 1154.70 | | |
| 252 | 1208.98 | | | | | | | | | 252 | 1208.98 | 295 | 1208.98 | | |
| 257 | 1267.13 | | | | | | | | | 257 | 1257.52 | 297 | 1257.52 | | |
| 262 | 1329.59 | | | | | | | | | 262 | 1307.80 | 302 | 1307.80 | | |
| 267 | 1396.60 | | | | | | | | | 267 | 1361.53 | 307 | 1361.53 | | |
| 272 | 1468.41 | | | | | | | | | 272 | 1419.24 | 312 | 1419.24 | | |
| 277 | 1545.51 | | | | | | | | | 277 | 1480.82 | 317 | 1480.82 | | |
| 282 | 1628.07 | | | | | | | | | 282 | 1547.19 | 322 | 1547.19 | | |
| 287 | 1716.46 | | | | | | | | | 287 | 1617.73 | 327 | 1617.73 | | |
| 292 | 1811.27 | | | | | | | | | 292 | 1693.83 | 332 | 1693.83 | | |
| 297 | 1912.98 | | | | | | | | | 297 | 1775.03 | 337 | 1775.03 | | |
| 302 | 2021.60 | | | | | | | | | 302 | 1861.86 | 342 | 1861.86 | | |
| 307 | 2137.68 | | | | | | | | | 307 | 1954.71 | 347 | 1954.71 | | |
| 312 | 2261.83 | | | | | | | | | 312 | 2054.23 | 352 | 2054.23 | | |
| 317 | 2394.34 | | | | | | | | | 317 | 2160.26 | 357 | 2160.26 | | |
| | | | | | | | | | | 322 | 2273.62 | 362 | 2273.62 | | |
| | | | | | | | | | | 327 | 2394.65 | 367 | 2394.65 | | |

APPENDIX C

Upper Shelf Energy Evaluation

Background:

The low upper shelf Charpy energy concern is associated with the determination of acceptable reactor vessel toughness when the vessel is operating at normal temperatures of 525°F or higher (the "upper shelf" of measured fracture toughness).

In 1973, in an effort to improve the quality of reactor pressure vessel integrity and to base the assessment of vessel integrity on a theoretical rather than an empirical basis, the concept of fracture mechanics techniques was implemented through ASME activities and NRC regulation. These requirements are included in 10CFR50, Appendix G, "Fracture Toughness Requirements". 10CFR50 Appendix G requires utilities to submit an analysis at least 3 years prior to the time that the upper shelf energy of any of the reactor vessel material is predicted to drop below 50 ft-lb as measured by Charpy V-notch specimen testing. One source of the irradiated materials that can be used to make this prediction on a plant specific basis is the reactor vessel surveillance capsule program. The surveillance capsules contain material identical to or representative of the critical reactor vessel materials that would be irradiated during plant operation. The surveillance capsules are attached inside the reactor vessel at locations designed to provide a higher irradiation rate than the reactor vessel itself, thus providing an irradiation "lead" factor that allows for prediction of future vessel irradiation damage.

There are three methods that can be applied to estimate the upper shelf energy:

- o Use of Revision 2 of Regulatory Criteria 1.99;
- o Use of plant specific surveillance capsule data; and
- o Use of alternative industry trend curves.

In the event that the 50 ft-lb requirement cannot be satisfied as stated in 10CFR50, Appendix G, or by alternative procedures acceptable to the NRC, a reactor may continue to operate provided all the following requirements of 10CFR50, Appendix G, paragraph V.C are satisfied:

- I. A volumetric examination of 100 percent of the beltline materials that do not satisfy the requirement of Section V.B of Appendix G is made, and any flaws are characterized according to Section XI of the ASME Code and as otherwise specified by the Director, Office of Nuclear Reactor Regulation.

2. Additional evidence of the fracture toughness of the beltline materials after exposure to neutron irradiation must be obtained from results of supplemental fracture toughness tests.
3. An analysis is performed that conservatively demonstrates, making appropriate allowances for all uncertainties, the existence of equivalent margins of safety for continued operation.

The issue of low upper shelf toughness has been a subject of active concern with the NRC for several years. In 1981, NUREG 0774 was issued. This document suggested an analysis procedure for determining the margins of safety present in reactor vessels. However, no definite criteria for acceptance margins were given. In 1982 a formal request was issued to the ASME Code Section XI committee to develop more specific criteria. In 1989 the ASME completed development of alternative criteria to define acceptable reactor vessel integrity when the Charpy upper shelf energy drops below 50 ft-lb. These criteria were transmitted to the NRC for their evaluation and incorporation into the regulations governing reactor vessel integrity.

Methodology:

The methodology presented in Regulatory Guide 1.99, Revision 2, was used to predict the changes in upper shelf energy of the McGuire Unit 1 reactor vessel beltline materials. For the materials contained in the reactor vessel surveillance program, the decrease in upper shelf energy was obtained by plotting the reduced plant surveillance data on Figure 2 of Regulatory Guide 1.99, Revision 2, and fitting the data with a line parallel to the existing lines as the upper bound of all the data. This line was used in preference to the existing graph to determine upper shelf energy values reported for the surveillance materials. For the beltline materials that were not in the surveillance program, the Charpy upper shelf energy was assumed to decrease as a function of fluence and copper content as indicated in Figure 2 of Regulatory Guide 1.99, Revision 2.

Results:

The results of the upper shelf energy calculations are given in Table C-1.

Conclusions:

Upper shelf energy values for each of the beltline region materials in the McGuire Unit 1 reactor vessel were calculated for 32 and 48 effective full power years (EFPY) of operation and the results presented in Table C-1. The results indicate that all of the beltline region materials will remain above the 50 ft-lb screening criteria for both 32 and 48 EFPY.

TABLE C-1

McGuire Unit 1 Beltline Material Upper Shelf Energy Values

| Material Description | Initial Upper Shelf Energy (ft-lb) | Upper Shelf Energy at 32 EFPY (ft-lb) | Upper Shelf Energy at 48 EFPY (ft-lb) |
|--|------------------------------------|---------------------------------------|---------------------------------------|
| Intermediate Shell B5012-1 | 101 | 91 | 90 |
| Intermediate Shell B5012-2 | 105 | 80 | 78 |
| Intermediate Shell B5012-3 | 112 | 88 | 86 |
| Lower Shell B5013-1 | 95 | 72 | 70 |
| Lower Shell B5013-2 | 115 | 92 | 90 |
| Lower Shell B5013-3 | 103 | 82 | 80 |
| Girth Weld | >126 | >101 | >98 |
| Intermediate Shell Longitudinal Weld Seams 2-442B & 2-442C | 112 | 69 | 65 |
| Intermediate Shell Longitudinal Weld Seam 2-442A | 112 | 71 | 66 |
| Lower Shell Longitudinal Weld Seams 3-442A & 3-442C | >90 | >59 | >57 |
| Lower Shell Longitudinal Weld Seam 3-442B | >90 | >58 | >56 |

APPENDIX D

Justification for Using Diablo Canyon Unit 2 Surveillance Weld
Data for the Prediction of the McGuire Unit 1 Lower Shell Longitudinal
Weld Seam Metal Mechanical Properties

Purpose:

The purpose of this appendix is to document an evaluation of the Diablo Canyon Unit 2 surveillance weld metal and the McGuire Unit 1 reactor vessel lower shell longitudinal weld seam metal to determine the feasibility of using the Diablo Canyon Unit 2 surveillance weld metal as a credible data source for the calculation of the adjusted RT_{NDT} of the limiting McGuire Unit 1 lower shell longitudinal weld seam.

Background:

Based on the calculational methods of Regulatory Guide 1.99, Revision 2, the limiting beltline material (in terms of RT_{NDT}) in the McGuire Unit 1 reactor vessel is the intermediate shell longitudinal weld seam. Thus, this material was chosen for the surveillance program weld metal. However, when surveillance data from the McGuire Unit 1 program is used to predict the adjusted RT_{NDT} of the intermediate shell longitudinal weld seams, it is no longer limiting. Applying the results of the McGuire Unit 1 surveillance program to calculate the adjusted RT_{NDT} of the intermediate shell longitudinal weld seams changes the limiting material to the lower shell longitudinal weld seam metal.

During the review of the draft report on the surveillance capsule V analysis, the Duke Power Company noticed that the limiting material for the generation of the heatup/cooldown curves had changed from the intermediate shell longitudinal weld seam to the lower shell longitudinal weld seam. This prompted a request to use Diablo Canyon Unit 2 surveillance weld data in the calculation of the RT_{NDT} for the limiting lower shell longitudinal weld seam and the subsequent request for the development of this appendix and the generation of new heatup/cooldown curves for McGuire Unit 1.

Later Westinghouse received a call from the Duke Power Company asking about the feasibility of using the Diablo Canyon Unit 2 surveillance weld data to predict the RT_{NDT} of the lower shell longitudinal weld seams of McGuire Unit 1. Since the lower shell longitudinal weld seam is the limiting material for the generation of the McGuire Unit 1 heatup and cooldown curves, a benefit in RT_{NDT} would give McGuire Unit 1 more operating margin when heating up and cooling down the plant.

Methodology:

The evaluation described in this appendix was performed utilizing the following methodology:

The evaluation of the Diablo Canyon Unit 2 surveillance weld metal and McGuire Unit 1 lower shell longitudinal weld seam data was based on the following:

- What weld wire heat number was used to fabricate the welds,
- What flux and flux lot number were used to fabricate the welds,
- What venter fabricated the welds and in what time frame,
- What heat treatment did each weld receive,
- Is the chemistry of both welds similar,
- Is the initial RT_{NDT} of both welds the same or relatively close,
- Is the initial upper shelf energy of both welds the same or relatively close,
- Is the geometry of both plants similar,
- Is the type of fuel in both plants the same,
- Are the fuel loading patterns in both plants similar (ie. low leakage, etc.),
- What is the projected 32 effective full power year surface fluence of each plant,
- What vessel inlet temperatures do the plants operate at,
- What are the differences in the capsule lead factors of both plants, and
- Can the criteria for credibility in Regulatory Guide 1.99, Revision 2, be met for McGuire Unit 1 when applied to the Diablo Canyon Unit 2 weld data ?

Development and documentation of the justification to use the Diablo Canyon Unit 2 surveillance weld data for the McGuire Unit 1 lower shell longitudinal weld seam metal mechanical property predictions was based on the answers to the above questions.

Evaluation:

The comparison of the Diablo Canyon Unit 2 surveillance weld metal relative to the McGuire Unit 1 lower shell longitudinal weld seam metal is summarized as follows:

What weld wire heat numbers, flux, and flux lot numbers were used to fabricate the welds ?

The Diablo Canyon Unit 2 surveillance weld is a Tandem weld fabricated with weld wire heat numbers 12008 and 21935 using Linde 1092 Flux Lot No. 3869.

The McGuire Unit 1 lower shell longitudinal weld seams are Tandem weld fabricated with weld wire heat numbers 12008 and 21935 using Linde 1092 Flux Lot No. 3889.

What vendor fabricated the welds and in what time frame ?

The Diablo Canyon Unit 2 surveillance weld was fabricated by Combustion Engineering, Inc. in the late 1960's and early 1970's.

The McGuire Unit 1 welds were also fabricated by Combustion Engineering, Inc. in the late 1960's and early 1970's.

What heat treatment did each weld receive ?

The Diablo Canyon Unit 2 surveillance weld metal post weld heat treatment was at $1150^{\circ}\text{F} \pm 25^{\circ}\text{F}$ for 40 hours and furnace cooled.

The McGuire Unit 1 lower shell longitudinal weld seams also received a post weld heat treatment of $1150^{\circ}\text{F} \pm 25^{\circ}\text{F}$ for 40 hours and furnace cooled.

Is the chemistry of both welds similar ?

The unirradiated chemistry of the Diablo Canyon Unit 2 surveillance weld and the McGuire Unit 1 Lower Shell Longitudinal Weld Seam metal is provided in Table D-1.

A review of the data presented in Table D-1 reveals that the chemistry of the Diablo Canyon Unit 2 surveillance weld metal is very similar to the chemistry of the McGuire Unit 1 lower shell longitudinal weld metal.

Is the initial RT_{NDT} of both welds the same or relatively close ?

The initial RT_{NDT} of the Diablo Canyon Unit 2 surveillance weld metal is -50°F .

The initial RT_{NDT} of the McGuire Unit 1 lower shell longitudinal weld seams is not known so a generic value of -56°F is used.

TABLE D-1

Unirradiated Chemistry of the Diablo Canyon Unit 2 Surveillance Weld and
the McGuire Unit 1 Lower Shell Longitudinal Weld Seams

| Element | Diablo Canyon Unit 2 | | McGuire Unit 1 ⁽⁶⁾ |
|---------|-------------------------------|---|-------------------------------|
| | CE ⁽⁷⁾ Analysis | Westinghouse ⁽⁸⁾ Analysis | |
| C | 0.16 | 0.13 | 0.11 |
| S | 0.010 | 0.010 | 0.011 |
| N | - | 0.008 | - |
| Co | - | 0.012 | - |
| Cu | 0.22 | 0.22 | 0.20 |
| Si | - | 0.22 | 0.15 |
| Mo | - | 0.47 | 0.55 |
| Ni | - | 0.83 | - |
| Mn | - | 1.32 | 1.38 |
| Cr | - | 0.031 | - |
| V | - | 0.001 | - |
| P | 0.015 | 0.017 | 0.015 |
| Sn | - | 0.010 | - |
| Al | - | 0.009 | - |

Is the initial upper shelf energy of both welds the same or relatively close ?

The unirradiated Diablo Canyon Unit 2 surveillance weld metal initial upper shelf energy is 124 ft-lb.

No documentation could be located to determine the unirradiated upper shelf energy of the McGuire Unit 1 lower shell longitudinal weld seams.

Is the geometry of both plants similar ?

Both Diablo Canyon Unit 2 and McGuire Unit 1 have a reactor vessel inner radius of 173 inches, a reactor vessel beltline thickness of 8.625 inches and a power rating of 3565 MWT, both are Westinghouse 4 loop NSSS plants, have neutron pads and the surveillance capsules are located at the same azimuthal angles.

Is the type of fuel in both plants the same ?

Both Diablo Canyon Unit 2 and McGuire Unit 1 use 17X17 rod array fuel assemblies.

Are the fuel loading patterns in both plants similar (ie. low leakage) ?

Diablo Canyon Unit 2 utilizes a low leakage fuel management scheme.

McGuire Unit 1 currently utilizes a low leakage fuel management scheme.

Is the projected surface fluence at 32 effective full power year (EFPY) relatively close ?

The Diablo Canyon Unit 2 projected clad/base metal interface fluence (n/cm^2 , $E > 1.0$ MeV) at 32 EFPY and various azimuthal angles is:

| | | | |
|---------------------------------------|--|--|--|
| $\frac{0^\circ}{9.83 \times 10^{18}}$ | $\frac{15^\circ}{1.46 \times 10^{19}}$ | $\frac{30^\circ}{1.19 \times 10^{19}}$ | $\frac{45^\circ}{1.70 \times 10^{19}}$ |
|---------------------------------------|--|--|--|

The McGuire Unit 1 projected clad/base metal interface fluence (n/cm^2 , $E > 1.0$ MeV) at 32 EFPY and various azimuthal angles is:

| | | | |
|--|---|---|---|
| $\frac{0^\circ}{1.332 \times 10^{19}}$ | $\frac{15^\circ}{1.969 \times 10^{19}}$ | $\frac{30^\circ}{1.459 \times 10^{19}}$ | $\frac{45^\circ}{2.016 \times 10^{19}}$ |
|--|---|---|---|

The difference in these fluence values is believed to be due to Diablo Canyon Unit 2 utilizing a low leakage loading pattern from the start of operation while a low leakage loading pattern was not initiated in McGuire Unit 1 until after several operating cycles.

What vessel inlet temperature do the plants operate at ?

Diablo Canyon Unit 2 operates with at vessel inlet temperature of approximately 545.1°F.

McGuire Unit 1 operates with at vessel inlet temperature of approximately 557.9°F.

What are the capsule lead factors for both plants ?

The surveillance capsule lead factors for Diablo Canyon Unit 2 and McGuire Unit 1 surveillance capsules is presented in Table D-2.

Based on the information provided in Table D-2, the lead factors of the surveillance capsules in both plants are essentially equivalent. However, when the lower average flux rate on the Diablo Canyon Unit 2 capsules is used with the higher average flux rate on the McGuire Unit 1 reactor vessel, the result is that the Diablo Canyon Unit 2 capsules actually have a slightly lower lead factor than the McGuire Unit 1 capsules.

| TABLE D-2 | | | | | |
|---|----------|-------------|--------------------------------|----------|-------------|
| Surveillance Capsule Lead Factors for Diablo Canyon Unit 2 and McGuire Unit 1 | | | | | |
| Diablo Canyon Unit 2 ⁽¹¹⁾ | | | McGuire Unit 1 ⁽¹³⁾ | | |
| Capsule | Location | Lead Factor | Capsule | Location | Lead Factor |
| U | 56° | 5.28 | U | 56° | 5.25 |
| V | 58.5° | 4.62 | V | 58.5° | 4.72 |
| W | 124° | 5.28 | W | 124° | 5.32 |
| X | 236° | 5.28 | X | 236° | 5.31 |
| Y | 238.5° | 4.62 | Y | 238.5° | 4.72 |
| Z | 304° | 5.28 | Z | 304° | 5.32 |

Can the credibility criteria of Regulatory Guide 1.99, Revision 2, be met for McGuire Unit 1 when applied to the Diablo Canyon Unit 2 surveillance weld metal ?

- 1) "Materials in the capsules should be those judged most likely to be controlling with regard to radiation embrittlement according to the recommendations of this guide."

When the results of the tested surveillance capsules from McGuire Unit 1 are applied in the calculation of the 32 EFPY adjusted RT_{NDT} 's of the McGuire Unit 1 beltline materials, the lower shell longitudinal weld metal becomes limiting. Hence, the weld metal in the Diablo Canyon Unit 2 surveillance program is the limiting material in the McGuire Unit 1 reactor vessel. Thus, this criteria is met.

- 2) "Scatter in the plots of Charpy energy versus temperature for the irradiated and unirradiated conditions should be small enough to permit the determination of the 30-foot-pound temperature and the upper-shelf energy unambiguously."

A review of the Charpy plots presented in the analyses of the two Diablo Canyon Unit 2 surveillance capsule tested to date was performed. The scatter in the plots of Charpy energy versus temperature for the irradiated and unirradiated conditions was judged to be small enough to permit the determination of the 30-foot-pound temperature and the upper-shelf energy unambiguously. Thus, this criteria is met.

- 3) "When there are two or more sets of surveillance data from one reactor, the scatter of ΔRT_{NDT} values about a best-fit line drawn as described in Regulatory Position 2.1 normally should be less than 28°F for welds and 17°F for base metal. Even if the fluence range is large (two or more orders of magnitude), the scatter should not exceed twice those values. Even if the data fail this criterion for use in shift calculations, they may be credible for determining decrease in upper-shelf energy if the upper shelf can be clearly determined, following the definition given in ASTM 185-82".

There are two sets of test data from the Diablo Canyon Unit 2 surveillance program. A review of the measured and predicted ΔRT_{NDT} 's in these analyses for the weld metal showed that the scatter in the ΔRT_{NDT} 's of the weld metal is less than 28°F. Thus, this criteria is met.

- 4) "The irradiation temperature of the Charpy specimens in the capsule should match vessel wall temperature at the clad/base metal interface within $\pm 25^\circ\text{F}$."

Both the Diablo Canyon Unit 2 surveillance program and the McGuire Unit 1 surveillance program are based on ASTM E185-73. Per ASTM E185-73, "Specimens shall be irradiated at a location in the reactor that duplicates as closely as possible the neutron-flux spectrum, temperature history, and maximum accumulated neutron fluence experienced by the reactor vessel." The Diablo Canyon Unit 2 and McGuire Unit 1 surveillance capsules were installed between the neutron pad and the reactor vessel wall in order to fulfill the requirements of ASTM E185-73. Based on the location of the capsules in the vessel, the

temperature should be the same as the vessel inlet water temperature and the temperature of the reactor vessel wall in the beltline region will also be the same as the vessel inlet water. The irradiation temperatures of the surveillance capsules is judged to be within $\pm 25^{\circ}\text{F}$ of the vessel wall temperature at the clad/base metal interface. Diablo Canyon Unit 2 operates at vessel inlet temperature of 545.1°F and McGuire Unit 1 operates at a vessel inlet temperature of 557.9°F . However, NRC currently believes that the irradiation damage of the material increases as the irradiation temperature of the material decreases. Therefore, the Diablo Canyon Unit 2 test data should be slightly more conservative than if the material were irradiated in the McGuire Unit 1 reactor vessel. Thus, based on this rationale, this criteria is also met.

- 5) "The surveillance data for the correlation monitor material in the capsule should fall within the scatter band of the data base for this material."

Neither the McGuire Unit 1 or the Diablo Canyon Unit 2 surveillance programs contain correlation monitor material. Therefore, this criteria is not applicable.

Results:

The evaluation of the Diablo Canyon Unit 2 surveillance weld metal and McGuire Unit 1 lower shell longitudinal weld seam metal results in the following:

Both the Diablo Canyon Unit 2 surveillance weld metal and the McGuire Unit 1 lower shell longitudinal weld seams are Tandem welds fabricated with weld wire heat numbers 21935 and 12008 using Linde 1092 Flux.

Both the Diablo Canyon Unit 2 surveillance weld metal and the McGuire Unit 1 lower shell welds were fabricated by Combustion Engineering, Inc. in the late 1960's / early 1970's.

Both the Diablo Canyon Unit 2 surveillance weld metal and the McGuire Unit 1 lower shell longitudinal weld seams had a post weld heat treatment of $1150^{\circ}\text{F} \pm 25^{\circ}\text{F}$ for 40 hours and were furnace cooled.

A review of the available data for both the Diablo Canyon Unit 2 surveillance weld metal and the McGuire Unit 1 lower shell welds indicates that the weld metal chemistry is similar.

The initial RT_{NDT} of the Diablo Canyon Unit 2 surveillance weld metal is measured and is -50°F. The initial RT_{NDT} of the McGuire Unit 1 lower shell weld seams is a generic value of -56°F. A higher initial RT_{NDT} value is conservative, thus, the use of -50°F for the initial RT_{NDT} of the McGuire Unit 1 lower shell longitudinal weld seams is conservative and acceptable.

The initial upper shelf energy of the Diablo Canyon Unit 2 surveillance material was measured to be 124 ft-lb. No data for initial upper shelf energy of the McGuire Unit 1 lower shell longitudinal weld seams could be located. Therefore, this criterion was not used for this evaluation.

Both plants have vessels with a beltline thickness of 8.625 inches and an inner radius of 173 inches, both have four loops, both have 17X17 rod array fuel assemblies, both plants have neutron pads and the surveillance capsules in both plants are located at the same azimuthal angles and at the same distance from the center of the core. Thus, Diablo Canyon Unit 2 and McGuire Unit 1 have similar geometry.

Both Diablo Canyon Unit 2 and McGuire Unit 1 have a power rating of 3565 MWt and both plants are currently using a low leakage core loading pattern.

The projected 32 full effective power year (EFPY) fluence (n/cm^2 , $E > 1.0$ MeV) of the McGuire Unit 1 reactor vessel beltline material is higher than that for Diablo Canyon Unit 2. However, since the neutron flux rate of the Diablo Canyon Unit 2 surveillance capsules is less than the neutron flux rate of the McGuire Unit 1 surveillance capsules, the data obtained from the Diablo Canyon Unit 2 surveillance program should give a better prediction of the McGuire Unit 1 vessel beltline materials than the McGuire Unit 1 surveillance program because the integrated average lead factors are slightly lower.

The vessel coolant inlet temperature of the Diablo Canyon Unit 2 reactor vessel is 545.1°F and the vessel coolant inlet temperature of the McGuire Unit 1 reactor vessel is 557.9°F. The current belief is that a lower irradiation temperature causes greater damage to the material. Thus, the lower operating temperature of Diablo Canyon Unit 2 makes its surveillance results slightly conservative when applied to the McGuire Unit 1 reactor vessel beltline materials.

The applicable credibility criteria of Regulatory Guide 1.99, Revision 2, for judging the credibility of surveillance data are met for McGuire Unit 1 when applied to the Diablo Canyon Unit 2 surveillance weld metal.

Conclusions:

Based on the above evaluation, using the Diablo Canyon Unit 2 surveillance weld data to predict the mechanical properties of the McGuire Unit 1 lower shell longitudinal weld seam metal is justified and is recommended for calculations of the irradiated mechanical properties of the McGuire Unit 1 lower shell longitudinal weld seam material.